A role for neutrophil granulocytes as afferent signals in immune-to-brain communication during systemic and localized organ-specific lung inflammation

Inaugural Dissertation

submitted to the

Faculty of Veterinary Medicine

in partial fulfillment of the requirements

for the Doctor of Philosophy-PhD Degree

of the Faculties of Veterinary Medicine and Medicine

of the Justus Liebig University Giessen

by

Jessica Kate Hernandez

of

Houston, Texas, USA

Giessen 2024

From the Institute of Veterinary Physiology and Biochemistry

Dean: Prof. Dr. Dr. Stefan Arnhold

of the Faculty of Veterinary Medicine of the Justus Liebig University Giessen

Supervisor and Committee Member: Prof. Dr. Christoph Rummel

Co-supervisor and Committee Member: Prof. Dr. Klaus-Dieter Schlüter

Committee Member: Prof. Dr. Martin Hadamitzky

Chair and Committee Member: Prof. Dr. Ralph Schermuly

Date of Doctoral Defense: 04.07.2024

“Failure is the condiment that gives success its flavor.”

Truman Capote

Table of contents

Table of contents

Table of contents

I. Introduction

It is well know that information can be transmitted from the periphery to the brain and that this immune-to-brain communication plays an important role in maintaining normal brain function as well as regulating immune responses. Primarily, studies have focused on communication via the humoral route, namely through circulating immune mediators including lipid derived signaling, as well as through neuronal transmission (Rummel 2016). Moreover, evidence indicates that not only are peripheral immune cells capable of infiltrating the brain but, once there, they are also influencing the inflammatory process and modulating brain function (Pflieger et al. 2018). Specifically, the potential for neutrophil granulocyte (NG) recruitment to the brain and their role in immune-to-brain communication is the main focus of this dissertation project.

Traditionally viewed as pro-inflammatory cells, little is actually known about the effect NGs can have on the central nervous system (CNS) despite the fact that they have been shown to infiltrate the brain under certain conditions, such as during systemic inflammation (Bohatschek et al. 2001). Additionally, not only are they trafficking to the brain but effects have been seen of NGs impacting depressive-like behaviors. As such, Aguilar-Valles and colleagues (2014) have shown that depletion of NGs inhibited depression-like behaviors observed in septic-like inflammation surviving mice (Aguilar-Valles et al. 2014). This information alone would encourage further investigation into NG contributions to immune-to-brain communication. Interestingly, there is also evidence of an anti-inflammatory potential of NGs. Studies have found that NGs produce anti-inflammatory immune-mediators of the so-called cytokine family, namely, interleukin (IL)-1 receptor antagonist (ra) as well as inducible nitric oxide synthase (NOS) (Schröder et al. 2006, Garcia-Bonilla et al. 2014). These reports lend credence to the idea that NGs could be playing a more beneficial role than previously thought.

The pro- or anti-inflammatory capacity of NGs may well have broad implications, including a contribution to the resolution of the sickness response experienced during infection or inflammation. For example, NGs can undergo a type of programmed cell death known as NETosis during which neutrophil extracellular traps (NETs) composed of chromatin fibers and granule proteins are released from the cell and form a web-like

structure that traps and neutralizes bacterial and viral factors (Brinkmann et al. 2004, Boeltz et al. 2019). However, NETs can also be detrimental and have been linked to exacerbating immune responses in such diseases as rheumatoid arthritis and Type 1 diabetes mellitus (Delgado-Rizo et al. 2017). Recently Al-Kuraishy and colleagues (2022) even found that NGs and NETs played a role during lung inflammatory insults with critical complications in acute lung injury (ALI) inducing hyper-inflammation during coronavirus disease 2019 (COVID-19) infection (Al-Kuraishy et al. 2022). The dual nature of NETs and their potential to be pro- or anti-inflammatory makes them a particularly interesting topic and research continues into the role they could be playing during inflammation as well as a variety of other metabolic, autoimmune, and inflammatory conditions. Moreover, neutropenia is a common side effect of chemotherapy and neutropenic fever is a severe clinical status of unknown origin (Lyman et al. 2014). Following chemotherapy it is not uncommon for patients to contract bacterial infections that result in an intense and enduring fever, and possibly even sepsis, during which the function of NGs remains largely unknown (Pizzo 1993, Schiel et al. 2003). Therefore, a better understanding of NGs may lead to new therapeutic options and better quality of life for those cancer patients showing neutropenia.

Overall, immune-to-brain communication during systemic or organ (lung) inflammation affects the brain and can, potentially, exacerbate ongoing brain pathology such as stroke or cerebral ischemia (D'Mello et al. 2009, McColl et al. 2007, Perry et al. 2007, Spencer et al. 2007) . Here, the so far largely unexplored role of the NG response during systemic or lung inflammation when stimulated by the bacterial mimetic lipopolysaccharide (LPS) is investigated.

1.1 The systemic inflammatory response

Anyone that has scrapped a knee or had that unfortunate pleasure of being stuck in bed due to an unruly infection has experienced some degree of inflammation first hand. Whether suffering from swelling and redness or nausea, fever, loss of appetite, or lethargy all are covered under the umbrella of symptoms resulting from inflammation (Hart 1988, Nathan 2002). Specifically, the inflammatory response refers to the body’s

local defense mechanism using cellular and humoral components against a pathogen or insult in an attempt to return to homeostasis (Levy 1996).

Multiple different tissue types are able to show an inflammatory response and once triggered by a combination of pathogens and/or pathogen-associated molecular patterns (PAMP), the first defense is mounted by the immune system. To mimic such an acute inflammatory response, LPS, for example, can be used as a stimulant (Bucklin et al. 1993, Hu and Pasare 2013). A primary component of the outer membrane of gram-negative bacteria, released during division or bacterial lysis, the endotoxin LPS is a well-known and frequently applied inducer of inflammation in animals and humans (Freudenberg and Galanos 1990, Lasselin et al. 2020). After administration of LPS, both animals and humans release pro-inflammatory cytokines and chemokines, which will recruit NGs to the site of experimental trauma (i.e., LPS-injection) where the first attempts at neutralization begins (Levy 1996, Serhan 2017). It is during this stage when individuals experience the typical manifestations of sickness mentioned above (Dantzer et al. 2008). As the immune response continues, a cascade effect is activated not only to neutralize the source of the infection but to then operate in a negative feedback loop where the later phases work to terminate the process through the release of anti-inflammatory cytokines and clearance of pro-inflammatory mediators (Shimada et al. 1998). However, it is important to bear in mind that resolution of inflammation is a complex process involving many additional immunoresolvent factors other than cytokines (Serhan et al. 2007). Lipid derivatives known as specialized pro-resolving mediators (SPM) are one such example that aid in cell clearance and cessation of inflammation (Sugimoto et al. 2019). SPM such as resolvins (Rv) stop NG infiltration, induce macrophage cleanup, and encourage tissue restoration (Serhan et al. 2015, Abdolmaleki et al. 2020). An overview of the initiation and resolution of local inflammation is shown in Figure 1. Furthermore, it is important to note that communication via inflammatory mediators, i.e., cytokines, not only occurs amongst immune cells but can also transport important inflammatory information to the brain by interacting with other cell types such as endothelial and glial cells as well but this will be discussed in more detail in section 1.3.1 (Xu et al. 2020, Benveniste and Benos 1995).

Although heavily regulated, it is possible for a local inflammatory reaction to become systemic. When an infectious agent is more severe or the infection has spread beyond the abilities for the local inflammatory response to control, inflammatory mediators can be found in circulation (Rummel et al. 2004). In such circumstances, systemic bacterial growth and overproduction of cytokines results in permeability of the vasculature and a life-threatening systemic infection known as sepsis (see section 1.8) (Stephens et al. 1988, Bone et al. 1997). During sepsis, the body experiences systemic inflammation known as the acute phase response (APR) (Baumann and Gauldie 1994). In addition to the recruitment of NGs and monocytes, inflammatory mediators also enter the bloodstream. These stimulate the release of acute phase proteins (APP), activate the hypothalamic-pituitary-adrenal axis (HPA), and elicit behavioral changes (Baumann and Gauldie 1994, Gruys et al. 2005). The APP released from the liver assist in clearing the infection and modulating the immune response. Moreover, both the activation of the HPA axis and the behavioral changes demonstrate the level of communication that occurs with the brain during the APR (Dantzer 2001, Gruys et al. 2005, Hart 1988). This communication between the periphery and the brain is key because during sepsis inflammatory mediators and peripheral immune cells can interact with the CNS and cause inflammation in the brain (Meneses et al. 2019).

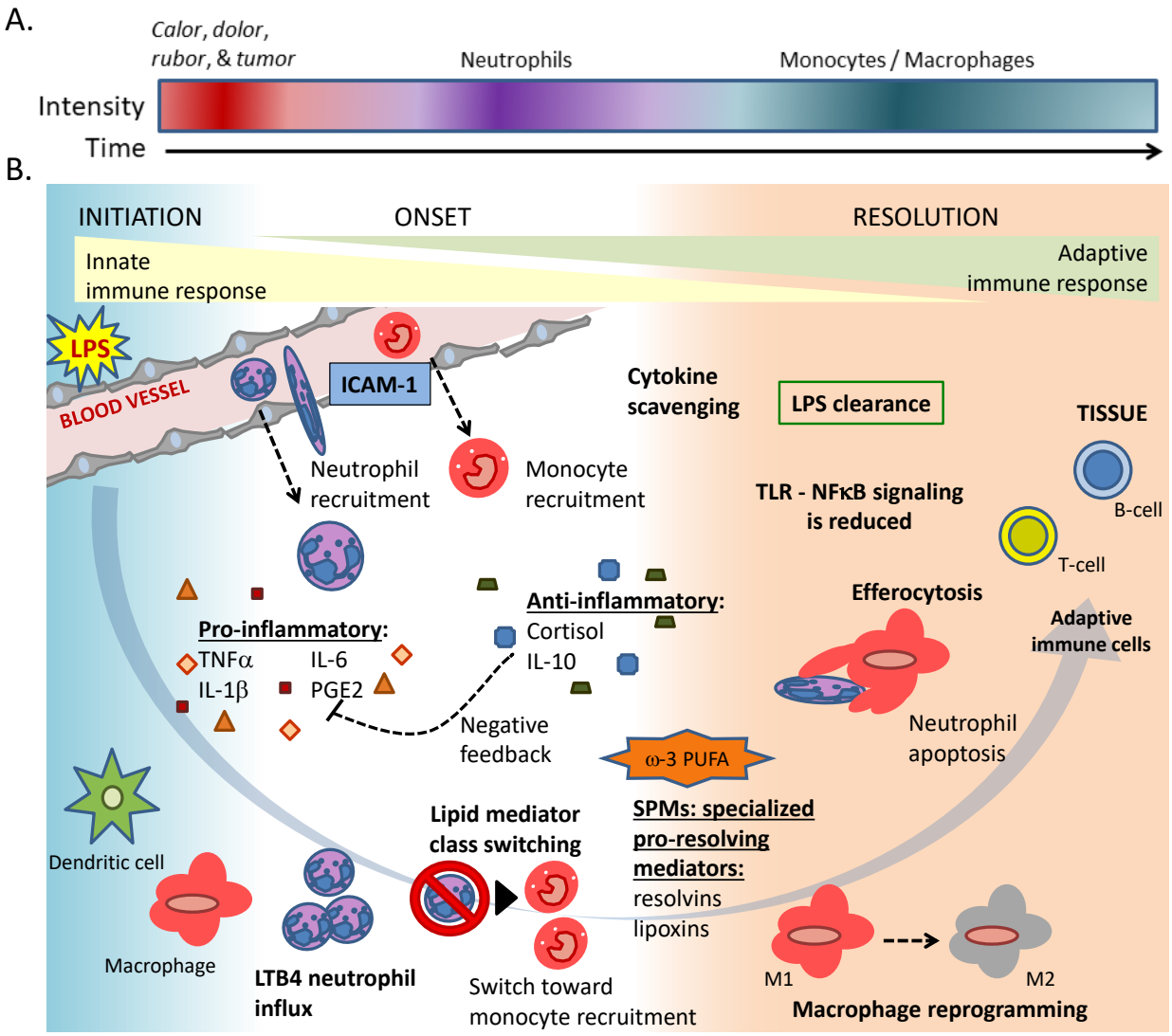

Figure 1: Process of the inflammatory response

A stimulant such as infection or injury can initiate inflammatory responses; the three stages of inflammation are characterized by initial signs of inflammation [calor, dolor, rubor, & tumor] following initiation, increase in neutrophil granulocyte (NG) recruitment during onset, and monocyte and macrophage influx during resolution (A). Here, the bacterial mimic lipopolysaccharide (LPS) triggers the response through toll-like receptor (TLR) 4 and activation of the inflammatory transcription factor nuclear-factor-κ-B (NFκB). The resulting cascade produces a self-limiting innate immune response that ends in resolution with generation of adaptive immunity (B). Adhesion molecule: intercellular adhesion molecule-1 (ICAM-1); cytokines: tumor necrosis factor (TNF)α, interleukin (IL) 1β, 6, and 10; hormones: cortisol; lipid mediators: prostaglandin E2 (PGE2), leukotriene B4 (LTB4), resolvins, and lipoxins. An original figure created with references from Sugimoto et al. (Sugimoto et al. 2019).

1.2 The inflammatory cascade of innate immunity

After suffering an inflammatory event, the ability to mobilize a defense is crucial in order to minimize damage and to ensure return to homeostasis as quickly as possible. The APR primarily achieves this through a choreographed cascade composed of molecular and cellular components carefully regulated throughout (Gilroy et al. 2003).

1.2.1 Inflammatory cells

The key components to a successful APR are the cells of the innate immune response. It is monocytes and macrophages that first come into contact with the inflammatory stimulus through pattern-recognition receptors (PRRs) and release an initial burst of cytokines (Auffray et al. 2007). Concurrently, local cells begin to die and release damage-associated molecular patterns (DAMP) (McDonald et al. 2010). Together these are the first steps toward initiating the cytokine cascade. Meanwhile, tissue damage and cytokines encourage efforts at repair and barrier formation through coagulation to minimize the spread of infectious agents (Kambas et al. 2008). From here, the process builds and the monocytes differentiate into activated M1 macrophages. These M1 macrophages push the cascade onwards as the cytokines they release interact with local cells, such as endothelial cells, and a more robust second wave of cytokines is released (Baumann and Gauldie 1994, Verreck et al. 2004). The inflammatory mediators being released include tumor necrosis factor (TNF)α, IL-1β, and prostaglandin (PG) E2, which will be discussed in more detail in section 1.2.2.

With the second wave of cytokines and release of DAMPs, NGs and plasma proteins are now being heavily recruited to the site of trauma to facilitate pathogen clearance (Pittman and Kubes 2013). The influence of the endothelial cells is highlighted once again when they are activated to express adhesion molecules such as intercellular adhesion molecule (ICAM)-1 (Dustin et al. 1986). Combined with an increased vessel permeability, NGs and leukocytes are drawn to the site of trauma where they begin to “stick to” vessel walls and extravasate into the tissue (Ding et al. 1999). The heavy influx of NGs and their role in the immune response is the focus here and is the reason why special attention will be paid to this inflammatory cell in section 1.2.1.1.

The next steps involve the gradual flip of a switch as the release of cytokines progresses to an anti-inflammatory profile, including IL-10 and SPMs (see section 1.2.2.5 and 1.2.3.4), and the self-limiting process begins. During the resolution of inflammation, NG recruitment is replaced with a preference for monocytes, as those NGs present start to undergo an apoptotic cell death or return to circulation (Hughes et al. 1997). Macrophages now possess an anti-inflammatory M2 phenotype that produce IL-10 and phagocytize dying NGs in a process known as efferocytosis (Savill et al. 1989, Verreck et al. 2004). Finally, remaining macrophages will drain from the tissue via the lymphatic system (Schif-Zuck et al. 2011).

1.2.1.1 Neutrophil granulocytes

NG are a subtype of bone marrow derived granulocytes and are the most abundant cell type in circulation, making up approximately 40-70% of leukocytes (Actor 2012). Characterized by a multi-lobed nucleus and cytoplasmic granules they serve a primarily phagocytic purpose (Carbone et al. 2017). The granules of NGs can be divided into four categories, namely, azurophilic, specific, gelatinase, or secretory that are characterized by their protein contents and ability to be exocytosed (Pham 2006). Additionally, NGs can also be polarized into different subsets, which express different functional roles and have been termed as tumor-associated neutrophils (TAN). These subpopulations are the N1 and N2 NG groups, which are designated as pro-inflammatory and immunosuppressive, respectively, and are covered in more detail in section 1.2.1.1.1 (Fridlender et al. 2009). Though short lived, NGs are the first line of defense of the APR, and are the most heavily recruited cell type to sites of inflammation. Originally, they may have been seen as one-dimensional but new experimental evidence provided insights into their abilities and broader functional significance.

Along with monocytes and macrophages, NGs also express PRRs and are able to detect PAMPs, such as LPS, that stimulate migration (Fan and Malik 2003). Activation of the PRRs along with the initial cytokines release initiates NG migration known as the extravasation cascade. The main steps of this process are: capture, rolling, adhesion, crawling, and migration i.e., extravasation (Ley et al. 2007). To start with, NGs need to be recruited to the site of inflammation, which is achieved through the expression of

selectins and their receptors on both endothelial cells and NGs where they serve as one of the regulators of NG capture and subsequent rolling following a cytokine gradient (Lawrence et al. 1994). Next, adhesion occurs when rolling stops and the NG prepares for extravasation. Moderators of adhesion are triggered by the second wave of cytokines and include adhesion receptor like integrins as well as the previously mentioned ICAM-1 (Lowell and Berton 1999). At this point, NGs will move on to crawling, which is a brief precursor before the final step when NGs look for an ideal site to pass through the endothelial cell barrier (Phillipson et al. 2006). Finally, once positioned, a combination of chemoattractants and endothelial signaling allow the NG to pass through the endothelium to the tissue (Cinamon et al. 2004).

Once NGs have successfully infiltrated the site of inflammation, their role in cellular defense begins. When activated, NGs main role is to identify and phagocytize pathogens while simultaneously releasing pro-inflammatory cytokines (Cicco et al. 1990, Fujishima et al. 1993). Phagocytosis can occur through an oxygen-dependent or -independent manner when an opsonized bacteria or immune complexes activate the plasma membrane receptors of NGs, thus, triggering invagination and engulfment of the pathogen (Weissmann et al. 1980). In an oxygenated environment the azurophilic granules, which contain antimicrobial enzymes like myeloperoxidase (MPO), are the primary granule involved within the phagolysosomes (Pham 2006). Once activated, increased oxygen consumption leads to the generation of reactive oxygen species (ROS) by nicotinamide adenine dinucleotide phosphate (NADPH) oxidase, ROS in particular require careful regulation as they are very cytotoxic and unspecific and, thus, capable of damaging host tissue (Follin and Dahlgren 1992). One such ROS utilized during phagocytosis is hydrogen peroxide, which MPO uses along with chloride ions, to produce the highly cytotoxic hypochlorous acid to aid in pathogen breakdown (Hirche et al. 2005). Alternatively, through antimicrobial peptides and enzymes also stored within azurophilic and specific granules, such as defensins, cathepsins, elastase, and lysosozyme, that do not necessitate the production of ROS; pathogens can be broken down via an oxygen-independent system (Kobayashi et al. 2018). Additionally, NGs can also undergo a process called NETosis to trap and kill pathogens but this will be detailed later in section 1.2.1.1.2.

As NG accumulation peaks, the APR enters the beginning stages of resolution, when a negative feedback loop leads to NG removal and return to homeostasis (Serhan et al. 2007). In addition to the lipid mediators mentioned earlier, NGs also aid in the synthesis of SPMs like lipoxins (LX) and Rvs that play key roles in the resolution process and are synthesized at the site of inflammation (see section 1.2.3.4) (Lehmann et al. 2015). Finally, once the inflammatory agent is removed, NGs need to exit the tissue. This can happen through three different processes: reverse migration, draining through the lymphatic system, or efferocytosis, with this being the most common method. The process of efferocytosis is triggered by SPMs and composed of two parts. To start with, the NGs undergo a programmed cell death after which they are phagocytized by macrophages (Savill et al. 1989).

1.2.1.1.1 Tumor-associated neutrophils: N1 vs. N2

A more recent topic of interest are TANs, identified as N1 or N2, that can be classified according to their phenotypes, which have anti- or pro-tumorigenic properties respectively. Early on an association was noticed between NGs and tumors where the levels of polymorphonuclear cells rose proportionally with the metastatic potential of tumors in rats (Welch et al. 1989). Further studies were able to identify heterogeneous populations of NGs that had been polarized by certain factors, such as type 1 interferons (IFN) or transforming growth factor (TGF)-β, in the microenvironment (Fridlender et al. 2009, Pylaeva et al. 2016). During early tumorigenesis pro-inflammatory and anti-tumorigenic N1 NGs remain near the periphery of the tumor and have a more suppressive effect on tumor activity due to their production of cytotoxic mediators (Brandau et al. 2013, Mishalian et al. 2013). During later stages of tumorigenesis when NGs were also localized within tumors, their profiles switch to an immunosuppressive and pro-tumorigenic N2 phenotype that facilitates such effects as tumor invasion and angiogenesis through the release of oncostatin M, matrix metalloprotease type 9, and hepatocyte growth factor to name a few (To et al. 2002, Wislez et al. 2003, Queen et al. 2005, Nozawa et al. 2006, Mishalian et al. 2013). Work done by Bellocq and colleagues in 1998 already shows an association of increased NG infiltration into bronchioloalveolar carcinomas with worse prognoses in these patients (Bellocq et al. 1998).

In addition to their role in cancer, these NG subsets could also contribute to the pathogenesis of several autoimmune diseases. For example, NGs can impact disease through altered immune functions, adhesion and migratory abilities and/or a primed status, which contributes to their role in chronic inflammation in diseases such as neuromyleitis optica, multiple sclerosis (MS), and rheumatoid arthritis in patients (Cedergren et al. 2007, Naegele et al. 2012, Hertwig et al. 2016) have been identified. However, more research is required to understand the different physiological conditions under which NG subsets can exist as well as their potential impact on disease states and their progression or resolution. Yet, determination of N1 and N2 NGs phenotypes is largely restricted due to the lack of validated surface markers (Sagiv et al. 2016).

1.2.1.1.2 What are NETs?

In 1996 Takei and colleagues discovered that NGs treated with phorbol 12-myristate 13-acetate (PMA) were not undergoing typical apoptosis but instead organelles remained intact while the membrane became increasingly permeable (Takei et al. 1996). Building on this research, the process of NETosis or the generation and release of fibers comprised of nuclear and granule contents by activated NGs to extracellularly capture and kill pathogens was elucidated (Brinkmann et al. 2004). There are currently three known forms of NETosis: suicidal, vital with the release of nuclear DNA (vital nuclear), and vital with the release of mitochondrial DNA (vital mitochondrial).

Traditionally, the formations of suicidal and vital mitochondrial NETosis are both ROS dependent and rely on the NADPH oxidase enzyme (NOX) complex to form while the vital nuclear form of NETosis is ROS independent (Fuchs et al. 2007, Yousefi et al. 2009, Branitzki-Heinemann et al. 2016). However, the requirement of oxygen in the process of NETosis is still not fully understood. Different stimuli, such as Methyl-β-cyclodextrin (CD), have been shown to induce NET formation under hypoxic conditions while PMA or LPS stimulated NET induction is ROS dependent (Neumann et al. 2014, Fuchs et al. 2007). Together, these data indicate that the stimuli being used can prompt different types of NET formation. Following is a brief explanation of the steps involved in ROS dependent suicidal NETosis.

After activation of the NOX complex and generation of ROS, the nucleus begins to experience histone cleavage, citrullination, and subsequent decondensation of chromatin followed by the dissolution of the nuclear membrane as chromatin enters the cytoplasm and starts to combine with cytoplasmic granules and proteins (Li et al. 2010, Papayannopoulos et al. 2010, Fuchs et al. 2007). At this point, rupture of the plasma membrane is the final step needed to release the net-like structures into the extracellular space (Fuchs et al. 2007). An example of the steps is shown in Figure 2. In both vital models, the membranes are not lost and only nuclear or mitochondrial DNA is released.

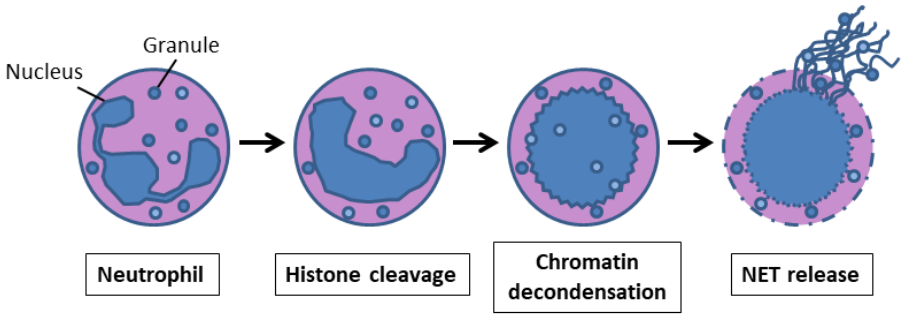

Figure 2: Steps of NETosis

When a neutrophil is activated and undergoes NETosis neutrophil elastase containing granules migrate to the nucleus and cleave histones. This is followed by chromatin decondensation via histone citrullination and cellular depolarization. Finally, the breakdown of the nuclear membrane and rupture of the plasma membrane results in release of a chromatin and granule protein mixture into the extracellular space.

Ideally, NETs would serve their protective role without causing any harm but they have been shown to contribute to the pathogenesis of some disease states. Enhanced NET formation as well as the release of extracellular autoantigens like citrullinated peptides and pro-inflammatory molecules by NETs can, for example, accumulate in the synovial fluid of patients with rheumatoid arthritis, likely promoting inflammation and generation of specific autoantibodies (Assi et al. 2007, Khandpur et al. 2013) . Similarly, in non-obese diabetic (NOD) mice NGs can be recruited to pancreatic islets where they undergo NETosis and release cathelicidin-related antimicrobial peptides that contribute to initiation of diabetes (Diana et al. 2013). What's more, circulating levels of neutrophil elastase and proteinase 3, both of which can be found in granules of NGs, are elevated

in patients suffering from type 1 diabetes mellitus while ROS has proven to be an effective inducer of pro-inflammatory cytokines that contribute to pancreatic cell destruction as well as activation of adaptive immunity (Padgett et al. 2013, Wang et al. 2014b). Therefore, an excessive immune response can contribute to the induction of chronic inflammation and, in the case of type 1 diabetes mellitus, increased NG infiltration and NETosis in the pancreas could even contribute to instances of mild peripheral neutropenia that persists for years (Mitroulis et al. 2011b, Khandpur et al. 2013, Valle et al. 2013, Wang et al. 2014b). Most recently, connections have been made between NETs and the severity and infectivity of COVID-19. For example, it was demonstrated that prolonged NET formation may play a role in the development of ALI and contribute to enhanced cell to cell fusion and entry of COVID-19 into host cells (Al-Kuraishy et al. 2022, Hong et al. 2022).

1.2.2 Cytokines and signaling pathways

In order to initiate the inflammatory response, there needs to be an initial trigger such as PAMPS and DAMPs (see also section 1.1 and 1.2). PAMPs and DAMPs have been characterized as evolutionarily conserved molecules associated with alive or dead pathogens or dying host cells, respectively (Medzhitov and Janeway 1997, McDonald et al. 2010). They are specifically recognized by PRRs on immune cells or other cell types (Carbone et al. 2017). PRRs are highly conserved among species and do not require immunologic memory unlike other receptors that are generated as a part of adaptive immunity, although, recent studies have found that innate immune cells do have some capacity for short-lived memory to stimuli they have had prior exposure to (Akira et al. 2006, Sherwood et al. 2022). One specific family of PRRs are the Toll-like receptors (TLRs) that each recognize distinct microbial PAMPs. LPS, for example, is a component of the cell wall of gram-negative bacteria and is very efficient at activating the immune response through TLR4 (Medzhitov et al. 1997, Shimazu et al. 1999).

Recognition by the PRRs is the first step in inducing an intracellular signaling cascade, such that it carriers the signal across the plasma membrane, with the ultimate goal of eliciting an anti-pathogen response (Poltorak et al. 1998). Once initiated, the cascade will activate transcription factors and subsequently the expression of genes responsible

for the synthesis of cytokines and other inflammatory mediators (Akira and Takeda 2004, Triantafilou et al. 2004, Akira et al. 2006).

1.2.2.1 Signaling via the NFκB pathway

Nuclear-factor-κ-B (NFκB) is a key transcription factor involved in the regulation of expression of many inflammatory proteins when signaled through PRRs such as TLRs (Ghosh et al. 1998, Akira and Takeda 2004). For this purpose, a hetero- or homodimer composed of p50 and p65 subunits, NFκB translocated from the cytoplasm into the nucleus (Verma et al. 1995). In fact, NFκB is one of the pivotal mechanisms in how the innate immune response is able to rapidly mount a defense once an inflammatory insult is detected. Maintained in the cytoplasm of most cell types ,NFκB is held in its inactive form, bound with the inhibitor proteins NFκB inhibitor α (iα), and ready to respond immediately during signaling (Baeuerle and Baltimore 1988). Once a pathogen is detected, cellular signals lead to the phosphorylation and proteolytic degradation of the NFκBiα inhibitors releasing NFκB, which can then translocate into the nucleus (Henkel et al. 1993, Karin and Ben-Neriah 2000). In monocytes and macrophages, once NFκB has reached the nucleus, it induces the production of not only pro-inflammatory cytokines like TNFα, IL-1β, and IL-6, some of which serve as further activators of NFκB themselves, but also of the NG chemoattractant chemokine [C-X-C motif] ligand (CXCL) 1 and pro-inflammatory enzymes like cyclooxygenase (COX)-2 (Huang et al. 2007, Kwon et al. 2013, Liu et al. 2017). Since the NFκB pathway is responsible for such an array of cellular processes, careful regulation is crucial. Therefore, a self-limiting process is initiated through the NFκB driven synthesis of new NFκBiα that is capable of entering the nucleus and inactivating NFκB (Zabel and Baeuerle 1990, Zabel et al. 1993); NFκBiα being frequently used as a marker of activated NFκB signaling (Damm et al. 2012).

1.2.2.2 TNFα

First discovered by Carswell and colleagues (1975) in the serum of mice infected with bacillus Calmette-Guérin, TNF was found to be released from host cells and was toxic to two mouse sarcoma cell lines, establishing its name (Carswell et al. 1975). Since then,

TNFα has been associated with multiple biological process including inflammation, immunomodulation, and fever (Bradley and Pober 1996, Dinarello et al. 1986, Wedgwood et al. 1988). Derived from the pro-TNFα precursor, mature TNFα is released after an inflammatory stimulus or trauma from a variety of cells, e.g., activated monocytes and macrophages (Tang et al. 1996). One of the first cytokines to appear in the bloodstream, TNFα can stimulate signaling pathways, including NFκB, through receptors TNFR1 and TNFR2. On the one hand, TNFR1 can be expressed on a variety of cells in humans and the TNFα-TNFR1 complex produces a primarily pro-inflammatory response that stimulates genes or apoptosis and cell death (Wajant and Scheurich 2011, Tartaglia et al. 1993, Aggarwal 2003). On the other hand, TNFR2 has only been found on immune and endothelial cells in humans and the TNFα-TNFR2 complex has more anti-inflammatory qualities such as by promoting T-cell activation or migration (Aggarwal 2003, Kafrouni et al. 2003). Typically released quickly followed by rapid degradation the initial peak of TNFα can only be measured in circulation during early onset inflammation; however, depending on the stimulant used, a later peak has also been recorded, for example, being released from mouse bone marrow derived mast cells (Janský et al. 1995, McCurdy et al. 2001).

1.2.2.3 IL-1β

Much like TNFα, IL-1β is another inflammatory mediator that influences fever and inflammatory responses (Hsi and Remick 1995, Opp and Krueger 1991, Dinarello 1996). The inactive precursor pro-IL-1β is synthesized following PAMP recognition then cleaved by IL-1β converting enzyme to produce the mature active form (Thornberry et al. 1992). Acting through IL-1 receptor 1, IL-1β stimulates the release of pro-inflammatory cytokines, adrenocorticotropic hormone (ACTH), and induces leukocytosis (Dinarello 2004b). Again, IL-1β is primarily released early in the inflammatory process, following TNFα, and can be measured during early onset inflammation (Janský et al. 1995).

1.2.2.4 IL-10

As a notable anti-inflammatory cytokine, IL-10 limits the pro-inflammatory response to prevent damage and promotes a return to homeostasis (Gazzinelli et al. 1996). As an

activator of the STAT3 pathway (see section 1.2.2.5), IL-10 signals through the IL-10 receptor (Tan et al. 1993). This receptor is most prominent on monocytes and macrophages but it can also be found on other immune cells and in the brain. Overall, in monocytes and macrophages, IL-10 inhibits the production of pro-inflammatory cytokines and soluble mediators such as IL-1β, TNFα, IL-6, and PGE2 (Fiorentino et al. 1991, Niiro et al. 1994, Marfaing-Koka et al. 1996). Ledeboer and colleagues have also found that production of IL-10 and its receptor expression by rat microglia and astrocytes *in vitro* help to modulate glia-mediated responses during inflammation (Ledeboer et al. 2002). Interestingly, IL-10 enhances the production of IL-1ra and diminishes the effect of IL-1β in NGs (Cassatella et al. 1994). Other studies have also shown that IL-10 could inhibit the production of PG in NGs, specifically in work done by Niiro and colleagues (1997) using LPS-stimulated NG cultures. (Niiro et al. 1997).

1.2.2.5 Signaling via the STAT3 pathway

The Janus kinase-signal transducer and activator of transcription (JAK-STAT) cascade, of which STAT3 is a part, is essential for the transmission of information and generation of the immune response (Darnell et al. 1994). Once the cascade is initiated, STAT3 is phosphorylated by Janus kinase and forms a homodimer, through interactions between two monomers, before translocating into the nucleus to regulate gene expression (Yu et al. 1995). Notably the JAK-STAT cascade can be activated toward two opposing responses, pro-inflammatory through IL-6 or anti-inflammatory through IL-10 (Braun et al. 2013). During inflammation and IL-6 stimulation, STAT3 is an important regulator of pro-inflammatory cytokines such as IL-6 (Chen et al. 2012, Damm et al. 2013). Additionally, STAT3 will also influence expression of inflammatory enzymes such as COX-2 and microsomal prostaglandin E synthase (mPGES) (Rummel et al. 2006, Rummel et al. 2011, Eskilsson et al. 2014). Interestingly, stimulation by IL-10 promotes suppression of macrophage and NG activity, which helps prevent chronic inflammation (Takeda and Akira 2000). Finally, the STAT3 pathway has a built-in self-regulatory mechanism using the suppressor of cytokine signaling (SOCS) 3 which operates in a negative feedback loop to suppress STAT3 phosphorylation (Nicholson et al. 2000). Indeed, SOCS3-mRNA expression can be applied as a marker of activated STAT3 signaling (Rummel 2016).

1.2.2.6 NFIL-6

The final transcription factor involved in the cytokine cascade that will be covered here is nuclear factor (NF)-IL-6. NF-IL6 is particularly relevant since it can be activated by a range of pro-inflammatory cytokines such as IL-6, IL-1β, or TNFα as well as through treatment with LPS (Kishimoto et al. 1992). Once phosphorylation and dimerization occurs, NF-IL6 is able to translocate into the nucleus where it contributes to regulation of gene transcription (Metz and Ziff 1991, Ramji and Foka 2002). Not only does NF-IL6 regulate IL-1β and TNFα but, together with NFκB, NF-IL6 synergistically regulates the expression of IL-6 (Natsuka et al. 1992, Matsusaka et al. 1993, Zhang and Rom 1993). Like NFκB and STAT3, NF-IL6 also regulates mediator synthesis and is required for the synthesis of PGE2 via induction of its rate limiting enzymes COX-2 and mPGES (Uematsu et al. 2002, Schneiders et al. 2015). In addition to its expression by macrophages and endothelial cells, the expression of NF-IL6 by cells of the CNS like astrocytes, microglia, and neurons means that the nuclear translocation of NF-IL6 has emerged as an important brain cell activation marker during inflammation (Ramji and Foka 2002, Damm et al. 2011, Rummel 2016). Interestingly, studies have shown that through the production of SOCS3 and reduction of NFκBiα expression, NF-IL6 is able to influence STAT3 and NFκB signaling pathways, respectively (Borland et al. 2009, Cappello et al. 2009). Overall, such data supports NF-IL6 being an important inflammatory transcription factor.

1.2.3 Lipid mediators

When the inflammatory cascade is initiated and the APR is underway, lipid mediator synthesis can be activated resulting in lipid compounds and derivatives capable of exerting influence and regulating the inflammatory reaction (Heller et al. 1998). These lipids function to progress both pro- and anti-inflammatory aspects of inflammation as well as contributing to its ultimate resolution (Serhan et al. 2014).

1.2.3.1 Polyunsaturated fatty acids

A source of increasing interest is the connection between inflammation and polyunsaturated fatty acids (PUFA), predominantly reliant on eicosanoids. These

important lipid mediators are primarily generated PUFAs derived from the phospholipids of cell membranes (Calder 2006b). Predominantly acquired from the omega (ω) 6-PUFA arachidonic acid (AA), eicosanoids can also be metabolites from ω-3-PUFA eicosapentaenoic acid (EPA) and docosahexaenoic acid (DHA). In the brain, AA is predominantly present while levels of EPA and DHA can be increased through dietary supplementation, such as with fish oil (Lee et al. 1985). Indeed, studies have found that an increased intake of ω-3 PUFA will result, to a degree, in their replacing AA in cell membrane phospholipids (Gibney and Hunter 1993). This is significant because many of the eicosanoids synthesized from AA push toward a pro-inflammatory profile, including PG and leukotrienes (LT). Those synthesized from ω-3 PUFA exert a weakened pro-inflammatory effect or, in the case of Rv, an anti-inflammatory profile (Endres et al. 1989, Serhan et al. 2000, Serhan et al. 2002). An overview of PUFA synthesis and lipid mediator metabolism is shown in Figure 3.

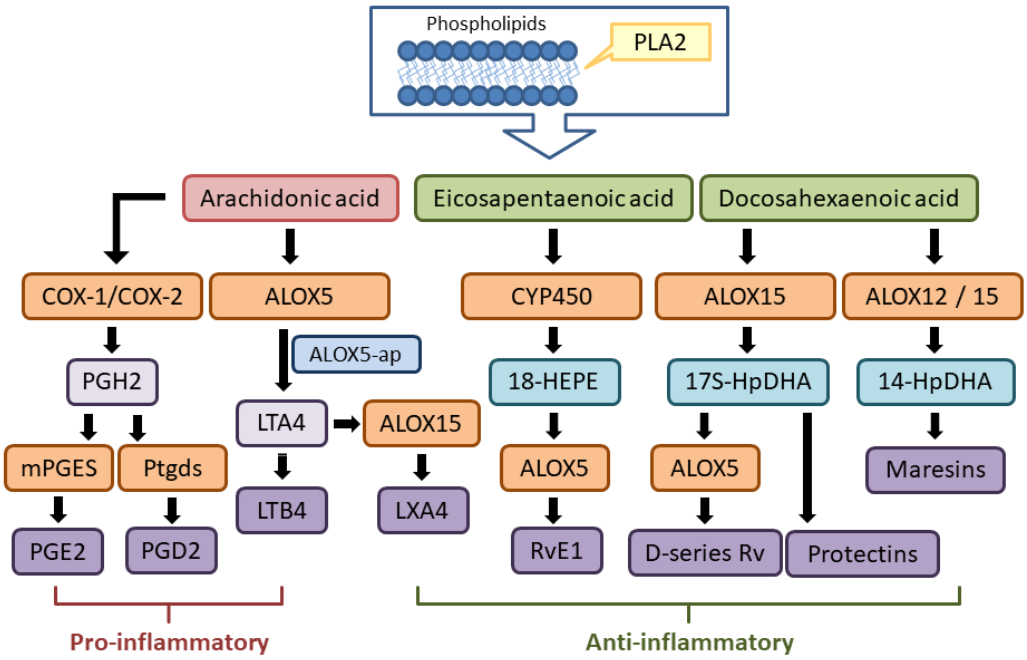

Figure 3: PUFA pathways for lipid mediator synthesis

A schematic representation of the synthesis pathways for the three major polyunsaturated fatty acids: ω-6 arachidonic acid, ω-3 eicosapentaenoic acid, and ω-3 docosahexaenoic acid is shown here after they have been released from phospholipids. The lipid mediators important for pro- or anti-inflammatory actions are shown along with the enzymes required for their synthesis. Enzymes: Cytosolic phospholipase A_2 (PLA2), cyclooxygenases (COX)-1/-2, arachidonate lipoxygenases (ALOX) 5/12/15,

cytochrome P450 (CYP450), microsomal prostaglandin (PG) E synthase (mPGES), PGD2 synthase (Ptgds); ALOX5-activating protein (ALOX5-ap); Precursors: PGH2, leukotriene (LT) A4; Metabolites: 18-hydroxyeicosapentaenoic acid (18-HEPE), 17-hydroperoxy-DHA (17S-HpDHA), 14-HpDHA; and lipid mediators: PGE2, PGD2, LTB4, lipoxin (LX) A4, resolvin (Rv) E1, D-series resolvins (Rv), protectins, and maresins.

1.2.3.1.1 ω-6 vs. ω-3 PUFAs during inflammation

PUFA are characterized based on where the first of their double bonds occurs, i.e., at the third (ω-3) or sixth (ω-6) to last carbon atom. The diet of an individual can greatly influence the concentration of each of these PUFA within the cell membrane, for instance, individuals consuming a typical western diet have a significantly higher concentration of ω-6 PUFA present (Rett and Whelan 2011). Furthermore, the composition of cell membrane phospholipids is capable of exerting a strong influence on both the cellular response and function during inflammation through lipid mediators (Innes and Calder 2018).

The ω-6-PUFA AA represents about 18% of the total PUFA in peripheral blood mononuclear cells (PBMCs) and, as mentioned above, is a key producer of eicosanoids by way of cellular activation (Kew et al. 2003, Rees et al. 2006). The process begins when AA is cleaved by phospholipase A2 (PLA2) from the cell membrane to be targeted by enzymes like COX and lipoxygenases (LOX) to form eicosanoid mediators (see Figure 3) (Lewis et al. 1990, Tilley et al. 2001). The resulting mediators, such as PG and LT, have predominantly pro-inflammatory effects and, for example, play a role in inducing fever, pro-inflammatory cytokine production, leukocyte recruitment, and degranulation but will be discussed in more detail later in sections 1.2.3.2 and 1.2.3.3 (Palmer et al. 1980, Sha'afi et al. 1981, Hoover et al. 1984, Coceani et al. 1986, Petrova et al. 1999). However, the anti-inflammatory role that AA-derived eicosanoids play in inflammation should also be taken into account. While a major pro-inflammatory mediator, PGE2 is also capable of regulating the inflammatory cascade and aiding in resolution (Kunkel et al. 1988, Petrova et al. 1999, Innes and Calder 2018). Indeed, PGE2 has been shown to induce a negative feedback loop inhibiting cytokine production

as previously shown in primary neuroglial cell cultures during LPS-induced inflammation (Simm et al. 2016).

In contrast, ω-3 PUFA like EPA and DHA are found at much lower amounts in PBMCs than ω-6 PUFA like AA (Kew et al. 2003). Nonetheless, by increasing the consumption ω-3 PUFA the proportions present in phospholipids of PBMCs can be increased at the expense of AA (Yaqoob et al. 2000). As the levels of ω-3 PUFA increase, less AA is available for eicosanoid synthesis and, therefore, levels of AA derived PG and LT production are also decreased (Lee et al. 1985, Trebble et al. 2003). It is important to keep in mind that EPA competes for the same enzymes, COX and arachidonate 5-lipoxygenase (ALOX5), to generate ω-3 PUFA derived eicosanoids but the difference here is that these eicosanoids are less potent pro-inflammatory mediators (Goldman et al. 1983, Lee et al. 1984, Bagga et al. 2003). Meanwhile, the COX-2 generated E-series Rv from EPA and DHA derived D-series Rv (Figure 3) have demonstrated anti-inflammatory capacities but this will be discussed in more detail later in section 1.2.3.4 (Serhan et al. 2000, Serhan et al. 2002, Hong et al. 2003). Though these actions alone are substantial in altering the inflammatory profile, studies have found that when sufficient quantities of fish oil are ingested there was a reduction in leukocyte chemotaxis, adhesion molecule expression, and ROS (Calder 2006a).

1.2.3.2 Prostaglandins

Responsible for some of the key symptoms of inflammation, PGs, and particularly PGE2, are instrumental in the APR. Stimulated by pro-inflammatory cytokines, the levels of cytosolic PLA2 enzyme increase and the process of eicosanoid synthesis begins (Zhang et al. 2008). As PLA2 levels rise, it works to cleave AA free from the cell membrane to be metabolized by COXs; specifically COX-1, which is constitutively expressed, and COX-2 that is induced during inflammation e.g. via the NFκB pathway (O'Neill and Ford-Hutchinson 1993, Williams and DuBois 1996). Both COX isoforms convert AA into PGH2, which is a common substrate for a series of PGs in monocytes as well as platelet derived thromboxane A2 (Bockman 1981, Paul et al. 1999). The common PG precursor PGH2 can be converted by a variety of synthase enzymes to

form PGs including, but not limited to, mPGES or PG D2 synthase (Ptgds) to produce PGE2 and PGD2, respectively (see Figure 3) (Ricciotti and FitzGerald 2011).

PGE2 is one of the most prevalent PGs and is a particularly important immune mediator, regulated by COX-2, and responsible for many symptoms of inflammation (Park et al. 2006, Takai et al. 2013). Comprised of four receptors (EP1-4), PGE2 is able to illicit multiple responses depending on which receptor is activated, for example: EP1 primarily deals with the mediation of pain, EP2 and 4 signal inflammatory responses, and some anti-inflammatory responses are mediated through EP3 (Kurihara et al. 2001, Stock et al. 2001, Honda et al. 2009, Yao et al. 2009). Additionally, by signaling through neurons predominantly in the median preoptic region of the hypothalamus, PGE2 acts as a pyrogen to induce fever via EP3 and EP4 receptors, but this will be discussed in section 1.8.1 (Engblom et al. 2003, Machado and Saper 2022, Osaka 2022). However, PGE2 has been shown to modulate the inflammatory response in that it inhibits production of TNFα in cultured blood stimulated with LPS (Kunkel et al. 1988, Petrova et al. 1999). PGE2 has also been identified as an inducer of LXs, SPMs, that aid in the resolution of inflammation (Innes and Calder 2018). As a result of the impact PGE2 has on the immune response, it is unsurprising that the synthesis pathway has a long history with anti-inflammatory therapeutic treatments, namely nonsteroidal anti-inflammatory drugs (NSAIDs). By inhibiting COXs activity, NSAIDs, such as ibuprofen and acetylsalicylic acid, effectively block the synthesis of PGs to act as analgesics and antipyretics (Vane 1971, Kerola et al. 2009).

Another prominent eicosanoid, PGD2, performs homeostatic functions as well as promoting inflammation. Originally discovered at high levels in the brains of rats it was soon clear that PGD2 functioned within the CNS to regulate several bodily functions like sleep, body temperature, and hormone release (Abdel-Halim et al. 1977). As far as the pro-inflammatory role of PGD2 is concerned, studies involving intra-dermal injects of PGD2 into the forearms of volunteers resulted in the development of prolonged erythema, a rash caused by inflamed capillaries (Flower et al. 1976). Additionally, PGD2 has been identified as a contributor to allergic reactions and asthma by promoting eosinophilia and T lymphocyte recruitment (Fujitani et al. 2002). However, a variety of metabolites can also be derived from PGD2 and some, like the PGJ2 family, have

decidedly anti-inflammatory effects that contribute to the resolution of inflammation (Trivedi et al. 2006). Although contrary to the more characterized roles of PGs, it has been observed that treatment with COX inhibitors, such as NSAIDs, will initially ameliorate symptoms of inflammation but also stall resolution and exacerbate symptoms later on (Gilroy et al. 1999).

1.2.3.3 Leukotrienes

In addition to PG, free AA can likewise be metabolized by LOX, specifically ALOX5, to form LT. Working together with ALOX5-activating protein (ap), two groups of LT are generated from the intermediate LTA4: LTB4 and Cysteinyl LT. Here, the focus will be on LTB4 (see Figure 3) (Peters-Golden and Henderson 2007). Found in a variety of cells, including NGs and monocytes, LTB4 signals through LTB4 receptor 1 (LR) and LTB4 receptor 2 (LR2) (Le Bel et al. 2014). Expressed predominantly on immune cells, LR is bound with a higher-affinity than LR2 and it is through this receptor that pro-inflammatory LTB4 acts as a chemoattractant and activator of immune cells including NGs (Ford-Hutchinson et al. 1980, Yokomizo et al. 1997, Miyahara et al. 2006). As a promoter of inflammation, LTB4 induces immune cell influx, chemotaxis, phagocytosis, and degranulation (Tager et al. 2000, Woo et al. 2002, Gaudreault et al. 2005). Moreover, LTB4 can increase the release of pro-inflammatory cytokines from activated immune cells, namely, IL-1β and chemokine [C-C motif] ligand (CCL) 2 from monocytes and IL-8 from NGs (Rola-Pleszczynski and Lemaire 1985, Kuhns et al. 2001, Huang et al. 2004). The low-affinity LR2 is expressed on most cells and is mainly associated with protective barrier functions (Saeki and Yokomizo 2017). Interestingly, the anti-inflammatory potential of LR2 has been studied using models of allergic airway inflammation and it was found to play a protective role in bronchial epithelial cells (Liu et al. 2018).

1.2.3.4 Specialized pro-resolving mediators

Now that the major pro-inflammatory lipid mediators have been discussed, it is important to also look at those mediators that primarily perform an anti-inflammatory and pro-resolving role. SPMs are a subset of signaling molecules that play an important role in the resolution of inflammation (Serhan et al. 2015). This group of SPMs includes LX, Rv,

protectins, and maresins. Within this group, LXA4 is one of the few SPMs derived from AA; ω-6 PUFA AA-derived metabolites are typically pro-inflammatory. The Rv to be discussed include RvE1 and the D-series of Rv metabolized from EPA and DHA, respectively (Serhan et al. 2015). Lastly, protectins and maresins are both metabolized from DHA (see Figure 3 for PUFA synthesis pathways) (Park et al. 2020). Before further details are introduced for SPMs, one final point should be addressed. Due to the fact that SPMs are present at lower levels than typical mediators and that the signaling pathways through which they operate have not been fully elucidated, some questions have been raised on their exact biological relevance (Schebb et al. 2022). In the following sections, I hope to supply evidence supporting why it is important not to dismiss the significance of SPMs and their role in the resolution of inflammation.

1.2.3.4.1 Lipoxins

Interest in LX increased after their role in the resolution of inflammation became apparent, particularly in relation to NGs. Work by Godson and colleagues (2000) found that the LOX-derived eicosanoid LXA4, which is metabolized along with LTB4 by LTA4, is an important inducer of NG clearance by stimulating the phagocytosis of apoptotic NGs (efferocytosis) *in vitro* (Godson et al. 2000, Serhan 2005). Additionally, LXA4 will restrict the entry of NGs to sites of inflammation and thereby inhibit NG related injury (Takano et al. 1998). Both actions can be connected to activation of the LXA4 specific receptor (ALX), which elicits cell-type-specific responses. Activation of ALX by LXA4 in NGs inhibits NG migration while the same interaction in monocytes promotes chemotaxis and activation (Maddox et al. 1997). In so far as the benefits of treating with LXA4 are concerned, in a mouse model of sepsis, where cecal ligation and puncture (CLP) were used to induce systemic inflammation, a combined treatment of LXA4 with antibiotics not only reduced NG infiltration but also inhibited pro-inflammatory cytokines such as IL-1β, TNFα, and IL-6 as well as reducing bacterial loads (Walker et al. 2011, Ueda et al. 2014). Finally, the administration of LXA4 in rats prior to injection with carrageenan in the hind paw, an established model of peripheral inflammation, attenuated nociception and is investigated as an avenue for pain regulation (Svensson et al. 2007).

1.2.3.4.2 Resolvins

Among the family of Rvs, RvE1 is synthesized from EPA through a process that utilizes the enzymes CYP450 and ALOX5. The production of the DHA derived D-series of Rvs involves ALOX15 as well as ALOX5 (Serhan et al. 2015). As mentioned before, Rvs are compelling regulators in the resolution of inflammation acting through two prominent G-protein coupled receptors: chemerin receptor 23 (CR) and the LR (Arita et al. 2007, Ohira et al. 2010). Unlike the LR, CR is expressed on a variety of tissue types including organs, like the liver, and other cells such as dendritic cells, macrophages, endothelial cells, and even NGs (Gantz et al. 1996, Samson et al. 1998b, Goralski et al. 2007, Parolini et al. 2007, Arita et al. 2005, Kaur et al. 2010).

RvE1 has been shown to have a significant impact on NGs during models of inflammation. As such, RvE1s ability to bind to the LR on polymorphonuclear cells attenuates LTB4 pro-inflammatory properties, thus, dampening its impact and regulating inflammation (Arita et al. 2007). In addition, it has been established that treatment with aspirin and EPA leads to the formation of RvE1, through the intermediary 18R-hydroxyeicosapentaenoic acid (HEPE), and inhibits the transendothelial migration of NGs *in vitro* and in an *in vivo* mouse model, treated with aspirin and 18R-HEPE, into a dorsal air pouch (Serhan et al. 2000, Arita et al. 2005). Most recently, we have even detected up-regulated levels of 18-HEPE in primary sensory circumventricular organ (CVO) cultures stimulated with LPS, a promising lead for their potential role in brain inflammation (Pflieger et al. 2022). In addition, the production of the pro-inflammatory cytokines IL-1β, TNFα, and IL-6 as well as superoxides produced by NGs can be inhibited by aspirin-stimulated biosynthesis of RvE1 at least partially through the CR (Hasturk et al. 2006, Oh et al. 2011). Likewise, RvE1 has reduced NG accumulation in lung tissue as well as bronchoalveolar lavage fluid (BALF) and decreased levels of pro-inflammatory cytokines IL-1β, IL-6, and HMGB-1 in lung tissue during pneumonia (Seki et al. 2010). Therefore, treatment with RvE1 could represent a future therapeutic option in the treatment of ALI such as in the ongoing battle against COVID-19 related lung inflammation (Serhan et al. 2022).

On the other hand, the D-series of Rv are able to bind to the G protein coupled receptor (GPCR) 32 found on macrophages to boost the phagocytosis of NGs (Krishnamoorthy et al. 2010). Importantly, since DHA is necessary for neural development, it is present in rather high levels in the brain as well as in the retina and the phospholipid membrane of NGs (Tou 1986, Bazan et al. 1993). The D-series Rv have been shown to inhibit LPS-induced pro-inflammatory cytokines i.e., TNFα, IL-6, and IL-1β produced by microglia *in vitro* (Rey et al. 2016). Moreover, studies performed in mice and humans establish an impact of D-series Rv on NG levels in exudate as well as their ability to transmigrate across endothelial cells, respectively (Serhan et al. 2002, Sun et al. 2007). In addition, RvD2 can contribute to protective effects in mouse models of sepsis, specifically, by reducing leukocyte recruitment, bacterial load, and inhibiting mediators of inflammation like IL-1β, IL-6 and TNFα, ultimately improving survival rates (Spite et al. 2009).

1.2.3.4.3 Protectins and maresins

Along with the D-series of Rv, DHA derived protectins and maresins are converted by hydrolase enzymes via ALOX12 and ALOX15 and are present at sites of inflammation (Basil and Levy 2016). Maresins are primarily produced in monocytes and macrophages (Deng et al. 2014). Among protectins, protectin D1 (PD1) is of particular interest and has been found in a variety of human cell types, also known as neuroprotectin (NP)D1 when produced in neural systems (Mukherjee et al. 2004). Indeed, we were recently able to show that NPD1 is also released from primary neuroglial cell cultures of CVOs during acute LPS-induced inflammation (Pflieger et al. 2022). The DHA pathway and subsequent production of NPD1 acts as a strong inhibitor of leukocyte infiltration, NFκB activation, and COX-2 induction as previously shown in a mouse model of stroke and by *in vitro* treatment of neural cell cultures inhibiting IL-1β induced NFκB and COX-2 expression (Marcheselli et al. 2003). Moreover, PD1 contributes to mediation of inflammation by upregulating expression of chemokine [C-C motif] receptor type (CCR)5 on polymorphonuclear cells to bind and clear inflammatory chemokines (Ariel et al. 2006). In addition, NPD1 has shown neuroprotective potential through modulation of amyloid-β peptides e.g. promoting brain cell survival by reducing apoptosis and promoting anti-apoptotic proteins in an *in vitro* model of Alzheimer's disease (Lukiw et al. 2005). Maresins, on the other hand, reduce levels of the pro-inflammatory cytokines IL-

1β, TNFα, IL-6, and IFNγ in mouse models of inflammatory bowel disease as well as inhibit NG infiltration and heighten efferocytosis in mouse peritonitis (Serhan et al. 2012, Marcon et al. 2013). In addition, maresins can also inhibit NG migration and ROS production as shown in LPS-stimulated cultures of bone-marrow derived macrophages (Marcon et al. 2013). Finally, Serhan and colleagues (2021) showed that injured planaria exposed to the maresin MaR1 regenerated tissue at an accelerated rate, thus, demonstrating a promising role for maresins in wound healing (Serhan et al. 2012).

1.3 Communication between the periphery and the brain

Although the brain has been considered to be an immune-privileged organ, protected by the selectively permeable blood-brain barrier (BBB), there is clear evidence for communication with the periphery involving components of the immune system (Medawar 1946, Abbott et al. 2010, Banks 2012, 2019). The cells that comprise the brain not only include antigen presenting cells like perivascular macrophages and dendritic cells but also microglia, which are capable of responding to inflammatory stimuli (Dantzer et al. 2008, Perry and Teeling 2013). Moreover, communication is required to regulate CNS controlled sickness responses during inflammation where information is delivered to the brain via three different pathways: the neuronal, humoral, and cellular routes (Pflieger et al. 2018). Using these pathways, bidirectional communication is achieved between the brain and immune system.

The neuronal pathway is one of the early alert systems that initially transmits inflammatory signals to the brain through cytokine interactions with peripheral nerves (Watkins et al. 1995, Ross et al. 2000). It also explains why brain induced sickness responses such as fever during moderate systemic inflammation fail to occur or are at least attenuated after the abdominal vagus nerve is severed (Goehler et al. 2000, Roth and Souza 2001). The autonomic nervous system forms a pathway between the periphery and brain by way of afferent neurons (aSN), followed by the relay of information from neural circuits through efferent neurons (eAN) (Hall et al. 1990, Kenney and Ganta 2014). Activated immune cells and the release of pro-inflammatory cytokines will prompt aSN in the periphery and conduct information to the brain where eAN are the conduit for brain-to-periphery communication, which culminates in the release of

regulatory molecules (Chavan et al. 2017). By releasing regulatory molecules and neurotransmitters, the nervous system achieves near instantaneous communication with the brain (Chavan et al. 2017, Kenney and Ganta 2014). The other pathways, humoral and cellular, will be discussed in more detail in the sections below (1.3.1, 1.3.2).

1.3.1 Humoral Immune-to-brain communication

The humoral route of communication involves the transfer of information via blood borne mediators (Dantzer et al. 2000). Here, once a pathogen is detected and the inflammatory response is initiated, the pro-inflammatory cytokines or lipid mediators being released into the bloodstream travel to the brain to exert their influence (Banks 2005, Steiner et al. 2006). Since large proteins like cytokines cannot indiscriminately pass through the BBB in large quantities, interactions with the brain can only occur at areas that allow for it (Dantzer et al. 2000). Such sites include CVOs which lack a tight BBB, through active transendothelial transport, or by stimulating perivascular cells that comprise the BBB (Roth and Blatteis 2014).

Characterized as either sensory or secretory, the sensory CVOs: *area postrema* (AP), *organum vasculosum of the laminae terminalis* (OVLT), and subfornical organ (SFO), are able to detect cytokine signals (Johnson and Gross 1993, Roth et al. 2004, Banks 2005). Specifically, the OVLT is of interest due to its location and connection to the preoptic-anterior hypothalamic area (POA) where the fever response is generated (Lazarus et al. 2007). Although cytokine interactions at the “leaky” brain structures are important, it is not their only access into the brain. Proinflammatory cytokines like IL-1β, TNF, and IL-6, which all significantly contribute to inflammatory responses, have been shown to be actively transported across the BBB at low levels (Banks 2005). Lastly, endothelial cells and perivascular macrophages of the BBB and the cerebral vasculature express PRRs and cytokine receptors (Schiltz and Sawchenko 2003, Matsumura and Kobayashi 2004). By binding these receptors, the stimulated cells can provoke a response in the brain through the secretion of secondary mediators including lipophilic PGE2 (Rummel et al. 2005, Eskilsson et al. 2014).

1.3.2 Cellular Immune-to-brain communication

At this point, literature has seen the evolution of an immune privileged brain via a tight BBB to one capable of communicating through neuronal and immune mediators. Building upon this work, more studies have additionally shown that there are several different conditions during which immune cells traffic to the brain: bacterial meningitis, MS, and septic encephalopathy to name a few. During such conditions, the BBB can become “leaky” and more permeable (Kim 2003, Engelhardt 2006, Schweighöfer et al. 2016). However, increased permeability is not required, as studies have found evidence of low levels of immune cells crossing the BBB even while it remains intact. For example, Wolburg and colleagues (2005) found that during a mouse model of MS mononuclear cells were able to infiltrate the brain via a transcellular pathway that left endothelial tight junctions intact (Wolburg et al. 2005). As a result, the idea of the BBB has begun to evolve to think of it more as a blood-brain interface capable of more complex interactions with other parts of the body than originally thought possible (Banks 2016).

Monocytes and macrophages have been recognized as one of the cell types important for immune-to-brain communication. Not only during disease or infection but models of psychological stress have also been able to induce monocyte trafficking to the brain after which they differentiate into pro-inflammatory IL-1β producing macrophages and influence the development of anxiety like behaviors (Wohleb et al. 2013, Sawada et al. 2014, McKim et al. 2018). With stress there is an induced release of catecholamines which, subsequently, increases levels of circulating monocytes and NGs (Powell et al. 2013, McKim et al. 2018). It is predominantly from these circulating populations that cells are recruited to the brain (Powell et al. 2013, McKim et al. 2018). Within the brain, macrophages are primarily located in the perivascular space as well as the meninges (Bechmann et al. 2001, Wohleb et al. 2013). The perivascular cells also contribute to activation of the HPA axis, which functions as one of the moderators of inflammation (Serrats et al. 2010).

NGs are of particular importance for the present study. During infection or inflammation, endothelial cells of the brain can be activated by circulating inflammatory mediators to

express ICAM-1, a crucial adhesion molecule involved in NG extravasation into the brain (Bohatschek et al. 2001). Therefore, it is unsurprising that during studies when mice received an intracerebral injection of LPS or IL-1β, trafficking of monocytes and NGs were detected in the brain (Andersson et al. 1992b, Anthony et al. 1997). What's more, the recruitment of NGs into the brain is time-dependent and region specific with NGs congregating near ventricles, meninges, the hemisphere commissure, and some other specific structures (Andersson et al. 1992a, Andersson et al. 1992b, Rummel et al. 2010). Notably, specific brain regions have demonstrated an ability to express chemokines specific for NG recruitment and could explain some of the localization of NGs being seen during inflammation (Sakamoto et al. 1996, Rummel et al. 2010). When it comes to the role that these NGs are playing in the brain, Aguilar-Valles and colleagues (2014) found that depressive-like symptoms were ameliorated through NG depletion during septic-like inflammation (Aguilar-Valles et al. 2014). Experiments performed by Stoolman and colleagues (2014) also showed that the symptoms of disease could be improved by impeding NG recruitment during an atypical mouse model of MS (Stoolman et al. 2014). Conversely, *in vitro* experiments involving human NGs were found to secrete the anti-inflammatory cytokine IL-1ra suggesting an anti-inflammatory potential of these cell types (Schröder et al. 2006). Together, these data indicate that NGs are capable of entering the brain and transmitting information that alters brain function and pathology.

1.4 Hypothalamic-Pituitary-Adrenal axis

Another pathway utilized by the immune system for communication with the brain is the HPA axis, whose primary role is regulating the adaptive stress response. Involving the endocrine, nervous, and immune systems, the stress response is activated by a real or perceived threat to homeostasis; once activated, certain physiological changes start to take place involving the regulation of metabolism, the autonomic nervous system, and immunity (Chrousos 2009).

The HPA axis is made up of the hypothalamus, pituitary, and adrenal glands and works to stimulate the release of glucocorticoids (Chrousos 1995). During an infection, an increase in circulating pro-inflammatory cytokines TNFα, IL-1, and IL-6 can stimulate the

HPA axis by activating the hypothalamus and pituitary (Sapolsky et al. 1987, Bernardini et al. 1990, Perlstein 1993). Located within the hypothalamus is the paraventricular nucleus (PVN), a structure comprised of three different types of neurons: parvocellular, neurosecretory magnocellular, and long-projecting neurons (Tasker and Dudek 1991). Together, these neurons are responsible for the secretion of hormones, including corticotropin-releasing hormone (CRH) and arginine vasopressin (AVP), as well as regulating autonomic and somatosensory functions (Herman and Tasker 2016). The hormones CRH and AVP stimulate the pituitary and, thus, activate the second stage of the HPA axis, namely, the pituitary. The pituitary gland includes the anterior and posterior lobe. The anterior lobe produces a variety of hormones important for growth and reproduction but in the context of this axis its production of adrenocorticotropic hormone (ACTH) is most relevant (Sheng et al. 2020). The anterior pituitary is stimulated by the CRH of the hypothalamus and will in turn secrete ACTH. Finally we come to the adrenal glands, located on the kidneys, the adrenal cortex region of the glands are stimulated by circulating ACTH and the synthesis and release of glucocorticoids is initiated (Chrousos 1995). Cortisol is the main glucocorticoid secreted in humans, corticosterone being the equivalent in rodents, and is able to transmit information all over the body including to the brain resulting in effects on cardiac output, blood pressure, and glucose levels, inhibiting activated immune cells among other things (Stephens and Wand 2012). While these affects are beneficial during stressful situations that require a “fight-or-flight” response, prolonged activation of the HPA axis can have serious ramifications on an individual’s health.

As such, studies have shown links between chronic stress and, for example, increased risks for cardiovascular disease, cognitive issues, and a chronic inflammatory status (McEwen and Sapolsky 1995, Konstantinos and Sheridan 2001, Cohen et al. 2012, Han et al. 2016). Therefore, a negative-feedback loop serves as an off-switch for the HPA axis to prevent overstimulation (Stephens and Wand 2012). During times of stress when levels of circulating cortisol are high it will bind with glucocorticoid receptors and inhibit production of CRH and ACTH in the hypothalamus and pituitary, respectively, and tones down the process through negative-feedback (Reul and Kloet 1985).

1.5 Lung-brain interaction

At this point, multiple means of immune-to-brain communication to develop the sickness response have been discussed during systemic inflammatory insults. The influence of organ specific infection or inflammation on the brain remains less clear. The lungs, for instance, can produce many of the same inflammatory mediators as the brain and when released into the bloodstream would come in contact with the CNS (Gonzalvo et al. 2007). There have been connections described linking lung microbiota with the immune reactivity of microglia in the brain (Hosang et al. 2022). Furthermore, susceptibility to lung inflammation and/or infection is a common problem seen in patients that have suffered from brain injuries while peripheral inflammation can modify brain function and even aggravate certain pathologies (Perry et al. 2007, Vermeij et al. 2013, Sahu et al. 2018, Allgire et al. 2021). Outside of an injury or infection the lung-brain interaction can already be impacted by circumstances like lifestyle choices (both good and bad) or psychological stress that can cause levels of systemic or brain inflammation (Cooney et al. 2013, Krüger et al. 2015, Madore et al. 2020).

The capacity for information to pass between the lung and the brain is particularly clear when we look at patients that have suffered from acute respiratory distress syndrome (ARDS) or from a traumatic brain injury. Amongst patients with ARDS, there have been reported side effects related to memory, concentration, and processing impairments while a traumatic brain injury increased vulnerability to ALI (Hopkins et al. 2004, Vermeij et al. 2013). Conditions such as ALI and ARDS involve an inflammatory process in the lungs that is mediated by the pro-inflammatory cytokines IL-1β and TNFα (Goodman et al. 2003a). Like with other inflammatory incidents during ALI and ARDS, NGs are heavily recruited and traffic into the lungs. Persistent NG influx has been associated with increased mortality in septic patients (Steinberg et al. 1994). In fact, in patients suffering from diffuse lung injury in combination with radiation induced leukopenia, resolution of the leukopenic status leads to an increase in lung dysfunction (Rinaldo and Borovetz 1985).

More recently, emerging evidence shows that the global pandemic involving the acute respiratory syndrome COVID-19 can not only result in damage to multiple organs but

also in neurological manifestations (Mao et al. 2020). Some COVID-19 patients have reported headaches, anosmia, encephalopathy, coma, and even stroke (Chou et al. 2021, Gentile et al. 2022). These neurological pathologies were typically observed during more severe infections possibly resulting from viral invasion of the brainstem by means of neuronal routes or an exaggerated systemic immune response (Chou et al. 2021, Gentile et al. 2022). Indeed, studies have shown that during certain upper respiratory virus infections, for example, with respiratory syncytial virus (RSV), viral particles were detectable in the hippocampus causing inflammation in the brain (Mao et al. 2022). RSV infections can lead to the development of neurological disorders such as encephalitis and encephalopathy. Moreover, such viral infection may as well impact neuronal function i.e., release of neurotransmitters and even cause remodeling of neural networks (Mao et al. 2022). Building on this framework, there have been several studies, which show that alterations of lung function can impact the brain. For example, the unique microbiota of the lung has been identified as a means of lung to brain signaling (Khatiwada and Subedi 2020, Hosang et al. 2022). Smoking and lung infections increase the risk for MS and, using a rat model of lung experimental autoimmune encephalomyelitis, it was shown that dysregulation of the microbiota can alter susceptibility to MS (Hosang et al. 2022). In fact, unlike the gut microbiome, even a moderate shift in the rats' lung microbiome influenced microglial reactivity in the brain (Hosang et al. 2022). During infection with COVID-19, it has been hypothesized that the lung microbiome could have a similar impact and altering the lung microbiome may represent a potential therapeutic strategy for the future (Khatiwada and Subedi 2020). Overall, the lung-brain route of communication is able to transfer information under multiple conditions and should be considered in the search to treat or prevent neurological pathologies during ALI, ARDS, and serious respiratory infections including severe COVID-19 cases.

In addition, psychological impacts need to be considered during lung inflammation. For example, association of psychological conditions including depression, posttraumatic stress disorder (PTSD), and panic disorder (PD) with lung inflammation/ALI have been established (Bienvenu et al. 2012, Lewkowich et al. 2020, Allgire et al. 2021). While LPS-induced depressive-like symptoms have been attributed to the innate immune

response and circulating cytokines during systemic inflammation detailed mechanisms during ALI remain to be investigated (Dantzer et al. 2008, Lasselin et al. 2020). Notably, ALI can increase levels of NOX derived ROS, which are also elevated in humans and animal models of depression (Zhang et al. 2015, Hirose et al. 2016, Nadeem et al. 2017). NOX is found in NGs, which, as previously mentioned, are recruited during ALI (Steinberg et al. 1994). With this information in mind, Nadeem and colleagues (2017) analyzed NOX-2 levels in NGs and the brain in an LPS-induced ALI mouse model. The authors revealed that NOX-2 levels in NGs and neurons correlated with the degree of depressive symptoms (Nadeem et al. 2017). Based on these results, we see that the capacity to transfer inflammatory information is not restricted to cytokines but can similarly occur through immune cells, specifically NG migration to the brain. Recent work has also demonstrated an association between PTSD and PD with lung inflammation and asthma (Allgire et al. 2021, Lewkowich et al. 2020). While the mechanisms are not yet known, there is evidence that a house dust mite asthma model caused increased fear behaviors in mice (Lewkowich et al. 2020). Moreover, these authors showed modulation of microglial functions in several CVOs prompting a new avenue of research for fear-associated conditions (Lewkowich et al. 2020).

1.6 Circumventricular organs

The CVOs are several brain structures which characteristically lack a tight BBB. Thus, they are able to detect circulating signal molecules (Roth et al. 2004). Located around the third and fourth ventricles, the CVOs are separated from the CSF by specialized ependymal cells (tanycytes) that control brain exposure to circulating molecules (Langlet et al. 2013). Of the structures characterized as CVOs, the OVLT, SFO, and AP, as stated earlier, are sensory CVOs with neuronal connections to other regions of the brain and serve as an important interface for communication between the periphery and CNS (Johnson and Gross 1993).

1.6.1 The organum vasculosum of the lamina terminalis

Of particular importance is the OVLT, in rodents it is located on the rostral end of the third ventricle and extends to the optic chiasma (Szabó 1983). Largely comprised of astrocytes but also containing microglia, neurons, and endothelial cells, the OVLT is

divided into three sections and includes the rostromedial vascular region, dorsal cap covering the rostrocaudal vascularized region, and the periventricular tissue surrounding the central vascular plexus (McKinley et al. 2003). Respectively, these brain structures show an extensive capillary plexus with neurosecretory terminals, neural projections into the PVN, and neural networks extending to the hypothalamus and PVN (McKinley et al. 2003). Contact of immune mediators with the OVLT is one of the first steps in thermoregulation due to the close proximity to the preoptic area and median preoptic nucleus (MnPO), a thermosensitive region of the hypothalamus (Boulant 2000, McKinley et al. 2003). In fact, stimulation with the circulating pro-inflammatory mediators IL-1β, TNFα, IL-6, and PGE2 have all been able to activate brain cells in the OVLT, an effect that was also replicated with LPS treatment (Matsuda et al. 1992, Harré et al. 2003, Ott et al. 2010).

1.7 Sickness response

The behavioral changes and symptoms we experience as a result of infection are known cumulatively as the sickness response and are the ultimate result of communication between the immune system and the brain (Dantzer et al. 1998). Sickness behaviors can include components such as lethargy, anorexia, adipsia, weakness, and shivering as well as symptoms like suffering from a febrile response (Hart 1988, Kent et al. 1992b). Benjamin Hart (1988) was one of the first researchers to reveal the connection between fever and behavioral patterns in animals and humans during infection and inflammation. He came to the conclusion that the behaviors were not a side effect of experiencing fever but rather a strategy to facilitate survival supporting, for example, fever induction during infection (Hart 1988). Today, the scope of sickness behaviors has evolved to include several aspects such as mental health disorders, deficits related to learning and memory, and psychological factors (Kelley and Kent 2020, Lasselin 2021).

In order to link the development of the sickness response with immune-to-brain communication, the means of communication had to be established. To start with, certain cytokines have been linked with the induction of sickness behaviors by injecting IL-1, IL-2, and IFNα systemically (Dantzer and Kelley 1989). However, to test whether the development of the sickness response is truly not reliant upon an initial febrile

response remained to be seen. Moving forward, rats injected with a combination of IL-1 and its antagonist IL-1ra allowed Kent and colleagues (1992) to determine that different receptor mechanisms were required for IL-1-stimulated behavioral or febrile effects (Kent et al. 1992a). Moreover, the viral and bacterial mimics polyinosinic:polycytidylic acid and LPS have been shown to impact the febrile and sickness responses through different pathways or demonstrate a dissociation between the development of fever and sickness behaviors, respectively (Fortier et al. 2004, Damm et al. 2013). Together, these data indicate a wider range of information that the immune system is capable of transmitting to the brain and its ability to have not only pharmacological but also physiological effects.

1.8 Sepsis

Sepsis is a very severe diagnosis resulting from a systemic inflammatory response due to an infection in circulation and a strong activation of the immune system that can progress to septic shock and multiple organ failure (Bone et al. 1997). As a result, sepsis and its complications are one of the leading causes of mortality in intensive care units (Semmler et al. 2008, Parrillo 1993). Although aggressive fluid administration and support to maintain organ function can increase survival rates, it is not uncommon for survivors of the initial insult to suffer from severe long-term impairments such as organ dysfunctions, recurrent infections, and even impaired cognitive functions (Gentile et al. 2012, Biff et al. 2013, Corrêa et al. 2015, Karampela and Fragkou 2022). Currently, more work is being done to understand and treat septic patients more effectively but the complexity of the condition is still an obstacle when it comes to diagnosis and treatment. While the pathogenesis of sepsis involves a multifaceted interaction between the host response and infectious agent, the initial process begins with recognition of PAMPs and DAMPs by PRRs (Salomao et al. 2012). However, unlike a typical inflammatory response, instead of clearing the infectious agent, they evade destruction and, in turn, the host response can become dysregulated and detrimental. At this point, homeostasis is completely disrupted and the immune systems attempts to compensate results in simultaneous severe inflammation and immune suppression (Schiel et al. 2003, Wiersinga et al. 2014).

Severe inflammation is elicited by the release of inflammatory mediators from leukocytes, and activation of complement, and coagulation factors (Guo and Ward 2005, Wiersinga et al. 2014). Chief among the pro-inflammatory cytokines elevated during sepsis are TNFα and IL-1β (Waage et al. 1989, Lv et al. 2014). As these pro-inflammatory cytokines are being released, there is also excessive complement activation, in particular via the complement factor C5a (Guo and Ward 2005). Not only will C5a increase inflammation and contribute to organ failure by promoting NG survival, formation of NOX, and further cytokine release; but C5a also causes T cell apoptosis and immunodeficiency (Guo et al. 2000, Perianayagam et al. 2004, Joseph et al. 2017). Additionally, the high levels of circulating pro-inflammatory cytokines and NOX derived ROS can reach the brain, activate glial cells, and damage the BBB (Tsao et al. 2001, Comim et al. 2011a, Mina et al. 2014). Lastly, sepsis promotes a pro-coagulant status namely via tissue factor, which can be released in NETs, and limited activity of anti-coagulant pathways (Kambas et al. 2012, Levi and van der Poll 2017). As a consequence, septic patients can be at risk for thrombosis and hemorrhage (Mitroulis et al. 2011a, Kambas et al. 2012, Claushuis et al. 2016).

1.9 Thermoregulation during inflammation

1.9.1 Fever

Most are familiar with the defensive mechanism of fever, the controlled increase of core body temperature in response to infection, having experienced it at some point or even dealt with a sick pet (Kluger et al. 1975). Though some might associate fever as a mammalian response, it has been observed in vertebrates ranging from birds to fish and even reptiles (Kluger 1979). Long connected with disease it was not until an extensive survey by Dr. Wunderlich in 1871, which recorded the temperatures of thousands of healthy and sick patients, was fever characterized as a core body temperature that exceeds 38°C (Wunderlich CA 1871). Since then, knowledge about the febrile response has exponentially increased and more is understood about core body temperature, for example, some degree of variation occurs between individuals and as of yet an exact set point for core body temperature has not been determined (Obermeyer et al. 2017). Therefore, a more accurate characterization of fever would be the increase of the core

body temperature by 1-4°C (Saper and Breder 1994). Through the coordinated elevation of the thermoregulatory indifferent temperature, the body is able to induce the febrile response via a step-wise process. Even though the increase in core body temperature is a response to PAMPs or exogenous pyrogens, this is not the signal that initiates fever. Instead, it is also the pyrogenic cytokines secreted during inflammation that transmit the necessary information to initiate the febrile response (Dinarello 2004a, Akira et al. 2006). Together, pyrogenic cytokines and LPS travel to the POA where they act to induce expression of PGE2, the key mediator of fever (see section 1.2.3.2) (Engblom et al. 2003, Blomqvist and Engblom 2018).

1.9.1.1 Generation of the febrile response

To begin with, stimulation with LPS will activate the TLR4 pathway, the mechanisms of which will be discussed in more detail later, and lead to secretion of the main pyrogenic cytokines TNFα, IL-1β, and IL-6 (see section 1.2.2), produced in the same order as listed (Laflamme and Rivest 2001). Moreover, by acting through the NFκB and STAT3 signaling pathways (see section 1.2.2), these cytokines will ultimately lead to PGE2 production from macrophages or brain endothelial cell by means of the rate limiting enzyme COX-2 (see section 1.2.3.2) (Park et al. 2006). IL-6 dependent PGE2 synthesis by way of the COX-2-pathway in endothelial cells in particular is a key mediator of inflammation-induced fever; moreover, inhibition of IL-6 signaling on endothelial cells will attenuate the fever response (Rummel et al. 2006, Eskilsson et al. 2014, Wilhelms et al. 2014). Once the complement cascade is initiated an initial release of PGE2 is seen from the Kupffer cells (Kc) in the liver and alveolar macrophages in the lung shortly after stimulation (Hespeling et al. 1995, Blatteis et al. 2004a, Steiner et al. 2006). It has been proposed that the Kc PGE2 can act more locally by binding to EP receptors, such as EP3, on hepatic vagal afferents and signal directly to the POA via the neuronal communication pathway (Ushikubi et al. 1998, Li and Blatteis 2004, Li et al. 2006). At this point, the exogenous pyrogens led to the release of pyrogenic cytokines and PGE2, some of which stimulated the neuronal communication pathway, leak into circulation, and reach the OVLT. Now the final threshold left is activation of the POA.

1.9.1.2 Development of fever in the brain

By systematically injecting different brain regions with pyrogenic cytokines, the POA was identified as the major thermoregulatory control region. It was clear that injections to the POA of rabbits caused more intense fevers that developed more rapidly compared to other regions (Cooper et al. 1967). Similarly, when PGE2 was injected into the POA, near the third ventricle, it also elicited a fever response in rats (Stitt 1991, Scammell et al. 1996a). The POA has an intricate network of cold-sensitive (C) and warm-sensitive (W) neurons that control for cold defense (i.e., heat gain) or heat defense (i.e., heat loss) respectively (Morrison and Nakamura 2019). The neuronal axons extend through the dorsomedial hypothalamic nucleus (DMH) to the raphe pallidus nucleus (RPA) in the brainstem and transmit signals to effector organs (Nakamura 2011). Under normal conditions the core body temperature is maintained but as neuronal and humoral fever signals travel to the POA the thermoregulatory set-point is increased as C neurons become activated while W neurons are inhibited leading to the activation of thermoregulatory mechanisms to preserve heat (Cannon et al. 1998, Ogoina 2011). Recently, a study by Osterhout and colleagues (2022) characterized a neuronal population within the ventral medial POA that contributes to sickness symptoms, including temperature, during LPS-induced systemic inflammation (Osterhout et al. 2022).

The pathway to most physiological processes is rarely simple and straight forward and the generation of fever is not different. In order for fever signals to reach the POA they first need to overcome the BBB. As mentioned previously, there are a few ways of humoral immune-to-brain communication that can lead to this transfer of information. However, one of the most promising routes could be through CVOs like the OVLT (Lazarus et al. 2007). Indeed, studies in a variety of mammals, sheep, guinea pigs, and rats, have shown that ablation of the anteroventral wall of the third ventricle including the OVLT can suppress LPS-induced fever (Blatteis et al. 1983, Blatteis et al. 1987, Hunter 1997). Since the permeability of the CVOs has been well documented (see section 1.6) the cells of the OVLT could receive information from exogenous pyrogens and the pyrogenic cytokines. In fact, endothelial cells of the OVLT have been shown to express receptors for TNFα and IL-1β constitutively while IL-6 receptors were seen in the

endothelial cells of rats following peripheral LPS stimulation. (Vallières and Rivest 1997, Schiltz and Sawchenko 2003, Matsumura and Kobayashi 2004). Cultures of the rat OVLT treated with IL-6, TNFα, IL-1β, and even LPS, elicited a response in intracellular levels of calcium in neurons (Ott et al. 2010). Additionally, the same CVO endothelial cells will also express the PGE2 precursor enzyme mPGES constitutively and can be induced into expressing COX-2 (Matsumura and Kobayashi 2004, Eskilsson et al. 2014). The expression profile of these cells implies that although some circulating PGE2 may be transported across the BBB, there is a network in place to locally synthesize PGE2 in these structures as well (Steiner et al. 2006, Roth and Blatteis 2014). Together these data outline a process where pyrogenic cytokines are detected by the cells of the OVLT, which leads to production and release of COX-2 by the endothelial cells, and catalyzes production of PGE2. However, this is only one possible pathway for PGE2 synthesis and subsequent febrile response. As previously mentioned, PGE2 released from liver Kc could transmit initial inflammatory signals to the POA through vagal afferents (Blatteis et al. 2004b, Li et al. 2006).

Signaling by PGE2 through EP3 and EP4 receptors on gamma-aminobutyric acid (GABA) and glutamatergic neurons within the POA inhibits tonic release of GABA to other brain sites, including the DMH and RPA, and pushes forward a fever response (Nakamura 2011, Osaka 2022). However, it has been hypothesized that signaling is restricted to the glutamatergic neurons, as supported by Machado and colleagues (2020), where inhibitory interneurons of the DMH and RPA are disinhibited and allow for fever production (Machado et al. 2020). Ultimately, activation of these neurons leads to signal transmission from the DMH and RPA to effector organs of thermogenesis, which generate heat through the adrenergic autonomic pathway, i.e., vasoconstriction and thermogenesis in brown adipose tissue (BAT), and somatic pathways, i.e., shivering, as well as behavioral modifications that preserve heat (Cannon et al. 1998, Ogoina 2011, Nakamura 2011).

1.9.2 Hypothermia

Conversely, infection can also result in a decrease of core body temperature through a regulated hypothermic response (Garami et al. 2018). To most individuals fever is what

we think of when it comes to sickness or an infection but there are certain circumstances under which it may not be beneficial to have a fever and instead hypothermia could be better served to minimize damage and restore homeostasis (Romanovsky et al. 1997, Liu et al. 2012). Systemic inflammation has been shown to illicit both febrile and hypothermic responses, however, hypothermia typically occurs during very severe cases in both humans and in animal models (Blanqué et al. 1996, Romanovsky et al. 1997, Drewry et al. 2015). In general, the mechanics to generate hypothermia are not entirely dissimilar to those required for fever. Once again, thermoeffectors, which in the case of hypothermia are known as cryogenic cytokines, will transmit information to initiate physiological and behavioral changes but the exact mechanisms are not as well understood as those for fever development (Romanovsky 2004, Garami et al. 2018).

When looking at hypothermia using a high dose LPS model of systemic inflammation, TNFα appears as an important mediator (Blanqué et al. 1996). Since elevated levels of TNFα are present in circulation during early phases of systemic inflammation it has been studied as a key contributor that could act as both a pyrogenic or cryogenic cytokine (Leon 2004). In fact, in experiments performed by Leon and colleagues (1997-98), using the aforementioned LPS model, it was observed that TNFR knock-out (KO) mice had attenuated hypothermia but still developed fevers (Leon et al. 1997, Leon et al. 1998). Meanwhile, neutralization with TNF-binding protein during high dose LPS-induced systemic inflammation lead to faster recovery from hypothermia and ultimately fever generation in rats (Töllner et al. 2000). Therefore, given a significantly strong stimuli, it is likely that during the initial stages of inflammation TNFα has the potential to switch from a pyrogenic to cryogenic cytokine as occurs with a severe dose of LPS (Bibby and Grimble 1989, Leon et al. 1997, Leon et al. 1998, Töllner et al. 2000).

Once initiated, the body temperature is lowered through a combination of cold-seeking behaviors and physiological changes (Romanovsky et al. 1996, Romanovsky 2004, Almeida et al. 2006). For example, a reduction in thermogenesis as opposed to targeted heat loss is a major contributor to hypothermia while peripheral vasodilation also contributes to this regulated response (Derijk et al. 1994, Romanovsky et al. 1996). Nevertheless, when it comes to analysis of hypothermia, it is crucial to acknowledge the role of ambient temperature in thermoregulation. On the one hand, it is established that,

during LPS-induced systemic inflammation, rats housed in a neutral or warm environment had a polyphasic febrile response (Derijk et al. 1994, Steiner et al. 2004). On the other hand, rats housed in a cool environment that received a similar LPS dose experienced hypothermia (Derijk et al. 1994, Scammell et al. 1996b, Steiner et al. 2004). The same influence of ambient temperature has also been observed in mice (Rudaya et al. 2005). In order to avoid a confounding factor, housing should be held at the animals thermoneutral zone which, for mice, is approximately 30°C (Gordon 1985).

Even though hypothermia cannot clear pathogens as effectively as a febrile response, there is still evidence that supports its' having beneficial properties (Rumbus et al. 2017, Garami et al. 2018). Comparisons between rats, which received systemic inflammation via *Escherichia coli* or LPS showed that, when hypothermia occurred, survival rates where significantly higher than groups with fever (Liu et al. 2012). While hypothermic rats, which received *E. coli*, did have an elevated level of bacteria in their liver overall many other symptoms were reduced: endotoxemia, NG infiltration of the lung, and organ dysfunction compared to febrile groups (Liu et al. 2012). In human studies, patients suffering from septic ARDS had improved oxygenation and survival after induction of a therapeutic mild hypothermia (Villar and Slutsky 1993). One explanation for these benefits could be attributed to the high energy cost required for fever generation. During moderate to severe infection, when energy levels are low, the benefits of a febrile response can be outweighed by its high energy costs whereas a hypothermic response leaves room for energy conservation (Rumbus and Garami 2019). However, the "choice" between fever and hypothermia seems to involve some flexibility. As such, Fonseca and colleagues (2016) reported seeing a regulated form of spontaneous transient hypothermia in septic patients that appears as a normal phase in systemic inflammation (Fonseca et al. 2016).

Even given these advantageous properties, hypothermia during sepsis is still viewed as a severe condition that should be monitored carefully. If the core body temperate drops too low and results in extreme hypothermia consequences could include organ failure and neurological dysfunction (Kushimoto et al. 2013, Drewry et al. 2015, Rumbus et al. 2017). Further research is still required in order to fully grasp the complex role of hypothermia and its contributions to sepsis.

1.10 Experimental model

1.10.1 LPS induced inflammation

Comprised of a hydrophilic polysaccharide and a hydrophobic lipid it is the polysaccharide chain of LPS that will be recognized by the immune system (Erridge et al. 2002). The hydrophobic lipid portion, otherwise known as lipid A, is unique as it is comprised of a conserved molecular structure recognized across mammalian innate immune systems (Akira et al. 2006). Monocytes and macrophages will recognize LPS through cluster of differentiation (CD)14 and TLR4 (Frey et al. 1992, Shimazu et al. 1999). The APP LPS binding protein is an initial contributor to the LPS-receptor interaction, although not required, and by recruiting LPS accelerates the process of LPS-CD14 binding (Hailman et al. 1994). Since CD14 lacks a cytoplasmic signaling domain it requires a secondary receptor in order to convey the LPS signal across the plasma (Ulevitch and Tobias 1995). TLR4 fulfills this purpose, as it is unable to identify LPS without the assistance of CD14 and, along with myeloid differentiation factor (MD)-2, a TLR4-MD-2 complex is formed (Shimazu et al. 1999, Akashi et al. 2000). In summary, the two receptors will come together to form the CD14-TLR4-MD-2 complex to recognize LPS and transfer the signal (da Silva Correia et al. 2001). The end result is stimulation of the immune response through LPS-induced activation of the NFκB pathway (see section 1.2.2.1) and ultimately the release of pro-inflammatory cytokines (Chow et al. 1999). The series of steps that must be fulfilled in order for the immune response to recognize and respond to LPS are yet another form of self-regulation that prevents an excessive cytokine response. Notably, the presence of TLR4 and CD14 are not limited to the periphery, both receptors have been found in the brain and, specifically, in the CVOs (Laflamme and Rivest 2001, Chakravarty and Herkenham 2005).

The popularity of LPS as a model for inflammation is attributed to its ability to accurately mimic a bacterial infection and has been used to induce both systemic and local inflammation (Rummel et al. 2005, Rummel et al. 2006, Damm et al. 2011). In its purified form it is possible to adjust the dosage and, thus, regulate the severity of exposure depending on the concentration and serotype of the LPS batch (Thomas et al. 2014). Importantly, the effect of LPS can vary among species, for example, mice have a

relatively high tolerance and thus typically require a higher concentration of LPS (Sauter and Wolfensberger 1980, Redl et al. 1993). Therefore, the species used is an important consideration when designing an experiment with LPS-induced inflammation.

1.10.2 *Fat-1* mouse model

With growing evidence supporting the beneficial, anti-inflammatory role of ω-3 PUFA (see section 1.2.3.1) it is becoming increasingly important to have an accurate research model to study their impact during inflammation. Traditionally, these studies have been carried out through dietary supplementation where animals can be fed identical diets that have only had alterations to the PUFA profile (Sperling et al. 1987, Watanabe et al. 2004). In theory, this is an ideal model that would accurately mirror a therapeutic approach relying on oral delivery of ω-3 PUFA. However, with all the components that go into a balanced diet, it is unlikely that different batches of animal feed would have identical compositions, thus, adding confounding factors. The problem with ω-3 PUFA enriched diets are magnified when looking at nutritional studies in humans who have even more varied diets (Gu et al. 2018). Moreover, the ω-3- and ω-6 PUFAs are themselves derived from different sources, such as fish or vegetable oils, that each contribute unique bioactive compounds, which add further confounding factors between the groups (Kang 2007). In addition to problems with consistency between diets there is also a stability issue as PUFA are prone to oxidation at room temperature (RT) (Kang 2007). Together, these issues point toward a necessity for a more reliable means of testing ω-3 PUFA.

The development of a mouse strain capable of synthesizing ω-3 PUFA would present an ideal solution to many of the problems associated with PUFA dietary supplementation. Surprisingly, the journey towards a transgenic mouse line started with the roundworm *C. elegans*. These simple animals possess a PUFA desaturase, *fat-1* gene, that is lacking in mammals and is able to convert ω-6 PUFA to ω-3 PUFA by introducing a double bond into the ω-3 carbon of the hydrocarbon chain (Spychalla et al. 1997). By isolating the *fat-1* gene and transferring it into mice Kang and colleagues were able to create the transgenic *fat-1* mouse (Fat) which endogenously produce ω-3 PUFA (Kang et al. 2004). When raised on an ω-6 high and ω-3 deficient diet alongside unaltered control mice the

Fat mice where shown to have ω-3 enriched tissues throughout the body and alterations to the overall ratios of ω-6/ω-3 PUFA while levels still remained physiologically relevant (Kang et al. 2004, Orr et al. 2010). These changes were even observed in the brain where the ratio of ω-6/ω-3 PUFA were reduced from 3.9 to 0.8 (Kang et al. 2004). Given these alterations to the PUFA profile further examination showed that the total amount of PUFA remained the same in both Fat and control mice (Kang 2007). While a transgenic mouse lacks the therapeutic relevance of dietary supplementation, it does solve many of the issues with the former. Additionally, Fat mice experience approximately the same brain level of ω-3 PUFA enrichment as those mice that have been placed on a fish oil diet (Orr et al. 2010).

1.11 Key objective

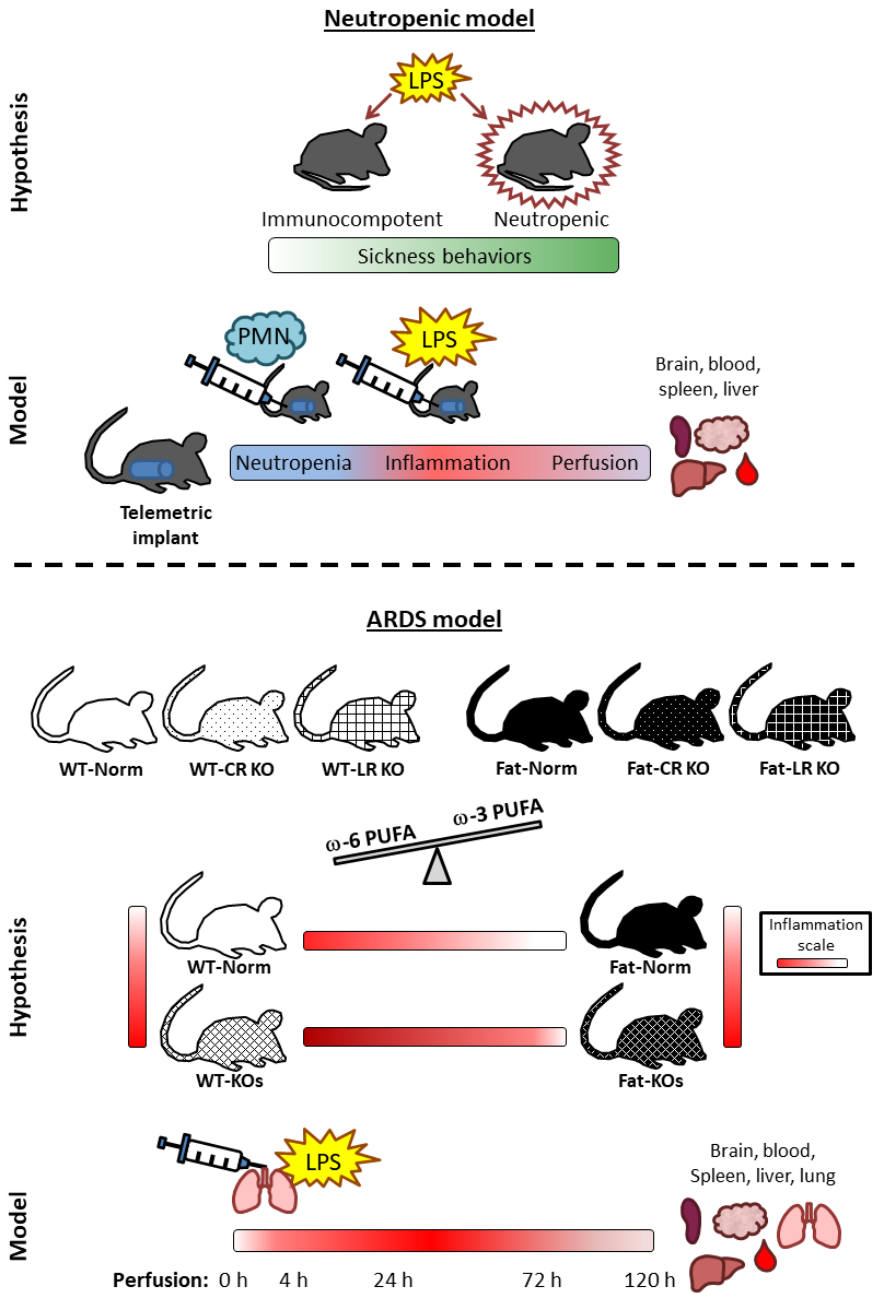

Figure 4: Hypothesis and model for neutropenic and ARDS experiments

A schematic representation and experimental approach to two models of systemic and localized organ-specific lung inflammation under separate conditions: neutropenia or ω-3 PUFA enrichment combined with resolvin receptor knock-out (KO) mice. Abbreviations: anti-polymorphonuclear serum (PMN), lipopolysaccharide (LPS); C57BL6/N mice (WT), chemerin receptor 23 (CR), leukotriene B4 receptor (LR), unmodified mice (Norm), transgenic Fat-1 mice (Fat).

To study the impact of NGs on the development of the sickness response and their overall importance during systemic and localized organ-specific lung inflammation, I have endeavored to address the following questions:

- Does neutropenia have an effect on the magnitude and progression of systemic and brain inflammation?
    - What is the inflammatory mediator profile in circulation and in the brain?
    - Are inflammatory signaling pathways activated?
    - Are NGs trafficking to specific brain structures?
- How does neutropenia affect the sickness response after LPS-induced systemic inflammation?
    - Are normal behaviors such as activity or food and water intake altered?
    - What, if any, effects are there on thermoregulation?
    - Is the stress response activated?

Aim: These results will provide clarification of the pro- or anti-inflammatory role of NGs during LPS-induced systemic inflammation and to what extent they are involved in the development of the sickness response.

- Is NETosis contributing to inflammation in the brain during LPS-induced systemic inflammation?
    - Is LPS capable of inducing NETosis *in vitro*?
    - What inflammatory mediators do NETs release?
    - Does systemic inflammation lead to NET formation in the brain?
    - Does neutropenia impact the number of NETs found in the brain?

Aim: Here the aim is to determine if LPS treatment will result in NET formation and if said NETs are secreting inflammatory mediators that modulate inflammation in the brain during systemic inflammation.

- How does ω-3 PUFA enrichment impact inflammation and NG trafficking to the brain during LPS-induced ARDS?
- Does inhibition of RvE1 in ω-3 PUFA enriched Fat mice alter the inflammatory response or NG trafficking to the brain during ARDS?
    - Are inflammatory signaling pathways activated?
    - Do ω-3 PUFAs or RvE1 impact NG trafficking to specific brain structures?
    - What is the inflammatory mediator profile in the lung, systemically (in the liver), and in the brain during ARDS?
    - Do ω-3 PUFAs or RvE1 influence the inflammatory mediator profile in the lung, systemically (in the liver), and in the brain during ARDS?

Aim: The aim here is twofold, first, these results enable me to analyze the anti-inflammatory potential of ω-3 PUFAs on inflammation specifically their impact on the brain via the humoral pathway in immune-to-brain communication and NG recruitment and distribution during ARDS. Second, whether the ω-3 PUFA derivative RvE1 is contributing to the therapeutic potential of ω-3 PUFAs and impacting the brain over the course of ARDS.

II. Materials and methods

2.1 Material list

Table 1: Technical equipment

Device	Type	Manufacturer
Air conditioner (mice)	RC-E3	Mitsubishi, Minato, Japan
Airflow cabinet	UniProtect	Bioscape GmbH, Emmendingen, Germany
Autoclave	2540 E	Systec, Wettenberg, Germany
Automated hematology analyzer	ADVIA 2120	Siemens Healthcare GmbH, Erlangen, Germany
Centrifuge	Megafuge 1.0 R	Heraeus Sepatech GmbH, Osterode, Germany
Centrifuge	Micro 22R	Andreas Hettich GmbH and Co. KG, Tuttlingen, Germany
Centrifuge	Spectrafuge mini	Neo Lab, Heidelberg, Germany
Centrifuge for 96-well plate	Perfect spin P	Peqlab Biotechnologie GmbH, Erlangen, Germany
Climate chamber	10'US/+5 to +40 DU	Firma Weiss Umwelttechnik, Reiskirchen, Germany
CO_2-incubator	BB-15 function line	Thermo Scientific, Dreieich, Germany
Cryostat	CryoStar NX50	Thermo Scientific, Dreieich, Germany
Dataport	Dietscan analyzer	Accu Scan Instruments Inc., Columbus, OH, USA
Digital black/white camera	Spot insight, model 3.1.0	Visitron Systems GmbH, Puchheim, Germany
Flow cytometer	Accuri C6 plus	BD Biosciences, Heidelberg, Germany
Fluorescence microscope	BX50	Olympus Optical, Hamburg, Germany
Gooseneck lamp	KL 1500	Schott AG, Mainz, Germany
Heating mat		MarMed GmbH, Cölbe, Germany
Heating mat	Thermofol-Thermal foil	Thermo Flächenheizungs GmbH, Rohrbach, Germany
Hot air sterilizer	ED 115/E2	Binder GmbH, Tuttlingen, Germany
Ice-machine	Icematic F120 and D100	CastelMAC S.p.A., Castefrance Veneto, Italy
Light microscope	Olympus BX-41	Olympus Europa GmbH, Hamburg, Germany
Luminex Magpix® instrument		Luminex Corp, Austin, TX, USA
Microcentrifuge	Force 7	Denver Instrument, Bohemia, NY, USA
Microcentrifuge	D-6015	neoLab, Heidelberg, Germany
Microplate photometer	Digiscan	Asys Hitech, Eugendorf, Austria
Microscope	Fluovert FU	Leica Microsystems, Wetzlar, Germany
Microwave		Technostar
Molecular imager ®	ChemiDoc™ XRS imaging system	BioRad, Munich, Germany
Nano photometer	Nano photometer version 2.0	Implen GmbH, Munich, Germany
Perfusion system		Werkstatt Kerckhoff Institut, Bad Nauheim, Germany
pH-Meter	inoLab®7110	WTW GmbH, Weilheim, Germany
Pipettes	8-channel; 0.1-2.5 / 0.5-2 / 2-10 / 2-20 / 10-100 /	Eppendorf AG, Hamburg, Germany

	20-200 / 100-1000 / 200-1000	
Pipettes	20 / 200 / 0.5-2 ml	Gilson Inc., Middleton, WI, USA
Power supply	PowerPac™ 200	BioRad, Munich, Germany
Real-time PCR system	StepOnePlus™	Applied Biosystems, Foster City, Ca, USA
Safety bunsen burner	Fireboy eco	Integra Biosciences GmbH, Fernwald, Germany
Scale (food)	EK-200i	AD Instruments Ltd., Abingdon, UK
Scale (mice)	TB31000P-000D002	Sartorius AG, Göttingen, Germany
Scale (water)	EW-300G	AD Instruments Ltd., Abingdon, UK
Scales (dry materials)	P1210N, AE 50, and PM 2500	Mettler Toledo, Giessen, Germany
Shaker plate	Polymax 2040	Heidolph Instruments GmbH & CO. KG, Schwabach, Germany
Shaker plate	RotoMix type 50800	Thermo Fisher Scientific Inc., Walham, MA, USA
Shears	GT104/GH204	Aesculap, Tuttlingen, Germany
Stereo microscope	Stemi SV11	Carl Zeiss AG, Oberkochen, Germany
Stereo microscope with camera	SMZ-U	Nikon Düsseldorf, Germany
Sterile bench	Microflow biological safety cabinet	Thermo Scientific, Dreieich, Germany
Suction pump	Minni A	Leybold-Heraeus, Hanau, Germany
Tabletop stirrer and heater	RCT basic	IKA® Werke GmbH & Co, KG, Staufen, Germany
Telemetry- mouse temperature transmitter	TA-F10	Data Sciences International Inc., St. Paul, MN, USA
Telemetry- receiver plate	DSI PhysioTel™ RPC-1	Data Sciences International Inc., St. Paul, MN, USA
Telemetry-dataport	Matrix 2.0 (MX2)	Data Sciences International Inc., St. Paul, MN, USA
Thermoblock	Blockthermostat BT 100	Kleinfeld Labortechnik GmbH, Gehrden, Germany
Thermoblock	QBT	VWR, Darmstadt, Germany
Thermocycler	Mastercycler gradient	Eppendorf AG, Hamburg, Germany
Ultrapure water system for double deionized water (Aqua bidest.)	Milli-Q Biocel	Millipore, Eschborn, Germany
Ultrasonic homogenizer	SONOPLUS	Bandelin Electronic GmbH & Co KG, Berlin, Germany
Vortex mixer	VF and VF2	IKA® Werke GmbH & Co, KG, Staufen, Germany

Table 2: Laboratory equipment

Equipment	Type	Manufacturer
Beakers	Duran, different volume	Schott AG, Mainz, Germany
Glass flask with lid	Duran, different volumes	Schott AG, Mainz, Germany
Graduated cylinders	Class A, 100 and 250 ml	Roth GmbH, Karlsuhe, Germany
Magnetic stirring bar	PTFE, encapsulated	Roth GmbH, Karlsuhe, Germany
Screw top bottle	Nonsterile: 40 ml	Roth GmbH, Karlsuhe, Germany
Vial stands		Roth GmbH, Karlsuhe, Germany
Volumetric flasks	Class A, 1, 2, and 5 L	Roth GmbH, Karlsuhe, Germany

Table 3: Laboratory materials

Supplies	Type	Manufacturer
Aluminum foil	954.1	Roth GmbH, Karlsruhe, Germany
Centrifuge tubes	Sterile: 15 / 20 ml	Sarstedt AG and Co. KG, Nümbrecht, Germany
Disposable gloves- supergrip	900-2536	Henry Schein Vet GmbH, Hamburg, Germany
Disposable latex gloves	No. 1202	Unigloves GmbH, Troisdorf, Germany
Disposable nitrile gloves	7005 PFS	Showa Best Glove, Menlo, GA, USA
Dualfilter T.I.P.S.	0.1-10 / 0.5-20 / 2-100 / 50-1000 µl	Eppendorf AG, Hamburg, Germany
Lab wipes	Kimtech science delicate task wipes	Kimberley-Clark Europe Limited Surrey, UK
Lab wipes	Kimtech science precision wipes	Kimberley-Clark Europe Limited Surrey, UK
Multivette® PP-tube	600 ml, K3E	Sarstedt AG and Co. KG, Nümbrecht, Germany
Parafilm®	PM-996	Bemis Flexible Packaging, Neenah, WI, USA
Pasteur-pipette	Disposable	MAGV GmbH, Rabenau, Germany
Pipette tips- unfiltered	10 / 100 / 1000 µl	MAGV GmbH, Rabenau, Germany
PS-tube	Sterile: 12 / 15 / 50 ml	
Reaction tube	15 / 50 ml	Sarstedt AG and Co. KG, Nümbrecht, Germany
Reaction tube	0.5 / 1.5 / 2 ml	MAGV GmbH, Rabenau, Germany
Safe-lock tubes	Reagent vessel 3810, 0.5 / 1.5 / 2 ml	Greiner Bio-One GmbH, Frickenhausen, Germany
Scalpel blades	BB522	Aesculap-Werke AG, Tuttlingen, Germany
Serological pipette	Sterile: 5 / 10 / 25 ml	Sarstedt AG and Co. KG, Nümbrecht, Germany

Table 4: Software

Supplies	Type	Manufacturer
Accudiet	1.2	Accuscan Instruments Inc., Columbus, OH, USA
Adobe Photoshop	6	Adobe System Inc., San Jose, CA, USA
Citavi	6	Swiss Academic Software GmbH, Wädenswil, Switzerland
DietDat	1.7	AccuScan Instruments, Columbus, OH, USA
DietMax		AccuScan Instruments, Columbus, OH, USA
Fiji	win-64	National Institutes of Health, Bethesda, MD, USA
GraphPad Prism®	5 and 7	GraphPad Software, San Diego, CA, USA
Metamorph	7.7.5.0	Visitron Systems GmbH, Puchheim, Germany
Microsoft Office Excel	2010	Microsoft Corporation, Unterschleißheim, Germany
Microsoft Office Powerpoint	2010	Microsoft Corporation, Unterschleißheim, Germany
Microsoft Office Word	2010	Microsoft Corporation, Unterschleißheim, Germany
Ponemah	P3P	Data Sciences International Inc., St. Paul, MN, USA
SPSS® Statistics	26	IBM Corporation, Armonk, New York, USA
Veterinary Software	5.3.1-MS	

2.2 Experimental animals

Table 5: Mouse materials

Supplies	Type	Manufacturer
Bedding	H1 505 29	Ssniff Spezialdiäten GmbH, Soest, Germany
Biodegradable paper		MAGV GmbH, Rabenau, Germany
Feed	M-Z extrudate V1126	Ssniff Spezialdiäten GmbH, Soest, Germany
Filter tops		Ehret GmbH & Co. KG Labor and Pharmatechnik, Emmendingen, Germany
Mouse wooden chew sticks	ABEDD® wood chews size S, NGS E-021	Lab & Vet Service GmbH, Köflach, Germany
Nestlets		Ssniff Spezialdiäten GmbH, Soest, Germany
Operating instruments		Aesculap, Tuttlingen, Germany
Polycarbonate-cage	Type III	Ehret GmbH & Co. KG Labor and Pharmatechnik, Emmendingen, Germany
Rodent houses / tubes		Ehret GmbH & Co. KG Labor and Pharmatechnik, Emmendingen, Germany
Water bottle with nozzle		Ehret GmbH & Co. KG Labor and Pharmatechnik, Emmendingen, Germany

2.3 Mice

C57BL/6J mice were used for neutropenic experiments and NG cultures. Mice were obtained through in-house breeding with original breeding pairs obtained from Charles River Laboratories (Sulzfeld, Germany). All experiments were performed in accordance with the German animal protection law and the local Ethics committee “Regional Council Giessen” (ethics approval numbers GI 18/2 Nr. G 72/2017, 679_M).

2.3.1 Breeding

The mice were bred and maintained in Type III polycarbonate cages with a filter top and kept in an airflow cabinet at 22°C ± 1°C and 50 % ± 5 % humidity. Cages were lined with bedding and equipped with “mouse enrichment” that included a hiding place, nesting material (nestlets), and wooden mouse chews. Food and water were available *ad libitum*. Lighting was placed on a twelve-hour light/dark cycle with the daytime phase lasting from 07:00-19:00. Mating was done in trio breeding groups (i.e., two females and one male) and males were removed when it was clear females were pregnant. Pups remained with the mother until they were weaned, between 21-28 days, and then were separated by sex. Mice were kept in small groups of the same sex of up to eight animals until they entered experiments, with the exception of the breeding bucks, which need to be singularly housed when not breeding due to heightened aggression.

2.3.2 Health monitoring

To ensure that the mouse colony was healthy one mouse was sacrificed four times a year and tested for pathogens. The mice used were at least 12 weeks of age and were removed from housing before being humanely euthanized. Samples were collected and sent to the appropriate laboratories and testing facilities for analysis according to the hygiene and “Felasa” guidelines. Additionally, mice were monitored once a month by a qualified individual and checked daily by the animal care staff.

2.4 Neutropenia and LPS-induced severe systemic inflammation

Table 6: Experimental mouse materials

Supplies	Type	Manufacturer
Absorbable sutures	Surgicryl viol. DS19 1.5 meter USP4/0 75 cm	SMI AG, St. Vith, Belgium
Bedding	H1 505 29	Ssniff Spezialdiäten GmbH, Soest, Germany
Biodegradable paper		MAGV GmbH, Rabenau, Germany
Disposable surgical cap	Barettform	Henry Schein Vet GmbH, Hamburg, Germany
Disposable syringe	1 / 10 / 60 ml	BD Plastipak, Heidelberg, Germany
Disposable syringe	1 / 2 / 5 ml	Henry Schein Vet GmbH, Hamburg, Germany
Feed	M-Z extrudate V1126	Ssniff Spezialdiäten GmbH, Soest, Germany
Feed for experimental cages	M-Z meal V1126	Ssniff Spezialdiäten GmbH, Soest, Germany
Feed trays for experimental cages		Campuswerkstatt FB10, JLU Giessen, Germany
Filter tops		Ehret GmbH & Co. KG Labor and Pharmatechnik, Emmendingen, Germany
Heparin-Sodium	Heparin-sodium-2500-ratiopharm	Ratiopharm GmbH, Ulm, Germany
Leukosilk	01022-00	BSN-medical GmbH, Hamburg, Germany
Mouse wooden chew sticks	ABEDD® wood chews size S, NGS E-021	Lab & Vet Service GmbH, Köflach, Germany
Nestlets		Ssniff Spezialdiäten GmbH, Soest, Germany
Operating instruments		Aesculap, Tuttlingen, Germany
Pentobarbital	Pentobarbital-sodium	Boehringer Ingelheim Vetmedica GmbH, Ingelheim, Germany
Polycarbonate-cage	Type III	Ehret GmbH & Co. KG Labor and Pharmatechnik, Emmendingen, Germany
Rodent houses / tubes	Red, transparent	Ehret GmbH & Co. KG Labor and Pharmatechnik, Emmendingen, Germany
Scalpel blades	900-8946	Henry Schein Vet GmbH, Hamburg, Germany
Sterile disposable cannulas	26 G x 1/2"	B. Braun Melsungen AG, Melsungen, Germany
Swabs	HS-EuroGauze swab NS, 6 x 9 cm	Henry Schein Vet GmbH, Hamburg, Germany
Tunnel for feed tray		Campuswerkstatt FB10, JLU Giessen, Germany
Water bottle with nozzle		Ehret GmbH & Co. KG Labor and Pharmatechnik, Emmendingen, Germany
Water bottle with sipper tip for experimental cages		Ehret GmbH & Co. KG Labor and Pharmatechnik, Emmendingen, Germany
Weighing cage (for experiments)		Campuswerkstatt FB10, JLU Giessen, Germany

2.4.1 Experimental outline

To understand how neutropenia affects the sickness response during systemic inflammation a NG depleting antiserum, rabbit anti-polymorphonuclear serum (PMN), was used to reduce the levels of circulating NGs compared to immunocompetent control mice that had received normal rabbit serum (NRS). The experimental animals were males, aged between 6-8 weeks, weighing approximately 25-30g, and healthy. Males were selected as they are the standard model for immunological studies and because females have temperature fluctuations over the course of their estrous cycle that affect the profile of a fever response (Deeter et al. 1989, Kozak et al. 1997, Mouihate et al. 1998, Mouihate and Pittman 2003). To induce an inflammatory response, the bacterial mimic and PAMP LPS was utilized. Here, a high dosage of LPS (2.5 mg/kg) was able to mimic a sepsis-like response. A chronological sequence of the experimental outline is shown below.

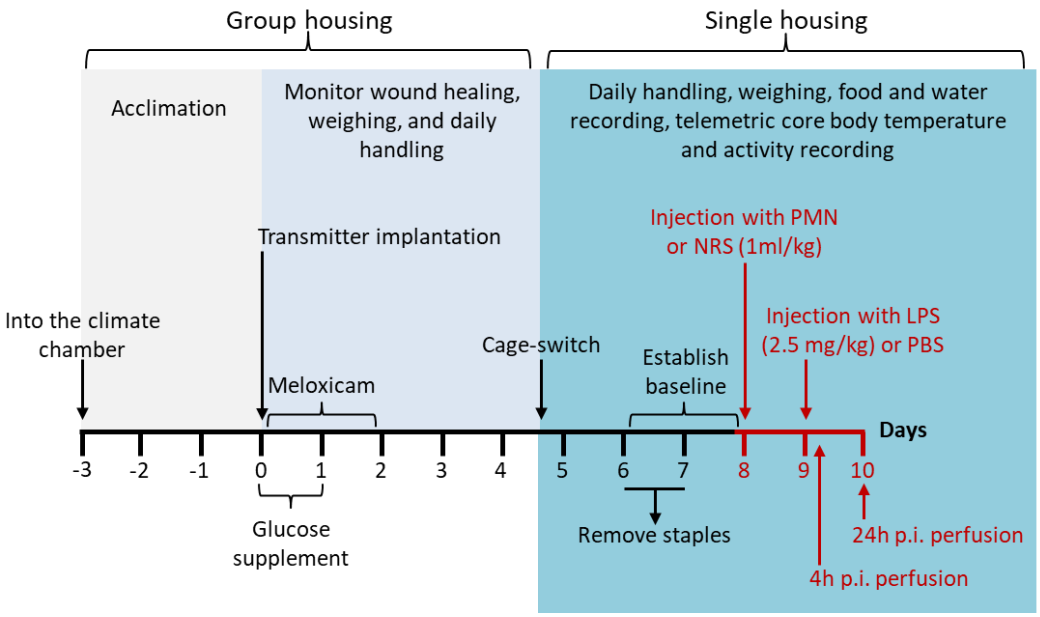

Figure 5: Timeline for experiments

Timing of transmitter implantation, cage switch, anti-polymorphonuclear serum (PMN) or normal rabbit serum (NRS) injection, lipopolysaccharide-(LPS) induced systemic inflammation, and perfusion.

2.4.2 Housing for experiments

Over the course of the experiment, the mice were kept in a temperature controlled climate chamber that was maintained at thermo-neutral 30°C ± 2°C and 50 % ± 5% humidity. As before, the light regime was set for a twelve-hour light/dark cycle that lasted from 7:00-19:00. Prior to the start of the experiment, the mice were given at least three days to acclimate to the new atmospheric conditions.

As detailed in the outline above, the mice remained group housed until approximately 3-5 days prior to the first injection. While group housed, the mice remained in polycarbonate cages (type III) with a filter top cover and enrichment; as stated previously in section 2.3.1, and with food and water available *ad libitum*. In rare cases some mice needed to be individually housed prior to the “cage switch” due to aggression.

When it was time for individual housing, the mice were put into the experimental cages. These cages were 42 x 28 x 15 cm (L x W x H) and were made of transparent Plexiglas. Air holes were placed into the lids which, combined with the transparency of the material, allowed the mice to have visual and olfactory contact with their conspecifics. Once again, the cages contained bedding and enrichment as well as food and water available *ad libitum*. In order to continuously record the consumption of food and water by a telemetric system, the water bottle and the food bowl were placed on scales located outside of the cage. The food was now offered in powdered form and was accessible via a tunnel to the food bowl and the water was available from a rodent sipper tip. The mice remained in this cage setup for the duration of the experiment.

Once in the climate chamber, the mice were checked on daily to make sure they had plenty of food and water and that there were no signs of fighting. After the transmitters were implanted with the laparotomy procedure, mice were handled and weighed at the same time daily and had their health status evaluated. Weights and health status were recorded approximately 5 days prior to the first injection in mice used for the preliminary dosage experiments, which did not receive a transmitter implantation. Daily handling also helped to habituate the mice for the experimental injections by getting them used to being restrained and experiencing light digital pressure on the sites for the intraperitoneal (IP) injections.

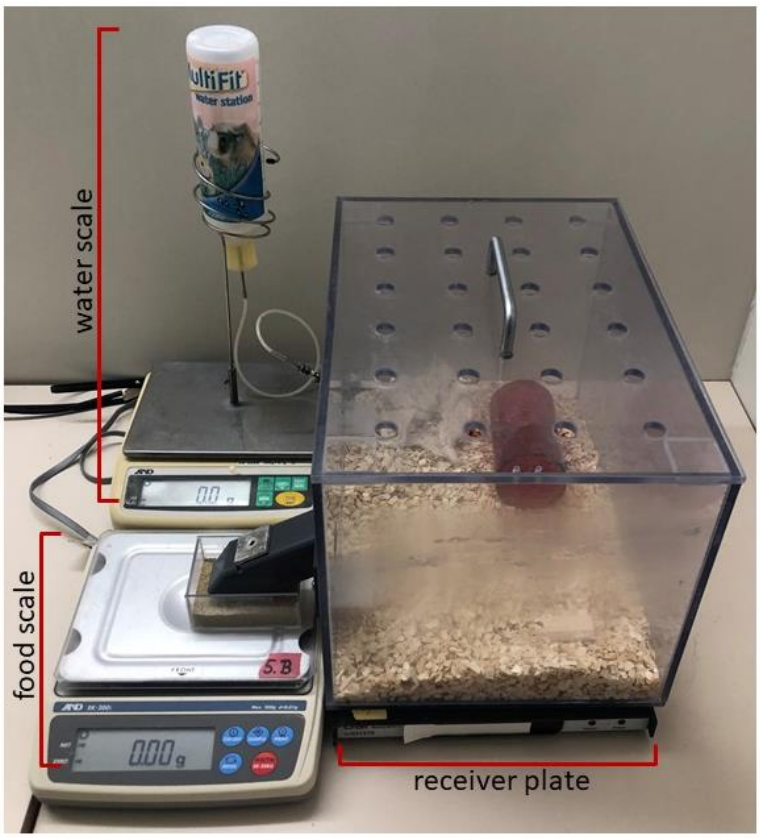

Figure 6: Cage setup for experimental housing

The cage is sitting on top of a receiver plate for the transmitter. The scales on the side record the feed and water intake connected to a telemetric system.

2.4.3 Transmitter implantation

After acclimating to the climate chamber environment (see section 2.4.2), the mice underwent laparotomy for transmitter implantation. Prior to surgery, each mouse received an oral dose of 1 drop, via syringe, of the analgesic meloxicam for pain management. Next, they were anesthetized using an antagonizable IP injection anesthesia. The volume was calculated based on a dosage of 10 ml/kg body weight using a solution composed of: 1 ml fentanyl, 1 ml midazolam, 0.5 ml medetomidine, and 7.5 ml of physiological saline. After the injection, the mouse was left in their cage for 10 min to give the anesthesia time to take effect. After 10 min, the mouse was moved to a cage free of bedding and kept under an infrared light while their blink reflex and flexor reflex, i.e., “toe pinch”, were checked. When both reflexes were absent the mouse was

prepped for surgery by applying artificial tears to the eyes and shaving the abdomen. All fur debris was removed before transferring the mouse to the clean surgical area. The final steps, before beginning surgery, were to gently expose the tongue, for the purpose of monitoring oxygenation, and to disinfect the abdomen of the mouse three times with iodine.

To begin the laparotomy, a small incision was made at the umbilicus and the skin was opened caudally approximately 2 cm exposing the *linea alba*. From here, the skin was briefly undermined to either side of the incision. At this point, it was now possible to open the abdominal cavity along the *linea alba* using micro-dissecting scissors. When the incision was wide enough the transmitter was inserted into the abdominal cavity towards the lower left flank. The incisions were closed in two phases, absorbable polyfilament sutures were used to close the *linea alba* and Michel clips were used to secure skin closure.

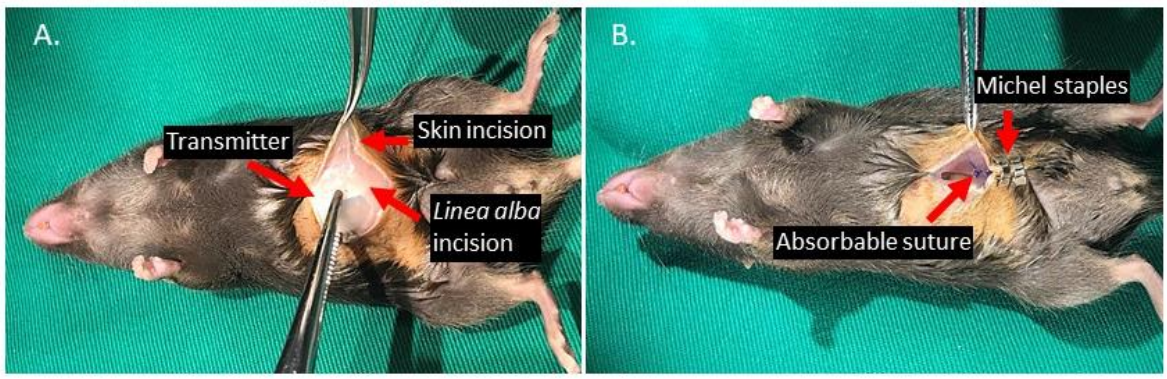

Figure 7: Laparotomy for transmitter implantation

The skin and *linea alba* are opened with two separate incisions and the transmitter is placed within the abdominal cavity (A). The *linea alba* is closed using absorbable sutures and the skin with Michel staples (B).

After the surgery was completed, the anesthesia antagonist was administered subcutaneously. The volume was calculated based on a dosage of 10 ml/kg body weight using a solution composed of: 5 ml flumazenil, 0.5 ml atipamezole, and 4.5 ml of physiological saline. The mouse was maintained under infrared light and monitored to

make sure it was alert and moving before being moved back into group housing in the home cage.

Table 7: Pharmaceuticals for laparotomy and recovery

Brand Name	Active Ingredient	Dosage	Manufacturer
Iodine solution	Povidone-iodine		B. Braun Melsungen AG, Melsungen, Germany
Isotone sodium chloride (NaCl)-solution 0.9 %	Sodium chloride		B. Braun Melsungen AG, Melsungen, Germany
Metacam oral 1.5 mg/ml (analgesic for mice)	Meloxicam	1 mg/kg, oral	Boehringer Ingelheim Vetmedica GmbH, Ingelheim, Germany
Thilo-Tears Gel	Carbomer		Alcon Pharma GmbH, Freiburg, Germany
antagonizable anesthesia			
Domitor® (1 mg/ml)	0.5 ml Medetomidin	10 ml/kg body weight, IP	Henry Schein Vet GmbH, Hamburg, Germany
Dormicum® (5 mg/ml)	1 ml Midazolam	10 ml/kg body weight, IP	Henry Schein Vet GmbH, Hamburg, Germany
Fentadon® (0.05 mg/ml)	1 ml Fentanyl	10 ml/kg body weight, IP	Dechra Veterinary Products Deutschland GmbH, Aulendorf, Germany
Isotone NaCl-solution 0.9 %	7.5 ml Physiological saline solution	10 ml/kg body weight, IP	B. Braun Melsungen AG, Melsungen, Germany
anesthesia antagonist			
Antisedan® (5 mg/ml)	0.5 ml Atipamezol	10 ml/kg body weight, s.c.	Henry Schein Vet GmbH, Hamburg, Germany
Flumazenil Hexal® (0.1 mg/ml)	5 ml Flumazenil	10 ml/kg body weight, s.c.	Henry Schein Vet GmbH, Hamburg, Germany
Isotone NaCl-solution 0.9 %	4.5 ml Physiological saline solution	10 ml/kg body weight, s.c.	B. Braun Melsungen AG, Melsungen, Germany

2.4.3.1 Recovery

Postoperative (post-op) care included the wounds being checked daily and careful monitoring for any signs of infection. The mice continued to receive an oral drop of meloxicam (1 mg/ml) for at least two days and longer if deemed necessary. Additionally, they also received a 15 % glucose agarose pad that acted as a “booster food” to help during the recovery process. Mice typically recovered from surgery, i.e., resumed normal

behavior and regained weight, within five days. The Michel clips were removed six-seven days post-op.

2.4.4 Telemetric & food and water recordings

While individually housed, it was possible to record physiological parameters of the mice. Each experimental cage was positioned on its own receiver plate, which, in combination with the transmitter assigned to it, allowed for continuous telemetric recordings of core body temperature and locomotor activity. Recordings were displayed in 5-minute intervals and could be checked without entering into the climate chamber i.e., without stressing the animals. The transmitters are battery operated and could be turned on/off by a hand-held magnet.

Once in experimental cages, it was also possible to continuously monitor food and water intake by telemetry (see section 2.4.2). Scales recorded data via the AccuDiet software; weights for food and water were also recorded by hand daily.

2.4.5 Anti-polymorphonuclear serum doses

Table 8: Pharmaceuticals for PMN/NRS injections

Description	Manufacturer
Rabbit anti-mouse polymorphonuclear serum Lot: 6326	Accurate Chemical and Scientific Co., Westbury, NY, USA
Normal rabbit serum Lot: 0925	Accurate Chemical and Scientific Co., Westbury, NY, USA
Dulbecco's phosphate buffered saline	PAA GmbH, Pasching, Austria

PMN was used to deplete NGs levels in circulation. Antibody targeted depletion of NGs is a well-established model for neutropenia and has been used successfully at the Institute of Veterinary Biochemistry and Physiology, Justus-Liebig-University Giessen following the protocol of Prof. Luheshi at the Neuroimmunology Laboratory of McGill University in Montreal, Canada (Aguilar-Valles et al. 2014). As an antiserum, it contains antibodies that target mouse polymorphonuclear cells, of which NGs are the most abundant, for clearance by the immune system. While the exact mechanism through

which this clearance occurs is unknown, it is likely that the NGs are broken down and phagocytosed by macrophages.

In order to ensure maximal reduction of NGs without causing lethality, a dose response with PMN was performed. As the distributor does not supply a concentration for the serum, the 5 ml stock was recorded as a dose of 5 ml/kg. Three different IP doses of PMN were tested: 5 ml/kg (undiluted), 2 ml/kg (2.5 fold dilution), and 1 ml/kg (5 fold dilution) with dilutions made using phosphate buffered saline (PBS) so that all doses could be administered uniformly according to bodyweight.

Table 9: Dilutions for PMN/NRS stocks

Concentration	PMN/NRS (ml)	PBS (ml)
5 ml/kg	1	-
2 ml/kg	0.4	0.6
1 ml/kg	0.2	0.8

2.4.6 Stimulation with LPS

Table 10: Stimulant for systemic inflammation

Description	Manufacturer
Dulbecco's phosphate buffered saline	PAA GmbH, Pasching, Austria
Lipopolysaccharide E. coli 0111:B4 lot: 078M4039V	Sigma-Aldrich Chemie GmbH, Munich, Germany

In order to mimic severe septic inflammation a model of LPS-induced (LPS: Escherichia coli serotype O111:B4) systemic inflammation was used. Mice received a 5 ml/kg IP injection of a high dose LPS at a concentration of 2.5 mg/kg. The LPS was diluted to the correct concentration in PBS, which also served as a control and was administered in the same injection volume. The same batch of LPS was used for all experiments and was stored in aliquots at -20°C.

2.4.7 Perfusion and sample collection

Mice were euthanized at two distinct time points, 4 h or 24 h post inoculation (p.i.) with LPS. Initially, the mice were put under deep anesthesia with an IP inoculation of 160

mg/kg pentobarbital. To verify that the mice were unconscious and had no pain response the blink reflex and flexor reflex were checked, respectively. When both reflexes were absent the abdomen then thoracic cavity was opened and the heart exposed. Using a 1 ml syringe with a heparinized 26 G needle, 0.6 ml - 1ml blood was quickly, but carefully, extracted from the right ventricle and stored on ice. Finally, the mouse was infused with five-seven ml of ice-cold isotonic saline resulting in death. The saline was pumped through the left ventricle while the right atrium was cut to allow for the outflow of blood. Ice-cold saline was used to reduce RNA degradation and preserve inflammatory mediators throughout the perfusion process.

Once the perfusion was complete, which took approximately 10 minutes, the head was detached and the brain removed. The cerebrum, cerebellum, and pituitary gland were identified and isolated. Tissues collected from the body cavity included the spleen, liver (left lateral lobe), and retroperitoneal subcutaneous adipose tissue. Immediately after collection, the brain and tissues were “snap frozen” using powdered dry ice and double wrapped in Parafilm® and aluminum foil for protection and insulation. The samples were stored at -80°C.

Once all tissues had been collected, the initial blood sample was inverted and samples were taken for a blood smear (see section 2.4.8.2) and hemocytometer counting to determine cellular populations and total cell numbers, respectively. The remaining blood was centrifuged at 8000 rpm for 10 min after which the plasma was collected and stored at -80°C.

2.4.8 Neutrophil granulocyte levels in serum

2.4.8.1 Hematological measurements

To identify how many NGs were in circulation, complete leukocyte analysis were performed. Whole blood samples were collected and evaluated with an automated hematology analyzer in collaboration with Prof. Dr. Natali Bauer (Central laboratory, small animal clinic, JLU). This technique was utilized to quickly determine the effectiveness of each dose of PMN but was not used after a dose was decided on due to the large quantity of blood required per test.

Immediately after perfusion, the blood samples were transported to the central laboratory, department of veterinary clinical sciences, clinical pathology and clinical pathophysiology, Justus-Liebig-University Giessen for analysis using their established protocol (Bauer and Moritz 2008). The hematology analyzer used operates by means of three different methods of hemoglobin measurement: flow cytometry, cyanmethemoglobin colorimetric method, and cyanide-free colorimetric method. Here the measurement of hemoglobin was based on a cyanide-free photometric measurement method and flow cytometry to determine hemoglobin concentration and red blood cell volume. An internal quality control was performed daily using human quality control material at three concentration levels. Calibration of the hematology instrument was performed annually by the manufacturer.

2.4.8.2 Leukocyte differentiation via peripheral blood smears

Table 11: Materials for blood smears and leukocyte counting

Supplies	Type	Manufacturer
Aqua bidest.		Millipore ultrapure water system
Giemsa solution		Merck KGaA, Darmstadt, Germany
May-Grünwald solution		Merck KGaA, Darmstadt, Germany
Disposable counting chamber	Neubauer improved, DHC-N01	Science Services GmbH, Munich, Germany
Leuko-TIC®	1:20 blue plus	Bioanalytic GmbH, Umkirch, Germany

A May-Gruenwald-Giemsa staining technique was used to identify and quantify the number of leukocytes in blood smears. This technique is two-fold; first, May-Gruenwald is a pH stain that targets the alkaline and acidic cellular components staining them either orange-red or blue, respectively. Second, Giemsa staining will stain all cellular components leaving the cytoplasm bluish and interacts with the May-Gruenwald stain to create a DNA complex, resulting in a purple nuclei stain. By analyzing the monolayer, it is possible to identify neutrophil-, basophilic-, and eosinophilic-granulocytes as well as lymphocytes and monocytes.

The collected blood was gently agitated to ensure a homogenous solution and 3 µl were collected by pipette and applied to a clean, un-coated glass slide. While holding another slide at a 45° angle the blood was gently smeared across. These samples were done in

replicates of 2-3 per animal and allowed to air-dry. Blood smears were stored at RT and protected from light until they were stained. The samples were stained in three separate batches to try to minimize variation as, due to the number of animals used, they could not all be stained at once. The staining protocol is shown in Table 12.

The evaluation was performed using a light microscope where 100 leukocytes were counted and identified per smear. From these numbers, the percentages of individual leukocyte populations could be determined, making it a useful technique to assess if a diminished NG response is occurring i.e., neutropenia. For each smear NGs, basophils, eosinophils, monocytes, and lymphocytes were distinguished. In some cases, multiple smears needed to be counted for one animal. When this was the case, the average values were calculated and used. All results were used in the statistical analysis unless an animal was excluded based on multiple parameters (i.e., absence of sickness behavior and verified by a lack of inflammatory cytokines measured by luminex assay).

Table 12: Protocol for blood smears

Solutions	Incubation time (min)
May-Grünwald solution	3
Aqua bidest.	1
Giemsa solution (40 ml Giemsa and 300 ml *Aqua bidest.*)	15
Aqua bidest.	1

In addition to analyzing different leukocyte populations, the total number of leukocytes in circulation was also determined for each animal. Using the Leuko-Tic® kit, blood was collected by 20 µl capillary tube and placed in a 1.5 ml tube with TIC® dye solution and inverted for 2 mins. Afterwards, the solution was applied to the Neubauer counting chamber with a chamber filling capillary tube and counted using a light microscope. Using the following formula where x is the number of leukocytes counted: (x*10*16*20)/64 I was able to determine the number of cells per µl. This technique was implemented after some experiments had already been performed and as a result, not all animals could be included. All results were used in the statistical analysis unless an animal was excluded based on multiple parameters (i.e., absence of sickness behavior

and verified by a lack of inflammatory cytokines measured by luminex assay) or there were not enough cells to count.

2.4.9 Immunofluorescence

Table 13: Materials for immunofluorescence

Supplies	Type	Manufacturer
Brush	Red sable hair	Renensis, Flensburg, Germany
Cover glass	24 x 60 mm, Nr. H878	Carl Roth GmbH & Co. KG, Karlsruhe, Germany
Glass slide	76 x 26 mm	Menzel GmbH und Co. KG, Braunschweig, Germany
Hellendahl staining jar	Glass	Carl Roth GmbH & Co. KG, Karlsruhe, Germany
Incubation box with lid	20 x 30 x 5 cm	Bochem instrumente GmbH, Wellburg, Germany
Lens tissue	101 020	Dörr GmbH, Neu-Ulm, Germany
Liquid blocking pen	Pap-pen, 5 mm tip width	Sigma-Aldrich Chemie GmbH, Munich, Germany
Microtome blade	MX35 ULTRA	Thermo Scientific, Dreieich, Germany
Nail polish	Commercial	Diverse
pH-indicator paper		Merck KGaA, Darmstadt, Germany
Plastic wrap	Commercial	Diverse
Slide box		MAGV GmbH, Rabenau, Germany
Slide folder	For 20 slides	LAT Labor und Analysen Technik GmbH, Garbsen, Germany

Table 14: Chemicals for immunofluorescence

Supplies	Manufacturer
4',6-Diamidin-2-phenylindol (DAPI)	MoBiTec, Göttingen, Germany
Aqua ad injectabilia (Aqua dest.)	B. Braun Melsungen AG, Melsungen, Germany
Citifluor AF1 (immunocytochemistry)	Citifluor Ltd., London, UK
Double deionized water *(Aqua bidest.)*	Millipore Reinstwassersystem
Ethanol- HPLC grade	Sigma-Aldrich Chemie GmbH, Munich, Germany
Normal donkey serum (NDS)	Biozol Diagnostica Vertrieb GmbH, Eching, Germany
Paraformaldehyde (PFA)	Sigma-Aldrich Chemie GmbH, Munich, Germany
Prolong gold with DAPI	Molecular Probes, Eugene, OR, USA
Sodium phosphate dibasic dihydrate	Honeywell International Inc., Charlotte, NC, USA
Sodium phosphate monobasic monohydrate	Honeywell International Inc., Charlotte, NC, USA
Triton X-100 (t-Octylphenooxypoly-Ethoxyethanol)	Sigma-Aldrich Chemie GmbH, Munich, Germany

Table 15: Solutions for immunofluorescence

Description	Preparation
20 % PFA stock solution	prepared in PBS at 60-65°C with constant stirring, then passed through a filter and allowed to cool
2 % PFA working solution	PFA stock solution is diluted with PBS
Blocking buffer	10 % NDS in PBS (0.1 M) and 0.3 % Triton X
DAPI incubation solution	1:8000 in PBS
PBS 0.1 M (pH = 7.2–7.4)	14 % Stock A + 36 % Stock B + 50 % *Aqua bidest.*
Sodium phosphate dibasic dehydrate (Stock B)	35.6 g in 1 L *Aqua bidest*.
Sodium phosphate monobasic monohydrate (Stock A)	27.6 g in 1 L *Aqua bidest*.

Immunofluorescence relies on antibodies targeting a specific antigen of interest that are then made visible by fluorescent labeling. The primary antibody (PAB) is developed in a “host species”, unrelated to the species of the tissue being used, and is primed to target an antigen of interest. Next, a fluorescently labeled secondary antibody (SAB) is used to aid in detection. The SAB is primed to target the antibodies of the PAB and can be visualized when the fluorescent label, fluorochrome, is excited by the respective wave length of light. Different fluorochromes require a specific wavelength for excitation, for example, Alexa488 excitation occurs between 460-490 nm while Cy3 requires 530-550 nm. It is crucial that the SAB has been developed in a “host species” that is different from both the PAB and that of the tissue; for example, if the tissue being stained comes from a mouse and the PAB is derived from a rabbit, then the SAB could come from a donkey. In this example, the donkey SAB was developed to target rabbit antibodies and will bind to the PAB, which in turn has bound to the antigen present in the mouse tissue. It is also possible to stain for two antigens of interest as long as the PABs were not generated in the same species, i.e., goat and rabbit, and the SABs do not use the same fluorochrome.

2.4.9.1 Neutrophil granulocyte infiltration into the brain

After analyzing NG levels in circulation, it was important to ascertain, to what extent, each dose of PMN affected NG infiltration into the brain. This was achieved through immunofluorescent staining of histological brain sections, a technique that has been very

well established at the Institute of Veterinary Biochemistry and Physiology, Justus-Liebig-University Giessen (Damm et al. 2013, Schneiders et al. 2015).

To evaluate differences in NG infiltration between treatments, several important brain structures were assessed: OVLT, SFO, choroid plexus (plexus), and the PVN. MPO was used as a marker for NGs, a component of myeloid cell granules; its use has been well-established (Haqqani et al. 1999). Additionally, the vascular endothelial cell marker von Willebrand factor (vWF) and the nuclear stain DAPI were also applied.

Moreover, during experiments, the same technique was used to gauge NG recruitment into the brain at 4 h and 24 h p.i. Focusing on the SFO and PVN, MPO was used to stain NG along with the nuclear DAPI counterstain.

To prepare the brain tissue for staining they first needed to be sliced by cryostat at a thickness of 20 μm. Afterwards, brain sections were stained. A detailed protocol of the staining procedure is shown below:

Table 16: Antibodies for neutrophil granulocyte infiltration staining

Antigen	Specification	Dilution	Product Information	Manufacturer
		primary antibodies		
MPO	Polyclonal IgG, rabbit	1:600	A0398	Dako Denmark A/S, Glostrup, Denmark
vWF	Polyclonal IgG, sheep	1:3000	SARTW-IG	Affinity Biologicals, Ancaster, Canada
		secondary antibodies		
Alexa 488, donkey	Anti-sheep	1:500	A11015	Life Technologies, Carlsbad, CA, USA
Cy3, donkey	Anti-rabbit	1:600	711-165-152	Jackson Immuno Research Europe Ltd., Newmarket, UK

Table 17: Protocol for neutrophil granulocyte infiltration staining

	Step	Procedure	Temperature	Time
Day 1	Thaw slides	in cryostat	-20°C	8-10 min
	Warm slides	on table, outline with blocking pen	RT	8-10 min
	Fixation	2 % PFA, in staining jar, on shaker plate	RT	10 min
	Wash	PBS, in staining jar, on shaker plate	RT	3 x 5 min
	Blocking	add blocking buffer, wrap incubation box with plastic wrap	RT	1 h
	Primary antibody	add vWF and MPO in blocking buffer wrap incubation box with plastic wrap	4°C	overnight
Day 2 **lights off**	Wash	PBS, in staining jar, on shaker plate	RT	3 x 5 min
	Secondary antibody	add Cy3 and Alexa 488 in blocking buffer wrap incubation box with plastic wrap and cover with aluminum foil	RT	2 h
	Wash	PBS, in staining jar, on shaker plate	RT	3 x 5 min
	DAPI	add, cover staining jar with aluminum foil on shaker plate	RT	10 min
	Wash	PBS, in staining jar, on shaker plate	RT	3 x 5 min
	Mount	Citifluor, 1-2 drops, apply cover glass	RT	
	Secure	apply nail polish to both ends to secure cover glass	RT	
	Store	protect from light	4°C	

2.4.9.2 NET formation in the brain

After NGs were identified in the brain, additional analyses were used to determine if they were undergoing NETosis. This was achieved through immunofluorescent staining of histological brain sections, a technique that has been very well established at the University of Veterinary Medicine Hanover and was carried out in collaboration with the lab of Prof. Dr. Maren von Köckritz-Blickwede (Buhr and Köckritz-Blickwede 2020). Selected slides were sent to Hannover and staining was performed by the lab of Prof. von Köckritz-Blickwede. I performed mean intensity analyses (detailed in section 2.7.5.2) of microscopic images provided by our collaborators of these brain sections.

NETosis is characterized by the release of decondensed chromatin fibers and granule proteins (Boeltz et al. 2019). Key indicators include a disruption of the nuclear membrane, histone citrullination, and the rupture of the plasma membrane and release

of extracellular traps. Therefore, by staining for the NET specific biomarker citrullinated histone H3 (H3Cit) and DNA/histone (DNA/His) complexes NETs were identified and quantified in the MnPO. A detailed protocol of the staining procedure is shown below:

Table 18: Blocking buffer for NET staining: prepared in tris-buffered saline

Description	Preparation
Bovine serum albumin	1 %
Cold water fish gelatin	2 %
Goat serum	5 %
Triton X-100	0.05 %
Tween 20	0.05 %

Table 19: Antibodies for NET staining

Antigen	Specification	Dilution	Product Information	Manufacturer
			primary antibody	
DNA/Histone H1	Mouse, monoclonal IgG2a	1:300	MAB3864	MilliporeSigma, Burlington, MA, USA
Histone H3 (citrulline R2+R8+R17)	Rabbit, polyclonal IgG	1:50	ab5103	Abcam, Cambridge, UK
			secondary antibody	
Alexa 633, goat	Anti-rabbit	1:500	A21070	Thermo Scientific, Dreieich, Germany
Alexa plus 488, goat	Anti-mouse	1:500	A32723	Invitrogen Co., Waltham, MA, USA

Table 20: Protocol for NET staining

	Step	Procedure	Temperature	Time
Day 1	Thaw slides	in cryostat	-20	8-10 min
	Warm slides	on table, outline with blocking pen	RT	8-10 min
	Fixation	2 % PFA	RT	10 min
	Wash	PBS	RT	3 x 5 min
	Blocking	add blocking buffer, wrap incubation box with plastic wrap	RT	1 h
	Primary antibody	add DNA/His and H3Cit, in blocking buffer, wrap incubation box with plastic wrap	4°C	overnight
Day 2 **lights off**	Wash	PBS	RT	3 x 5 min
	Secondary antibody	add Alexa plus 488 and Alexa 633 in blocking buffer, wrap incubation box with plastic wrap and cover with aluminum foil	RT	2 h
	Wash	PBS	RT	3 x 5 min
	DAPI/mount	Prolong gold with DAPI, 2 drops, cover glass	RT	10 min
	Store	protect from light	4°C	

2.4.10 Immunoassays

2.4.10.1 Magnetic luminex assay

Table 21: Materials for magnetic luminex assay

Supplies	Manufacturer
Magnetic luminex assay	BioTechne, Abingdon, Oxon, UK

To obtain comprehensive profiles of circulating cytokines, a luminex assay was performed. In doing so, seven different circulating cytokines were measured at once with only one sample of mouse plasma. The cytokine profile included granulocyte colony-stimulating factor (G-CSF), CCL5 (i.e., RANTES), CXCL1, CXCL2, TNF-α, IL-10, and IL-6. These immune mediators were chosen based on a literature search for NG related cytokines and chemokines important in the development of the sickness response and which could be impacted by neutropenia. Evidence showed that these mediators were altered during neutropenia or important during septic-like inflammation (Engel et al.

1994, Hynninen et al. 1995, Schönbohn et al. 1995, Miñano et al. 2004, Soares et al. 2008, Vänskä et al. 2012). Combined with the telemetric data, these analyses helped to gain better understanding of the sickness response for each treatment group. The luminex assay was carried out in the lab of Prof. Dr. Karsten Krüger, department of exercise physiology and sports therapy, Institute of Sports Science, Justus-Liebig-University Giessen.

Similarly to the immunofluorescent staining mentioned earlier, the magnetic luminex assay relies on the PAB targeting an antigen of interest; in this case the different cytokines, followed by a biotinylated SAB for visualization. However, the PAB is also bound to a magnetic bead and creates a “sandwich” complex where the antigen is bound by a PAB + bead followed by a SAB. Next, streptavidin-phycoerythrin will bind to the biotinylated site of the SAB and emit a measureable signal. The plate is read with a Luminex MAGPIX® system, which utilizes a magnet to hold the magnetic beads in place and two distinct light-emitting diodes (LEDs) to identify each antigen and the levels at which it is present.

Each bead is color coded and coated in PAB specific for one cytokine; therefore, the plate for this method contained seven different beads. The system is able to identify each bead and match it with the appropriate cytokine and uses the signal emitted by phycoerythrin to determine the magnitude. The plasma samples were diluted 1:2 and, in a few instances, the cytokine levels exceeded the detection limit. When this occurred, the measurements were excluded.

2.4.10.2 ELISA

Table 22: DetectX corticosterone ELISA kit

Supplies	Manufacturer
Coated 96-well plate	Arbor Assays, Ann Arbor, MI, USA
Plate sealer	Arbor Assays, Ann Arbor, MI, USA
Corticosterone standard	Arbor Assays, Ann Arbor, MI, USA
DetectX® corticosterone antibody	Arbor Assays, Ann Arbor, MI, USA
DetectX® corticosterone conjugate	Arbor Assays, Ann Arbor, MI, USA
Assay buffer concentrate	Arbor Assays, Ann Arbor, MI, USA
Dissociation reagent	Arbor Assays, Ann Arbor, MI, USA
Wash buffer concentrate	Arbor Assays, Ann Arbor, MI, USA
TMB substrate	Arbor Assays, Ann Arbor, MI, USA
Stop solution	Arbor Assays, Ann Arbor, MI, USA

In addition to the cytokines previously mentioned, corticosterone, a marker of the stress-induced HPA axis, was also measured in circulation at the 4 h and 24 h time points using an enzyme-linked immunosorbent assay (ELISA). This technique has been well established and published at the Institute of Veterinary Physiology at the Justus-Liebig-University Giessen (Koenig et al. 2014, Koenig et al. 2018).

Using an ELISA, it is possible to detect and measure a targeted antigen within the plasma sample. To start with, antibodies target the antigen of interest and, depending on the technique being applied; a detection antibody may be needed. Next, a chromogenic substrate is added, which will react with an enzyme located on one of the previous antibodies resulting in a color change. Using a microplate reader, it is possible to detect and measure the colorimetric reaction and, using a set of known standards of the targeted antigen, generate a logarithmic quantification that can be translated into calibration curves and used to calculate a linear regression analysis. Based on the linear regression of the standards, it is possible to assess the levels of antigen present in the samples.

Here, a sandwich ELISA method was utilized. In a sandwich ELISA, two antibodies are used to detect the antigen. First, a capture antibody is bound to the bottom of the microplate and binds to the antigen of interest. Next, a detection antibody is added that will also bind to the antigen but is conjugated to an enzyme that will react with the

substrate, typically tetramethylbenzidene (TMB), which changes color when oxidized by the enzyme horseradish peroxidase, and result in detection.

Table 23: Protocol for corticosterone ELISA

Step	Procedure
Preparation	solutions were prepared according to manufacturers' instructions
Load wells	add 50 ml of samples or standards
Non-specific binding (NSB) well	add 75 ml of assay buffer
Zero standard well	add 50 ml of assay buffer
Corticosterone conjugate	add 25 ml to each well
Corticosterone antibody	add 25 ml to each well, except NSB
Incubation	gently tap plate to mix, cover with plate sealer, shake on a plate shaker for 1 h
Wash	4 x with 300 ml wash buffer, tap plate dry on paper towels
Tetramethylbenzidine (TMB)	add 100 ml to each well
Incubation	30 min, without shaking
Stop	add 50 ml of stop solution
Read	measure in a plate reader at 450 nm

2.4.11 Reverse transcription real-time polymerase chain reaction

Table 24: Supplies for RT-qPCR

Supplies	Type	Manufacturer
Hearing protection earmuffs	1440	3M, Saint Paul, MN, USA
Micro amp 8-cap strips	N8010535	Thermo Fisher Scientific Inc., Waltham, MA, USA
Micro amp 8-tube strips	N8010580	Thermo Fisher Scientific Inc., Waltham, MA, USA
Micro amp 96-well support bases	N4379590	Thermo Fisher Scientific Inc., Waltham, MA, USA
Micro amp fast optical 96-well reaction plates	N4346907	Thermo Fisher Scientific Inc., Waltham, MA, USA
Micro amp optical adhesive films	N4311971	Thermo Fisher Scientific Inc., Waltham, MA, USA
Precision cuvette, Suprasil® quartz glass	105.202-QS	Hellma GmbH und Co. KG, Müllheim, Germany
Safety goggles		Infield Safety GmbH, Solingen, Germany

Table 25: Chemicals and reagents for RT-qPCR

Supplies	Manufacturer
Chloroform	Sigma-Aldrich Chemie GmbH, Munich, Germany
Deoxynucleotide mix (dNTPs)	Sigma-Aldrich Chemie GmbH, Munich, Germany
Diethylpyrocarbonate (DEPC)	Sigma-Aldrich Chemie GmbH, Munich, Germany
Dithiothreitol (DTT)	Thermo Fisher Scientific Inc., Waltham, MA, USA
Double deionized water (*Aqua bidest.*)	Millipore Reinstwassersystem
Ethanol absolute	Sigma-Aldrich Chemie GmbH, Munich, Germany
Isopropanol	Sigma-Aldrich Chemie GmbH, Munich, Germany
M-MLV reverse transcriptase (RT-enzyme)	Thermo Fisher Scientific Inc., Waltham, MA, USA
NucleoSpin™ RNA XS	Macherey-Nagel, Düren, Germany
Precision master mix with ROX	PrimerDesign Ltd., Southhampton, UK
Random hexamer	Thermo Fisher Scientific Inc., Waltham, MA, USA
RNaseZap™	Sigma-Aldrich Chemie GmbH, Munich, Germany
RT-buffer	Thermo Fisher Scientific Inc., Waltham, MA, USA
Taqman Gene Expression Master Mix	Thermo Fisher Scientific Inc., Waltham, MA, USA
Trizol reagent	Thermo Fisher Scientific Inc., Waltham, MA, USA

Table 26: Solutions for RT-qPCR

Description	Preparation
70 % Ethanol	70 % ethanol in DEPC water
DEPC water	0.1 % DEPC in *Aqua bidest.*
	stirred at RT for 24 h, autoclaved
Real time-PCR Mix	3.5 µl sterile H_2O
	5 µl Taqman Gene Expression Master Mix
	0.5 µl primer
Reverse transcription Mix 1	5 µl DEPC H_2O
	1 µl random hexamer
	1 µl dNTPs
Reverse transcription Mix 2	4 µl RT-buffer
	2 µl sterile H_2O
	2 µl DTT (0.1 M)
	1 µl RT-enzyme (M-MLV-RT)
Sterile water	autoclaved *Aqua bidest.*

Table 27: Primers list for neutropenic experiments

Gene	Assay ID	Manufacturer
CD68	Mm03047340_m1	Thermo Fisher Scientific Inc., Waltham, MA, USA
CD163	Mm00474091_m1	Thermo Fisher Scientific Inc., Waltham, MA, USA
COX-2	Mm00478374_m1	Thermo Fisher Scientific Inc., Waltham, MA, USA
CXCL1	Mm04207460_m1	Thermo Fisher Scientific Inc., Waltham, MA, USA
ELANE	Mm00469310_m1	Thermo Fisher Scientific Inc., Waltham, MA, USA
GAPDH	4352339E-1009032	Applied Biosystems, Waltham, MA, USA
IL-6	Mm00446190_m1	Thermo Fisher Scientific Inc., Waltham, MA, USA
IL-10	Mm00439614_m1	Thermo Fisher Scientific Inc., Waltham, MA, USA
mPGES	Mm00452105_m1	Thermo Fisher Scientific Inc., Waltham, MA, USA
NF-IL6	Mm00843434_s1	Thermo Fisher Scientific Inc., Waltham, MA, USA
NfκBiα	Mm00477798_m1	Thermo Fisher Scientific Inc., Waltham, MA, USA
SOCS3	Mm00545913_s1	Thermo Fisher Scientific Inc., Waltham, MA, USA
TNFα	Mm00443258_m1	Thermo Fisher Scientific Inc., Waltham, MA, USA

To look at the level certain pro- and anti- inflammatory and NG markers were expressed in the brain, their gene expression was analyzed via reverse transcription real-time polymerase chain reaction (RT-qPCR) in the hypothalamus as previously reported (Rummel et al. 2006, Damm et al. 2013). The variation in gene expression elucidates to what extent LPS and/or neutropenia effects their expression.

The first step in the process involves extracting ribonucleic acid (RNA) from the tissue with the Trizol method and converting it to DNA (cDNA). Trizol works in two parts: 1) solubilizes RNA and DNA and lowers the pH, and 2) denatures proteins to halt RNases. After undergoing sonication to homogenize the tissue in a Trizol solution, centrifugation, precipitation, and purification steps with ethanol (EtOH), the RNA is isolated, pelleted, and resuspended in diethyl pyrocarbonate (DEPC) water (table 28). Once the RNA is isolated, the concentration of each sample is determined with a nano-photometer and all samples are adjusted to an equal concentration of 250 ng/μl to ensure comparability. Now, RNA is reverse transcribed to cDNA using the Moloney murine leukemia virus-reverse transcriptase of an RNA-dependent DNA polymerase utilizing random hexamer primers as the starting points. All samples were stored at -80°C.

The next step requires amplification of the target gene using a primer pair specific to the corresponding gene. The primers anneal to the denatured cDNA and act as scaffolding

allowing the DNA polymerase to bind and assemble the cDNAs complementary strand. Most importantly, a Taqman® probe is what allows for later photometric determination. The probes carry two different fluorochromes known as the reporter and quencher, the reporter becomes excited and emits light while the quencher absorbs light emitted from the reporter.

At this point, it is possible to amplify the DNA in cycles and measure it in real time where a fluorescent signal is produced, which is proportional to the level of amplification. The higher the initial concentration of the gene, the sooner the fluorescent signal will be detected. The relative quantification (RQ) was determined based on the cycle threshold (ct) defined when amplification exceeds that of the background signal. Once the ct has been reached, the cDNA amplification becomes exponential and will double with each cycle and can be applied for relative quantification.

To reduce the effect of differences between individual animals, the RT-qPCR results were normalized to a control gene. When selecting a control, otherwise known as a housekeeping gene, it is important to find a gene that is continuously expressed at the same level in all samples and is not affected by the treatment group. In previous experiments performed by Dr. Fabian Pflieger at the Institute of Veterinary Physiology, Justus-Liebig-University Giessen, six different potential housekeeping genes were tested for the hypothalamus applying the same dose of LPS in mice (Pflieger 2021). Based on the results, GAPDH was selected as the most stable housekeeping gene between groups.

Table 28: RNA extraction protocol

	Step	Procedure	Time
Day 1	Homogenize samples	add 500 or 1000 ml ice-cold Trizol depending on weight (500 ml for < 50mg, 1000 ml for 50-100 mg tissue) sonicate, wash sonicator in-between samples: 100 % EtOH, DEPC-water briefly	10-15 sec
	Centrifuge	12000 x g, 4°C	10 min
	Isolation	collect supernatant in new 1.5 ml tube	
	Separation of nucleoproteins	leave at RT	5 min
	Dissolve denatured proteins	add 100 ml (500 ml Trizol) or 200 ml (1000 ml Trizol) chloroform and shake by hand	15 sec
	Separation	leave at RT	3 min
	Centrifuge	12000 x g, 4°C yield organic (DNA, proteins) and aqueous (RNA) phase	20 min
	Aqueous phase	add 250 ml (500 ml Trizol) or 500 ml (1000 Trizol) isopropanol into new 1.5 ml tube, add aqueous phase	
	RNA precipitation	vortex, incubate -20°C	overnight
Day 2	Centrifuge	12000 x g, 4°C	15 min
	Wash I	pour off supernatant, add 1 ml 70 % EtOH, vortex	3 sec
	Centrifuge	15000 x g, 4°C	10 min
	Wash II	pour off supernatant, add 1 ml 100 % EtOH, vortex	3 sec
	Centrifuge	15000 x g, 4°C	10 min
	Dry pellet	pour off supernatant, allow to dry upside down at RT	20-25 min
	Re-suspend pellet	add 10 or 20 ml DEPC water depending on pellet size	

Table 29: Reverse transcription protocol

Description	Temperature	Duration
7 µl RT-Mix 1 + 4 µl RNA sample	65°C	10 min
Blank 1: 7 µl RT-Mix 1 + 4 µl DEPC H_2O		
Keep samples on ice, add 9 µl RT-Mix 2	37°C	1 h
Blank 2: 9 µl RT-Mix 2 + 11 µl DEPC H_2O	90°C	5 min
	4°C	

Table 30: RT-qPCR protocol

	Step	Temperature	Time
	load 9 µl real time PCR-Mix + 1 µl cDNA Probe		
	activate DNA polymerase	50°C	2 min
	denaturation 1	95°C	10 min
Repeat x 39	denaturation 2	95°C	15 sec
(40 total cycles)	annealing and elongation	60°C	60 sec

2.5 Neutrophil granulocyte cultures

Table 31: Materials for cultures

Supplies	Type	Manufacturer
Cell culture plate	12 well, standard, flat base	Sarstedt AG & Co. KG, Nümbrecht, Germany
Cell culture plate	24 well, sterile, flat bottom	VWR International, Radnor, PA, USA
Cell strainer	100 µm	Sarstedt AG & Co. KG, Nümbrecht, Germany
Cover glasses	13 / 15 mm	MAGV Laborbedarf, Rabenau, Germany
Disposable counting chamber	Neubauer improved, DHC-N01	Science Services GmbH, Munich, Germany
Disposable syringe	10 ml	BD Plastipak, Heidelberg, Germany
Disposable syringe	1 ml	Henry Schein Vet GmbH, Hamburg, Germany
flexiPERM®	Micro 12, re-usable silicon insert	Sarstedt AG & Co. KG, Nümbrecht, Germany
Open-drop bell jar with mesh platform		
Operating instruments		Aesculap, Tuttlingen, Germany
Round-bottom polystyrene tubes	With caps, 5 ml	Stemcell Technologies, Vancouver, Canada
Sterile disposable cannulas	25 G x 1 ½ ''	Servoprax GmbH, Wesel, Germany
TC dish	35 / 100, standard	Sarstedt AG & Co. KG, Nümbrecht, Germany

Table 32: Chemicals for cultures

Supplies	Manufacturer
Dulbecco's PBS with Ca & Mg without phenol red	Capricorn Scientific GmbH, Ebsdorfergrund, Germany
Ethanol absolute	Sigma-Aldrich Chemie GmbH, Munich, Germany
Ethylenediaminetetraacetic acid (EDTA)	Fisher Scientific GmbH, Schwerte, Germany
Fetal calf serum (FCS)	Sigma-Aldrich Chemie GmbH, Munich, Germany
Hydrogen chloride	Carl Roth GmbH & Co. KG, Karlsruhe, Germany
L-glutamine	Fisher Scientific GmbH, Schwerte, Germany
Penicillin-Streptomycin (P/S)	Thermo Scientific, Dreieich, Germany
Poly-L-Lysine	Th. Geyer GmbH & Co. KG., Renningen, Germany
Roswell Park Memorial Institute (RPMI) 1640 without L-glutamine	Capricorn Scientific GmbH, Ebsdorfergrund, Germany
Sodium chloride (NaCl)	Merck KGaA, Darmstadt, Germany
Vetflurane 1000 mg/g	Virbac Pharmaceutical Co., Carros, France

2.5.1 Experimental outline

To better understand the role NGs play in the generation of the sickness response and their ability to undergo NETosis, they were isolated and cultured. Naïve NGs were collected from healthy male and female mice aged between 19-22 weeks old. The inflammatory stimulus LPS was used at three different doses in combination with the chemoattractant CXCL1. As a key mediator during severe systemic inflammation, CXCL1 contributes to NG migration and defenses as well as the expression of other inflammatory mediators (Jin et al. 2014). Using multiple concentrations of LPS (dose-response experiment), I determined if LPS was inducing a dose-dependent response in NG cultures.

2.5.2 Neutrophil granulocyte isolation

Table 33: Solutions for neutrophil granulocyte isolation

Description	Preparation
Preparation medium	10 % FCS + 1x P/S + 2 mM L-glutamine in RPMI
Isolation medium	10 % FCS + 2 mM L-glutamine + 2 mM EDTA in RPMI
Supplemented PBS	2 % FCS + 1 mM EDTA in PBS
Supplemented RPMI	2 mM L-glutamine in RPMI
0.2 % NaCl	0.4 g NaCl in 200 ml sterile water
1.6 % NaCl	3.2 g NaCl in 200 ml sterile water

Table 34: EasySep™ mouse neutrophil granulocyte enrichment kit

Supplies	Manufacturer
Biotin selection cocktail	Stemcell Technologies Inc., Vancouver, Canada
EasySep™ magnet	Stemcell Technologies Inc., Vancouver, Canada
Magnetic particles	Stemcell Technologies Inc., Vancouver, Canada
Mouse neutrophil enrichment cocktail	Stemcell Technologies Inc., Vancouver, Canada
Normal rat serum	Stemcell Technologies Inc., Vancouver, Canada

Through a laboratory rotation at the University of Veterinary Medicine Hannover in the lab of Prof. Dr. Maren von Köckritz-Blickwede, I learned how to isolate and culture NGs according to their long established protocol (Branitzki-Heinemann et al. 2020). The NGs were isolated from the tibia and femur of aged mice, which have higher levels of NGs, using an EasySep™ cell isolation kit.

The EasySep™ cell separation relies on a magnet-assisted process known as negative selection to yield purified cell populations. Negative selection utilizes a dual ended antibody complex to target and bind the undesirable cell populations. Magnetic particles are added and attach to the unbound end of the antibody complex. At this point, the mixture is inserted into a high powered magnet and labeled cells are attracted to the tube wall where the strong magnetic field holds them in place. The unlabeled population of interest, i.e., NGs, remains unbound and can be decanted into a separate tube. Once isolated, the NGs were counted and analyzed for purity or plated on poly-L-lysine coated glass coverslips. The complete protocol is shown below:

Table 35: Bone marrow derived NG isolation

Step	Procedure	Time
Prepare wells	attach glass coverslip to flexiPERM® well, add 30 µl of poly-L-lysine to well, cover in foil and store at 4°C	overnight
Wash	wash wells with sterile water, warm in CO_2 incubator until ready to plate cells	
Euthanize mouse	anesthetize mouse with Vetflurane, kill by cervical dislocation	
Remove hind legs	spray the mouse with 70 % EtOH, using surgical scissors make an incision along the inner thigh, flay the skin of the hind leg, remove leg by cutting at the acetabulofemoral joint, cut off foot at the talocrural joint and store leg in preparation media on ice, repeat with second leg	
Bone isolation	using surgical scissors and forceps separate upper and lower leg at the tibiofemoral joint, remove muscle and tissue from femur and tibia	
Sterilize and prepare bone	dip bone in 70 % EtOH, wash 3x in PBS, cut off the heads of both bones	
Bone marrow isolation	using 25G cannula and syringe with 10 ml isolation medium, insert cannula into the bone shaft and gently force marrow out into 100 µm filter inserted in a 50 ml tube	
Wash filter	using the plunger from a 1 ml syringe gently force bone marrow through the filter and rinse filter with remaining isolation medium from previous step	
Centrifuge	360 x g, 4°C	7 min
Lysate red blood cells	remove supernatant, add 10 ml 0.2 % NaCl	20 sec
Stop lysate	add 10 ml 1.6 % NaCl	
Centrifuge	360 x g, 4°C	10 min
Wash	remove supernatant, add 10 ml isolation medium	
Centrifuge	360 x g, 4°C	7 min
Re-suspend	remove supernatant, re-suspend in 1 ml supplemented PBS in 15 ml tube	

Table 36: EasySep™ neutrophil granulocyte isolation

Step	Procedure	Time
	using re-suspended cells from bone marrow isolation	
1	add 50 µl rat serum and 40 µl enrichment cocktail, mix and incubate 4°C	15 min
2	add 1 ml supplemented PBS	
3	centrifuge: 300 x g, 4°C	10 min
4	remove supernatant, re-suspend in 1 ml supplemented PBS	
5	add 50 µl biotin selection cocktail, mix and incubate 4°C	15 min
6	vortex magnetic particles	30 sec
7	add 150 µl magnetic particles, mix and incubate 4°C	10 min
8	add 300 µl supplemented PBS, move to round bottomed tube	
9	place tube into EasySep™ magnet, incubate	3 min
10	in one motion pick up magnet, while tube is still inserted, and pour out into new 15 ml tube	3 sec
11	count cells using disposable hemocytometer	

2.5.2.1 Purity of neutrophil granulocyte isolation

Table 37: Solutions for flow cytometry

Description	Preparation
Medium buffer	2 % NDS in PBS (0.1 M) and 1 mM EDTA
PBS 0.1 M (pH = 7.2–7.4)	14 % Stock A + 36 % Stock B + 50 % *Aqua bidest.*
Sodium phosphate dibasic dehydrate (Stock B)	35.6 g in 1 L *Aqua bidest*.
Sodium phosphate monobasic monohydrate (Stock A)	27.6 g in 1 L *Aqua bidest*.
antibody dilution	
Unstained	100 µl medium buffer
CD11b alone	1 µl CDllb + 99 µl medium buffer
Ly6G alone	1 µl Ly6G + 99 µl medium buffer
CD11b + Ly6G	1 µl CD11b + 1 µl Ly6G + 98 µl medium buffer
FITC IgG2b	1 µl FITC IgG2b + 99 µl medium buffer
PE IgG2a	1 µl PE IgG2a + 99 µl medium buffer

To verify the efficacy of the NG isolation technique, the isolated cells were tested using flow cytometry. By identifying specific cellular characteristics, it was possible to accurately determine the percent purity of NGs isolated from bone marrow through identifying $CD11b^{+}Ly6G^{+}$ cell populations.

Flow cytometry is a technique that utilizes lasers and fluorescent staining, similar to the immunofluorescent techniques discussed in section 2.4.9, to characterize and analyze the shape and surface antigen expression on a cell-by-cell basis in solution using a series of “gating strategies”. To accomplish this, cells flow past one or more lasers and, based on the disruption they cause to the laser stream or the fluorescence emitted, can be separated into different groups. The first gate is based on the size and complexity of the cells and is determined with the forward scatter (FSC) and side scatter (SSC), respectively, and does not require fluorescence. Size can be calculated based on the void left as the cell passes through the laser and the degree the laser scatters to the sides details the complexity or granularity of the cell. Once the desired population has been identified based on the first two parameters, it is possible to move on to the next gating strategy using fluorescence. Here, samples only stained with one of the fluorescent markers, i.e., single stains, or unstained samples are used to determine their emission strength. The gates are then set based on the emission for each marker. Now,

the cells can be grouped based on their fluorescent profile and it is possible to look at the expression for both antibodies in combination where cells could bind one, both, or neither antibody. An example of the gating strategy used is shown below in Figure 8.

Since mouse bone marrow derived NGs have been reported as presenting both medium and high FSC, both groups were included in the 'Granulocyte' population (Rambault et al. 2021). Flow cytometry and gating strategies were performed by Dr. Ivan Conejeros in collaboration with the lab of Prof. Dr. Anja Taubert at the Institute of Parasitology, Justus-Liebig-University Giessen.

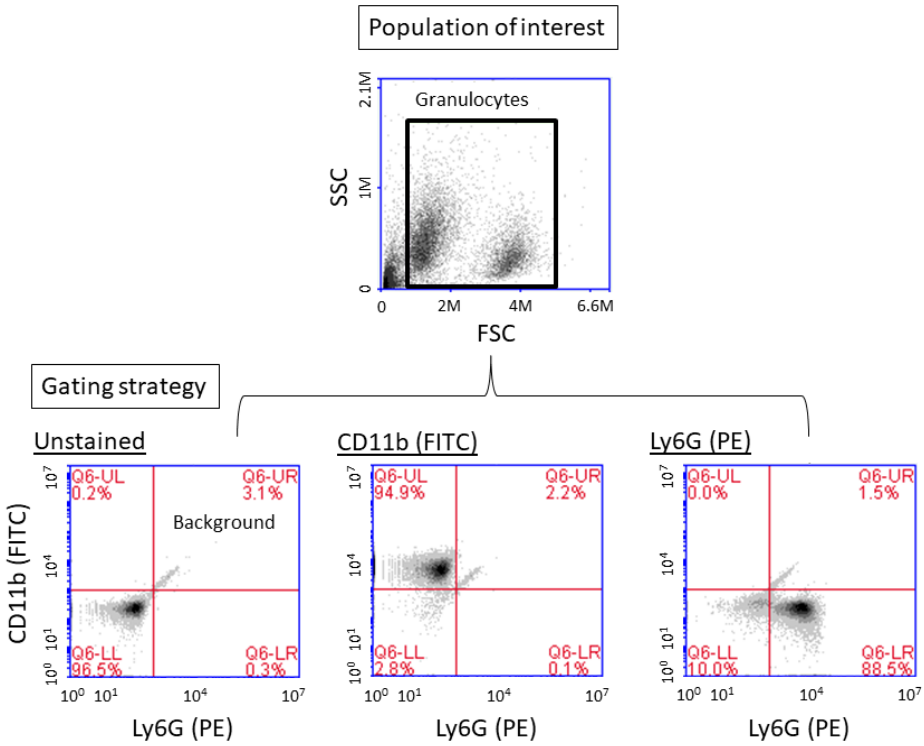

Figure 8: Gating strategies for CD11b: FITC and Ly6G: PE

The cells were gated on SSC vs. FSC for complexity and size in order to select the population of interest; these cells are labeled "Granulocytes". Unstained and single stains for CD11b (FITC) and Ly6G (PE) were used to determine the emission strength for each signal. Based on the emission strength the gates could be set for FITC vs. PE. Background signaling was identified as the percentage of $CD11b^{+}Ly6G^{+}$ cells in the unstained cells and are labeled as such.

Table 38: Antibodies for neutrophil granulocyte characterization

Antigen	Specification	Dilution	Product Information	Manufacturer
CD11b	Monoclonal M1/70, Rat, FITC	1:2000	553310	BD Biosciences, Heidelberg, Germany
Ly6G	Monoclonal 1A8, Rat, PE	1:2000	551461	BD Biosciences, Heidelberg, Germany
IgG2b	Monoclonal A95-1, κ isotype control, Rat, FITC	1:2000	553988	BD Biosciences, Heidelberg, Germany
IgG2a	Monoclonal R35-95, κ isotype control, Rat, PE	1:2000	553930	BD Biosciences, Heidelberg, Germany

Table 39: Staining protocol for flow cytometry

Step	Procedure	Temperature	Time
Prepare cells	add $2x10^5$ cells from EasySep™ isolation to six 2 ml eppi tubes	on ice	
Centrifuge	360 x g	4°C	5 min
Re-suspend	200 µl medium buffer	on ice	
	from here work with lights off		
Stain	add 10 µl of antibody dilution, one for each tube, incubate	on ice	45 min
Wash	add 1 ml cold PBS	on ice	
Centrifuge	360 x g	4°C	10 min
Re-suspend	add 300 µl medium buffer	on ice	

2.5.3 Treatment of neutrophil granulocyte cultures

Table 40: Stimulant for NETosis

Description	Manufacturer
Dulbecco's PBS	PAA GmbH, Pasching, Austria
Lipopolysaccharide E. coli 0111:B4 Lot: 078M4039V	Sigma-Aldrich Chemie GmbH, Munich, Germany
Methyl-β-cyclodextrin	Sigma-Aldrich Chemie GmbH, Munich, Germany

Cultures were treated with one of three LPS (Escherichia coli serotype O111:B4) doses: 1 µg/ml, 10 µg/ml, or 20 µg/ml in combination with 50 ng/ml of CXCL1. Work done by Neubert and colleagues (2019) showed that an LPS dose of 25 µg/ml but not 10 µg/ml was sufficient to induce NET formation in culture (Neubert et al. 2019). Boro and Balaji (2017) were able to stimulate inflammasome activation in macrophages by treating cells

with 50 ng/ml of CXCL1 (Boro and Balaji 2017). The goal of the dose response experiment was to determine if similar results were observed with the LPS batch and/or which dose was sufficient to induce NETs in combination with CXCL1. The same batch of LPS was used for all experiments and was stored in aliquots at -20°C. The NET inducer CD was used as a positive control and the diluent PBS served as the negative control as previously reported (Henneck et al. 2022). The treatments were added immediately after plating NGs cultures and incubated for 3 h in a humidified atmosphere composed of 5 % CO_2 and maintained at 37°C. The incubation time was taken from the established protocol of Prof. Dr. Maren von Köckritz-Blickwede based on NG viability in culture and the length of time it takes for NET formation to occur (Hoppenbrouwers et al. 2017, Boeltz et al. 2019, Henneck et al. 2022). After 3 h, the supernatants were collected and stored at -20°C and the cells were fixed with 4 % PFA.

Table 41: Treatment preparations for neutrophil granulocyte cultures

Treatment dose	Stock Concentration (in RPMI)	Preparation
CXCL1 50 ng/ml	1800 ng/ml	add 10 µl to cells in 350 µl
Cyclodextrin 5mM	35 mM	add 50 µl to cell in 300 µl
LPS 1 µg/ml	7 µg/ml	add 50 µl to cell in 300 µl
LPS 10 µg/ml	70 µg/ml	add 50 µl to cell in 300 µl
LPS 20 µg/ml	140 µg/ml	add 50 µl to cell in 300 µl

2.5.4 NET formation *in vitro*

Table 42: Solutions for NET immunofluorescence

Description	Preparation
Blocking buffer	5 % NDS in PBS (0.1 M) and 0.5 % Triton X
DAPI incubation solution	1:5000 in PBS
PBS 0.1 M (pH = 7.2–7.4)	14 % Stock A + 36 % Stock B + 50 % *Aqua bidest.*
Sodium phosphate dibasic dehydrate (Stock B)	35.6 g in 1 L *Aqua bidest*.
Sodium phosphate monobasic monohydrate (Stock A)	27.6 g in 1 L *Aqua bidest*.

Here, the immunofluorescent technique described in section 2.4.9 was used to evaluate NET formation in culture. DNA/His, MPO, and DAPI were used to identify when a NG underwent NETosis (section 2.4.9.2). NETs were determined based on the release of

nuclear DNA and DNA/His and the expression of MPO. In addition, when a NET was touching another NG it was also counted. A detailed protocol of the staining procedure is shown below:

Table 43: Antibodies for NET staining

Antigen	Specification	Dilution	Product Information	Manufacturer
		primary antibodies		
DNA/Histone H1	Mouse, monoclonal IgG2a	1:500	MAB3864	MilliporeSigma, Burlington, MA, USA
MPO	Polyclonal IgG, rabbit	1:500	A0398	Dako Denmark A/S, Glostrup, Denmark
		secondary antibodies		
Alexa 488, donkey	Anti-rabbit	1:500	A11015	Life Technologies, Carlsbad, CA, USA
Cy3, goat	Anti-mouse	1:1000	115-165-003	Jackson Immuno Research Europe Ltd., Newmarket, UK

Table 44: Fixation and staining protocol for NETs

Step	Procedure	Temperature	Time
	after 3 h treatment		
Wash	PBS, in 24-well plate	RT	3 x 5 min
Fixation	4 % PFA, in 24-well plate	RT	20 min
Wash	PBS, in 24-well plate	RT	3 x 5 min
Store	add 1 ml PBS and cover	4°C	up to 2 weeks
	immunofluorescence staining		
Blocking	add 300 µl blocking buffer	RT	20 min
Primary antibody	add 250 µl DNA/His and MPO in blocking buffer, cover and incubate in 24-well plate	RT	1 h
Wash	PBS, in 24-well plate	RT	3 x 5 min
	from here work with lights off		
Secondary antibody	add 250 µl Cy3 and Alexa 488 in blocking buffer, cover and wrap in aluminum foil, incubate in 24-well plate	RT	45 min
Wash	PBS, in 24-well plate	RT	3 x 5 min
DAPI	add 250 µl, cover and wrap in aluminum foil, incubate in 24-well plate	RT	10 min
Wash	PBS, in 24-well plate	RT	3 x 5 min
Mount	apply 1 drop of Citifluor to slide, dip cover glass in water briefly, dry on filter paper; place on Citifluor drop, cell side down, to mount	RT	

2.5.5 Cytokine production *in vitro*

Table 45: Materials for bioassays

Description	Type	Manufacturer
Disposable counting chamber	Neubauer improved, DHC-N01	Science Services GmbH, Munich, Germany
Tissue culture flask	Sterile with filter, 50 / 75 / 250 / 550 ml	Sarstedt AG und Co. KG, Nümbrecht, Germany
Tissue culture plate	Sterile, with coverplate 96	Sarstedt AG und Co. KG, Nümbrecht, Germany

Table 46: Chemicals and reagents for bioassays

Description	Manufacturer
3-[4,5-Dimethylthiazol-2yl] 2,5-Diphenyl-Tetrazolliumbromide (MTT)	Sigma-Aldrich Chemie GmbH, Munich, Germany
Actinomycin D	Sigma-Aldrich Chemie GmbH, Munich, Germany
Dulbecco's PBS	Capricorn Scientific GmbH, Ebsdorfergrund, Germany
Fetal calf serum (FCS)	Capricorn Scientific GmbH, Ebsdorfergrund, Germany
Gentamicin	Capricorn Scientific GmbH, Ebsdorfergrund, Germany
Glutamine	Capricorn Scientific GmbH, Ebsdorfergrund, Germany
Heparin-Sodium-25000-ratiopharm	Ratiopharm GmbH, Ulm, Germany
Hydrochloric acid (HCl)	Merck KGaA, Darmstadt, Germany
IL-6 standard	National Institute for Biological Standards and Control, Potters Bar, UK
Isopropanol	Merck KGaA, Darmstadt, Germany
Mercaptoethanol	Merck KGaA, Darmstadt, Germany
Penicillin-Streptomycin (P/S; 5000 IU/ml)	Capricorn Scientific GmbH, Ebsdorfergrund, Germany
RPMI-Medium	Capricorn Scientific GmbH, Germany, Ebsdorfergrund
TNFα standard	National Institute for Biological Standards and Control, Potters Bar, UK
Trypsin (25 %)	Capricorn Scientific GmbH, Ebsdorfergrund, Germany

Table 47: Solutions for bioassays

Description	Preparation
Assay and growth medium (TNFα)	500 ml RPMI 55 ml FCS 5 ml P/S 5 ml Glutamine
Assay medium (IL-6)	45 ml RPMI 4 ml FCS 0.5 ml Glutamine (200 nM) 125 µl Mercaptoethanol (200 nM) 65 µl Gentamicin (10 ng/ml)
Growth medium (IL-6)	assay medium (IL-6) 50 I.U. IL-6 standard/ml
Isopropanol-HCl solution	4 ml HCl (2N) 196 ml Isopropanol
MTT solution	0.1 g MTT 20 ml PBS

The pro-inflammatory cytokines TNFα and IL-6 were each measured in the supernatants of cultured NGs following treatment. These bioassay techniques are well established in the Institute of Veterinary Physiology at Justus-Liebig-University Giessen (Peek et al. 2020). Both bioassays require a cell line to determine the level of cytokine present; TNFα is measured with a murine fibrosarcoma cell line (MF; WEHI 1674 subclone13) while IL-6 requires a B9 hybridoma cell line (B9). When TNFα, in combination with actinomycin, is added to the MF cells it has a cytotoxic effect and the relation of TNFα present to living cells is inversely proportional (Espevik and Nissen-Meyer 1986). IL-6 has a proliferative effect on the B9 cells and the relation of IL-6 present to living cells is directly proportional (Lansdorp et al. 1986). After treating the respective cell lines, MTT tetrazolium salt is added and results in a colorimetric effect that can be quantified.

To begin with, both bioassays required the cell lines to be thawed, grown, and passaged until cell numbers were high enough to be cultured in a 96-well plate (MF:50,000 cells/well, B9: 5,000 cells/well). The cells were maintained and incubated at 37°C, 95 % humidity, and 5% CO_2 unless otherwise stated. Once the 96-well plates were prepared, the standards and samples were added in duplicate and incubated for 24 h (TNFα) or 72 h (IL-6) after which the MTT tetrazolium salt was added for an additional 4 h. Afterwards,

the reaction was stopped by adding an isopropanol-hydrochloric acid and the plates were left at RT for 12 h before photometric measurements were taken with an ELISA plate reader. Based on the known standards and linear regression analysis, the amounts of TNFα and IL-6 were calculated.

The cells were grown and the practical application of measuring the samples was completed in two batches with the help of Ms. Jolanta Murgott.

2.6 LPS-induced ARDS

2.6.1 Experimental outline

Previous work performed in our lab has shown that ω-3 PUFA play a protective role during systemic inflammation (Pflieger 2021) and it is hypothesized that leukocyte trafficking could contribute to those effects. Indeed, the ω-3 PUFA derived metabolite RvE1 has been shown to alter transendothelial migration and recruitment of NGs into the dorsal air pouch and *in vitro* (Serhan et al. 2000, Arita et al. 2005). Here, I aimed to identify through which receptor RvE1 may modulate NG recruitment to the brain with therapeutic potential during LPS-induced ARDS. For this purpose, resolving receptor deficient mice were used. The KO mice were bred on a C57BL/6N background with (Fat) or without (WT) the *fat-1* transgene. Transgenic Fat mice endogenously produce ω-3 PUFA via a desaturase derived from *C. elegans*, thus, are genetically enriched in ω-3 PUFA (Kang 2007). WT and Fat mice were crossed either with mice that lacked the CR (CR KO) or the LR (LR KO) as has been done in other studies (Tager et al. 2000, Cash et al. 2008). RvE1 can mediate its effects via both of these receptors i.e., CR and LR (Arita et al. 2007, Ohira et al. 2010).

The experimental animals were males and females, aged between 10-13 weeks, weighing approximately 22-25g, and healthy. To induce an inflammatory response, mice received an i.t. instillation of LPS (10 μg/mouse) and were sacrificed at multiple time-points after stimulation to primarily investigate its effects on lung inflammation (0h, 4h, 24h, 72h, and 120h after stimulation). The animal experiments were carried out in the lab of Prof. Dr. med. Konstantin Mayer, Center for Internal Medicine, Justus-Liebig-University Giessen. In the scope of the 3R principle (Russell and Burch 1960), the brains

were collected from these mice at the end of the experiment in the framework of the FCMH initiative “Lung-brain axis in health and disease”. In addition to ongoing investigation of lung inflammation by the group of Prof. Mayer, Prof. Sommer, and Prof. Hecker, I assessed the role of RvE1 on lung-brain communication.

2.6.2 Mice

C57BL/6N wild-type (WT-Norm) and the Fat mice (Fat-Norm) were crossed with KO mice resulting in: WT-CR KO, WT-LR KO, Fat-CR KO, and Fat-LR KO and used for all experiments. WT mice were obtained through in-house breeding with original breeding pairs obtained from Charles River Laboratories (Sulzfeld, Germany); Fat knock-in line were originally provided by Prof. Kang, Boston, Massachusetts, USA; CR KO line were originally provided by Prof. M. Barns, Takeda Cambridge, UK; and LR KO lines were originally purchased from Jackson Laboratory (Bar Harbor, ME, USA). Crossbreeding of WT and Fat mice with both lines of KO mice were performed in the lab of Prof. Dr. med. Konstantin Mayer. All experiments were performed in accordance with the German animal protection law and the local Ethics committee “Regional Council Giessen” (ethics approval numbers GI 20/10 Nr. G 46/2017).

2.6.3 Stimulation with LPS

Table 48: Stimulant for ARDS

Description	Manufacturer
Lipopolysaccharide E. coli 0111:B4	Sigma-Aldrich Chemie GmbH, Munich, Germany

In order to mimic ARDS, a model of LPS-induced (LPS: Escherichia coli serotype O111:B4) localized organ-specific lung inflammation was used. Mice were anesthetized using an antagonizable IP injection anesthesia. The volume was calculated based on a dosage of 0.25 mg/kg body weight medetomidine using a solution composed of: 75 µl medetomidine and 1.125 ml of physiological saline. The depth of anesthesia was tested by checking the tail reflex at the base and flexor reflex. When both reflexes were absent, the mouse was prepped by applying artificial tears to the eyes and receiving orotracheal intubation with a 22 G indwelling venous catheter. Afterwards, mice received i.t.

instillation of 10 μg LPS diluted to the correct concentration in 50 μl sterile NaCl 0.9 % administered in three portions (10 μl, 20 μl, 20 μl).

After LPS was administered, the anesthesia antagonist was given subcutaneously. The volume was calculated based on a dosage of 0.25 mg/kg body weight atipamezole using a solution composed of: 15 μl atipamezole and 1.185 ml of physiological saline. Once fully awake, the mouse received the analgesic tramadol using a solution composed of: 2.5 mg tramadol dissolved in 100 ml drinking water. The mouse received 1 drop orally via syringe followed by tramadol enriched drinking water for 24 h. The same batch of LPS was used for all experiments and was stored in aliquots at -20°C.

Table 49: Pharmaceuticals for i.t. instillation

Brand Name	Active Ingredient	Dosage	Manufacturer
Bepanthen eye and nose salve (5g)			Roche, Eppstein-Bremthal, Germany
		antagonizable anesthesia	
Domitor® (1 mg/ml)	Medetomidin	0.25 mg/kg body weight, IP	Vetoquinol GmbH, Ismaning, Germany
		anesthesia antagonist	
Antisedan® (5 mg/ml)	Atipamezol	0.25 mg/kg body weight, s.c.	Zoetis, Berlin, Germany
		analgesic	
Tramal®	Tramadol		Grunenthal Pharma AG, Aachen, Germany

2.6.4 Euthanasia and tissue collection

After 0 h, 4 h, 24 h, 72 h, or 120 h p.i. with LPS the experimental mice were euthanized. This was done by putting the mice under deep anesthesia with an IP inoculation of 16 mg/kg body weight xylazine hydrochloride and 100 mg/kg body weight ketamine hydrochloride. Once it was verified by flexor response that the mice were under deep anesthesia, the mice were euthanized by blood withdrawal. The abdomen was opened and blood was removed from the caudal vena cava.

Once the mouse was deceased, the head was detached and the brain removed. The cerebrum, cerebellum, and pituitary gland were identified and isolated. Tissues collected from the body cavity included the lung, spleen, and liver (left lateral lobe). Immediately

after collection, the brain and tissues were “snap frozen” using powdered dry ice and double wrapped in Parafilm and aluminum foil for protection and insulation. The samples were brought back to our laboratory and stored at -80°C.

Table 50: Pharmaceuticals for euthanasia

Brand Name	Active Ingredient	Dosage	Manufacturer
Ketamin® 10 %	Ketamine hydrochloride	100 mg/kg body weight, IP	Medistar Arzneimittelvertrieb GmbH, Ascheberg, Germany
Xylazine 2 %	Xylazine hydrochloride	16 mg/kg body weight, IP	CEVA Tiergesundheit GmbH, Düsseldorf, Germany

2.6.5 Magnetic luminex assay: lung and liver

Table 51: Materials for tissue homogenization

Description	Type	Manufacturer
cOmplete™ mini proteasehemmer-cocktail	04693124001	Bertin Technologies SAS, Berlin, Germany
Tissue homogenizer	Precellys 24	Bertin Technologies SAS, Berlin, Germany
Zirconium oxide beads	1.4 mm	Bertin Technologies SAS, Berlin, Germany

Table 52: Materials for luminex® assay

Description	Manufacturer
Bio-Plex 200	BioRad, Munich, Germany
Luminex® assay-Mouse premixed multi-analyte kit	R & D Systems Biotech Co., Minneapolis, MN, USA

To produce a comprehensive profile of cytokine levels in the tissue of the lung and liver, a luminex assay was, again, utilized (see section 2.4.10.1). The cytokines measured in both tissue homogenates included CCL5, CXCL1, CXCL5, IL-1β, IL-17, IL-10, and IL-6 while granulocyte-macrophage colony-stimulating factor (GM-CSF) and TNFα were only measured in the lung. Together, these immune mediators are markers for inflammation, both initiate and modulate the sickness response, and contribute to NG recruitment and activation (Donnelly et al. 1996, Matute-Bello et al. 2000, Ye et al. 2001, Jeyaseelan et al. 2004, Ballinger et al. 2006, Law et al. 2007, Sawant et al. 2015, Sahu et al. 2018). Through this analysis it was possible to compare differences in inflammation between groups for the affected lung tissue as well as changes in the systemic inflammatory

response using the livers as a proxy after i.t. LPS-stimulation (Crispe 2009). The tissue homogenates were diluted 1:2 and the luminex assay was carried out according to manufacturer's instructions in the lab of Prof. Dr. Natascha Sommer, department of pneumology, infectiology, gastroenterology, nephrology, and internal intensive care medicine, Institute of Internal Medicine, Justus-Liebig-University Giessen.

2.6.6 Reverse transcription real-time polymerase chain reaction

Table 53: Primers list for LPS-induced ARDS

Gene	Assay ID	Manufacturer
BDNF	Mm04230607_s1	Thermo Fisher Scientific Inc., Waltham, MA, USA
Cat	Mm00437992_m1	Thermo Fisher Scientific Inc., Waltham, MA, USA
CXCL1	Mm04207460_m1	Thermo Fisher Scientific Inc., Waltham, MA, USA
ELANE	Mm00469310_m1	Thermo Fisher Scientific Inc., Waltham, MA, USA
GAPDH	4352339E-1009032	Applied Biosystems, Waltham, MA, USA
GFAP	Mm01253033_m1	Thermo Fisher Scientific Inc., Waltham, MA, USA
IL-1β	Mm00434228_m1	Thermo Fisher Scientific Inc., Waltham, MA, USA
IL-1ra	Mm00446186_m1	Thermo Fisher Scientific Inc., Waltham, MA, USA
IL-10	Mm00439614_m1	Thermo Fisher Scientific Inc., Waltham, MA, USA
mPGES	Mm00452105_m1	Thermo Fisher Scientific Inc., Waltham, MA, USA
NF-IL6	Mm00843434_s1	Thermo Fisher Scientific Inc., Waltham, MA, USA
NfκBiα	Mm00477798_m1	Thermo Fisher Scientific Inc., Waltham, MA, USA
NOS2	Mm00440502_m1	Thermo Fisher Scientific Inc., Waltham, MA, USA
PGC-1α	Mm01208835_m1	Thermo Fisher Scientific Inc., Waltham, MA, USA
SOD1	Mm01344232_g1	Thermo Fisher Scientific Inc., Waltham, MA, USA
SOD2	Mm01313000_m1	Thermo Fisher Scientific Inc., Waltham, MA, USA
TFAM	Mm00447485_m1	Thermo Fisher Scientific Inc., Waltham, MA, USA

The RT-qPCR technique described in section 2.4.11 was repeated with the mice that received LPS-induced ARDS and all primers used are listed above. Genes were selected according to the following criteria: those related to oxidative stress, mitochondrial biogenesis, NG activation and recruitment, pro- and anti-inflammatory cytokines, signaling pathways, PG synthesis, neuronal and astrocyte activation. The goal being to evaluate NG trafficking, the brains inflammatory responses, as well as the extent glial cells were activated during ARDS in the hypothalamus.

2.6.7 Inflammation and neutrophil granulocyte trafficking to the brain during ARDS

The immunofluorescent technique described in section 2.4.9 was also applied to analyze the nuclear translocation of the inflammatory transcription factor NF-IL6 and NG infiltration to the brain. Evaluations were performed at two different sites, the OVLT and bifurcation separating the left and right hemisphere (BIF), which are exemplarily taken representative for the overall reaction of the hypothalamus and cortex respectively i.e., brain structures with intact or leaky BBB. A schematic of the brain structures is given in Figure 9.

Once again, MPO was used to stain NGs and NF-IL6 nuclear translocation was assessed as a marker for genomic brain cell activation (Damm et al. 2011). Tissues were stained with MPO + NF-IL6, NF-IL6 + vWF, or MPO + ICAM-1 as well as DAPI. The previously mentioned staining protocol was used here with minor modifications as shown in Table 55.

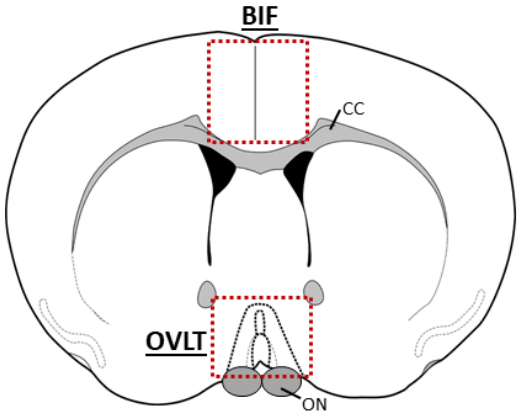

Figure 9: Schematic representation of the *organum vasculosum of the laminae terminalis* (OVLT) and the bifurcation (BIF)

The optical nerve (ON) was used as a structural marker for the OVLT while the corpus callosum (CC) was used for the BIF. The red outlines show the approximate field of view analyzed.

Table 54: Antibodies for inflammatory markers in the brain

Antigen	Specification	Dilution	Product Information	Manufacturer
primary antibodies				
ICAM-1	Polyclonal IgG, goat	1:500	sc-1511	Santa Cruz Biotechnology, Santa Cruz, CA, USA
MPO	Polyclonal IgG, rabbit	1:600	A0398	Dako Denmark A/S, Glostrup, Denmark
MPO	Polyclonal IgG, goat	1:200	AF3667	R & D Systems Biotech Co., Minneapolis, MN, USA
NF-IL6	Polyclonal IgG, rabbit	1:5000 / 1:1000	sc-150	Santa Cruz Biotechnology, Santa Cruz, CA, USA
vWF	Polyclonal IgG, sheep	1:3000	SARTW-IG	Affinity Biologicals, Ancaster, Canada
secondary antibodies				
Alexa 488, donkey	Anti-sheep	1:500	A11015	Life Technologies, Carlsbad, CA, USA
Cy3, donkey	Anti-rabbit	1:600	711-165-152	Jackson Immuno Research Europe Ltd., Newmarket, UK

Table 55: Staining protocols for neutrophil granulocytes and NF-IL6

Staining Combination	Step	Procedure	Temperature	Time
MPO + ICAM-1	Thaw slides	in cryostat	-20°C	30 min
	Warm slides	skip this step		
	EtOH Fixation	100 % EtOH, in staining jar in cryostat	-20°C	15 min
	Drying	dry with hairdryer	RT	5 sec
	Wash	PBS	RT	3 x 5 min
	PFA Fixation	2 % PFA, in staining jar on shaker plate	RT	10 min
	Blocking	add blocking buffer (0.01 % Triton X), wrap incubation box with plastic wrap	RT	1 h
	Primary antibody	add MPO (rabbit) and ICAM-1 in blocking buffer wrap incubation box with plastic wrap	4°C	overnight
	from this point the steps adhere to the original protocol			
NF-IL6 + vWF	Blocking	add blocking buffer (0.01 % Triton X), wrap incubation box with plastic wrap	RT	1 h
	Primary antibody	add NF-IL6 and vWF in blocking buffer wrap incubation box with plastic wrap	4°C	overnight
	all other steps adhere to the original protocol			
MPO + NF-IL6	Blocking	add blocking buffer (0.01 % Triton X), wrap incubation box with plastic wrap	RT	1 h
	Primary antibody	Add MPO (goat) and NF-IL6 in blocking buffer wrap incubation box with plastic wrap	4°C	overnight
	all other steps adhere to the original protocol			

2.7 Statistics and analysis

2.7.1 Experimental design

To appropriately test for the effects of both neutropenia and LPS on the generation of the sickness response, mice were divided into four experimental groups that received PMN or NRS and LPS or PBS (NRS+PBS, PMN+PBS, NRS+LPS, and PMN+LPS). The mice were sacrificed and analyses were performed at 4 h and 24 h p.i. with LPS. The 4 h time-point was selected based on analyses of the 24 h core body temperature response for the first set of experiments. The time-point 4 h shows the beginning of a temperature drop after LPS-stimulation in the NRS and PMN groups. This second set of experiments was used to investigate if changes could already be detected due to NG depletion within LPS-stimulated treatment groups before the temperature separation began to occur.

Mice that received LPS-induced ARDS were divided into six groups that were unmodified (Norm) and CR or LR KO on a WT or Fat background (WT-Norm, Fat-Norm, WT-CR KO, Fat-CR KO, WT-LR KO, or Fat-LR KO). The mice were sacrificed and analyses were performed at five time-points: 0 h, 4 h, 24 h, 72 h, and 120 h p.i. to assess the influence of ω-3 PUFAs and the two RvE1 receptors over the course of ARDS. WT and Fat groups were compared to each other within each group: Norm, CR KO, and LR KO. Additionally, the WT and Fat mice from CR KO and LR KO groups were compared to the respective Norm group but not to each other for each time point.

2.7.2 Evaluation of hematological measurements

This method was only used with the preliminary mice that were sacrificed 24 h p.i. with LPS to identify an efficient dose of PMN: The number of NGs were normalized to the total leukocyte count for each animal and the percentage was determined. The percentages of NGs were compared between groups pretreated with NRS or PMN by unpaired t test. Outlier analyses were performed using the ROUT method (Motulsky and Brown 2006) but no exclusions were necessary. All statistical analyses were performed using the GraphPad Prism 5 software.

2.7.3 Evaluation of core body temperature, activity, & food and water intake

The telemetric and food and water intake systems provided continuous recordings of the core body temperature and activity over the course of the experiment. Animals with core body temperatures inconsistent with what had been previously observed within their treatment groups (i.e., LPS treated mice that did not develop hypothermia) were excluded from all analysis following confirmation by luminex assays that the inflammatory cytokine profile was also absent indicating a failure of LPS-injection. In accordance with these standards, 4 mice were excluded: 2 PMN+LPS (24 h), 1 NRS+LPS (24 h), and 1 PMN+LPS (4 h). Discrepancies in numbers presented for temperature and activity graphs and food and water intake are explained by technical difficulties with the system when it failed to record. The recordings were separated into three 24 h time blocks: 1) baseline, 2) p.i. PMN/NRS, and 3) p.i. LPS/PBS; recordings started two hours prior to the injections, were extracted in 15 min intervals, and plotted as curves. In the case of the 4 h time-point these mice were graphed in combination with those from the 24 h time-point up till 4 h p.i. with LPS.

To analyze, time blocks 1 and 2 were divided into 12 sections beginning at -48 h and -23 h p.i. with LPS respectively and covering a span of two hours, i.e., consisting of eight measurements per sections. An exception was made for the final sections, which only included five measurements. Time block 3 was separated into two units where the first included the mice from both the 4 h and 24 h time-point (1-4 h p.i.) and the second was only those mice from the 24 h time-point (4-24 h p.i.). The first unit was divided into three one-hour sections, each consisting of four measurements except the third, which had five measurements. The second unit was divided into 10 sections, each consisting of eight measurements except for the tenth, which contained nine. Each interval was then analyzed using a two-factorial analysis of variance (ANOVA) with repeated measures over time. The factors were defined as condition (i.e., PMN induced neutropenia) and treatment (i.e., treatment with LPS). A Holm-Bonferroni post-hoc was performed to correct for multiple testing and evaluate main effects and interactions; p-values were listed from smallest to largest and compared to corresponding adjusted p-value (adjusted p-value= (raw p-value) / (number of tests+1) - rank number.). All statistical analyses were performed using the IBM SPSS Statistics 26 or 29 software.

2.7.4 Evaluation of body weights

Body weights were recorded daily and were used to measure the impact of PMN and LPS. Weights were collected and graphed at three time points: 24 h after inoculation with NRS or PMN (0 h p.i.), 4 h p.i. with LPS, and 24 h p.i. with LPS. To calculate the percentage of body weight change the weights were compared to a baseline weight collected 24 h prior to their first injection of NRS or PMN. Mice used for the 4 h and 24 h time points were grouped together to analyze differences in body weights after NRS or PMN injections. For the 4 h and 24 h recordings the mice were grouped together based on those sacrificed at 4 h or 24 h p.i. At 0 h p.i. the weights were divided into two groups that received either NRS or PMN and were compared by a Mann-Whitney test. For the body weights collected at 4 h and 24 h p.i., the body weights were divided into treatment groups and compared by two-way ANOVA with the factors condition (i.e. PMN induced neutropenia) and treatment (i.e. treatment LPS) and a Tukey post-hoc test. Outlier analyses were performed using the ROUT method (Motulsky and Brown 2006) but no exclusions were necessary. All statistical analyses were performed using the GraphPad Prism 7 software.

2.7.5 Evaluation of blood smears and total leukocyte populations

To quantify the percentage of different leukocyte populations in the blood smears 100 leukocytes were counted and it was noted how many lymphocytes, monocytes, eosinophils, basophils, and NGs there were. In some instances, it was not possible to count 100 leukocytes and the percentage was based on the leukocytes that could be counted but when less than 50 leukocytes were present, these mice were excluded. Based on the exclusion criteria, three mice were removed from the 24 h time point (1 each from the groups PMN+LPS, PMN+PBS, and NRS+PBS). Total leukocyte populations were reported as cells/μl. Twice counting was not possible due to low cell numbers for an unknown reason so at the 4 h time point the groups NRS+LPS and PMN+LPS both had one mouse excluded. Each time-point was analyzed separately. The percentages of cells in each group were compared by two-way ANOVA with the factors condition (i.e. PMN induced neutropenia) and treatment (i.e. treatment LPS) and a Tukey post-hoc test. Outlier analyses were performed for both tests using the ROUT

method (Motulsky and Brown 2006) but no exclusions were necessary. All statistical analyses were performed using the GraphPad Prism 7 software.

2.7.6 Evaluation of immunofluorescence

In all instances where immunofluorescence was used, brain sections were exposed to the optimal wave length of light and an image was collected. For each experiment, either quantitative or semi-quantitative measurements of fluorescent signals were assessed. When a semi-quantitative evaluation was used, the level of nuclear signals present were scored for each section on a scale from 0-4: 0 = none, 1 = single or very few, 2 = low density, 3 = moderate density, 4 = high density; ¼ scores were assigned when slightly more or less than average signals were present but not enough to move up or down an entire level i.e. 1.25 or 1.75 where a score of 1.25 has slightly more signal than 1 and 1.75 has slightly less signal than 2. All evaluations were carried out with Adobe Photoshop (version 6) unless otherwise stated. Statistical analyses were performed only if at least n = 3 per group were assessed using the GraphPad Prism 7 software unless otherwise stated. Outlier analyses were performed using the ROUT method (Motulsky and Brown 2006) and all exclusions specified.

2.7.6.1 Evaluation of neutrophil granulocyte infiltration into the brain during LPS-induced severe systemic inflammation

When determining the effect of different doses of PMN on NG recruitment into the brain during preliminary experiments, 10x magnification images were taken of the OVLT, SFO, Plexus, and PVN; the structures were clearly identified and the level of MPO expression was evaluated based on the semi-quantitative scale (0-4), covered previously in section 2.7.5, within each structure. For each structure, 1-12 sections per animal with between 1-3 animals per group were analyzed. In some instances, fewer than 3 mice or 3 sections were only collected per brain structure due to damage to the brain, or insufficient number of slides and only one section was collected for the structure. These results are specified in Supplementary Table 1 and referenced in the figure legend to highlight this limitation. Additionally, as multiple brain sections were present per slide, occasionally > 5 sections per animal were analyzed. Since 3 animals or more could not be collected for all brain structures, descriptive data are presented as

means (per animal) of the means (per group). The overall effect of PMN treatment on NG recruitment to the brain was assessed by pooling the means (per animal) of the PMN or NRS pretreated groups regardless of brain structure. The semi-quantitative scores were compared by t-test.

After preliminary experiments, the recruitment of NGs into different brain structures at 4 h and 24 h p.i. was also assessed. Focusing on the SFO and PVN 40x or 20x images were taken of the structures, respectively, and the number of NGs were counted manually. For each structure, 1-4 sections per animal with between 4-8 animals per group were analyzed. Results are presented as means (per animals) of the means (per group). Analyses of NGs were compared by two-way ANOVA with the factors condition (i.e. PMN induced neutropenia) and treatment (i.e. treatment with LPS) followed by a Tukey post-hoc test. The following values were excluded based on the outlier analysis: SFO 24 h (1 PMN+PBS, 1 PMN+LPS) and PVN 24 h (1 PMN+PBS).

2.7.6.2 Evaluation of NET formation in the brain

NET formation in the brain was evaluated at the level of the MnPO, 40x images were taken of the upper cap of the MnPO structure and the raw integrated density (Raw IntDen) of each color channel were measured for the entire image using Fiji software (Win-64) 1-2 sections per animal with between 4-5 animals per group were analyzed. Results are presented as means (per animals) of the means (per group). The ratio of DNA/His and H3Cit in relation to DAPI were calculated and compared by two-way ANOVA with the factors condition (i.e. PMN induced neutropenia) and treatment (i.e. treatment with LPS) and a Tukey post-hoc test.

2.7.6.3 Evaluation of NET formation in vitro

When looking at NETs *in vitro* pictures were taken at 20x magnification in five locations in each well: the center, upper left, upper right, lower left, and lower right corner of each well. Using Fiji software (Win-64) the total numbers of cells were counted in each image while NETs were counted manually. Criteria to categorize a NG as having undergone NETosis included one or more of the following: an enlarged or irregular nucleus, loss of shape, processes extending from the cell including DNA/His, MPO, and/or nuclear DAPI. The percentage of NETs per image were calculated and the average was taken for the

five images per well. Five independent experiments with 2-4 wells per treatment group were analyzed. The mean of each well of the mean of each treatment of the mean of all five experiments were compared by one-way ANOVA and a Newman-Keuls post-hoc test. All statistical analyses were performed using the GraphPad Prism 5 software.

2.7.6.4 Evaluation of inflammation and neutrophil granulocyte trafficking to the brain during ARDS

The assessment of MPO and NF-IL6 was performed at the level of the BIF and OVLT but at different magnifications; quantitative assessment of MPO was performed at 10x magnification while the semi-quantitative assessment of NF-IL6 was done at a 20x magnification. To start with, a 10x image was taken of the BIF that included the upper portion of the cortex, equally dived between the left and right hemisphere, extending downward until the corpus callosum. From here, MPO was counted within the field of view for each brain (1-13 sections per animal with between 2-6 animals per group in the BIF were analyzed). 10x images of the OVLT were taken to include the lower half of the cortex extending downward until the ocular nerve. Once again, MPO was counted within the field of view for each brain. 1-10 sections per animal with between 2-5 animals per group in the OVLT were analyzed. When less than 3 animals per group were available, no statistical analyses was performed but descriptive data is presented.

For the assessment of NF-IL6, it was necessary to use a higher magnification, 20x, but the procedure for taking the image was the same for both structures as with the 10x magnification. Now, the fluorescent expression of NF-IL6 was evaluated using a semi-quantitative assessment, stated previously in section 2.7.5, for each structure. 1-8 sections per animal with between 1-5 animals per group in the both structures were analyzed.

Overall, the goal was to collect 3 sections per animals with 3 animals per group, but for WT-Norm at 4 h and Fat-CR KO at 120 h only 2 mice were available. In a few instances, due to damage to the brain or insufficient number of slides, only one section or animal could be collected for a structure and these results are highlighted in the figure legends to reflect this limitation. Since multiple brain slices were present per slide, occasionally mice have >5 sections per animal. Tables detailing the number of mice and sections per

group are presented in Supplementary Tables 2-7. Both evaluations were compared by two-way ANOVA with the factors condition (i.e. Norm, CR KO, or LR KO) and treatment (i.e. ω-3 PUFA (Fat) enrichment) and a Tukey post-hoc test. When less than 3 animals per group were available, no statistical analyses was performed but descriptive data is presented.

2.7.7 Evaluation of bio- and immunoassays

2.7.7.1 Evaluation of magnetic luminex assays

The concentrations of cytokines for neutropenic and ARDS experiments were determined according to manufacturer's instructions for the assay using the standards. For the neutropenic experiments, the cytokine or corticosterone concentrations were shown in either ng/ml or pg/ml. Each cytokine was analyzed by two-way ANOVA with the factors condition (i.e. PMN induced neutropenia) and treatment (i.e. treatment with LPS) and a Tukey post-hoc test. Outlier analyses were performed using the ROUT method (Motulsky and Brown 2006) and the following values were excluded. From the cytokine values in the serum at 4 h: **CCL5** (1 NRS+PBS), **IL-10** (1 NRS+PBS, 1 PMN+PBS, 1 NRS+LPS), **IL-6** (1 PMN+PBS), **TNFα** (1 NRS+PBS, 2 PMN+PBS) and 24 h: **CCL5** (2 NRS+PBS), **CXCL1** (1 NRS+LPS), **CXCL2** (1 PMN+PBS), **IL-10** (3 NRS+PBS, 2 PMN+PBS), **IL-6** (4 NRS+PBS, 4 PMN+PBS, 3 NRS+LPS, 1 PMN+LPS). From the corticosterone values in the serum at 24 h: 1 PMN+PBS was excluded. All statistical analyses were performed using the GraphPad Prism 7 software.

For ARDS experiments, the cytokine concentrations were presented as the fold change of values normalized to WT-Norm 0 h controls. Parameters measured from the tissue homogenates (lung and liver) were normalized to the protein amount of each sample before the fold change was normalized to WT-Norm 0 h. If a cytokine was not detectable or showed a smaller quantity than the detectable range, these sample values were set to 0. Each cytokine was analyzed by two-way ANOVA with the factors condition (i.e. Norm, CR KO, or LR KO) and treatment (i.e. ω-3 PUFA (Fat) enrichment) and a Tukey post-hoc test. Outlier analyses were performed using the ROUT method (Motulsky and Brown 2006) and the following values were excluded in the liver: **IL10** at 24 h: 1 WT-CR KO /

CXCL1 at 24 h: 1 WT-Norm, 1 Fat-CR KO; 72 h: 1 WT-Norm / **IL-17** at 24 h: 1 WT-CR KO). All statistical analyses were performed using the GraphPad Prism 7 software.

2.7.7.2 Evaluation of bioassays

The analyses of cytokines in the supernatant of *in vitro* bone marrow derived NG cultures were calculated by comparing the samples effect on the established cell line to that of the known standards. Due to variations between samples and to control for differences between cultures that were treated at different times, the cytokine concentrations were presented as a percentage change. To control for high variations in analytes between experiments, samples were compared to the LPS 20 μg/ml control, which was assigned 100%. Five independent experiments with 2-4 wells per treatment group were analyzed and the mean of each well of the mean of each treatment of the mean of all five experiments were analyzed and compared by one-way ANOVA and a Newman-Keuls post-hoc test. Outlier analyses were performed using the ROUT method (Motulsky and Brown 2006) but no exclusions were necessary. All statistical analyses were performed using the GraphPad Prism 7 software.

2.7.8 Evaluation of RT-qPCR data

The RQ values were used to compare target genes from the RT-qPCR analysis. To start with, RQ values were normalized to the lowest expression in the control group (NRS+PBS 4 h, NRS+PBS 24 h, or 0 h WT-Norm) for each target gene and assigned a value of 1. All other values were shown as a multiple of the expression (Yuan et al. 2006). For ARDS experiments, the values were presented as the fold change of RQ values normalized to WT-Norm 0 h controls. RT-qPCR for target genes were analyzed for all groups in the experiment on one day to limit variation. Analyses were performed using a two-way ANOVA with the factors condition (i.e., PMN induced neutropenia) and treatment (i.e., treatment with LPS) for neutropenic experiments. ARDS experiments used the factors condition (i.e., Norm, CR KO, or LR KO) and treatment (i.e., ω-3 PUFA (Fat) enrichment). A Tukey post-hoc test was used for both neutropenic and ARDS experiments. Outlier analyses were performed using the ROUT method (Motulsky and Brown 2006). All statistical analyses were performed using the GraphPad Prism (Version 7; GraphPad Software, San Diego, CA, USA).

Following outlier analyses the following exclusions were made for the neutropenic experiments at 4 h: **CD68** (1 NRS+PBS, 1 NRS+LPS), **NF-IL6** (1 NRS+PBS), **SOCS3** (1 NRS+PBS) and 24 h: **CD68** (1 PMN+PBS, 1 PMN+LPS), **COX2** (1 NRS+PBS), **CXCL1** (2 NRS+PBS, 1 PMN+LPS), **Elane** (1 NRS+PBS, 1 PMN+PBS), **IL-6** (2 NRS+PBS), **IL-10** (1 NRS+PBS), **mPGES** (1 NRS+PBS), **NF-IL6** (1 PMN+PBS), **NFκBiα** (1 NRS+PBS), **SOCS3** (2 NRS+PBS), **TNFα** (2 NRS+PBS). For samples where a value could not be determined, they were removed from the data set (4 h: **CXCL1**- 2 NRS+PBS / **IL-6**- 1 NRS+PBS / **IL-10**- 2 NRS+PBS, 2 PMN+PBS and 24 h: **IL-6**- 1 NRS+LPS / **IL-10**- 2 NRS+PBS, 2 PMN+PBS, 3 NRS+LPS).

The following outlier exclusions were made for the ARDS experiments: **SOD1** at 72 h: 1 WT-Norm / **Elane** at 0 h: 1 Fat-Norm; 24 h: 1 Fat-CR KO, 1 Fat-LR KO; 72 h 1 Fat-CR KO / **IL-10** at 24 h: 1 Fat-CR KO / **IL-1β** at 0 h: 1 WT-Norm / **IL-1ra** at 0 h: 1 WT-Norm, 1 WT-CR KO / **NF-IL6** at 0 h: 1 Fat-Norm / **mPGES** at 72 h: 1 Fat-Norm. For samples where a value could not be determined they were removed from the data set (**Elane** at 0 h: 1 WT-Norm, 2 Fat-LR KO; 24 h: 1 Fat-Norm; 72 h: 1 WT-Norm/ **IL-10** at 0 h: 3 WT-Norm, 3 Fat-Norm, 1 WT-CR KO, 2 Fat-CR KO, 1 Fat-LR KO; 24 h: 4 WT-Norm, 1 Fat-Norm, 1 WT-CR KO, 2 WT-LR KO, 1 Fat-LR KO; 72 h: 1 WT-Norm, 1 Fat-Norm, 2 WT-CR KO, 1 Fat-CR KO, 2 WT-LR KO, 1 Fat-LR KO).

2.7.9 Evaluation of flow cytometry data

To start with, cells were gated on size and complexity using SSC vs. FSC. Those cells that were larger and more complex were gated and preceded to the next step. From here, double positive expression of CD11b, leukocyte receptor, and Ly6G, NG cell surface protein were used to identify NGs. The gating strategies to determine expression level for CD11b and Ly6G were based on single stained cells, stained with either CD11b alone (FITC) or Ly6G alone (PE). Once the gates were set, a sample stained for both CD11b and Ly6G were analyzed and the percentage of $CD11b^{+}Ly6G^{+}$ cells calculated. The gating strategy was set using the described procedure (see section 2.5.2.1) with unstained and single stained samples for each. Unstained samples of the same cells were used to subtract basal background expression and samples were analyzed by acquiring at least 1000 events per sample.

III. Results

3.1 *In vivo* models of neutropenia during LPS-induced severe systemic inflammation

3.1.1 Characterization of anti-polymorphonuclear serums' ability to deplete neutrophil granulocytes

In order to study the impact of neutropenia during severe systemic inflammation, it was crucial to identify an effective dose of PMN that sufficiently depleted NGs. Using three different doses of PMN, i.e., 1, 2, or 5 ml/kg, the dose, which significantly reduced NGs in circulation and infiltration into the brain without causing lethality, was determined at 24 h p.i. with LPS. After a PMN dose was selected leukocyte levels continued to be recorded during experiments at 4 h and 24 h p.i. with LPS.

3.1.1.1 Neutrophil granulocytes in circulation

Following injections with LPS (24 h), increased levels of circulating NGs were observed in control mice that received NRS. In comparison, mice that were given IP injections with 1 ml/kg (p = 0.0204) or 2 ml/kg (p = 0.0003) PMN had reduced levels of circulating NGs by approximately 25% (Figure 10, A-B). Between these two groups, in preliminary experiments, mice given a dose of 1 ml/kg had a 100% survival rate while at 2 ml/kg it was only 75% (Figure 10, C). Levels of circulating NGs were not measured in mice that received 5 ml/kg because the dose was too severe and proved lethal (Figure 10, C). Therefore, 1 ml/kg was the only dose sufficient to induce neutropenia without causing lethality. The dose of antiserum was chosen according to previous studies (Aguilar-Valles et al. 2014). Thus, lethality was unexpected and amendments of the ethics approval were approved to reduce the dose and timing, and to adjust the animal protocol accordingly.

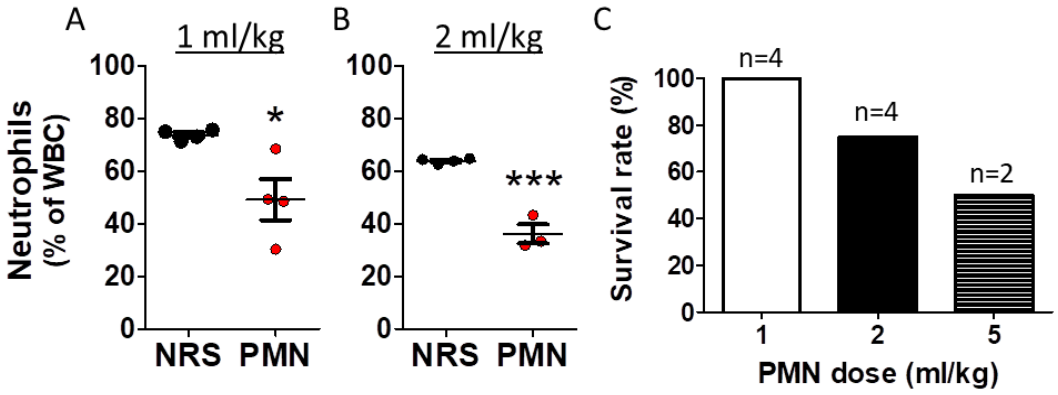

Figure 10: PMN dose of 1 ml/kg reduced NGs in circulation with the highest survivability rate after LPS-stimulation

Hematological measurements of neutrophil granulocytes (NG) in circulation following 1 or 2 ml/kg dose of anti-polymorphonuclear serum (PMN; A, B) and the survival rate of mice after 1, 2, or 5 ml/kg dose of PMN (C) i.e., deaths / per group were 0/4 (1 ml/kg), 1/4 (2 ml/kg), and 1/2 (5 ml/kg) . Mice received an intraperitoneal (IP) injection with normal rabbit serum (NRS) or PMN followed by an IP injection with lipopolysaccharide (LPS, 2.5 mg/kg) 24 h later and were sacrificed after 24 h. Both 1 and 2 ml/kg doses significantly reduced the levels of circulating NGs compared to NRS control mice but 1 ml/kg was the only dose that showed no lethality. n= 3-4 (A,B), 'n' for figure C are shown in the graph. *p<0.05, ***p<0.001.

3.1.1.2 Neutrophil granulocyte infiltration into the brain

Semi-quantitative evaluation of preliminary immunofluorescent staining of several brain structures showed recruitment of NGs 24 h p.i. with LPS in control mice that received NRS. Mice that were given IP injections with 1 ml/kg (p = 0.0129) or 2 ml/kg (p = 0.0061) PMN had, overall, reduced levels of NG recruitment into the brain (Figure 11, F, H). Since the 1 ml/kg dose was sufficient to inhibit NG recruitment into the brain, and reduce circulating NGs as seen previously, it was selected as the experimental dose. Although in some instances fewer than 3 mice could be evaluated for each brain structure, the staining served a preliminary purpose to evaluate NG recruitment to the brain when selecting the dose of PMN to be used.

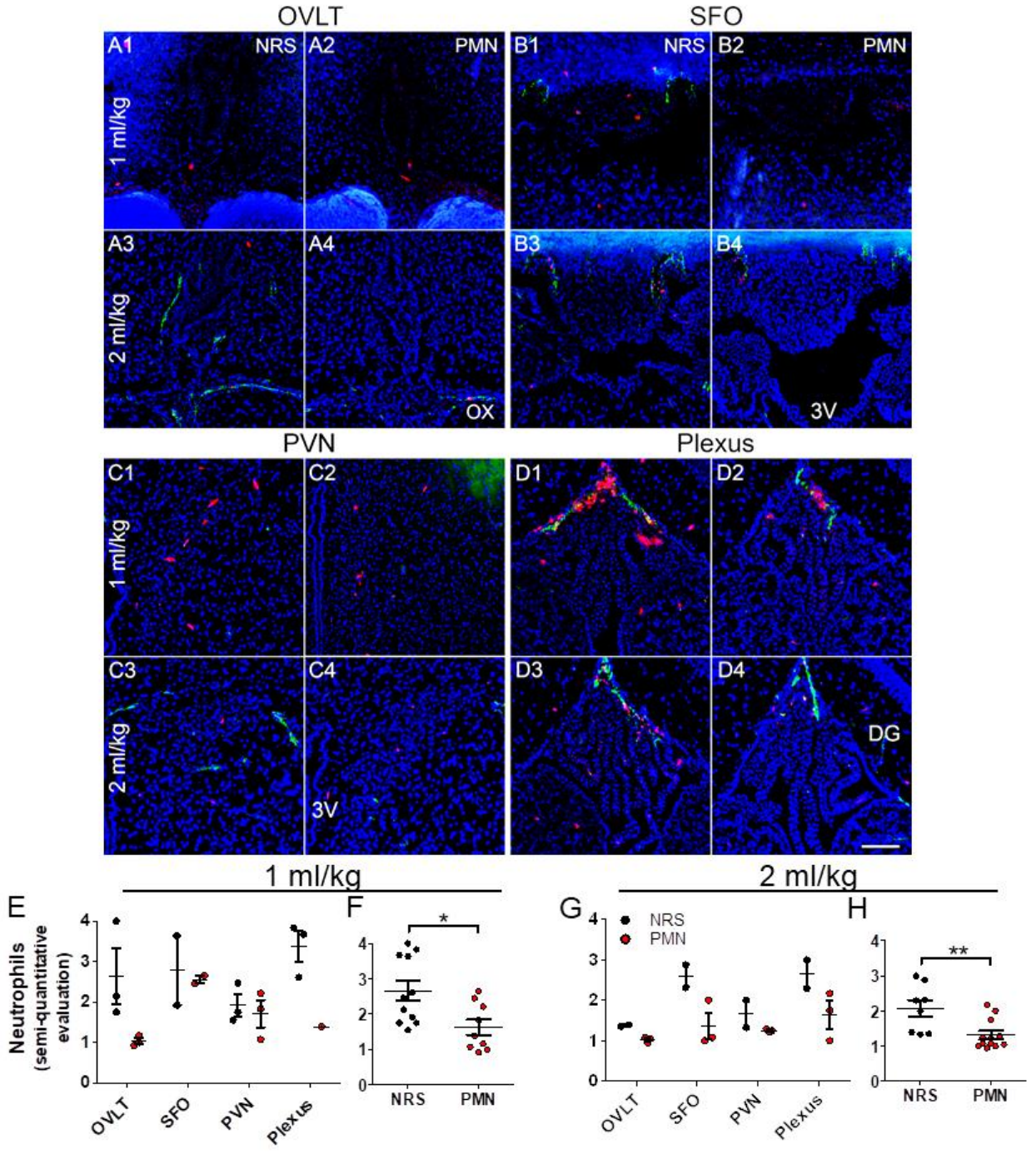

Figure 11: PMN dose of 1 ml/kg may reduce NG recruitment into several brain structures after LPS-stimulation

Sections of the brain were analyzed at the level of the *organum vasculosum of the laminae terminalis* (OVLT; A), subfornical organ (SFO; B), paraventricular nucleus (PVN; C), and choroid plexus (Plexus; D) for neutrophil granulocyte recruitment (NG; red) and were assessed by semi-quantitative evaluation (E-H). Mice received intraperitoneal (IP) anti-polymorphonuclear serum (PMN) or normal rabbit serum (NRS) at a dose of 1 ml/kg (1, 2) or 2 ml/kg (3, 4) followed by IP lipopolysaccharide (LPS, 2.5 mg/kg) 24 h later. At 24 h p.i. with LPS the mice were sacrificed and NG recruitment into the brain structures was compared

between mice that received PMN or NRS. Descriptive data for NG recruitment to the different brain structures are shown for 1 ml/kg (E) and 2 ml/kg (G). Overall effects of PMN regardless of structure are shown for 1 ml/kg (F) and 2 ml/kg (H). Pretreatment with PMN reduced overall NG recruitment compared to NRS control mice at both doses. Von Willebrand factor (green; C-F) depicts brain vasculature. DAPI (blue; C-F) visualizes the surrounding tissue. OX: optic nerve; 3V: third ventricle; DG: dentate gyrus. n= 1-3 per structure. n= 8-12 for NRS or PMN treatment overall. *p<0.05, **p<0.01. Scale bar in D4 = 100 μm and is representative for A-D.

3.1.1.3 Blood smears and leukocyte populations

Analysis of the total number of leukocytes in circulation (Figure 12) showed that PMN had a moderate impact on circulating levels. At 4 h and 24 h p.i. PMN pretreated mice had overall reduced levels of circulating leukocytes regardless of treatment with LPS (4 h p = 0.0013; 24 h p = 0.0123). After treatment with LPS circulating leukocytes were reduced at 4 h and 24 h p.i. regardless of pretreatment with NRS or PMN (4 h p = <0.0001; 24 h p = 0.0044). Overall, PMN may reduce total circulating leukocytes due to reduced levels of NGs.

Additionally, a main effect of PMN indicates reduced circulating NGs at 4 h and 24 h p.i. with minimal impact on other leukocyte populations (Figure 12). At 4 h p.i. LPS did not have a significant impact on NG populations but pretreatment with PMN did lower NG levels regardless of treatment with LPS (p = <0.0001). By 24 h p.i. an LPS effect was evident and increased the percentage of NGs regardless of pretreatment with NRS or PMN (p = <0.0001); additionally, PMN continued to cause an overall reduction in NGs (p = 0.0018). No effect of PMN was apparent on lymphocyte populations. Instead, LPS caused an overall reduction in the percentage of circulating lymphocytes at both 4 h p.i. (p = <0.0001) and 24 h p.i. (p = <0.0001) regardless of pretreatment with NRS or PMN. Finally, a moderate effect of PMN was present on monocytes. At 4 h p.i. LPS caused a significant increase in the percentage of monocytes (p = <0.0001) regardless of pretreatment with NRS or PMN. A PMN effect also signified increased circulating monocytes overall in mice regardless of treatment with LPS (p = 0.0037). By 24 h p.i., LPS still increased the percentages of circulating monocytes (p = 0.0005) and pretreatment with PMN maintained a modest effect that increased monocytes regardless of treatment with LPS (p = 0.0183). However, although the percentage of monocytes

may be higher in these PMN pretreated groups, the raw cell counts were actually lower compared to the NRS groups at 4 h (Figure 12, G-H) and 24 h p.i. (Figure 12, O-P) after treatment with LPS. Taken together, monocyte blood counts did not significantly change by PMN treatment. Eosinophil and basophil populations were also analyzed but were absent or present at extremely low numbers and, therefore, not addressed further (data not shown).

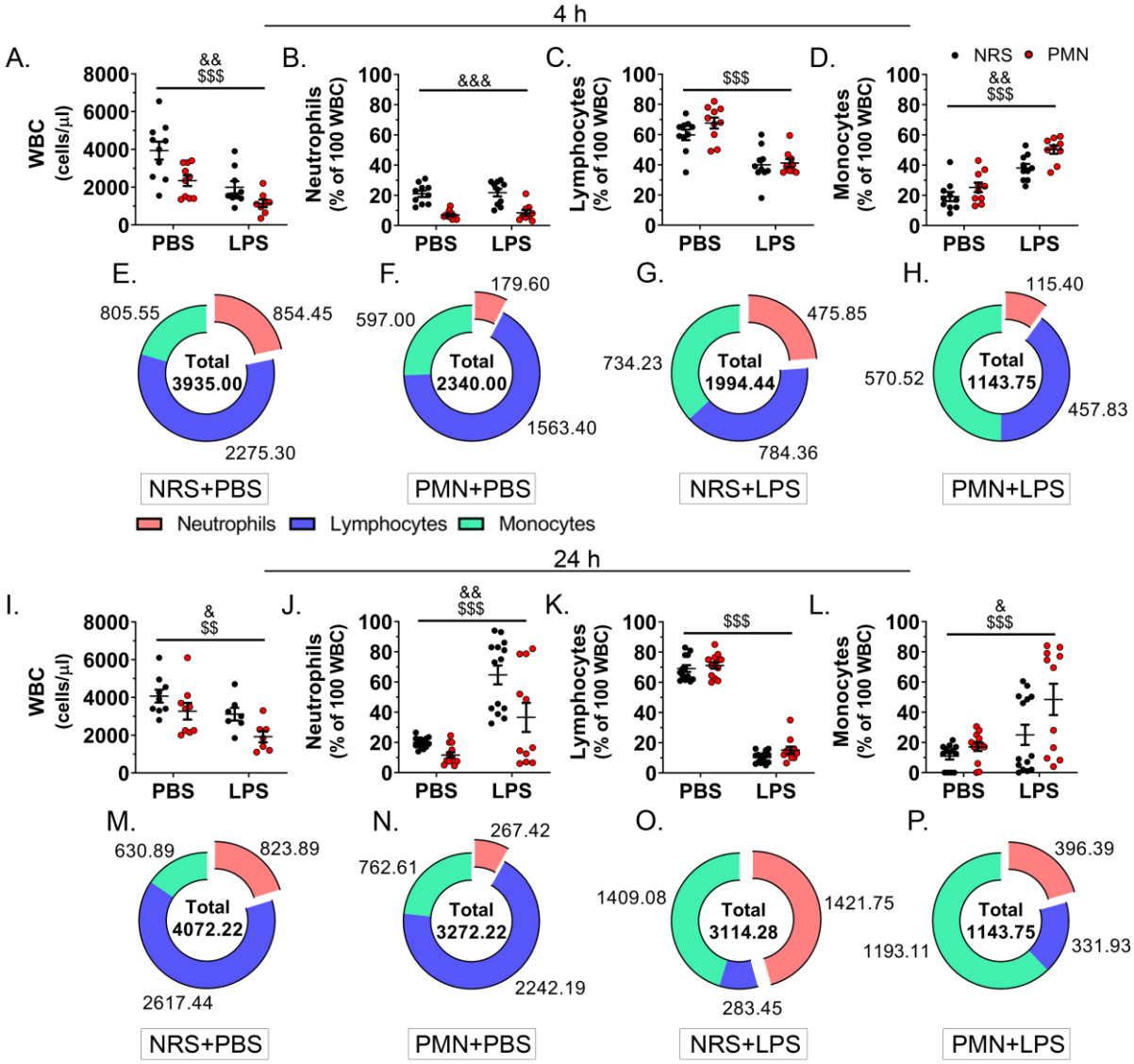

Figure 12: PMN decreases NG populations at 4 h and 24 h after LPS-stimulation

Blood smears were analyzed at different time points p.i. with lipopolysaccharide (LPS, 2.5 mg/kg) to compare populations of leukocytes (WBC) between mice treated with normal rabbit serum (NRS, 1 ml/kg) or anti-polymorphonuclear serum (PMN, 1 ml/kg). Total WBC counts (A, I) and populations of

neutrophil granulocytes (NG; B, J), lymphocytes (C, K), and monocytes (D, L) were compared between mice pretreated with NRS or PMN followed by phosphate buffered saline (PBS) or LPS after 4 h (A-D) or 24 h (I-L) p.i. Raw cell counts for total WBCs, NG (red), lymphocytes (blue), and monocytes (green) were shown for each treatment group at 4 h (E-H) and 24 h (M-P) p.i. Treatment with LPS increased circulating NGs at 24 h but not 4 h p.i. Regardless of the time point, PMN had an overall effect that indicated reduced NG levels. Lymphocytes were reduced by LPS at 4 h and 24 h p.i. with no effect of PMN. Monocytes were increased by LPS at 4 h and 24 h p.i. with an effect of PMN at each time point showing a moderate increase in circulating monocytes. Elevations in monocytes were not reflected in raw monocyte cell counts. n= 9-10 (4 h), 11-14 (24 h). & main effect of PMN; $ main effect of LPS. *p<0.05, **p<0.01, ***p<0.001.

3.1.2 Characterization of the role of neutrophil granulocytes on physiological parameters

The importance of NGs during severe systemic inflammation is not fully understood, therefore, to investigate the effects of neutropenia on the sickness response several different methods were employed. In addition to recording body weight and analyzing blood smears, it was possible to continuously monitor core body temperature, locomotor activity, and food and water intake over the course of the experiment using a telemetric system. In doing so, the generation and severity of the sickness response was assessed in detail.

3.1.2.1 Locomotor activity

The activity levels of the mice showed no differences between the baseline recordings of the groups that would be receiving either NRS or PMN (Figure 13 A). Following IP inoculation with PMN (p = 0.0314), there was a brief reduction in activity but otherwise no differences were observed between mice that received NRS or PMN (Figure 13 B). As expected, inoculation with LPS caused a significant difference in activity levels, which began approximately 1 h p.i. for mice that received NRS or PMN (Figure 13 C, Supplementary Table 8). After LPS, a fleeting impact of PMN occurred between 2-4 h p.i. but no other impact of PMN was observed. The impact of LPS was still present until approximately 22 h p.i. after which activity levels more resembled those of the mice that received PBS. From these data recordings, it is apparent that locomotor activity is altered by severe systemic inflammation as anticipated.

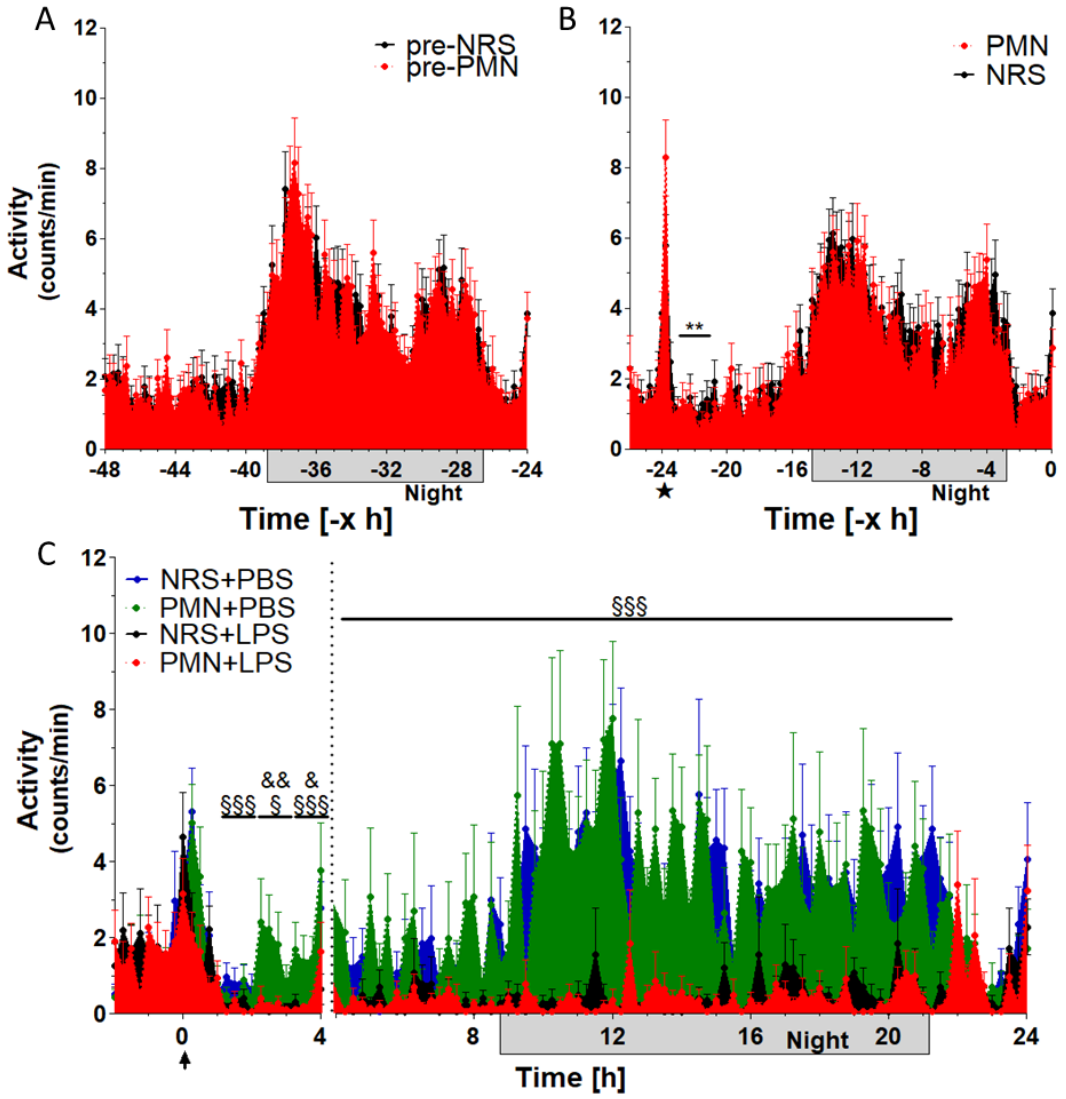

Figure 13: Locomotor activity levels are altered after LPS-stimulation

Telemetric recordings of activity were analyzed over the course of the experiment starting approximately 48 h prior to injection with lipopolysaccharide (LPS, 2.5 mg/kg) until mice were sacrificed at 4 h or 24 h p.i. with LPS. Baseline recordings showed no differences over 24 h between groups that would receive anti-polymorphonuclear serum (PMN, 1 ml/kg) or normal rabbit serum (NRS, 1 ml/kg; A). After intraperitoneal (IP) injection of PMN or NRS (1 ml/kg), indicated with ★, over the next 24 h the PMN mice had diminished activity immediately following the injection but this was short lasting and after which no other differences in activity were observed (B). 24 h after IP PMN or NRS mice received an IP injection of phosphate buffered saline (PBS) or LPS, indicated with ↑ (C). Immediately following the injection an impact of PMN was briefly observed while LPS caused a reduction in activity in both groups that lasted from 1-22 h p.i. The grey box indicates the night cycle. Prior to the dotted line indicates that the second cohort of animals (4 h time point) was included into the analyses of the locomotor activity; n= 47-48 (A-B), 23-24 (C; -2-4 h p.i.), 14 (C; 4-24 h p.i.). Image C: & main effect of PMN; § main effect of LPS. *p<0.05, **p<0.01, ***p<0.001.

3.1.2.2 Food and water intake

Both food (Figure 14) and water intake (Figure 15) were similarly affected by treatment with NRS or PMN and PBS or LPS. Baseline recordings showed no differences in food (Figure 14 A) or water (Figure 15 A) intake between groups that were receiving either NRS or PMN. Similarly, IP inoculation with PMN did not alter the consumption of food (Figure 14 B) or water (Figure 15 B) from the NRS controls. As seen with locomotor activity, IP inoculation with LPS caused a significant difference in both food (Figure 14 C) and water (Figure 15 C) intake (Supplementary Table 9), however, one difference was observed in the food intake that was not seen with water intake. From approximately 12-14 h p.i. food intake was significantly lower in both NRS (p = <0.0001) and PMN (p = <0.0001) groups that received LPS, additionally; treatment with PMN impacted the consumption of food and, specifically, increased the intake in PMN mice compared to NRS controls that received PBS (p = 0.0020) (Figure 14 C). Overall, the sickness responses experienced during severe systemic inflammation include anorexia and adipsia.

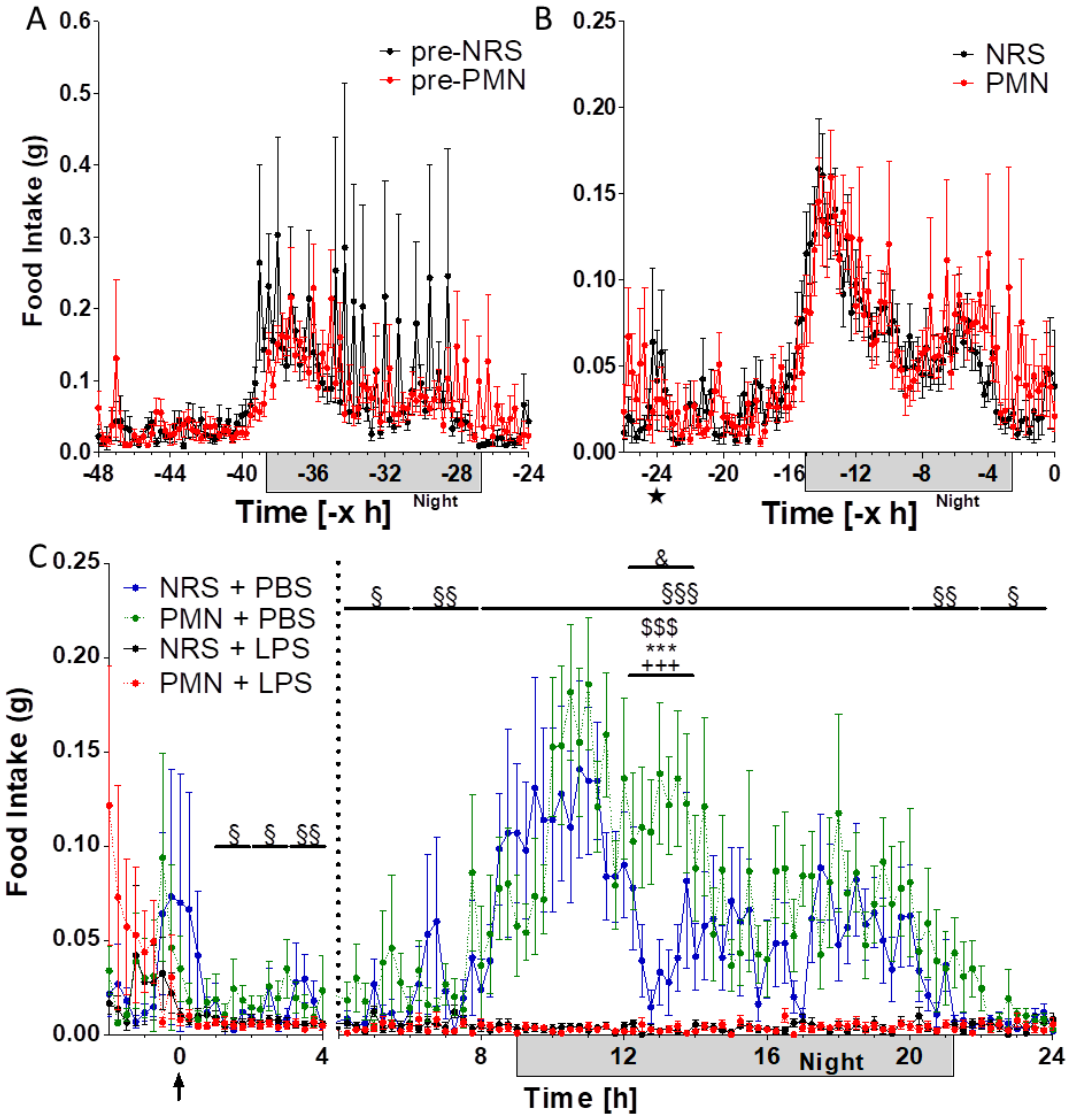

Figure 14: Anorexia occurs after LPS-stimulation

Telemetric recordings of food intake were analyzed over the course of the experiment starting approximately 48 h prior to injection with lipopolysaccharide (LPS, 2.5 mg/kg) until mice were sacrificed at 4 h or 24 h p.i. with LPS. Baseline recordings showed no differences over 24 h between groups that would receive anti-polymorphonuclear serum (PMN, 1 ml/kg) or normal rabbit serum (NRS, 1 ml/kg; A). After intraperitoneal (IP) injection of PMN or NRS (1 ml/kg), indicated with ★, over the next 24 h the food intake of the PMN mice did not differ from the NRS controls (B). 24 h after IP PMN or NRS mice received an IP injection of phosphate buffered saline (PBS) or LPS, indicated with ↑ (C). Immediately following the injection an impact of LPS was observed and persisted for the entirety of the experiment up to 24 h p.i. A short effect of PMN was briefly observed from approximately 12 -14 h p.i. at which point the PMN groups consumed more food than the NRS+PBS controls while LPS decreased food intake in both NRS and PMN groups. The grey box indicates the night cycle. Prior to the dotted line indicates that the second cohort of animals (4 h time point) was included into the analyses of food intake; n= 37-40 (A-B), 18-20 (C; -2-4 h p.i.), 12-13 (C; 4-24 h p.i.). Image C: & main effect of PMN; § main effect of LPS. $ NRS+PBS vs. NRS+LPS; * PMN+PBS vs. PMN+LPS; + NRS+PBS vs. PMN+PBS. *p<0.05, **p<0.01, ***p<0.001.

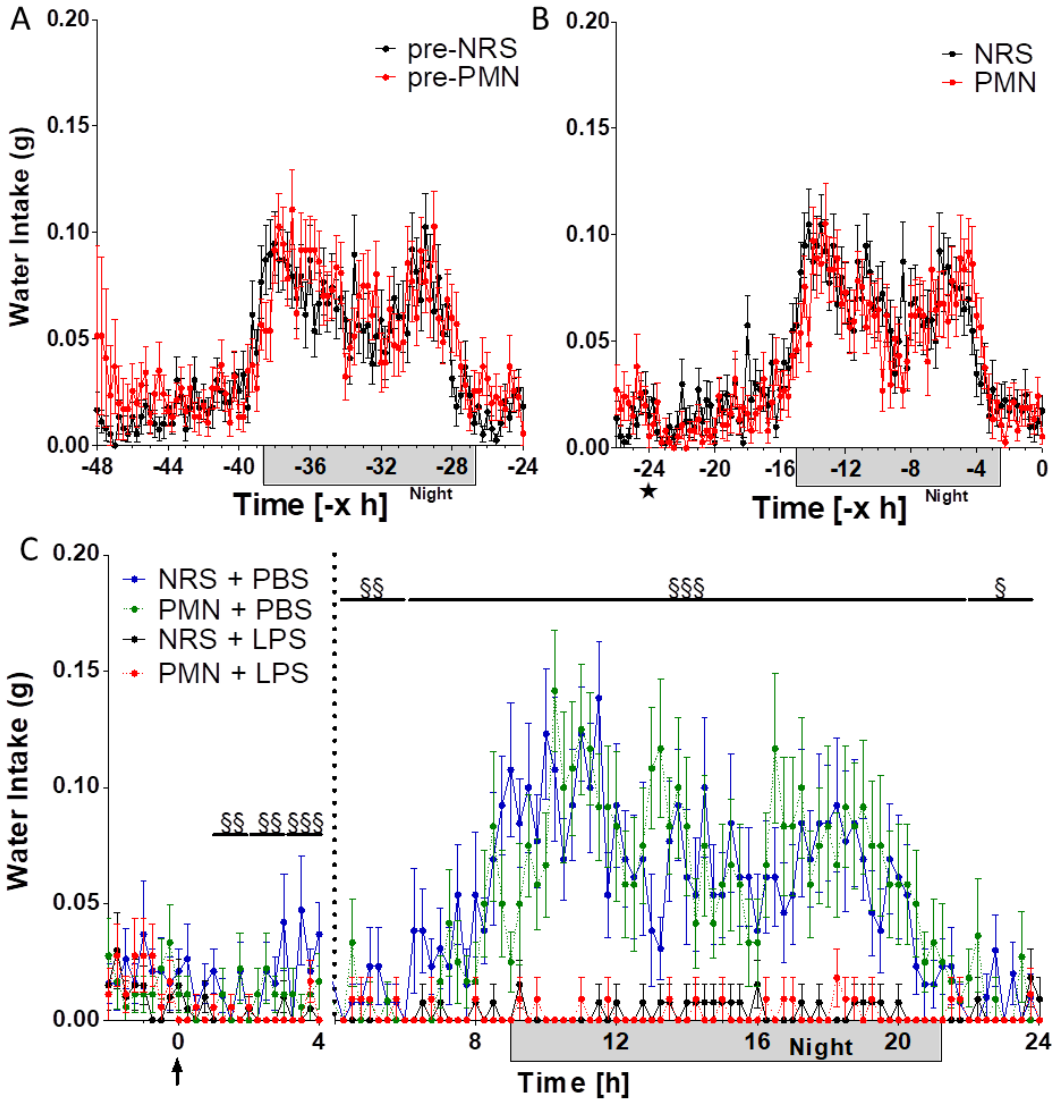

Figure 15: Adipsia occurs after LPS-stimulation

Telemetric recordings of water intake were analyzed over the course of the experiment starting approximately 48 h prior to injection with lipopolysaccharide (LPS, 2.5 mg/kg) until mice were sacrificed at 4 h or 24 h p.i. with LPS. Baseline recordings showed no differences over 24 h between groups that would receive anti-polymorphonuclear serum (PMN, 1 ml/kg) or normal rabbit serum (NRS, 1 ml/kg; A). After intraperitoneal (IP) injection of PMN or NRS (1 ml/kg), indicated with ★, over the next 24 h the water intake of the PMN mice did not differ from the NRS controls (B). 24 h after IP PMN or NRS mice received an IP injection of phosphate buffered saline (PBS) or LPS, indicated with ↑ (C). Immediately following the injection an impact of LPS was observed and persisted for the entirety of the experiment up to 24 h p.i. No effect of PMN on water intake was observed. The grey box indicates the night cycle. Prior to the dotted line indicates that the second cohort of animals (4 h time point) was included into the analyses of water intake; n= 37-40 (A-B), 18-20 (C; -2-4 h p.i.), 12-13 (C; 4-24 h p.i.). Image C: § main effect of LPS. §p<0.05, §§p<0.01, §§§p<0.001.

3.1.2.2.1 Body weight

Daily recordings of body weights (Figure 16) show that 24 h after inoculation with NRS or PMN (i.e., 0 h p.i. with LPS; Figure 16 A), PMN significantly reduced body weights compared to the NRS controls (p = 0.0001). Additionally, body weights were compared at 4 h (Figure 16 B) and 24 h p.i. (Figure 16 C). At 4 h p.i. a main effect of LPS was present that indicates an overall reducation in bodyweight regardless of pretreatment with NRS or PMN (p = <0.0001). By 24 h p.i. LPS significantly reduced body weights compared to the control groups that received PBS (NRS p = <0.0001; PMN p = <0.0001). Neither 4 h nor 24 h p.i. body weights were altered by PMN. Together, it appears that treatment with PMN antiserum to induce neutropenia elicits a subtle inflammatory response on its own resulting in a slight reduction in body weight, which is short lived.

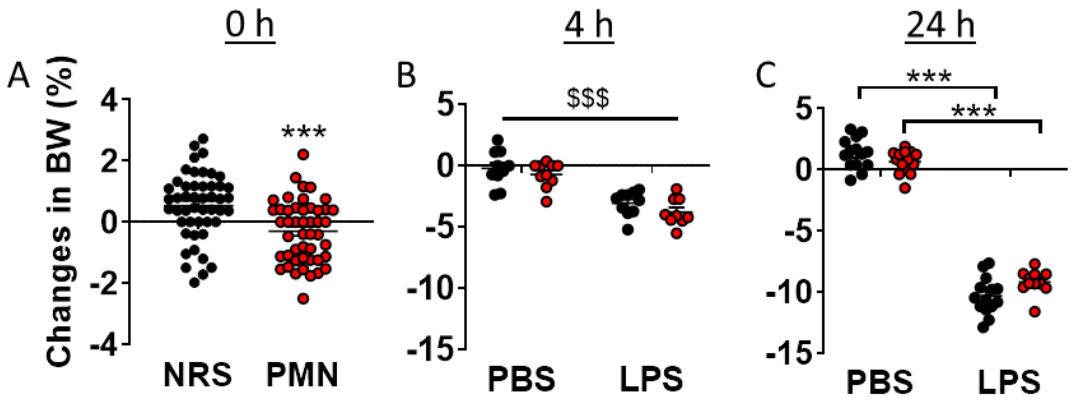

Figure 16: PMN decreases body weights prior to LPS-stimulation

By comparing body weights (BW) at several time points to their baseline BW, recorded -48 h p.i. with lipopolysaccharide (LPS, 2.5 mg/kg) or phosphate buffered saline (PBS), it was possible to compare treatment with normal rabbit serum (NRS, 1 ml/kg) and anti-polymorphonuclear serum (PMN, 1 ml/kg) at 0 h p.i. (A) as well as PBS and LPS after 4 h (B) or 24 h p.i. (C). PMN decreased BW in comparison to NRS 24 h after PMN/NRS treatment while treatment with LPS reduced body weights regardless of NRS or PMN pretreatment. n= 47-48 (A), 9-10 (B), 12-14 (C). ***p<0.001.

3.1.2.3 Core body temperature

Baseline recordings of core body temperature showed no differences between the groups that would be receiving either NRS or PMN (Figure 17 A). Following IP

inoculation with PMN (p = <0.0001) there was an acute fever that lasted approximately 3 h but otherwise no differences were observed between mice that received NRS or PMN (Figure 17 B). A strong effect of LPS appeared almost immediately following the inoculation (Figure 17 C, Supplementary Table 10). After LPS, both NRS and PMN mice developed a short lasting fever but by 2 h p.i. the temperature had begun to drop and continued to do so such that the mice became hypothermic. At 6 h p.i. the core body temperatures of the NRS and PMN groups began to deviate and while both temperatures continued to decline the PMN mice did so at an accelerated rate. This deviation ultimately resulted in the mice that received PMN maintaining a significantly lower core body temperature than those that received NRS from 10 h p.i. until the end of the experiment at 24 h p.i. Both groups temperature drop stopped at approximately 12 h p.i. and the mice began to recover, however, while the NRS groups' core body temperature climbed at a steady rate, the PMN groups' recovery was stunted and between 12 – 24 h p.i. only a marginal increase in temperature was observed. By 24 h p.i. the core body temperature of the NRS mice reached normal values while the PMN mice remained hypothermic. The temperature data suggests that neutropenia critically alters the thermoregulatory response during severe systemic LPS-induced inflammation.

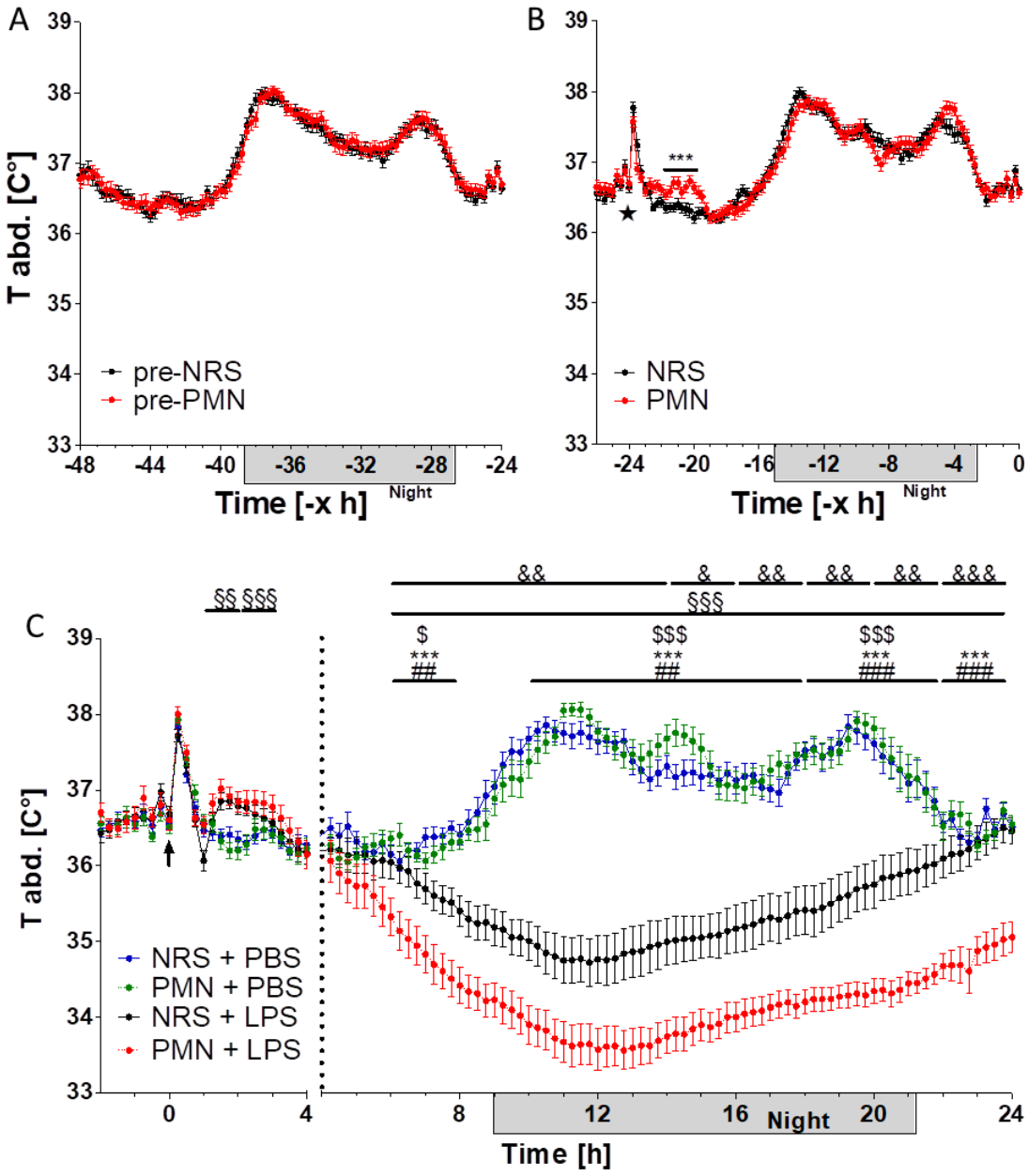

Figure 17: PMN exacerbates LPS-induced hypothermia

Telemetric recordings of core body temperature (T abd.) were analyzed over the course of the experiment starting approximately 48 h prior to injection with lipopolysaccharide (LPS, 2.5 mg/kg) until mice were sacrificed at 4 h or 24 h p.i. with LPS. Baseline recordings showed no differences over 24 h between groups that would receive anti-polymorphonuclear serum (PMN, 1 ml/kg) or normal rabbit serum (NRS, 1 ml/kg; A). After intraperitoneal (IP) injection of PMN or NRS (1 ml/kg), indicated with ★, over the next 24 h the PMN mice developed a short-lasting increase in T abd. compared to NRS counterparts (B). 24 h after IP PMN or NRS mice received an IP injection of phosphate buffered saline (PBS) or LPS, indicated with ↑ (C). Initially, LPS caused a short lasting fever in both groups until approximately 4 h p.i. when temperatures started to become hypothermic. At approximately 6 h p.i. PMN mice started to have more severe hypothermia, an effect which persisted until 24 h p.i., while the

temperature of the NRS mice ceased to be hypothermic at approximately 22 h p.i. Grey box indicates the night cycle. Prior to the dotted line indicates that the second cohort of animals (4 h time point) was included into the analyses of the febrile response; n= 47-48 (A-B), 23-24 (C; -2-4 h p.i.), 14 (C; 4-24 h p.i.). Image C: & main effect of PMN; § main effect of LPS. interactions: $ NRS+PBS vs. NRS+LPS; * PMN+PBS vs. PMN+LPS; # NRS+LPS vs. PMN+LPS. *p<0.05, **p<0.01, ***p<0.001.

3.1.3 Characterization of the role of neutrophil granulocytes in cellular communication with the brain

In furtherance of understanding the role NGs i.e., neutropenia, plays in the sickness response and immune-to-brain communication extensive analysis were performed at 4 h and 24 h p.i. with LPS. Important mediators of inflammation including pro- and anti-inflammatory cytokines as well as NG chemoattractants were analyzed in circulation and in the hypothalamus. Additionally, the expression of other transcription factors, target genes, and the humoral route of communication was also analyzed in the hypothalamus. Moreover, NET formation was examined at the level of the MnPO.

3.1.3.1 Inflammatory mediator levels in the periphery

Already at 4 h p.i. with LPS the mediators of inflammation in the periphery were altered as seen in Figure 18. LPS caused a significant overall increase in NG chemoattractants CCL5 (p = <0.0001), CXCL1 (p = <0.0001), and CXCL2 (p = <0.0001). The proinflammatory cytokines IL-6 (p = <0.0001) and TNFα (p = <0.0001) were also increased by LPS regardless of pretreatment with NRS or PMN; no effect of PMN was observed. The anti-inflammatory cytokine IL-10 was not only elevated by LPS (NRS p = 0.0298; PMN p = <0.0001) but, within this group, mice that received PMN had significantly higher levels than the NRS controls (p = 0.0052). No other PMN effects were observed for pro-inflammatory cytokines. Interestingly, a ratio of IL-10:TNFα showed that while LPS increased levels overall (p = <0.0001) pretreatment with PMN (p = 0.0471) had a modest main effect that may have enhanced these values compared to the NRS mice regardless of treatment with LPS.

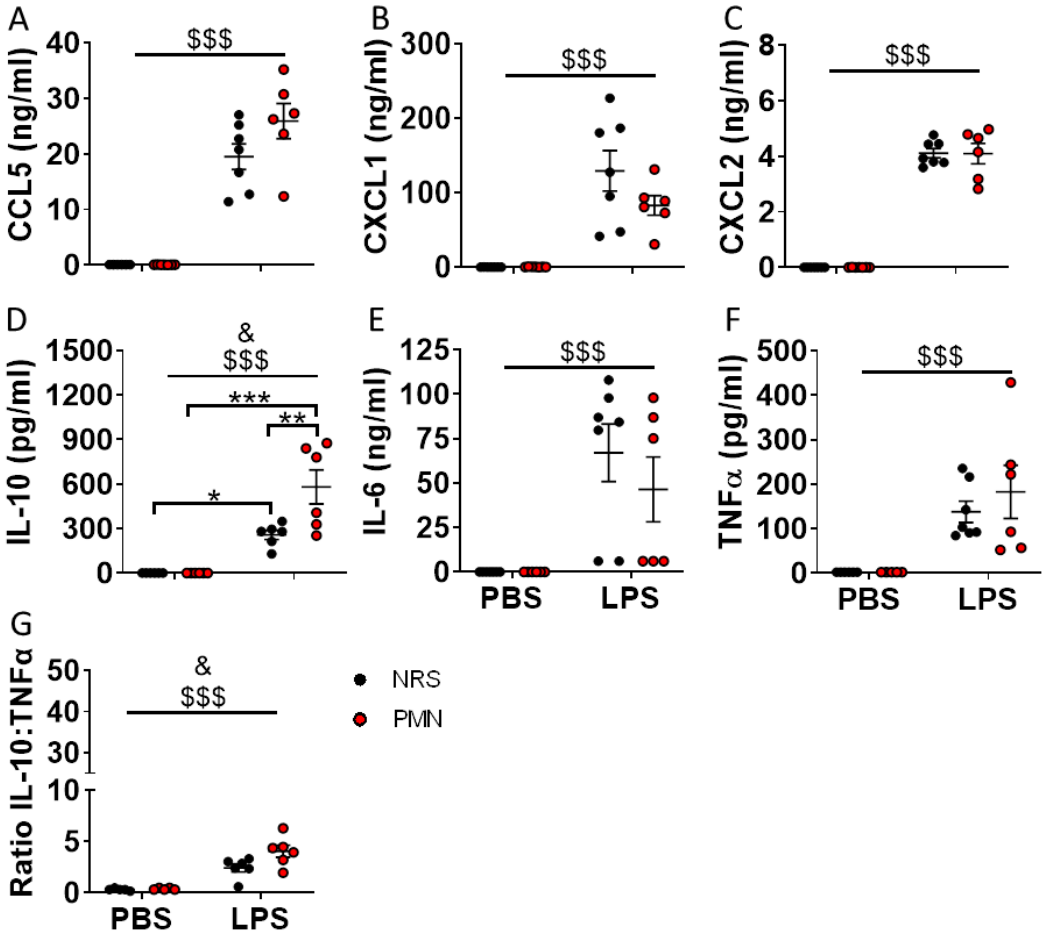

Figure 18: Neutropenia (PMN) exacerbated IL-10 plasma levels 4 h after LPS-stimulation

Plasma samples were collected 4 h p.i. with lipopolysaccharide (LPS, 2.5 mg/kg) and compared between groups that received normal rabbit serum (NRS, 1 ml/kg) or anti-polymorphonuclear serum (PMN, 1 ml/kg) as well as phosphate buffered saline (PBS) or LPS for circulating cytokines. The cytokines analyzed included neutrophil granulocyte chemoattractants: CCL5 (A), CXCL1 (B), and CXCL2 (C); anti-inflammatory cytokine: IL-10 (D); and pro-inflammatory cytokines: IL-6 (E) and TNFα (F). An additional comparison was made for the ratio of IL-10:TNFα (G). At 4 h p.i. LPS increased production of all cytokines regardless of pretreatment with NRS or PMN. However, for IL-10, PMN exacerbated circulating levels after LPS treatment. The IL-10:TNFα ratio was significantly altered by PMN. n=5-7, & main effect of PMN; $ main effect of LPS. *p<0.05, ***p<0.001.

At 24 h p.i. the alterations to the inflammatory mediators were still present although levels were not as high as those seen at 4 h p.i. (Figure 19). At the 24 h time point, LPS caused elevated levels of CCL5 (p = <0.0001) regardless of pretreatment with NRS or PMN. Additionally, levels of CXCL2 (NRS p = 0.0489; PMN p = <0.0001) and mice pretreated with PMN had significantly enhanced production of CXCL1 (p = <0.0001) during LPS-induced inflammation. The LPS-induced elevation of CXCL1 in PMN pretreated mice was exacerbated in comparison to their NRS counterparts (p = <0.0001). LPS-stimulated CXCL2 levels were also enhanced in PMN compared to NRS mice (p = <0.0001). Likewise, the LPS-induced increase in IL-10 (NRS p = <0.0001; PMN p = <0.0001) and TNFα (NRS p = 0.0167; PMN p = <0.0001) were also exacerbated in PMN pretreated mice (IL-10 p = 0.0072; TNFα p = <0.0001). Once again, the IL-10:TNFα ratio was altered after LPS stimulation overall (p = <0.0001), however, contradictory to the 4 h time point, now the PMN effect reduced the ratio regardless of treatment with LPS (p = 0.0407). Similar to CXCL1, IL-6 reached basal levels in the LPS-stimulated NRS group and only remained significantly elevated in the LPS-stimulated PMN group compared to the respective PBS control (p = <0.0001), which was significantly higher than the NRS mice (p = <0.0001). In summary, the LPS-induced increases in plasma mediators were enhanced in neutropenic versus immunocompetent mice indicating exacerbated immune responses.

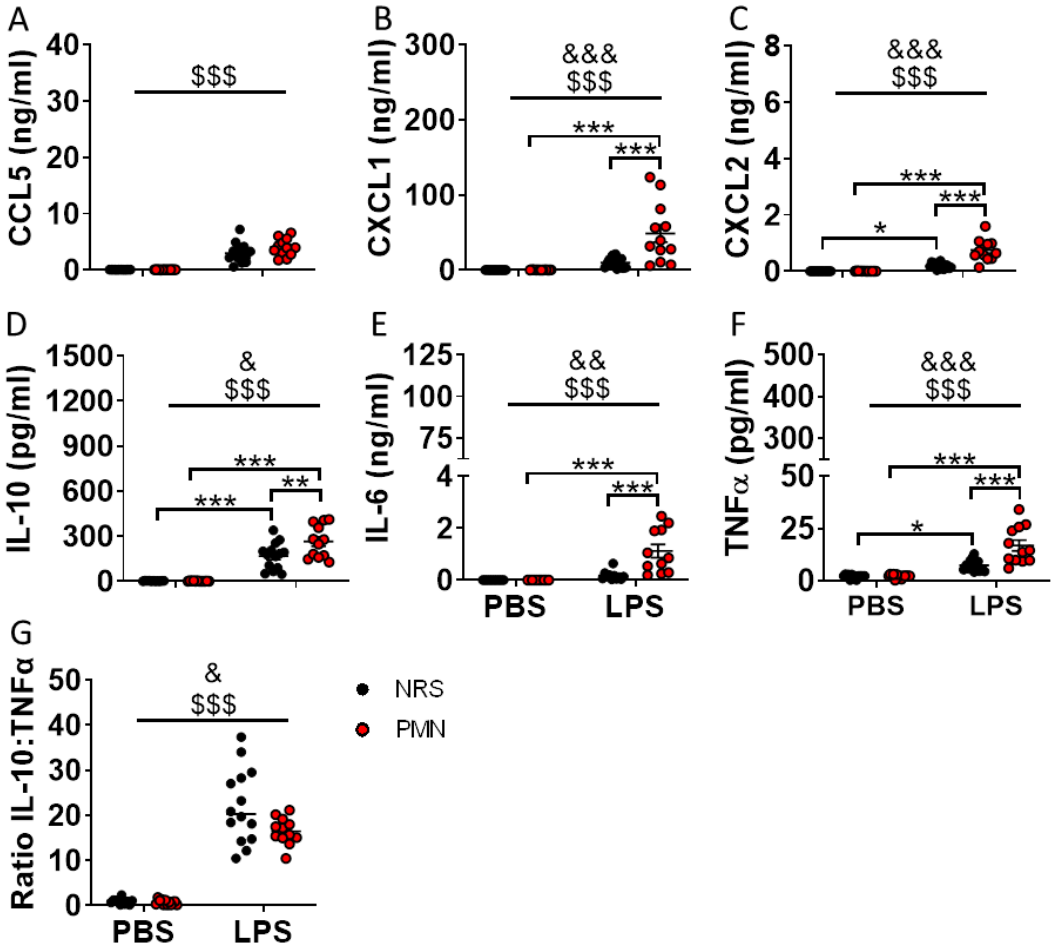

Figure 19: Neutropenia (PMN) exacerbated plasma cytokines 24 h after LPS-stimulation

Plasma samples were collected 24 h p.i. with lipopolysaccharide (LPS, 2.5 mg/kg) and compared between groups that received normal rabbit serum (NRS, 1 ml/kg) or anti-polymorphonuclear serum (PMN, 1 ml/kg) as well as phosphate buffered saline (PBS) or LPS for circulating cytokines. The cytokines analyzed included neutrophil granulocyte chemoattractants: CCL5 (A), CXCL1 (B), and CXCL2 (C); anti-inflammatory cytokine: IL-10 (D); and pro-inflammatory cytokines: IL-6 (E) and TNFα (F). An additional comparison was made for the ratio of IL-10:TNFα (G). At 24 h p.i. LPS significantly increased all analyzed circulating cytokines except for CCL5, where only an effect of LPS was present, and for CXCL1 and IL-6 in mice treated with NRS. Treatment with PMN exacerbated the production of CXCL1, CXCL2, IL-10, IL-6, and TNFα during inflammation. The IL-10:TNFα ratio was significantly altered by PMN. n=10-14, & main effect of PMN; § main effect of LPS. *p<0.05, **p<0.01, ***p<0.001.

3.1.3.2 Inflammatory mediator mRNA expression in the hypothalamus

Having observed changes in inflammatory marker protein levels in circulation due to neutropenia during LPS-induced severe systemic inflammation, my next aim was to assess markers for immune-to-brain signaling i.e., analyses of the brain inflammatory response.

3.1.3.2.1 Cytokine expression

The expression of mediators of inflammation in the hypothalamus did not show the same level of alterations as seen in plasma (Figure 20). At 4 h p.i., LPS caused a significant increase in the mRNA expression of anti-inflammatory IL-10 (p = 0.0011) and the pro-inflammatory cytokines IL-6 (p = <0.0001) and TNFα (p = <0.0001) regardless of pretreatment with NRS or PMN. Though, by 24 h p.i. the main effects were no longer present and no impact of either PMN or LPS was observed. Overall, while severe systemic inflammation caused an initial spike in mRNA expression of inflammatory mediators within the hypothalamus early on, the effect was not long lasting and was not impacted by neutropenia.

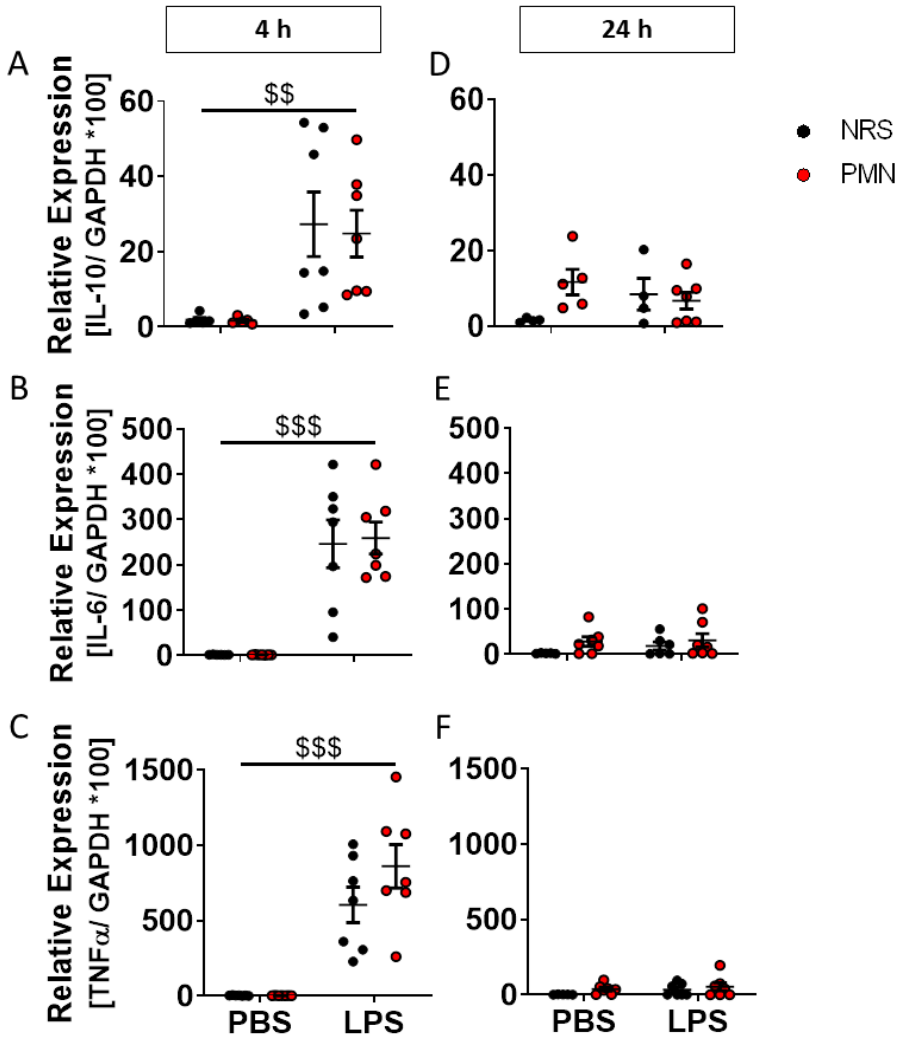

Figure 20: Hypothalamic mRNA expression of inflammatory mediators are increased 4 h after LPS-stimulation

The hypothalamus was analyzed for expression of cytokines as follows: IL-10 (A, D), IL-6 (B, E), and TNFα (C, F) 4 h (A-C) and 24 h (D-F) p.i. with lipopolysaccharide (LPS, 2.5 mg/kg) or phosphate buffered saline (PBS) in groups of mice pretreated with normal rabbit serum (NRS, 1 ml/kg) or anti-polymorphonuclear serum (PMN, 1 ml/kg). At 4 h p.i., LPS increased expression of all cytokines regardless of pretreatment with NRS or PMN. By 24 h p.i., the effects of LPS were no longer present and no impact of PMN was observed at either time point. n=5-7, $ main effect of LPS. *p<0.05, **p<0.01, ***p<0.001.

3.1.3.2.2 Transcription factor expression

To assess inflammatory signaling by cytokines in the brain, the hypothalamic expression of the transcription factors NF-IL6, NFκB i.e., its marker protein NFκBiα, and STAT3 i.e., its marker protein SOCS3 were measured at 4 h and 24 h p.i. with LPS (Figure 21). Consistent with previous studies (Rummel et al. 2006, Damm et al. 2011, Damm et al. 2013, Rummel 2016), LPS caused an overall increase in expression of all three transcription factors, regardless of pretreatment with NRS or PMN, at 4 h p.i. but no effect of PMN was observed (**NF-IL6**: p = <0.0001/ **NFκBiα**: p = <0.0001 / **SOCS3**: p = <0.0001). Moreover, at 24 h p.i., NFκBiα (p = 0.0358) and SOCS3 (p = 0.0425) showed an overall main effect of PMN. This data suggests some enhanced pro-inflammatory signaling in the brains of neutropenic animals.

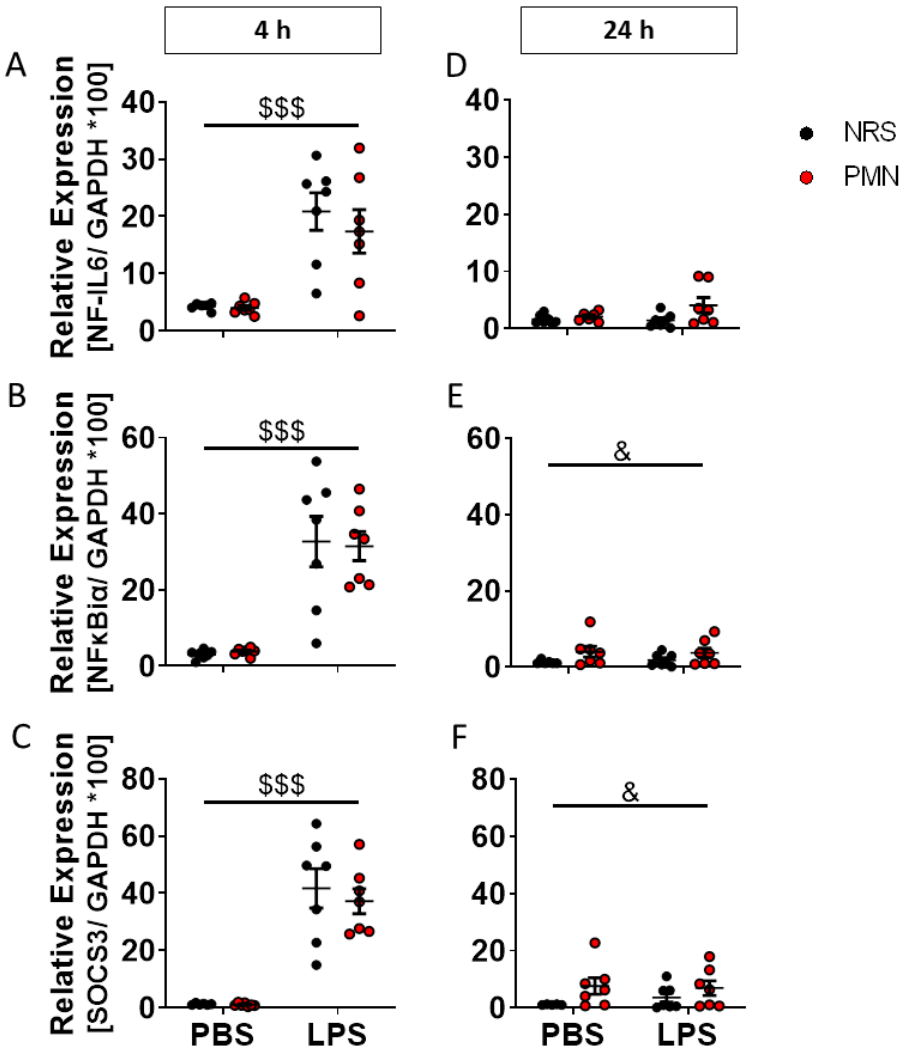

Figure 21: Hypothalamic mRNA expression of NFκBiα and SOCS3 altered by PMN 24 h after LPS-stimulation

The hypothalamus was analyzed for mRNA expression of inflammatory signaling: NF-IL6 (A, D), NFκBiα (B, E), and SOCS3 (C, F) 4 h (A-C) and 24 h (D-F) p.i. with lipopolysaccharide (LPS, 2.5 mg/kg) or phosphate buffered saline (PBS) in mice either pretreated with normal rabbit serum (NRS, 1 ml/kg) or anti-polymorphonuclear serum (PMN, 1 ml/kg). At 4 h p.i., LPS increased expression of all marker proteins for inflammatory signaling regardless of pretreatment with NRS or PMN. By 24 h p.i., the effects of LPS were no longer present but the expression of NFκBiα and SOCS3 were significantly altered by PMN. n=5-7, & main effect of PMN; $ main effect of LPS. *p<0.05, **p<0.01, ***p<0.001.

3.1.3.2.3 Target gene expression in the brain

The mRNA expression of important target genes of the inflammatory transcription factors NFκB, STAT3, and NF-IL6 related to the synthesis of PGE2 were altered in the hypothalamus as shown in Figure 22. The expression of COX-2 (p = <0.0001) and mPGES (p = <0.0001) both had a main effect of LPS that indicated an overall increase; no effect of PMN was observed. At 24 h p.i., there was no significant impact of LPS but PMN altered the expression of COX-2 (p = 0.0475) and mPGES (p = 0.0319). Overall, altered expression of PGE2 catalyzing enzymes caused by neutropenia may contribute to an exacerbated sickness response.

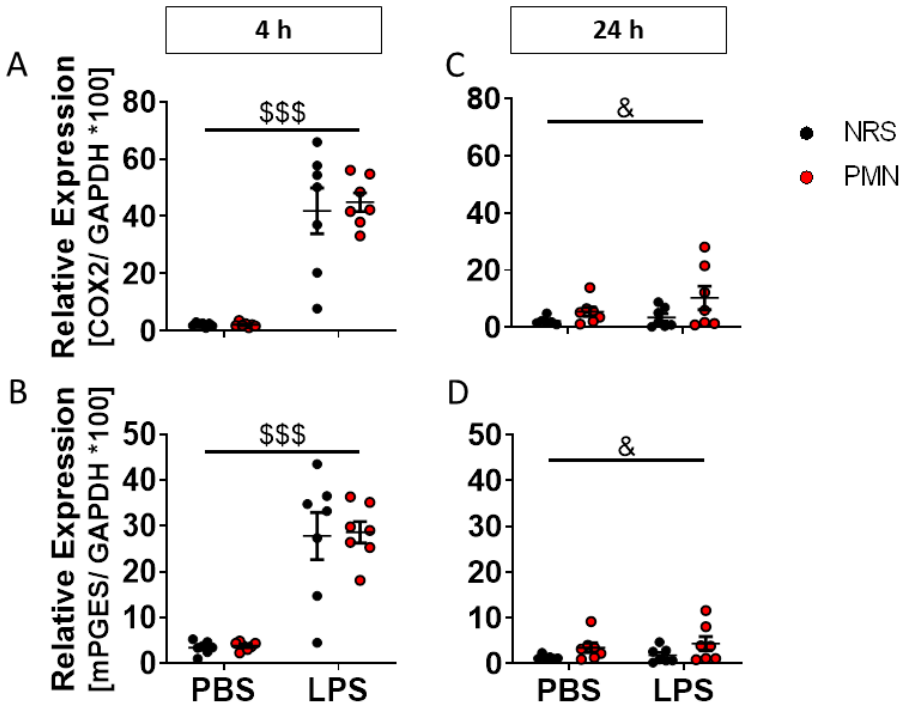

Figure 22: Hypothalamic mRNA expression of COX-2 and mPGES are altered by PMN 24 h after LPS-stimulation

The hypothalamus was analyzed for mRNA expression of the prostaglandin E2 catalyzing enzymes: COX-2 (A, C) and mPGES (B, D) 4 h (A-B) and 24 h (C-D) p.i. with lipopolysaccharide (LPS, 2.5 mg/kg) or phosphate buffered saline (PBS) in mice either pretreated with normal rabbit serum (NRS, 1 ml/kg) or anti-polymorphonuclear serum (PMN, 1 ml/kg). At 4 h p.i., LPS increased expression of both enzymes regardless of pretreatment with NRS or PMN. By 24 h p.i., the effects of LPS were no longer present but COX-2 and mPGES were significantly altered by PMN. n=6-7, & main effect of PMN; $ main effect of LPS. *p<0.05, ***p<0.001.

3.1.3.2.4 Expression of immune cell marker proteins

The impact of neutropenia on immune-to-brain communication during severe systemic inflammation assessed through the NG markers CXCL1 and Elane as well as the activated microglia/perivascular macrophage markers CD68 and CD163 is shown in Figure 23. The overall mRNA expression of CXCL1 (p = <0.0001) and Elane (p = <0.0001) were increased by a main effect of LPS while no effect of PMN was observed. At 24 h p.i., the LPS effect was no longer present. In contrast, 4 h after LPS-stimulation, a main effect of LPS (p = 0.0160) was observed for the expression of CD163, a marker protein for perivascular macrophages. No effect of LPS or PMN on the mRNA expression of CD68, used as a marker protein of activated microglia, was revealed at either time point.

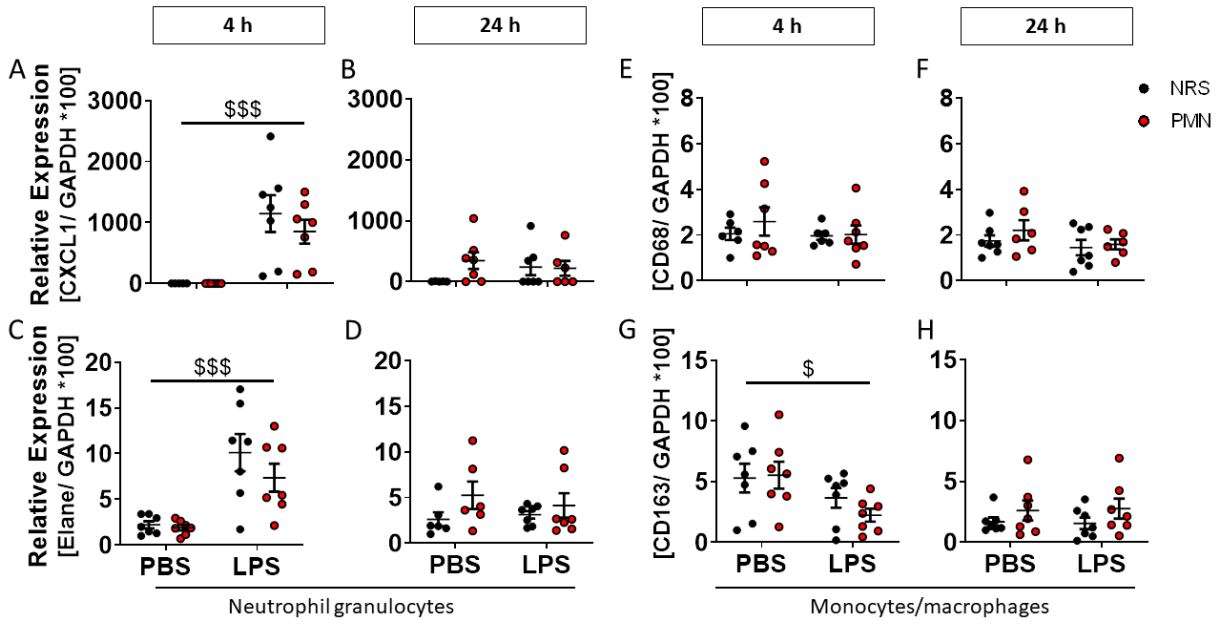

Figure 23: Hypothalamic mRNA expression of cellular marker proteins for NGs and perivascular macrophages are altered 4 h after LPS-stimulation

The hypothalamus was analyzed for expression of marker proteins for neutrophil granulocytes (NG): CXCL1 (A, B), Elane (C, D); and activated microglia/perivascular macrophages (MM): CD68 (E, F) and CD163 (G, H) 4 h (A, C, E, G) and 24 h (B, D, F, H) p.i. with lipopolysaccharide (LPS, 2.5 mg/kg) or phosphate buffered saline (PBS) in animals pretreated with either rabbit serum (NRS, 1 ml/kg) or anti-polymorphonuclear serum (PMN, 1 ml/kg). At 4 h p.i., LPS increased the expression of both NG marker proteins regardless of pretreatment with NRS or PMN. CD163 had an effect of LPS at 4 h p.i. that indicated reduced expression regardless of pretreatment with NRS or PMN. By 24 h p.i., the effects of LPS were no longer present and no impact of PMN was observed at either time point. n=5-7, $ main effect of LPS. *p<0.05, **p<0.01, ***p<0.001.

3.1.3.3 Immunohistochemical detection of neutrophil granulocyte recruitment to the SFO

To complement hypothalamic mRNA expression for marker proteins of NG recruitment to the brain during LPS-induced systemic inflammation on protein levels, I performed immunohistochemical MPO staining for NGs at the SFO (Figure 24). NG recruitment to this brain structure has previously already been shown 8 h after LPS-stimulation (Schneiders et al. 2015). Here, although NG recruitment to the SFO was low, LPS induced an increase in NG recruitment at 4 h p.i. (p = <0.0001) with LPS in mice pretreated with NRS. However, NG recruitment to the SFO was absent in the LPS-stimulated PMN group. Indeed, PMN significantly reduced levels of NG recruitment to the SFO (p = 0.0087) (Figure 24, K). The LPS-induced NG recruitment was no longer observed at 24 h p.i. but a main effect of PMN was still detected where these groups showed overall reduced NG recruitment regardless of treatment with LPS (p = 0.0101) (Figure 24, L).

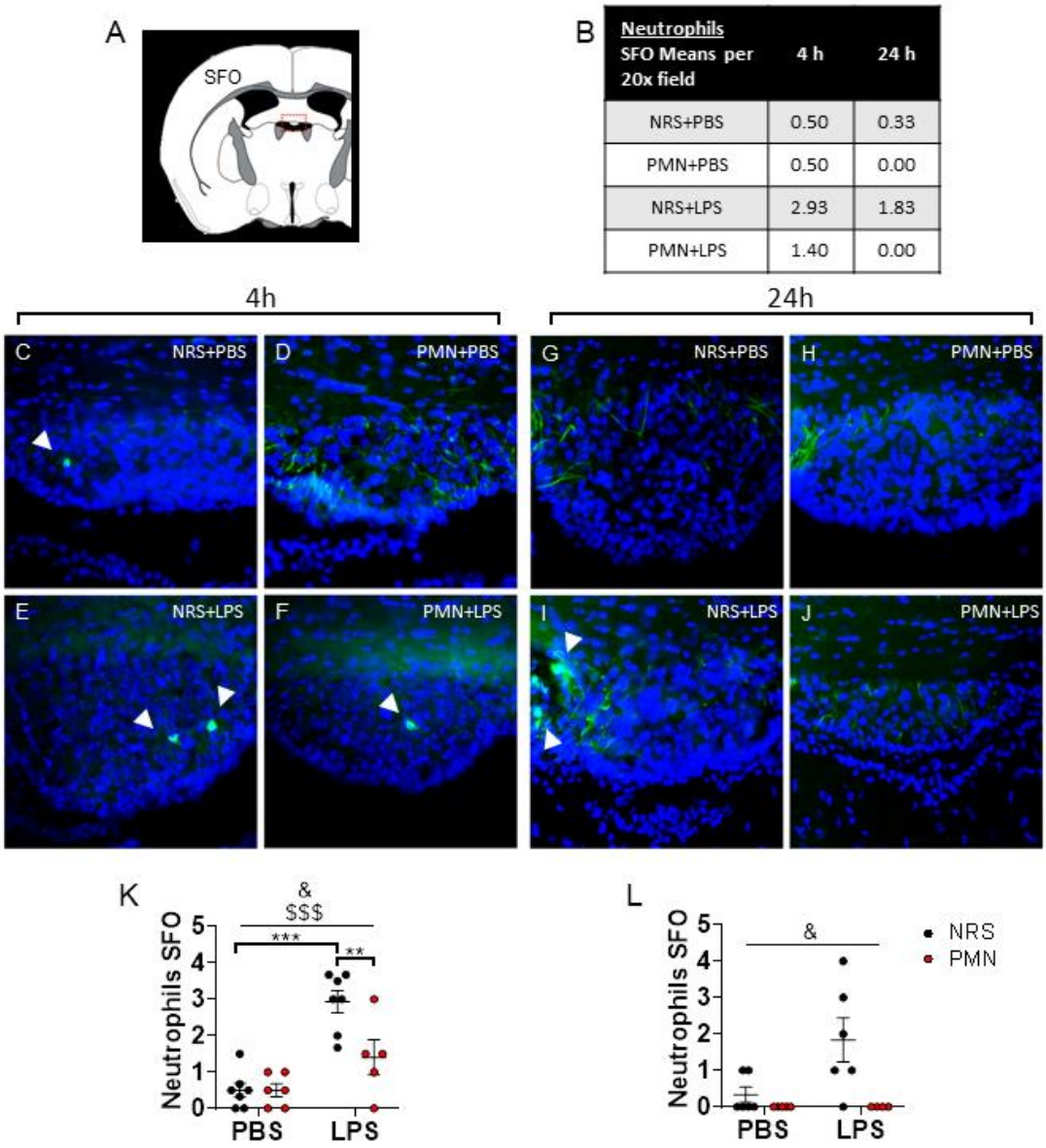

Figure 24: NG recruitment to the SFO is reduced by PMN after LPS-stimulation

Sections of the brain were analyzed at the level of the subfornical organ (SFO; A) and neutrophil granulocytes (NG; green, C-J) were counted per 20x field of view (B). Mice were evaluated at 4 h (C-F) and 24 h (G-J) p.i. with lipopolysaccharide (LPS, 2.5 mg/kg) or phosphate buffered saline (PBS) for mice pretreated with either normal rabbit serum (NRS, 1 ml/kg) or anti-polymorphonuclear serum (PMN, 1 ml/kg). Graphs detailing the number of NGs counted at 4 h (K) and 24 h (L) p.i. are also shown. LPS-induced increases in NG recruitment were observed at 4 h p.i. in mice pretreated with NRS but were significantly reduced in PMN pretreated mice. NG recruitment were not significantly increased at 24 h p.i. but were significantly altered by PMN. DAPI (blue; C-J) visualizes the surrounding tissue. n= 4-7 per group. Scale bar in C = 50 μm and is representative for (C-J); § interaction, & main effect of PMN, $ main effect of LPS. *p<0.05, **p<0.01, ***p<0.001.

3.1.3.4 Immunohistochemical detection of neutrophil granulocyte recruitment to the PVN

In addition to the SFO, the recruitment of NGs during LPS-induced systemic inflammation was assessed in another hypothalamic structure, namely, at the level of the PVN. Like the SFO, the PVN has previously been described to show enhanced staining for NGs during LPS-induced systemic inflammation (Pflieger et al. 2018). Here, the LPS-induced increase in NG recruitment observed at 4 h and 24 h p.i. was apparent in both groups as a main effect of LPS regardless if the mice received NRS or PMN (4 h p = <0.0001; 24 h p = <0.0001) (Figure 25). In contrast to the SFO, a PMN dependent reduction in NG recruitment was not revealed. Together, it seems that NG recruitment can vary by brain structure and even under neutropenic conditions; certain areas of the brain may be less altered and can still have significant NG interactions.

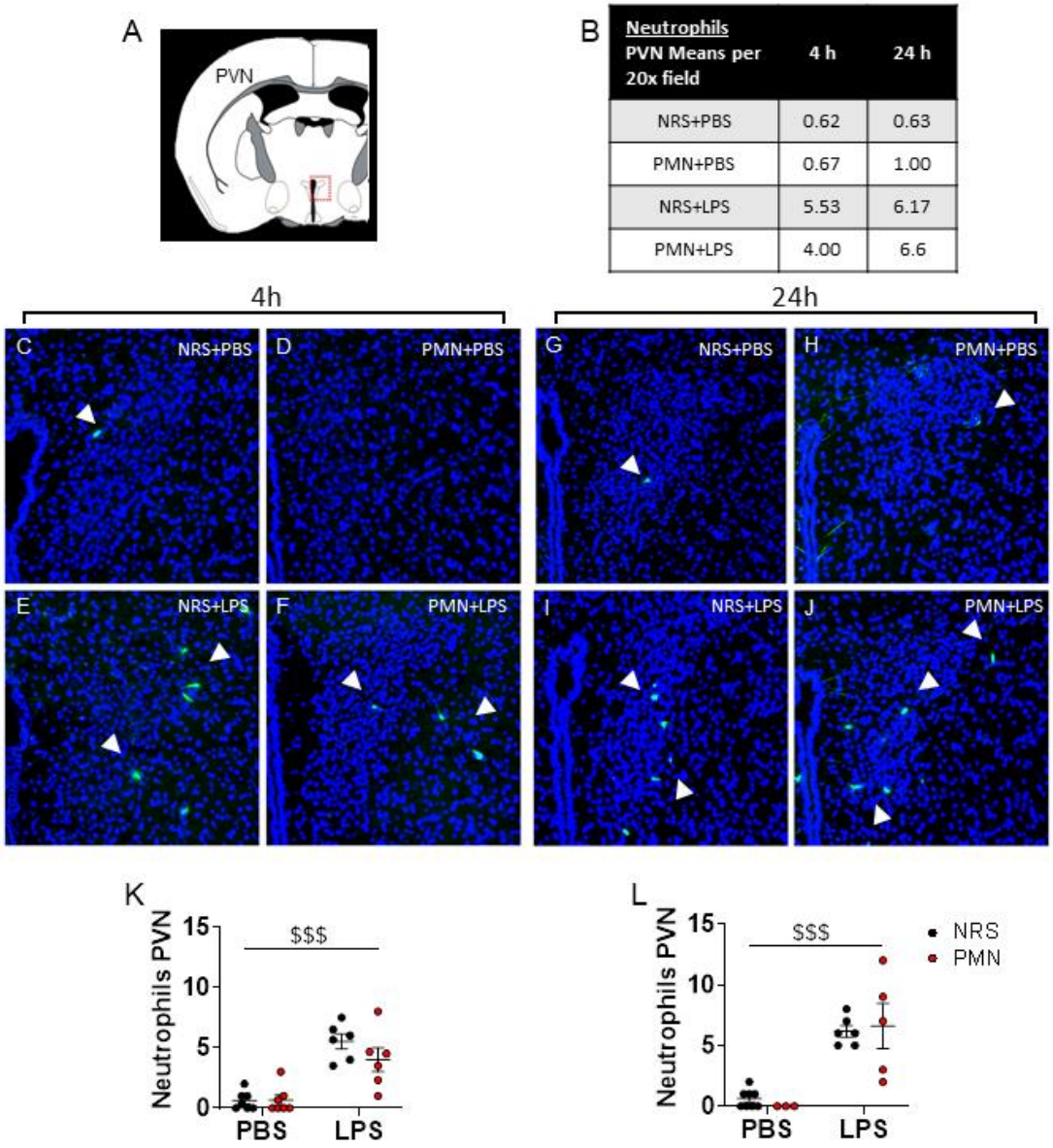

Figure 25: NG recruitment to the PVN is increased after LPS-stimulation

Sections of the brain were analyzed at the level of the paraventricular nucleus (PVN; A) and neutrophil granulocytes (NG; green, C-J) were counted for half of the PVN structure per 20x field of view (B). Mice were evaluated at 4 h (C-F) and 24 h (G-J) p.i. with lipopolysaccharide (LPS, 2.5 mg/kg) or phosphate buffered saline (PBS) pretreated either with normal rabbit serum (NRS, 1 ml/kg) or anti-polymorphonuclear serum (PMN, 1 ml/kg). Graphs detailing the number of NGs counted at 4 h (K) and 24 h (L) p.i. are also shown. LPS-induced increases in NG recruitment were observed at both time points regardless of pretreatment with NRS or PMN but no significant differences were observed between NRS or PMN pretreated mice. DAPI (blue; C-J) visualizes the surrounding tissue. n= 3-8 per group. Scale bar in C = 100 μm and is representative for (C-J). $ main effect of LPS. **p<0.01, ***p<0.001.

3.1.3.5 NET formation in the hypothalamus

To identify if NETs could be a stimulant for brain inflammatory responses and potentially contribute to the enhanced sickness response observed in the present study, NET formation was assessed in the hypothalamic MnPO, as this brain structure is known to be important for fever induction pathways (Boulant 2000, McKinley et al. 2003) (Figure 26). The ratio of the NET markers H3Cit and DNA/His to nuclear stain were compared between groups at 4 h and 24 h p.i. Altogether, no differences were determined between groups at either time point, although, H3Cit was significantly increased overtime regardless of treatment (p = 0.0321). These data suggest that neither LPS nor PMN had an effect on NET formation in the MnPO but NET formation may increase overtime during LPS-induced inflammation. Thus, NETs in the MnPO most likely do not contribute to observed exacerbation of brain inflammation and the sickness response in neutropenic animals.

A

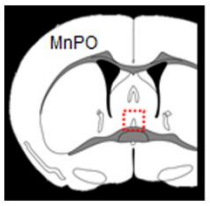

B

NET formation H3Cit per 40x field	4 h	24 h
NRS+PBS	11.91	11.42
PMN+PBS	12.87	19.81
NRS+LPS	13.63	19.51
PMN+LPS	9.20	19.13

C

NET formation DNA/His per 40x field	4 h	24 h
NRS+PBS	25.14	16.99
PMN+PBS	30.66	52.80
NRS+LPS	27.84	41.87
PMN+LPS	25.96	43.53

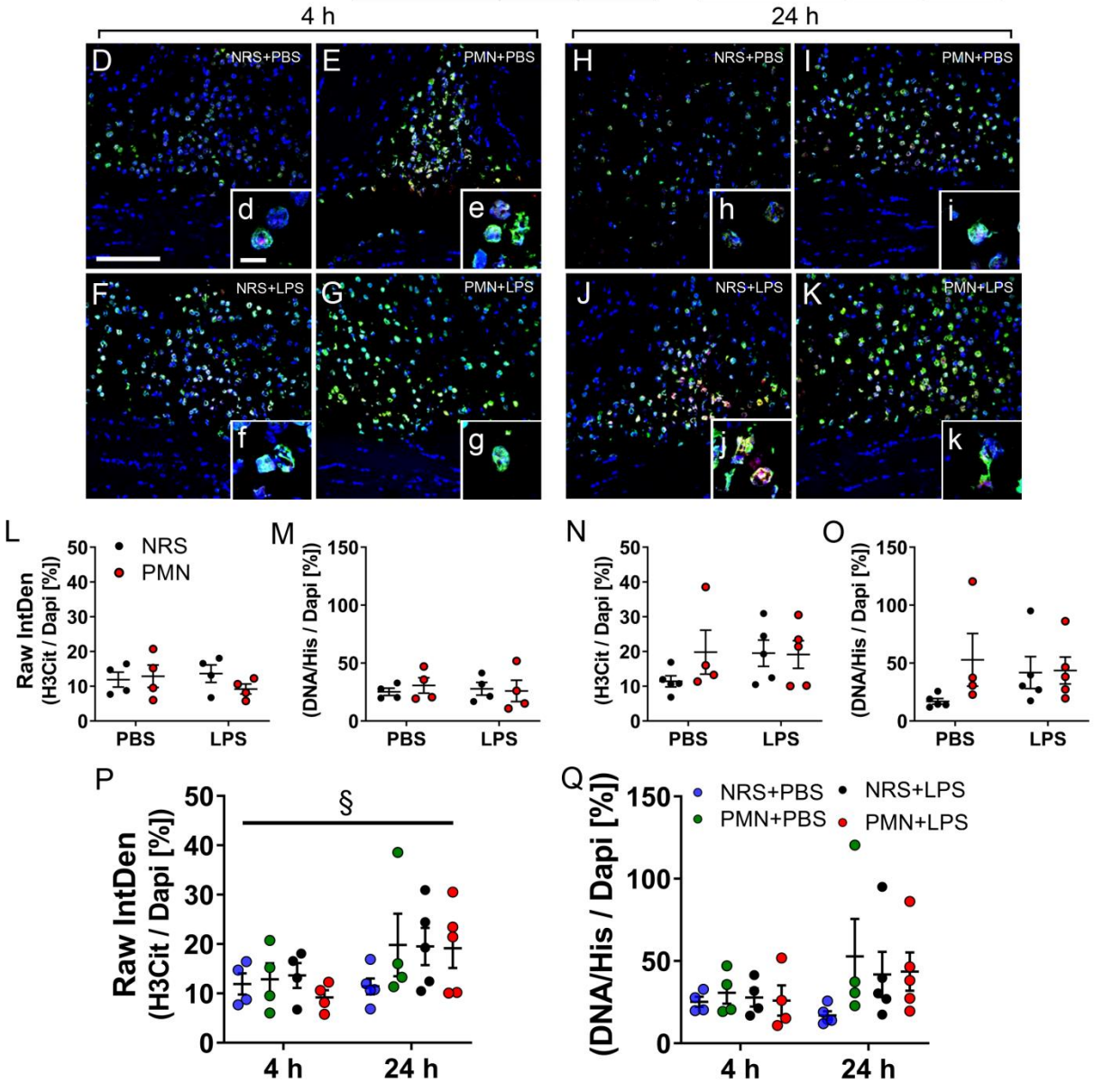

Figure 26: NET formation in the MnPO is unaffected by treatment with PMN or LPS after stimulation

Sections of the brain were analyzed at the level of the upper cap of the median preoptic nucleus (MnPO; A) by raw integrated density (Raw IntDen; B, C) for citrullinated histone H3 (H3Cit, red; D-K) and DNA/histone (DNA/His, green; D-K) immunoreactivity in relation to Dapi (blue; D-K). Mice were

evaluated at 4 h (D-G) and 24 h (H-K) p.i. with lipopolysaccharide (LPS, 2.5 mg/kg) or phosphate buffered saline (PBS) in mice pretreated either with normal rabbit serum (NRS, 1 ml/kg) or anti-polymorphonuclear serum (PMN, 1 ml/kg). Graphs detailing the distribution of H3Cit and DNA/His at 4 h (L, M) and 24 h (N, O) p.i. as well as differences in H3Cit (P) and DNA/His (Q) over time are also shown. No differences were observed in mice pretreated with PMN compared to NRS, additionally, LPS-induced inflammation did not alter the extent of NET formation. H3Cit was increased overtime regardless of treatment. n= 4-5 per group. Scale bar in D = 25 μm and is representative for (D-K); scale bar in d = 10 μm and is representative for insets (d-k). § main effect of time. § $p<0.05$.

3.1.3.6 Alterations to the HPA axis

Activation of the HPA axis appraised through circulating levels of corticosterone is shown in Figure 27. At 4 h p.i., LPS induced high levels of corticosterone in circulation compared to PBS counterparts (NRS p = <0.0001; PMN p = <0.0001). Additionally, at 4 h p.i., corticosterone levels were significantly lower in mice pretreated with PMN compared to NRS ($p = 0.0021$). By 24 h p.i., the LPS-induced elevated levels of corticosterone were still present (NRS p = <0.0001; PMN p = <0.0001) though appearing lower than what was observed at 4 h p.i. At the 24 h time point after LPS-stimulation, mice pretreated with PMN had higher levels of corticosterone compared to those treated with NRS ($p = 0.0281$). The results suggest that neutropenia dampens HPA axis activation during early stages of inflammation but exacerbates the later response i.e., prevents adequate depletion of circulating corticosterone during the resolution of inflammation.

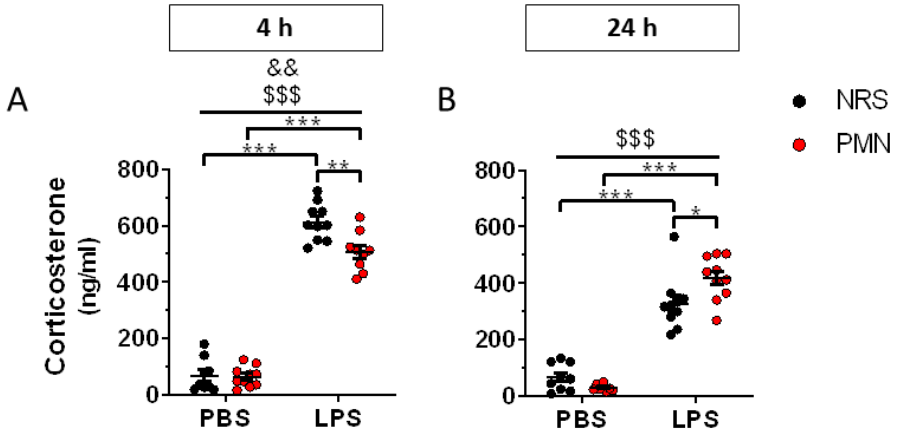

Figure 27: PMN dampens early corticosterone production but exacerbates this response at later stages after LPS-stimulation

Circulating levels of corticosterone were compared at 4 h (A) or 24 h (B) p.i. with lipopolysaccharide (LPS, 2.5 mg/kg) or phosphate buffered saline (PBS) in mice pretreated either with normal rabbit serum (NRS, 1 ml/kg) or anti-polymorphonuclear serum (PMN, 1 ml/kg). During LPS-induced inflammation PMN mice produced lower levels of corticosterone (4 h) that persisted in circulation at significantly higher levels than the NRS controls (24 h). n= 8-10; & main effect of PMN; $ main effect of LPS. *p<0.05, **p<0.01, ***p<0.001.

3.2 *In vitro* model of LPS-stimulated NET formation with bone marrow derived neutrophil granulocytes

3.2.1 Characterization of NETs *in vitro*

While I did not detect significant NET formation in the brain during systemic LPS-induced inflammation, I was interested if LPS was able to induce NETs potentially contributing to the peripheral and brain inflammatory response. For this purpose, *in vitro* cultures of bone marrow derived mouse NGs were performed. Using flow cytometry, I checked the purity of the bone marrow isolated and found it to be approximately 88.5% NGs, identified as $CD11b^{+}Ly6G^{+}$ cells, as shown in Figure 28. Additionally, when or if NETs are formed, are inflammatory mediators released that could exert influence on the inflammatory response? To test these parameters, NGs were treated with multiple doses of the serotype of LPS applied in the *in vivo* study with or without combination of CXCL1 to determine levels of NET formation. Previous studies have suggested that CXCL1 may

be essential in NET-formation (Jin et al. 2014). Supernatants of these cultures were analyzed for the pro-inflammatory cytokines TNFα and IL-6.

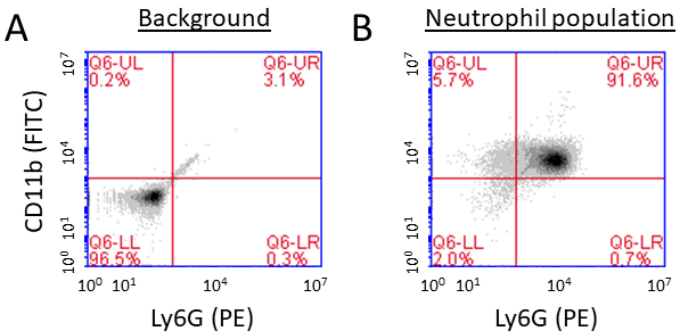

C

CD11b⁺Ly6G⁺ cells (%)	Unstained background (%)	Corrected CD11b⁺Ly6G⁺ (%)
91.6	3.1	88.5

Figure 28: Purity of NG isolations from bone marrow

Bone marrow derived cells were analyzed by flow cytometry to determine the purity of neutrophil granulocytes (NG). Immediately following EasySep™ isolation unstained control cells (A) were used to determine background staining for CD11b and Ly6G where $CD11b^+Ly6G^+$ cells were identified as NGs (B). The corrected $CD11b^+Ly6G^+$ population was determined by subtracting the unstained controls background staining from the total percentage of $CD11b^+Ly6G^+$ cells (C). Data obtained in cooperation with the Taubert Lab at JLU (Dr. Ivan Conejeros).

3.2.1.1 NET formation

Treatment with LPS at increasing concentrations was not sufficient to induce the formation of NETs *in vitro* (Figure 29). Overall, the morphology of NETs differed between groups. CD treatment was applied as a positive control and induced a high percentage of NET formation ($p = <0.0001$) but treatment with LPS at 1, 10, and 20 μg/ml with or without combination with CXCL1 (50 ng/ml) did not cause any significant shift from control wells treated with PBS. PMA served as another positive control but proved to be a weak inducer of NETs in the mouse NG cultures; therefore, CD replaced PMA as the positive control in further experiments. Although additional experiments need to be repeated with CD, these preliminary results indicate that LPS is not a strong inducer of NETosis.

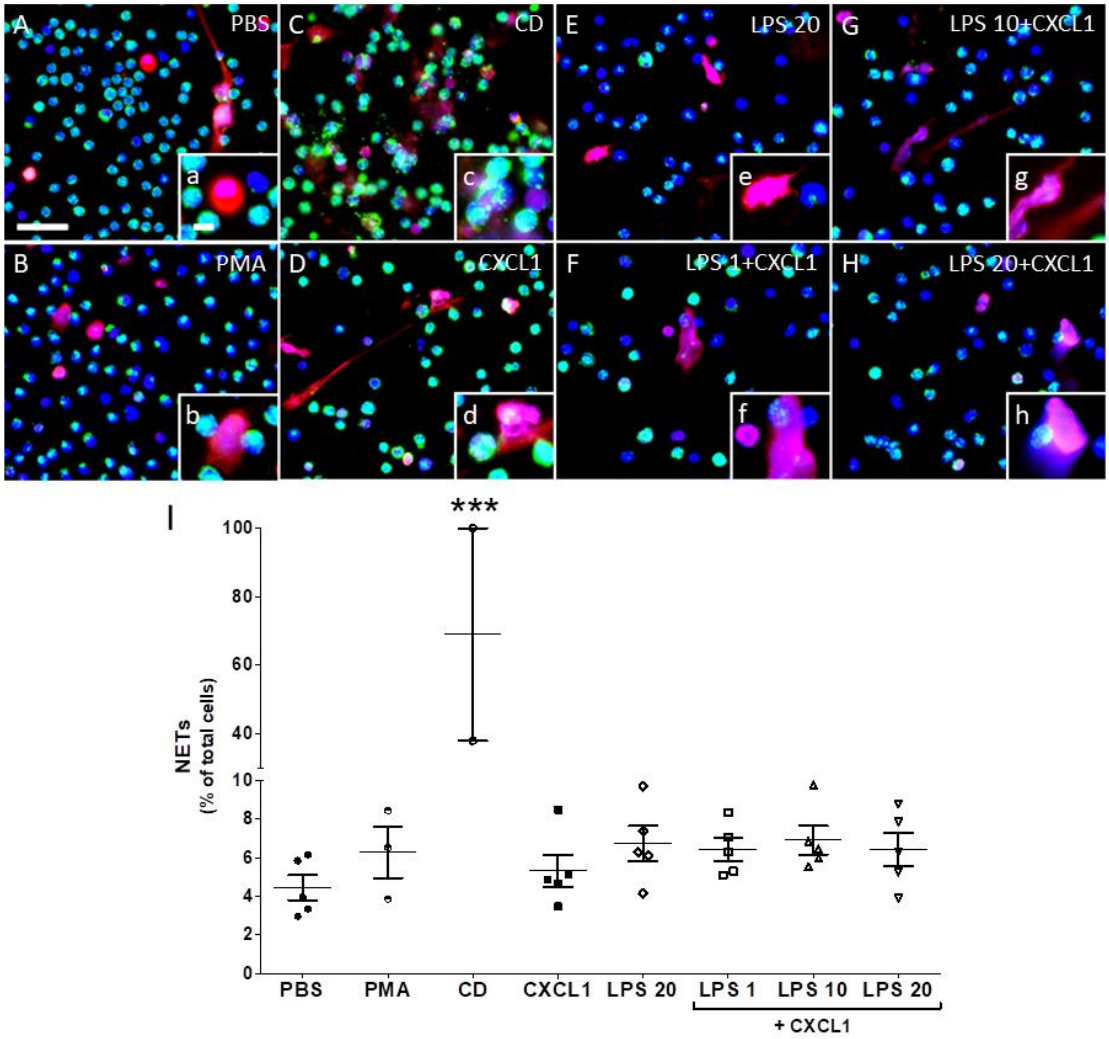

Figure 29: LPS failed to induce NET formation *in vitro* in a dose dependent manner

Bone marrow derived neutrophil granulocytes (NG) were isolated and cultured for 3 hours following treatment with lipopolysaccharide (LPS) at three different doses (1, 10, or 20 μg/ml) in combination with or without CXCL1 (50 ng/ml). Phosphate buffered saline (PBS) was used as a negative control and phorbol 12-myrisate a13-acetate (PMA; 25nM) was initially used as a positive control but was replaced with cyclodextrin (CD; 5mM) in the final two cultures. NETs were identified using DNA/histone complex (red) and myeloperoxidase (green; A-H). Abnormal NG shape and NET formation during each treatment is depicted in insets (a-h). All treatments except for CD failed to increase NET formation after 3 h. DAPI (blue; A-H) visualizes nuclear staining. Images represent the mean NET formation of each well (2-4 per experiment) of the mean of each treatment of the mean of all five independent experiments (except for PMA and CD, which only have an n=3 and n=2 respectively). The mean NET formation of each well of the mean of each treatment is reported as a percentage of total cells (I). ***$p<0.001$. Scale bar in A = 50 μm and is representative for A-H; Scale bar in a = 5 μm and is representative for a-h.

3.2.1.2 Release of mediators

TNFα and IL-6 release from cultured bone marrow derived NGs were quantified in supernatants to evaluate the inflammatory potential of NET formation. Treatment with LPS at increasing concentrations was not sufficient to significantly alter the release of TNFα or IL-6 from the control *in vitro* (Figure 30). Though treatment with LPS seemed to increase both cytokines, a high degree of variation prevented any significance.

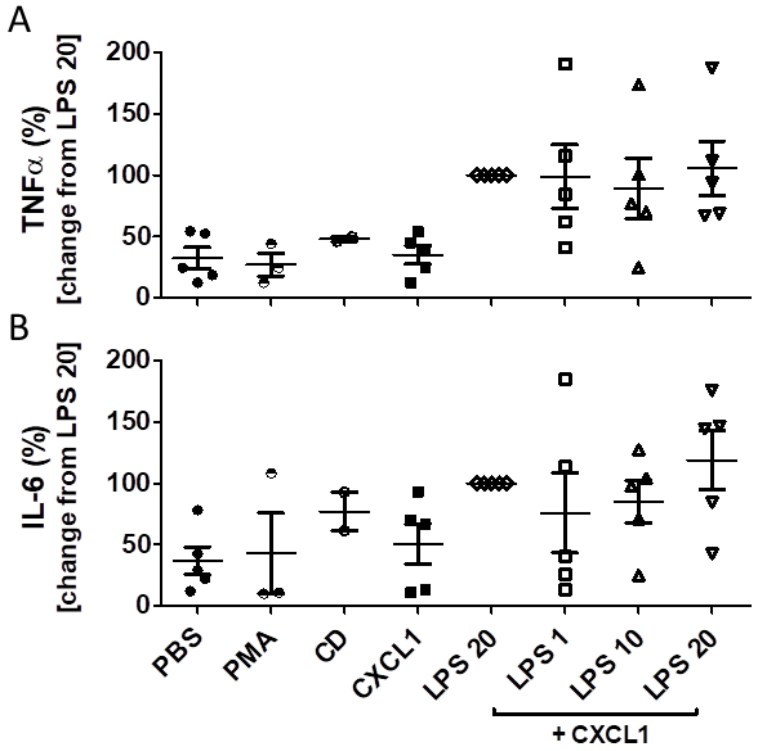

Figure 30: LPS failed to significantly increase the release of TNFα and IL-6 from NGs *in vitro* in a dose dependent manner

Bone marrow derived neutrophil granulocytes (NG) were isolated and cultured for 3 hours following treatment with lipopolysaccharide (LPS) at three different doses (1, 10, or 20 μg/ml) in combination with or without CXCL1 (50 ng/ml). PBS was used as a negative control and phorbol 12-myrisate a13-acetate (PMA; 25nM) was initially used as a positive control but was replaced with cyclodextrin (CD; 5mM) in the final two cultures. Levels of TNFα (A) and IL-6 (B) in the supernatant were measured and reported in reference to treatment with LPS 20 μg/ml. No differences in levels of TNFα or IL-6 were observed between any treatment and PBS control wells. The mean of each well (2-4 per experiment) of the mean of each treatment of the mean of all five independent experiments provided n=5 for all treatment groups except for PMA and CD which have an n=3 and n=2 respectively.

3.3 *In vivo* models of LPS-induced ARDS in ω-3 PUFA enriched and RvE1 receptor KO mice

3.3.1 Characterization of the role of ω-3 PUFA and RvE1 in humoral communication with the brain

To understand the impact of ω-3 PUFA and RvE1 receptors on the underlying mechanisms of the brain during LPS-induced ARDS, the humoral route of communication was extensively examined at three selected time points: 0 h, 24 h, and 72 h p.i. with LPS. To do so, mediators of inflammation in the periphery were analyzed in lung and liver tissues (as a marker for the systemic inflammatory response) by luminex assay. The selected mediators included pro- and anti-inflammatory cytokines as well as NG chemoattractants. Afterwards, the mRNA expression for markers for brain oxidative stress, immune cell trafficking, brain inflammatory responses (cytokines and signaling, enzyme of PG synthesis) and markers of neuroplasticity and glial activation were assessed in the hypothalamus.

3.3.1.1 Inflammatory mediator mRNA expression in the periphery

3.3.1.1.1 Lung

At the site of inflammation, i.e., the lung, mediators of inflammation appeared enhanced at 24 h p.i. These inflammatory mediators were modulated by genetic ω-3 PUFA enrichment and deficiencies of the RvE1 receptors over the course of inflammation (Figure 31). Main effects due to ω-3 PUFA enrichment and LR deficiency were already present at basal levels. However, as inflammation developed, effects at 24 h and 72 h p.i. became less frequent but, of those that remained, the majority occurred between the CR deficient mice and Norm controls (Figure 31 B).

At 0 h p.i., mice genetically enriched with ω-3 PUFAs (Fat background) had a strong impact on reducing the expression of nearly all inflammatory mediators although the effects were largely restricted to mice also deficient in the LR. In fact, IL-17 was the only mediator altered by ω-3 PUFA enrichment in the Norm controls (p = 0.0267).

Interestingly, ω-3 PUFA enrichment increased the levels of this cytokine. Overall, pro-inflammatory cytokines like IL-17 (p = 0.0010), IL-1β (p = 0.0366), and TNFα (p = 0.0266)); neutrophil chemoattractants GM-CSF (p = 0.0481) and CXCL5 (p = 0.0447); and the anti- inflammatory IL-10 (p = 0.0328) were all reduced in Fat-LR KO mice when compared to their Norm counterparts. IL-17 in particular was overall affected by LR deficiency, which decreased its levels in comparison to the Norm groups (Figure 31 B).

By 24 h p.i., only IL-10 was significantly reduced in CR KO mice on the WT background compared to WT-Norm controls (p = 0.0125) was the only specific change observed (Figure 31 A). However, several effects of ω-3 PUFA enrichment and the RvE1 receptors deficiency emerged. Compared to the 0 h time point, a stronger impact of CR was apparent at 24 h p.i. for IL-17 and IL-10 that decreased levels compared to Norm controls regardless of ω-3 PUFAs. The enrichment with ω-3 PUFAs also had its own effect and increased levels of CXCL1 in the Fat mice of the CR KO and Norm groups compared to WT. Now, the initially strong influence seen at basal levels in the Fat-LR KO groups had nearly vanished and an effect of the LR receptor deficiency only existed for IL-10 compared to Norm groups regardless of ω-3 PUFAs status. Additionally, between LR KO and Norm groups, ω-3 PUFA enrichment (Fat background) reduced levels of CXCL5 and IL-10 (Figure 31 B).

Finally, by 72 h p.i., a clear impact of the CR KO groups was present where deficiency in CR reduced the levels of most inflammatory mediators including IL-17, IL-1β, TNFα, GM-CSF, CXCL5, and IL-10 regardless of ω-3 PUFAs status (Figure 31 B). Although effects due to ω-3 PUFAs had come to an end at this point, the combination of ω-3 PUFA enrichment (Fat background) and CR deficiency lead to reduced levels of CXCL5 (p = 0.0463) and IL-10 (p = 0.0079) compared to Fat-Norm controls (Figure 31 A). During this late stage after LPS-stimulation, effects of the LR receptor had ceased entirely and significant differences between groups and overall main effects were no longer present.

Overall, predominantly at basal levels, genetic ω-3 PUFA enrichment (Fat background) did reduce inflammatory mediators in mice deficient in the RvE1 LR compared to Fat-Norm controls such as IL-17, IL-1β, TNFα, GM-CSF, CXCL5, and IL-10. However,

throughout inflammation CR deficiency had a more significant impact particularly during the late stage. At 72 h p.i., a robust effect of CR emerged when deficiency of this RvE1 receptor also decreased IL-17, IL-1β, TNFα, GM-CSF, CXCL5, and IL-10 in comparison to Norm control groups. One of the most consistent impacts of CR deficiency was for IL-10, which showed a prolonged reduction at 24 h and 72 h p.i. for this important anti-inflammatory cytokine compared to Norm controls.

A

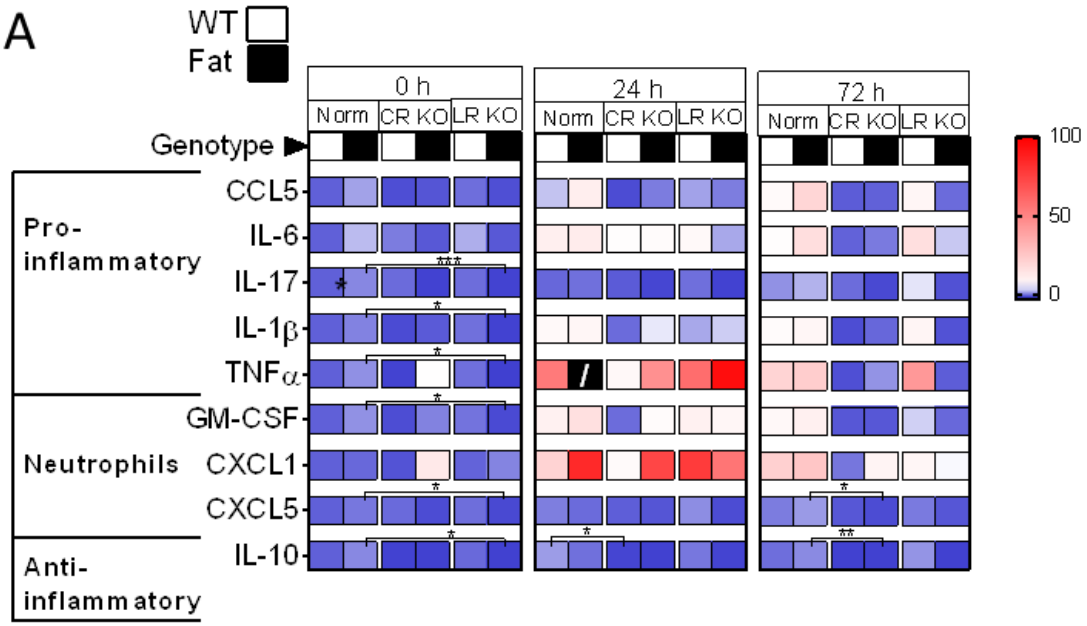

B

Time	Main effects	Group: Norm vs.	IL-17	IL-1β	TNFα	GM-CSF	CXCL1	CXCL5	IL-10
0 h	RvE1	LR KO	0.0064						
	ω-3 PUFAs	LR KO							
24 h	RvE1	CR KO	0.0334						0.0017
		LR KO							0.0372
	ω-3	CR KO					0.0321		
	PUFAs	LR KO						0.0374	0.0200
72 h	RvE1	CR KO	0.0465	0.0176	0.0477	0.0148		0.0098	0.0008
		LR KO							
	ω-3	CR KO							
	PUFAs	LR KO							

Figure 31: Changes in lung inflammatory mediators following LPS-induced ARDS

Luminex cytokine measurements from homogenized lung tissue assessing pro-inflammatory cytokines: chemokine (C-C motif) ligand 5 (CCL5), interleukin (IL)-6, IL-17, IL-1β, and tumor necrosis factor (TNF)α; neutrophil granulocyte chemoattractants: granulocyte-macrophage colony-stimulating factor (GM-CSF), chemokine (C-X-C motif) ligand (CXCL)1, and CXCL5; and the anti-inflammatory cytokine: IL-10. Unmodified control (Norm) mice as well as knock-out (KO) mice deficient in the RvE1 receptors chemerin receptor 23 (CR KO) or leukotriene B4 receptor (LR KO) were bred on a wild-type (WT) or genetically enriched ω-3 PUFA synthesizing Fat-1 (Fat) background. All mice were treated with lipopolysaccharide (LPS, 10 μg) via intra-tracheal (i.t.) instillation and were sacrificed at different time points: 0 h, 24 h, or 72 h p.i. (A). Impacts of ω-3 PUFAs and the CR and LR receptors are given for each time point to different extents. Significant alterations from ω-3 PUFAs and the RvE1 receptors are detected for IL-10. The main effects of ω-3 PUFAs and RvE1 receptor deficiencies and their p-values are shown in the table (B). The average fold change for each value was normalized to WT-Norm 0 h and shown as a value on the heat map. A white diagonal line through a black box is indicative of a value that exceeded the scaled range. n=3 except for the Fat-CR KO group at 0h where n=2; this group was excluded from the statistics but kept as a visually descriptive representation of data. *p<0.05, **p<0.01, ***p<0.001.

3.3.1.1.2 Liver

As a peripheral organ that responds to systemic inflammation, the liver was analyzed for changes in cytokine and NG chemoattractant protein levels in response to LPS-induced ARDS. The production of inflammatory mediators in the liver was far less pronounced in comparison to what had been observed in the lung (Figure 32). Almost all changes were restricted to main effects of either ω-3 PUFAs or RvE1 receptor deficiencies detected at 24 h p.i. with minor effects at the basal level and during late-stage inflammation (Figure 32 B).

A modest effect of CR KO-dependent increase in protein levels of CCL5 compared to the Norm groups was revealed while other inflammatory mediators remained unchanged. By 24 h p.i., more impacts of ω-3 PUFAs enrichment (Fat background) between the Norm and CR KO groups were evident as seen for the protein levels of CCL5, IL-17, and IL-10. An overall increase in CCL5 and IL-10 but decrease in IL-17 was observed when the ω-3 PUFA enriched mice (Fat background) were compared to WT mice from both Norm and CR KO groups. RvE1 receptor deficiencies did not have the same influence as ω-3 PUFAs at 24 h p.i. but, regardless of ω-3 PUFA status, groups lacking LR did have an overall increased level of IL-10 in comparison to Norm control groups. By late-stage inflammation, almost all differences had ceased and only a

minor reduction of the LR KO compared to Norm control groups for IL-17 remained (Figure 32 B).

Despite the weak activation observed in the liver, in addition to the main effects of ω-3 PUFA enrichment, there were several points at 24 h p.i. where inflammatory mediators were significantly changed in an ω-3 PUFA dependent manner. For instance, in the Norm controls ω-3 PUFA enrichment (Fat background) reduced levels of IL-17 (p = 0.0264). For IL-10, though the Norm controls were unaffected, CR deficiency in combination with ω-3 PUFA enrichment increased levels in the liver compared to the WT-CR KO group (p = 0.0027). In fact, both ω-3 PUFA enriched RvE1 receptor deficient KO groups had increased levels of IL-10 in comparison to the Fat-Norm controls (Fat-CR KO p = 0.0047; Fat-LR KO p = 0.0340). Overall, only modest impacts by ω-3 PUFAs and RvE1 receptors were revealed for a moderate systemic inflammatory response evidenced in the liver.

A

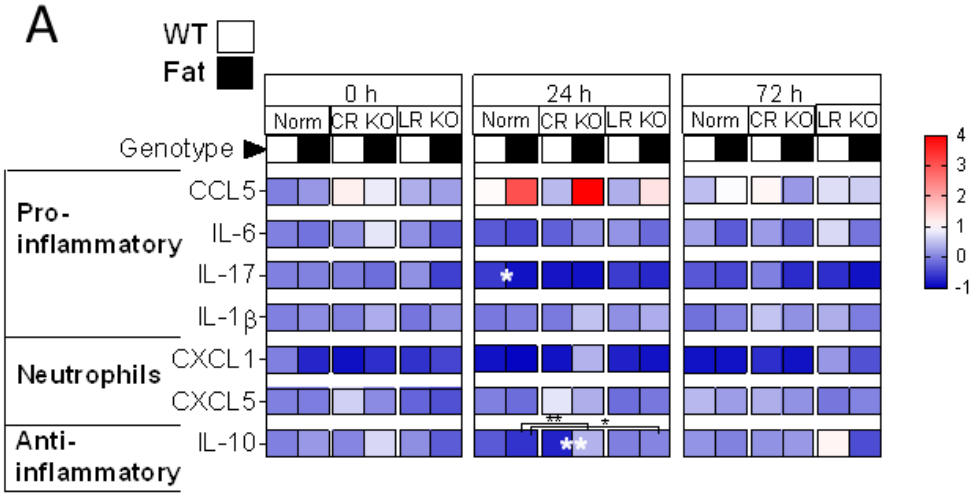

B

Time	Main effects	Group: Norm vs.	CCL5	IL-6	IL-17	IL-1β	CXCL1	CXCL5	IL-10
0 h	RvE1	CR KO	0.0336						
		LR KO							
24 h	RvE1	CR KO							
		LR KO							0.0065
	ω-3	CR KO	0.0355		0.0281				0.0347
	PUFAs	LR KO			0.0388				
72 h	RvE1	CR KO							
		LR KO			0.0045				

Figure 32: Changes in liver inflammatory mediators following LPS-induced ARDS

Luminex cytokine measurements from homogenized liver tissue evaluating pro-inflammatory cytokines: chemokine (C-C motif) ligand 5 (CCL5), interleukin (IL)-6, IL-17, and IL-1β; neutrophil granulocyte chemoattractants: chemokine (C-X-C motif) ligand (CXCL)1 and CXCL5; and the anti-inflammatory cytokine: IL-10. Unmodified control (Norm) mice as well as knock-out (KO) mice deficient in the RvE1 receptors chemerin receptor 23 (CR KO) or leukotriene B4 receptor (LR KO) were bred on a wild-type (WT) or genetically enriched ω-3 PUFA synthesizing Fat-1 (Fat) background. All mice were treated with lipopolysaccharide (LPS, 10 μg) via intra-tracheal (i.t.) instillation and were sacrificed at different time points: 0 h, 24 h, or 72 h p.i. (A). An impact of ω-3 PUFAs and the receptors CR and LR were most evident at 24 h p.i. but only a few significant differences between groups were present. The main effects of ω-3 PUFAs and RvE1 receptor deficiencies and their p-values are shown in the table (B). The average fold change for each value was normalized to WT-Norm 0 h and shown as a value on the heat map. n=3-5. *p<0.05, **p<0.01.

3.3.1.2 Inflammatory mediator mRNA expression in the hypothalamus

Since LPS-induced ARDS was sufficient to change inflammatory marker protein levels in the periphery and RvE1 receptor deficiency and ω-3 PUFA enrichment modulated this effect, my next aim was to evaluate markers for effects of lung inflammation on the brain.

3.3.1.2.1 Hypothalamic mRNA expression of marker proteins for oxidative stress

For oxidative stress, I analyzed the markers catalase (Cat), superoxide dismutase (SOD)1, SOD2, and nitric oxide synthase (NOS)2. Here, I found significant alterations by ω-3 PUFA enrichment and RvE1 receptor deficiencies over the course of inflammation (Figure 33). In particular, during the late stage of inflammation (72 h p.i.), ω-3 PUFA enrichment (Fat background) decreased the expression of NOS2 in the Norm controls (p = 0.0120) and all the markers of oxidative stress between Norm and CR KO groups regardless of RvE1 receptor expression. Fewer CR-dependent effects were present at the other time points except for NOS2. Indeed, starting at basal levels there was an early impact of CR deficiency on NOS2 expression, which caused a modest decrease compared to the Norm groups regardless of ω-3 PUFA status. By 24 h p.i., the CR KO induced reduction of NOS2 was still present and became significant between the CR KO and Norm controls on a WT background (p = 0.0133). This same effect persisted at 72 h p.i. where CR deficiency, in comparison to both Norm groups, continued to decrease the expression of NOS2 overall as well as between WT-CR KO and WT-Norm mice (p = 0.0049).

Deficiency in LR did not have as many effects as CR on the expression of markers of oxidative stress in the brain. At basal levels, ω-3 PUFA enrichment (Fat background) did increase expression of SOD2 (p = 0.0016) and caused an overall increase in its mRNA expression compared to Norm controls regardless of RvE1 receptor expression. In addition, LR deficiency in WT mice also caused a reduction in NOS2 expression from the WT-Norm controls at 72 h p.i. (p = 0.0068).

Further analysis of a marker of mitochondrial biogenesis and antioxidant effects (Wu et al. 1999, Kelly and Scarpulla 2004), namely mitochondrial transcription factor A (TFAM),

revealed a moderate influences of ω-3 PUFAs on TFAM mRNA expression. Between Norm and CR KO groups, ω-3 PUFA enrichment increased expression at 24 h p.i. and decreased expression at 72 h p.i. of TFAM regardless of RvE1 receptor expression. Moreover, ω-3 PUFAs enrichment did overall increase TFAM expression in Norm and LR KO groups.

In combination with the expression of the oxidative stress markers, these results showed ω-3 PUFA dependent alterations at basal levels and at 72 h p.i. particularly for SOD2, NOS2, and TFAM. Differences due to receptor deficiencies in relation to Norm mice were restricted to NOS2 with an earlier impact of CR at 24 h p.i. and CR and LR at 72 h p.i.

3.3.1.2.2 Hypothalamic mRNA expression of marker proteins for neutrophil granulocytes

During LPS-induced ALI, NGs can play a significant role in immune-to-brain signaling pathways (Nadeem et al. 2017). To gain insight into their recruitment to the hypothalamus during LPS-induced ARDS, I used the NG marker elastase (Elane) (Saadoun et al. 2012) and the NG chemoattractant CXCL1 (Figure 33). In doing so, I found main effects due to both RvE1 receptor deficiencies and ω-3 PUFA enrichment, the majority of which occurred at 24 h p.i. (Figure 33 B). For CXCL1, deficiencies in both CR and LR reduced expression, regardless of ω-3 PUFA enrichment, and ω-3 PUFAs increased expression regardless of RvE1 receptor status at 24 h p.i. Indeed, also at 24 h p.i., CXCL1 in Norm groups enriched with ω-3 PUFAs showed higher expression than the WT (p = 0.0248) and Fat-CR KO mice showed lower expression in comparison to Fat-Norm controls (p = 0.0111). LR deficiency alone reduced the expression compared to the Norm groups for elane at 24 h p.i. Aside from the 24 h effects, there was a minor alteration at basal levels between the Norm and CR KO mice where CR deficiency significantly reduced expression of CXCL1 regardless of ω-3 PUFAs. By 72 h p.i., all effects had ceased and no differences were detected between groups.

3.3.1.2.3 Hypothalamic mRNA expression of marker proteins for macrophages

Inflammation in the brain can lead to macrophage accumulation in the brain perivascular space and plexus (Corraliza 2014). Using the perivascular macrophage marker CD163 I carried out a preliminary analysis 24 h and 72 h after LPS-stimulation (Supplementary Figure 1) (Graeber et al. 1989, Galea et al. 2008). During late stage inflammation (72 h p.i.), Norm mice with ω-3 PUFA enrichment did have increased expression of CD163 compared to their WT counterparts. However, neither time point showed an effect of RvE1 receptors. Therefore, further analysis at 0 h p.i. were not performed.

3.3.1.2.4 Hypothalamic mRNA expression of pro- and anti-inflammatory cytokines

A selected panel of pro- and anti-inflammatory cytokines able to modulate inflammation during ARDS was used to determine cytokine expression in the hypothalamus. The cytokines evaluated included anti-inflammatory IL-10, pro-inflammatory IL-1β, and its antagonist IL-1ra (Figure 33) as well as pro-inflammatory IL-6 (Supplementary Figure 1). Unfortunately, IL-10 expression was difficult to detect and several samples were excluded due to 'undetermined' values, which possibly explains why significant differences were not detected. The preliminary investigation of IL-6 at 24 h and 72 h p.i. did not reveal significant differences between groups and, therefore, was not analyzed at 0 h. Otherwise, main effects and significant differences of ω-3 PUFAs and RvE1 were only detectable for the IL-1 family. Already at basal levels, ω-3 PUFA enrichment decreased expression of IL-1β in Norm and LR KO groups regardless of RvE1 receptor status. Additionally, ω-3 PUFA enrichment increased IL-1ra expression in the CR KO group (p = 0.0221), which was significantly higher than in the Fat-Norm controls (p = 0.0307).

By 24 h p.i., IL-1β expression was increased by ω-3 PUFA enrichment between LR deficient mice and Norm regardless of RvE1 receptor status. Moreover, IL-1β was significantly increased by ω-3 PUFA enrichment in Norm controls (p = 0.0148) and, in comparison, Fat-CR KO mice had a reduced expression (p = 0.0191). Overall, both CR and LR deficiency reduced the expression of IL-1β regardless of ω-3 PUFAs. Expression of IL-1ra was similarly increased by ω-3 PUFAs in Norm vs. CR and LR deficient groups

regardless of RvE1 receptor status. However, only the CR deficiency reduced expression compared to the Norm groups at 24 h p.i. (p = 0.0241). By 72 h p.i., all effects had ceased and no differences were detected between groups.

3.3.1.2.5 Hypothalamic mRNA expression of marker proteins for inflammatory signaling

The cytokines IL-1β and IL-6 can activate inflammatory signaling pathways via inflammatory transcription factors such as NF-IL6, NFκB, and signal transducer and activator of transcription (STAT)3 (see section 1.2.2) (Nadjar et al. 2005, Damm et al. 2011, Schneiders et al. 2015). The anti-inflammatory PPARγ pathway (peroxisome proliferator-activated receptor-α coactivator; PGC1α), which is increased in the brain during LPS-induced inflammation, is also utilized by lipid mediators for signaling (Koenig et al. 2014). Finally, I analyzed the PG precursor mPGES as it is another important target gene due to its role in fever development (Rummel et al. 2011). I evaluated the expression of NF-IL6, NFκB (via IκBα), PGC1α (Figure 33), and STAT3 (via suppressor of cytokine signaling (SOCS)3) during a preliminary analysis at 24 h and 72 h p.i. (Supplementary Figure 1) (Koenig et al. 2014). Only minor effects were detected. Interestingly, basal levels of NF-IL6 and PGC1α mRNA were differentially expressed due to genetic ω-3 PUFA enrichment (Figure 33 B). Regardless of RvE1 receptor status, NF-IL6 expression was reduced between Norm and CR KO groups while PGC1α was increased between Norm and LR KO groups by ω-3 PUFAs. Moreover, a modest impact of the LR deficiency to increase SOCS3 expression compared to Norm groups was revealed at 72 h p.i. (Supplementary Figure 1). No significant alterations were detected for NFκbiα but the apparent peak at 24 h p.i. indicates an overall increased inflammatory response in the brain. Together, ω-3 PUFAs have a modest influence on mRNA expression of NF-IL6 and PGC1α at basal levels while mPGES remained unchanged.

3.3.1.2.6 Hypothalamic mRNA expression of marker proteins for neuroplasticity and astrocytes

To identify activation and function within the hypothalamus, I analyzed the expression of brain-derived neurotrophic factor (BDNF), astrocytic marker protein glial fibrillary acidic

protein (GFAP) (Figure 33) and microglial activation marker CD68 (Bauer et al. 1994, Damoiseaux et al. 1994) (Supplementary Figure 1). Expression of BDNF and CD68 were unaffected by ω-3 PUFAs or RvE1 receptors but CR deficiency did alter GFAP at the basal level and again during late-stage inflammation (Figure 33; Supplementary Figure 1). Specifically, ω-3 genetically enriched mice deficient in CR (Fat-CR KO) had increased expression of GFAP compared to Fat-Norm controls at 0 h p.i. (p = 0.0162) and again at 72 h p.i. (p = 0.0480). Moreover, at 72 h p.i., ω-3 PUFA enrichment increased expression of GFAP in the CR KO mice (p = 0.0146). Changes in CD68 mRNA expression were not detected at 24 h or 72 h p.i., thus, I omitted further analyses (Supplementary Figure 1). These results suggest that genetic ω-3 PUFA enrichment impacts GFAP mRNA expression but only in mice deficient in CR.

3.3.1.2.7 Summary of findings for inflammatory mediator expression

During LPS-induced ARDS, I found that ω-3 PUFAs exerted a broader effect on inflammatory markers in the hypothalamus than the RvE1 receptors, although, receptor effects still occurred in most groups. Overall, the most robust impacts of receptor deficiencies occurred at 24 h p.i. for the CR KO group, in particular for the expression of NOS2, CXCL1, and IL-1β compared to Norm controls. Few effects remained during the late stage of inflammation (72 h p.i.) and those that persisted in CR KO mice were predominantly isolated to ω-3 PUFA effects on markers for oxidative stress and GFAP.

A

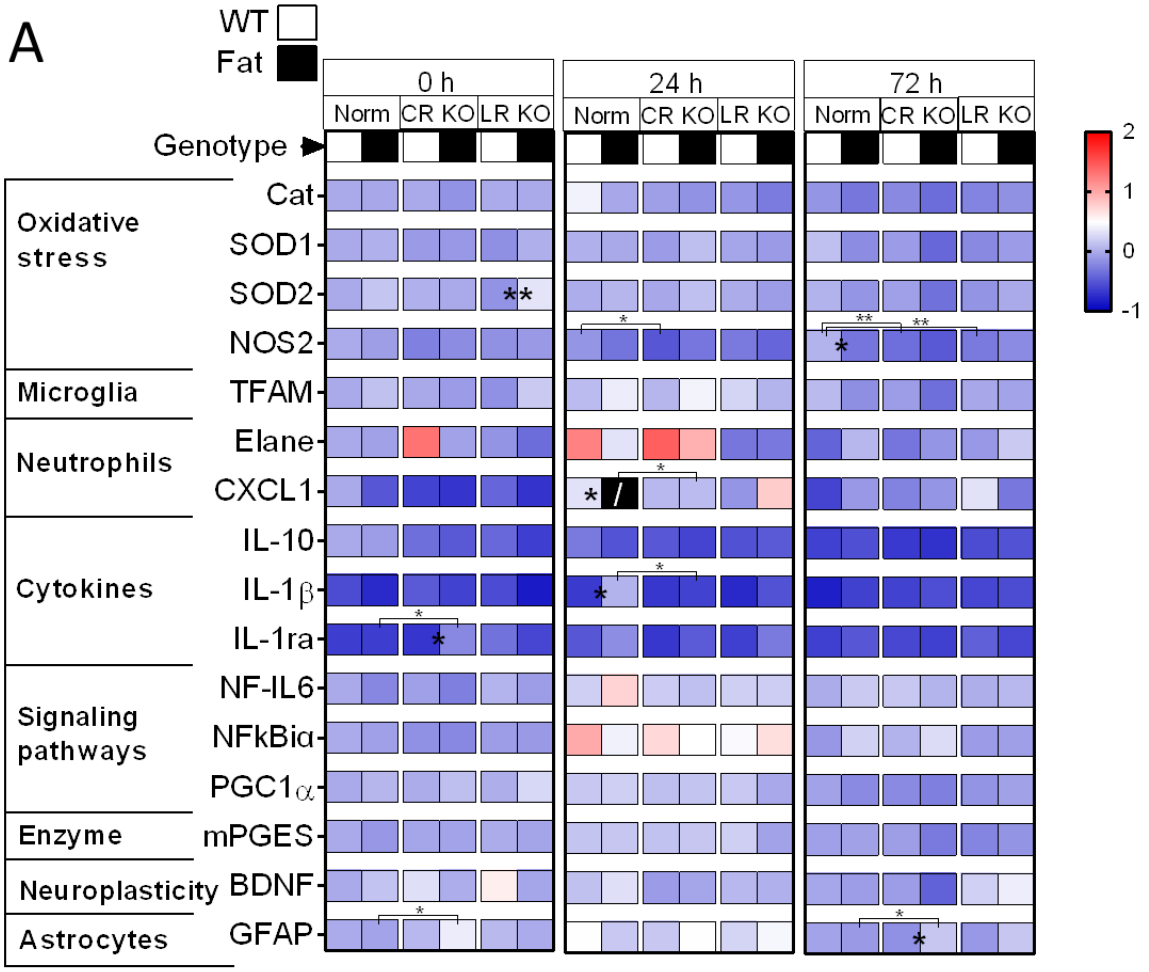

B

Time	Main effects	Group: Norm vs.	Cat	SOD1	SOD2	NOS2	TFAM	Elane	CXCL1	IL-1β	IL-1ra	NF-IL6	PGC1α	GFAP
0 h	RvE1 receptor	CR KO				0.0172			0.0261					0.0112
		LR KO												
	ω-3 PUFAs	CR KO									0.0347	0.0380		
		LR KO			0.0005		0.0268			0.0286			0.0280	
24 h	RvE1 receptor	CR KO				0.0275			0.0152	0.0268	0.0385			
		LR KO						0.0440	0.0380	0.0346				
	ω-3 PUFAs	CR KO					0.0487		0.0275	0.0126	0.0241			
		LR KO							0.0118	0.0044	0.0156			
72 h	RvE1 receptor	CR KO				0.0008								
		LR KO												
	ω-3 PUFAs	CR KO	0.0077	0.0178	0.0463	0.0029	0.0404							
		LR KO												

Figure 33: Changes in hypothalamic mRNA expression of inflammatory mediators following LPS-induced ARDS

RT-qPCR analysis of the hypothalamus for expression of markers for oxidative stress: catalase (Cat), superoxide dismutase (SOD)1, SOD2, and nitric oxide synthase (NOS)2; mitochondrial dysfunction:

transcription factor A, mitochondrial (TFAM); neutrophil granulocyte trafficking: elastase, neutrophil expressed (Elane) and chemokine (C-X-C motif) ligand (CXCL)1; anti-inflammatory cytokines: interleukin (IL)-10 and IL-1 receptor antagonist (ra); pro-inflammatory cytokine: IL-1β; signaling pathways: nuclear factor (NF)-IL6, NFκB via IκBα (iα), and PPARγ via peroxisome proliferator-activated receptor-α coactivator (PGC1α); Enzymes required for prostaglandin expression: microsomal prostaglandin E synthase (mPGES); neuroplasticity: brain-derived neurotrophic factor (BDNF); and astrocyte activation: glial fibrillary acidic protein (GFAP). Unmodified control (Norm) mice as well as knock-out (KO) mice deficient in the RvE1 receptors chemerin receptor 23 (CR KO) or leukotriene B4 receptor (LR KO) were bred on a wild-type (WT) or genetically enriched ω-3 PUFA synthesizing Fat-1 (Fat) background. All mice were treated with lipopolysaccharide (LPS, 10 μg) via intra-tracheal (i.t.) instillation and were sacrificed at different time points: 0 h, 24 h, or 72 h p.i. (A). The main effects of ω-3 PUFAs and RvE1 receptor deficiencies and their p-values are shown in the table (B). An impact of ω-3 PUFAs and the receptors CR and LR are apparent at each time point but for the mRNA expression of different marker proteins. The average fold change for each value was normalized to WT-Norm 0 h and shown as a value on the heat map. A white diagonal line through a black box is indicative of a value that exceeded the scaled range. After excluding outliers and undetermined values n=3-6, only IL-10 had fewer samples (n=1-5) therefore this group was excluded from the statistics but kept as a visually descriptive representation of data. *p<0.05, **p<0.01.

3.3.1.3 Immunohistochemical detection of inflammatory transcription factor expression at the OVLT, a brain structure with a leaky BBB, and the bifurcation, a brain structure with a complete BBB

NF-IL6 immunoreactivity served as a marker of humoral immune-to-brain signaling to further evaluate genomic brain cell activation (Rummel 2016); immunohistochemical detection of nuclear NF-IL6 signals was carried out at the level of the OVLT (see section 1.6.1) and BIF. These brain structures were selected based on the composition of the surrounding BBB where the OVLT is a brain structure with a leaky BBB, known to detect circulating mediators, and the BIF as a brain structure with a complete BBB (Bredehöft et al. 2019). Unfortunately, due to low n-numbers, damaged brain structures, or a combination of both, I was not always able to collect enough structures for all groups to perform statistical analyses (i.e., WT-Norm and Fat-CR KO). Therefore, descriptive data is presented for preliminary analysis.

In the OVLT, semi-quantitative evaluations of NF-IL6 immunoreactivity did not appear different between time points (Figure 34) or for CR KO (Figure 35) and LR KO mice (Figure 36). Low detection levels of nuclear NF-IL6 signaling suggest little genomic activation per section. Overall, significant changes in OVLT NF-IL6 immunoreactivity by

ω-3 PUFA enrichment or RvE1 receptor deficiency were not detected. In combination with the modest systemic inflammatory response identified in the liver, these results suggest that circulating cytokines may only modestly contribute to immune-to-brain communication during LPS-induced ARDS.

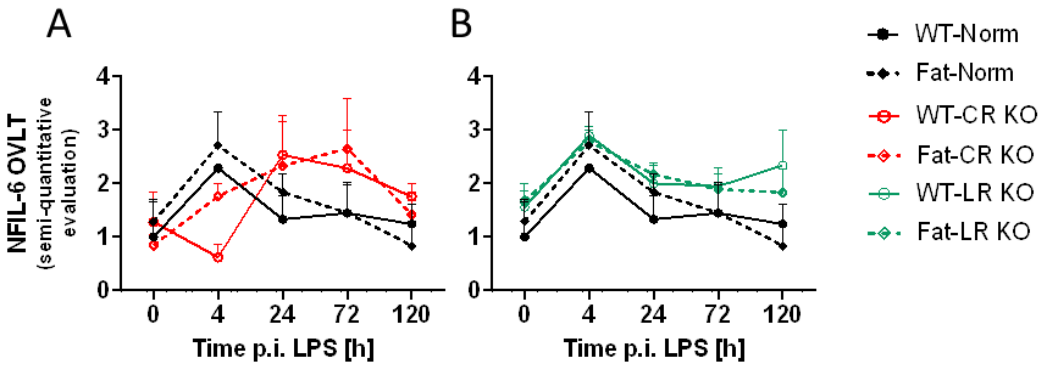

Figure 34: NF-IL6 immunoreactivity at the level of the OVLT in Norm, CR KO, and LR KO mice over time after LPS-induced ARDS

Analysis of the brain at the level of the *organum vasculosum of the lamina terminalis* (OVLT) for nuclear factor (NF)-interleukin (IL) 6 immunoreactivity on a semi-quantitative scale ranging from 0-4 (A-B). Unmodified control mice (Norm, black) were compared to two different RvE1 receptor knock-out (KO) mice, i.e., chemerin receptor 23 (CR KO; A, red) and leukotriene B4 receptor (LR KO; B, green). All mice were bred on wild-type (WT; solid line) or genetically enriched ω-3 PUFA synthesizing Fat-1 (Fat; dashed line) background. All mice were treated with lipopolysaccharide (LPS, 10 μg) via intra-tracheal (i.t.) instillation and were sacrificed at different time points: 0 h, 4 h, 24 h, 72 h, and 120 h p.i. Immunofluorescent staining was used to analyze sections using an antibody for NF-IL6. The immunoreactivity was assessed by semi-quantitative evaluation (see section 2.7.6). n= 1-5. Due to low n-numbers statistics were not performed but the data was presented as a visually descriptive representation.

A

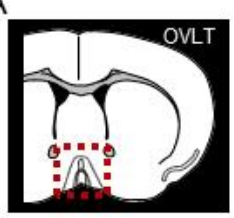

B

NF-IL6 OVLT Semi-quantitative Evaluation	0 h	4 h	24 h	72 h	120 h
WT-Norm	0.75	2.75	0.25	1.00	0.75
Fat-Norm	0.75	2.00	1.25	1.00	0.75
WT-CR KO	1.75	0.75	2.75	2.25	2.00
Fat-CR KO	0.75	1.75	2.25	2.75	1.25

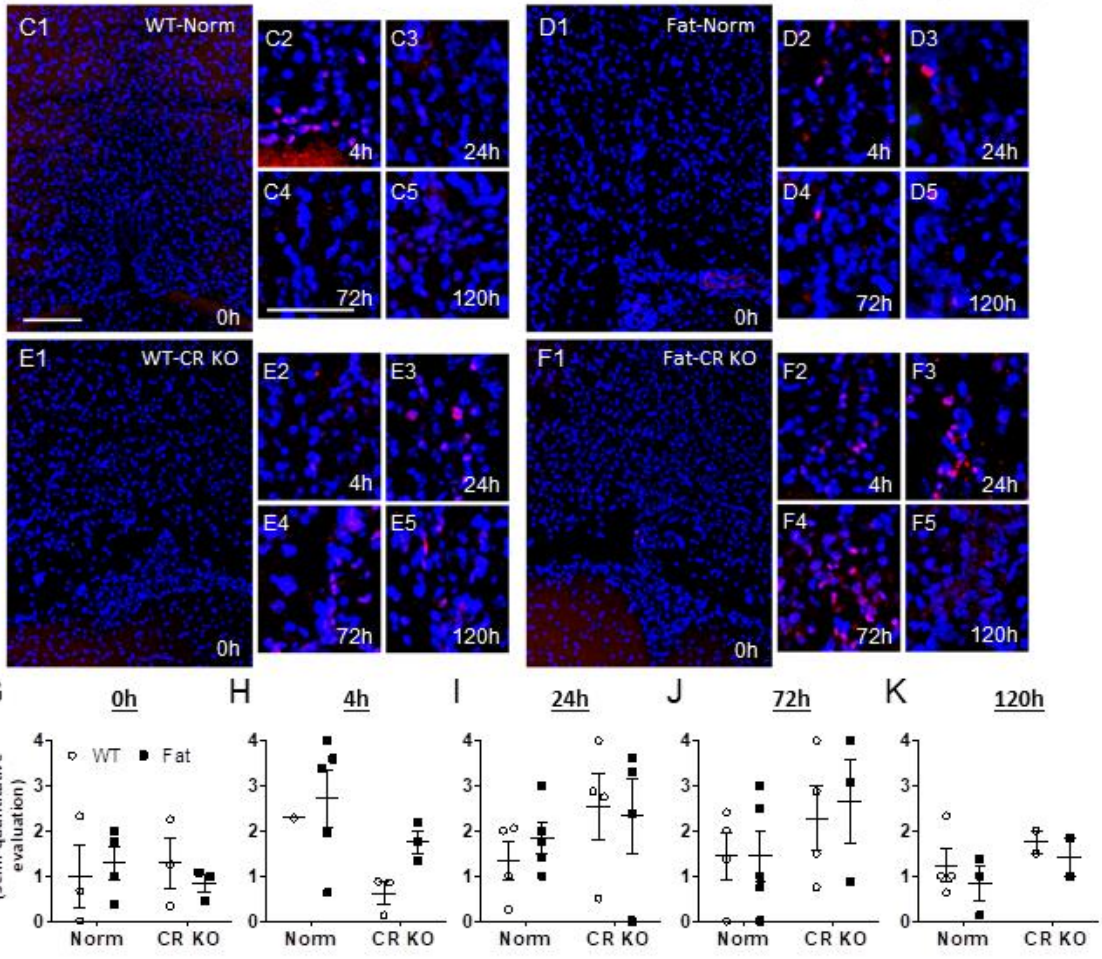

Figure 35: LPS-induced ARDS NF-IL6 immunoreactivity at the level of the OVLT in Norm vs. CR KO mice was not significantly altered

Analysis of the brain at the level of the *organum vasculosum of the lamina terminalis* (OVLT; A) for nuclear factor (NF)-interleukin (IL) 6 (red, C-F) immunoreactivity on a semi-quantitative scale ranging from 0-4 (B). Unmodified control mice (Norm; C, D) were compared to the RvE1 chemerin receptor 23 knock-out mice (CR KO; E, F) on a wild-type (WT; C, E) or genetically enriched ω-3 PUFA synthesizing Fat-1 (Fat; D, F) background. All mice were treated with lipopolysaccharide (LPS, 10 μg) via intra-tracheal (i.t.) instillation and were sacrificed at different time points: 0 h, 4 h, 24 h, 72 h, and 120 h p.i. At each time point, Norm (WT-/Fat-) groups were compared to CR KO (WT-/Fat-) groups (G-K). Statistics were performed when n ≥ 3 but the data was presented as a visually descriptive representation when n<3. No differences were observed between groups. Staining also shows: Von Willebrand factor (green; C-F)

depicting brain vasculature; DAPI (blue; C-F) visualizes surrounding tissue. n= 1-5. For C1, D1, E1, and F1 a representative scale bar shown in Figure C1 = 100 µm; For C2-C5, D2-D5, E2-E5, and F2-F5 a representative scale bar shown in Figure C4 = 50 µm.

A

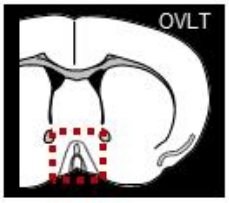

B

NF-IL6 OVLT Semi-quantitative Evaluation	0 h	4 h	24 h	72 h	120 h
WT-Norm	0.75	2.75	0.75	1.00	0.75
Fat-Norm	0.75	2.00	1.25	1.00	0.75
WT-LR KO	1.75	3.00	2.00	2.00	2.25
Fat-LR KO	1.75	2.75	2.25	2.00	1.75

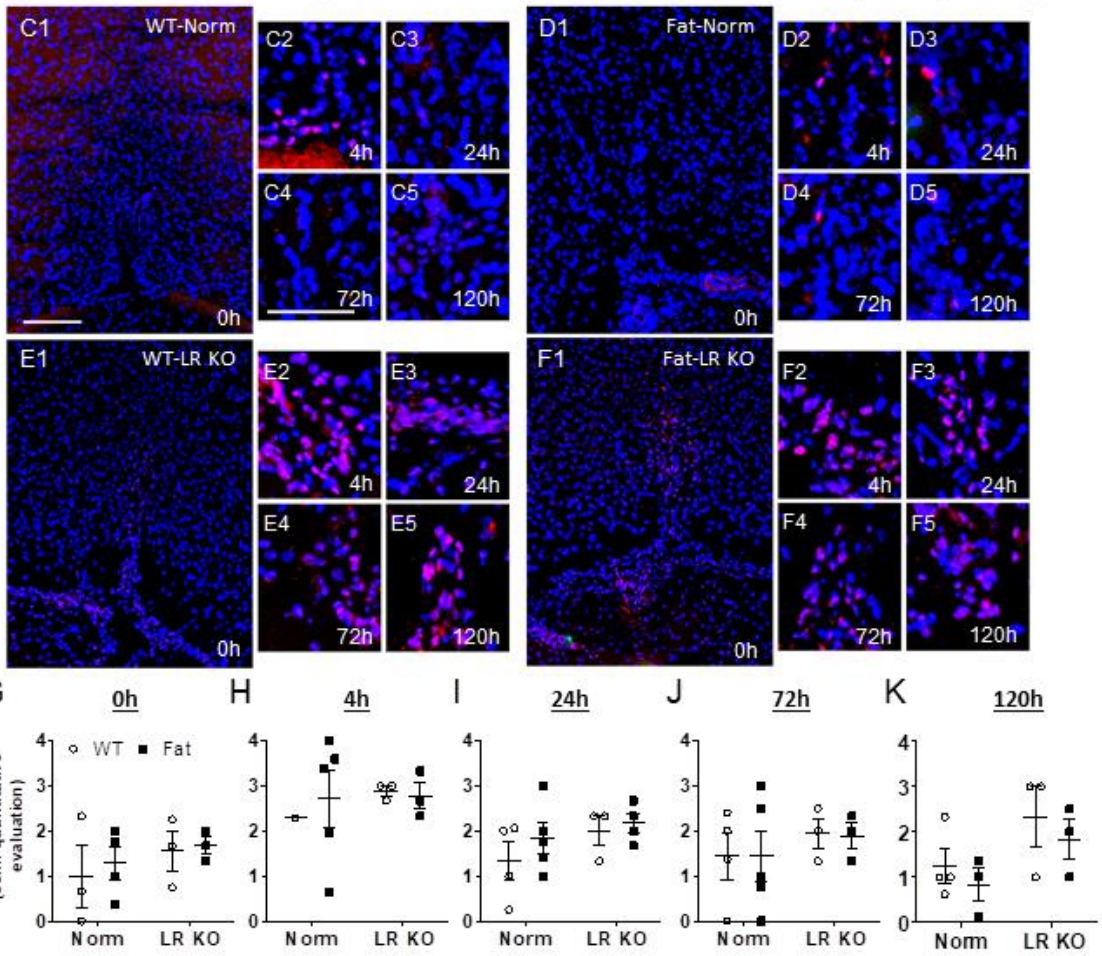

Figure 36: LPS-induced ARDS NF-IL6 immunoreactivity at the level of the OVLT in Norm vs. LR KO mice is not significantly altered

Analysis of the brain at the level of the *organum vasculosum of the lamina terminalis* (OVLT; A) for nuclear factor (NF)-interleukin (IL) 6 (red, C-F) immunoreactivity on a semi-quantitative scale ranging from 0-4 (B). Unmodified control mice (Norm; C, D) were compared to the RvE1 leukotriene B4 receptor

knock-out mice (LR KO; E, F) on a wild-type (WT; C, E) or genetically enriched ω-3 PUFA synthesizing Fat-1 (Fat; D, F) background. All mice were treated with lipopolysaccharide (LPS, 10 μg) via intra-tracheal (i.t.) instillation and were sacrificed at different time points: 0 h, 4 h, 24 h, 72 h, and 120 h p.i. At each time, point Norm (WT-/Fat-) groups were compared to LR KO (WT-/Fat-) groups (G-K). Statistics were performed when n ≥ 3 but the data was presented as a visually descriptive representation when n < 3. No differences were observed between groups. Staining also shows: Myeloperoxidase (green; E, F) visualizes neutrophil granulocytes; DAPI (blue; C-F) visualizes surrounding tissue. n= 1-5. For C1, D1, E1, and F1 a representative scale bar shown in Figure C1 = 100 μm; For C2-C5, D2-D5, E2-E5, and F2-F5 a representative scale bar shown in Figure C4 = 50 μm. Please note, the data on WT-Norm and Fat-Norm controls is displayed again from Figure 35 for comparison.

Unlike the OVLT, semi-quantitative evaluation of NF-IL6 immunoreactivity at the level of the BIF seemed to show a peak in NF-IL6 immunoreactivity in WT and Fat- Norm groups at 4 h p.i. (Figure 37). As I had previously observed that ω-3 PUFA enrichment in CR deficient mice caused moderate alterations to NF-IL6 mRNA expression in the hypothalamus (Figure 33), immunofluorescence of the BIF showed that a deficiency in RvE1 CR but not genetic ω-3 PUFA enrichment status may increase immunoreactivity at 24 h p.i. (p = 0.0197) (Figure 38). However, in LR KO mice, the RvE1 receptor dependent increase was only significant at 0 h p.i. (p = 0.0098) (Figure 39). Together, a modest increase in NF-IL6 activation at 4 h after LPS-induced ARDS may be identified for the BIF suggesting a moderate but low systemic inflammatory response (Figure 32) capable of contributing to minor humoral signals to the brain in the current model.

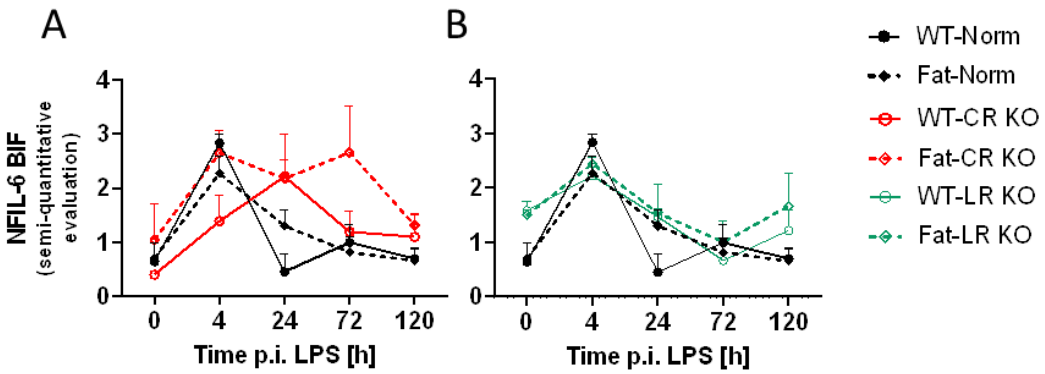

Figure 37: NF-IL6 immunoreactivity at the level of the BIF in Norm, CR KO, and LR KO mice over time after LPS-induced ARDS

Analysis of the bifurcation (BIF) for nuclear factor (NF)-interleukin (IL) 6 immunoreactivity on a semi-quantitative scale ranging from 0-4 (A-B). Unmodified control mice (Norm; black) were compared to two different RvE1 receptor knock-out (KO) mice, i.e., chemerin receptor 23 (CR KO; A, red) or leukotriene B4 receptor (LR KO; B, green). All mice were bred on a wild-type (WT; solid line) or genetically enriched ω-3 PUFA synthesizing Fat-1 (Fat; dashed line) background. All mice were treated with lipopolysaccharide (LPS, 10 μg) via intra-tracheal (i.t.) instillation and were sacrificed at different time points: 0 h, 4 h, 24 h, 72 h, and 120 h p.i. Immunofluorescent staining was used to analyze sections using an antibody for NF-IL6. n= 2-5 per group. Due to low n-numbers statistics were not performed but the data was presented as a visually descriptive representation.

A

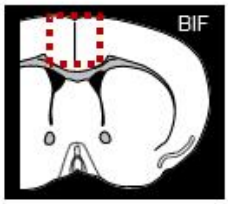

B

NF-IL6 BIF Semi-quantitative Evaluation	0 h	4 h	24 h	72 h	120 h
WT-Norm	0.75	2.75	0.25	1.00	0.75
Fat-Norm	0.75	2.00	1.25	1.00	0.75
WT-CR KO	0.75	1.25	2.25	1.25	1.00
Fat-CR KO	1.00	2.75	2.25	2.75	1.25

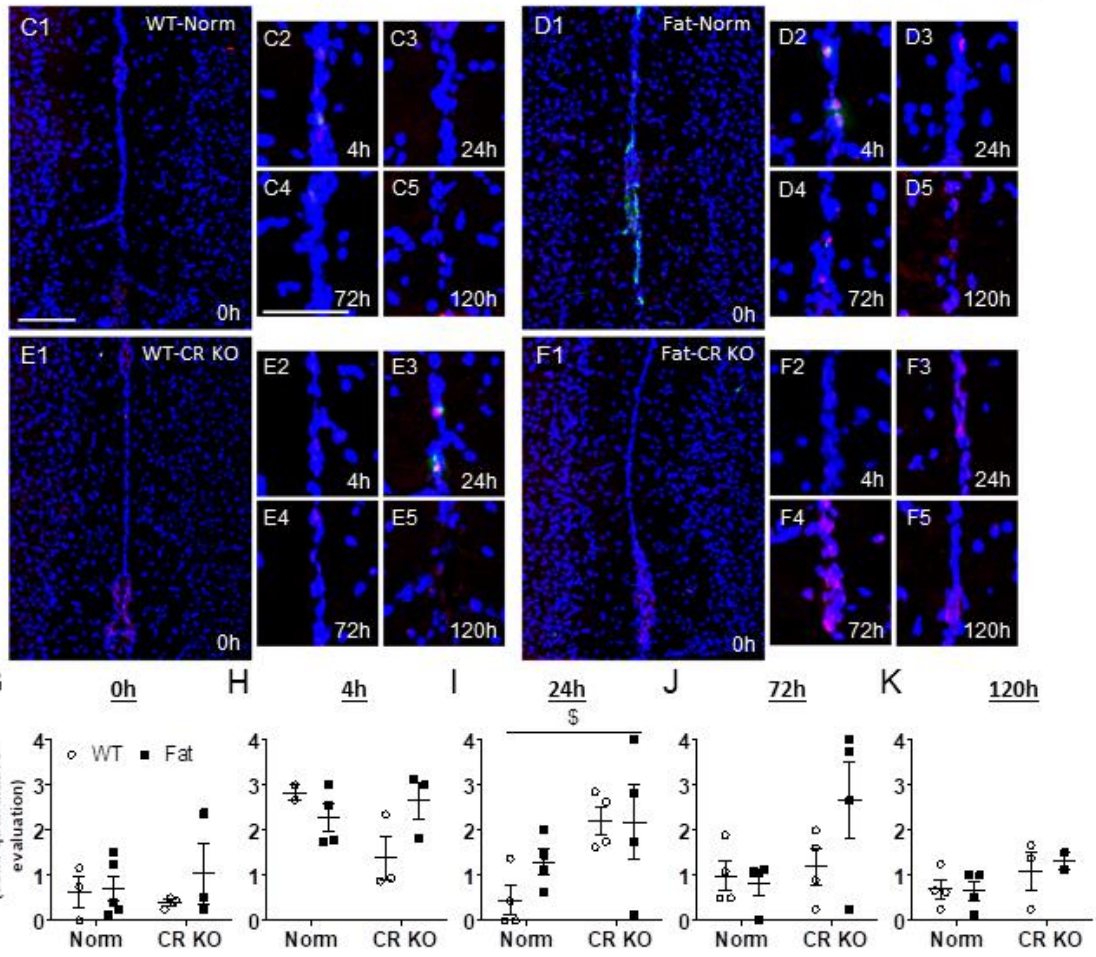

Figure 38: LPS-induced ARDS NF-IL6 immunoreactivity at the level of the BIF in Norm vs. CR KO mice is significantly altered at 24 h p.i.

Analysis of the bifurcation (BIF; A) for nuclear factor (NF)-interleukin (IL) 6 immunoreactivity (NF-IL6; red, C-F) on a semi-quantitative scale ranging from 0-4 (B). Unmodified control mice (Norm; C, D) were compared to the RvE1 chemerin receptor 23 knock-out mice (CR KO; E, F) on a wild-type (WT; C, E) or genetically enriched ω-3 PUFA synthesizing Fat-1 (Fat; D, F) background. All mice were treated with lipopolysaccharide (LPS, 10 μg) via intra-tracheal (i.t.) instillation and were sacrificed at different time points: 0 h, 4 h, 24 h, 72 h, and 120 h p.i. At each time point, Norm (WT-/Fat-) groups were compared to CR KO (WT-/Fat-) groups (G-K). Statistics were performed when n ≥ 3 but the data was presented as a visually descriptive representation when n < 3. At 24 h p.i with LPS CR KO mice had increased NF-IL6 immunoreactivity in comparison to Norm controls regardless of ω-3 PUFA enrichment. Staining also

shows: Von Willebrand factor (green; C-F) depicting brain vasculature; DAPI (blue; C-F) visualizes surrounding tissue. n= 2-5. $ main effect Norm vs. CR KO. For C1, D1, E1, and F1 a representative scale bar shown in Figure C1 = 100 μm; For C2-C5, D2-D5, E2-E5, and F2-F5 a representative scale bar shown in Figure C4 = 50 μm. $ p<0.05.

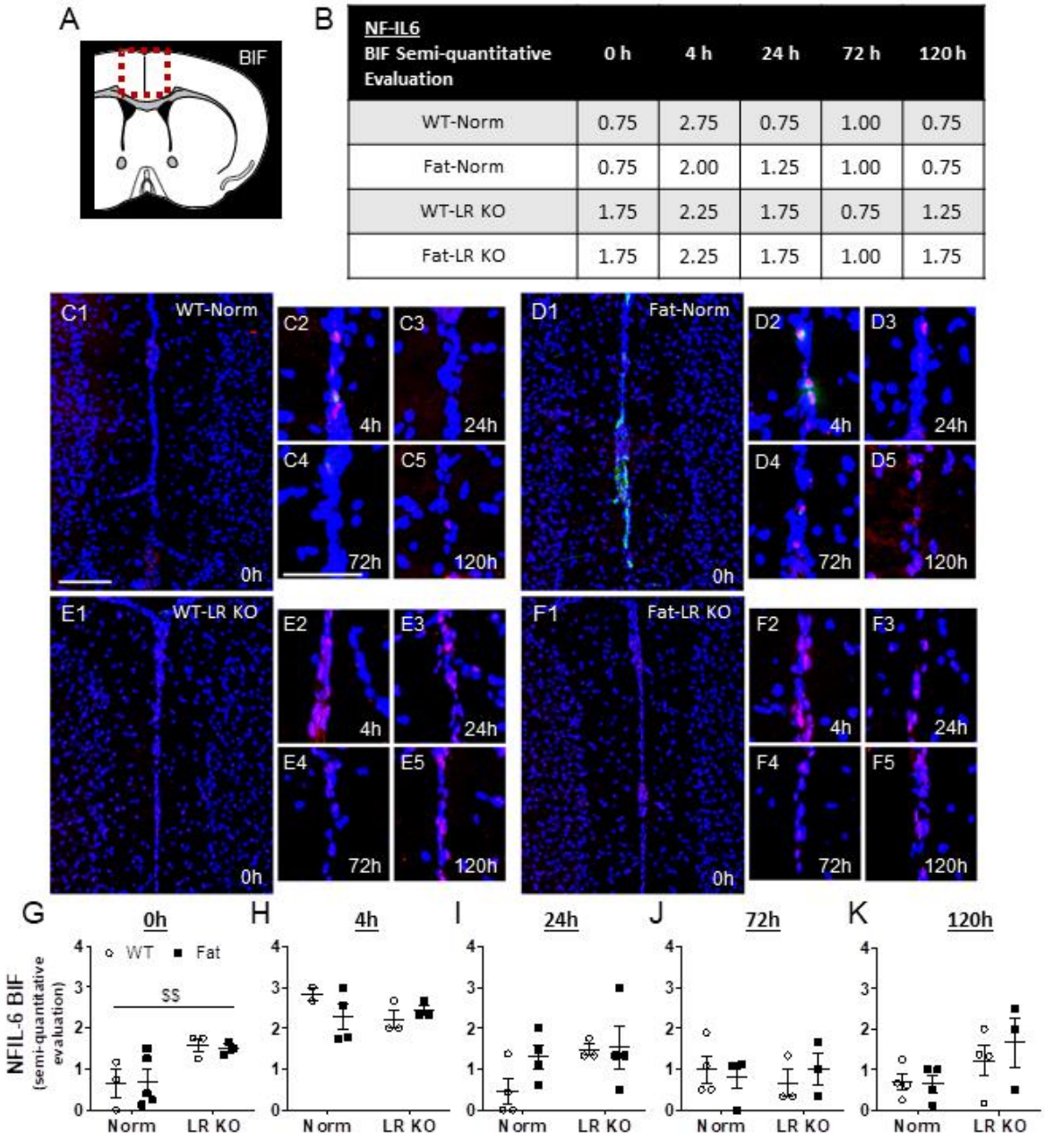

NF-IL6 BIF Semi-quantitative Evaluation	0 h	4 h	24 h	72 h	120 h
WT-Norm	0.75	2.75	0.75	1.00	0.75
Fat-Norm	0.75	2.00	1.25	1.00	0.75
WT-LR KO	1.75	2.25	1.75	0.75	1.25
Fat-LR KO	1.75	2.25	1.75	1.00	1.75

Figure 39: LPS-induced ARDS NF-IL6 immunoreactivity at the level of the BIF in Norm vs. LR KO mice is significantly altered at 0 h p.i.

Analysis of the bifurcation (BIF; A) for nuclear factor (NF)-interleukin (IL) 6 immunoreactivity (NF-IL6; red, C-F) on a semi-quantitative scale ranging from 0-4 (B). Unmodified control mice (Norm; C, D) were

compared to the RvE1 leukotriene B4 receptor knock-out mice (LR KO; E, F) on a wild-type (WT; C, E) or genetically enriched ω-3 PUFA synthesizing Fat-1 (Fat; D, F) background. All mice were treated with lipopolysaccharide (LPS, 10 μg) via intra-tracheal (i.t.) instillation and were sacrificed at different time points: 0 h, 4 h, 24 h, 72 h, and 120 h p.i. At each time point, Norm (WT-/Fat-) groups were compared to LR KO (WT-/Fat-) groups (G-K). Statistics were performed when n ≥ 3 but the data was presented as a visually descriptive representation when n < 3. At 0 h p.i with LPS LR KO mice had increased NF-IL6 immunoreactivity in comparison to Norm controls regardless of ω-3 PUFA enrichment. Staining also shows: Von Willebrand factor (green; C, D) depicts brain vasculature; DAPI (blue; C-F) visualizes surrounding tissue. n= 2-5. $ main effect Norm vs. LR KO. For C1, D1, E1, and F1 a representative scale bar shown in Figure C1 = 100 μm; For C2-C5, D2-D5, E2-E5, and F2-F5 a representative scale bar shown in Figure C4 = 50 μm. $$ p<0.01. Please note, the data on WT-Norm and Fat-Norm controls is displayed again from Figure 38 for comparison.

3.3.1.4 Immunohistochemical detection of neutrophil granulocyte recruitment to the OVLT and bifurcation

To expand on the hypothalamic mRNA expression of markers for NG recruitment to the brain during LPS-induced ARDS (Figure 33), I performed immunohistochemical staining using MPO to identify NGs at two different brain structures: the OVLT and BIF. During early systemic inflammation, MPO staining is a useful tool to identify NG recruitment to the brain (Pflieger et al. 2018). As with NF-IL6, low n-numbers for the groups WT-Norm and Fat-CR KO meant that the analysis were presented as preliminary descriptive data.

The peak of NG recruitment to both brain structures appeared to occur at 4 h p.i. in WT-Norm controls but was reduced by ω-3 PUFA enrichment (i.e., Fat-Norm, Figure 40). Additionally, although recruitment of NGs to the OVLT was low, CR deficiency was able to increase NG recruitment in comparison to the Norm groups regardless of ω-3 PUFA enrichment at basal levels (p = 0.0340) (Figure 41) but LR deficiency only exerted a minor increase at 120 h p.i. (p = 0.0136) (Figure 42). Descriptive analyses of alterations between Norm and CR KO mice may indicate a modulatory role for RvE1 receptors in NG recruitment to the OVLT.

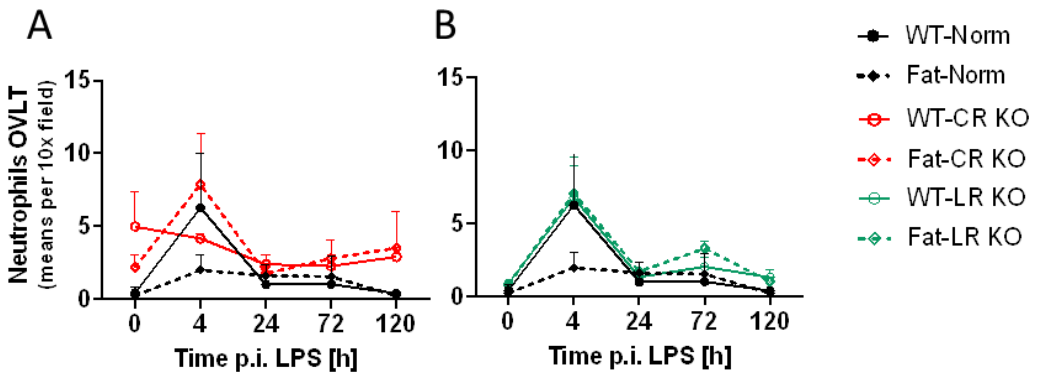

Figure 40: NG recruitment at the level of the OVLT in Norm, CR KO, and LR KO mice over time after LPS-induced ARDS

Analysis of the brain at the level of the *organum vasculosum of the lamina terminalis* (OVLT) for neutrophil granulocyte (NG) recruitment to the brain (A-B). Unmodified control mice (Norm; black) were compared to two different RvE1 receptor knock-out (KO) mice, i.e., chemerin receptor 23 (CR KO; A, red) or leukotriene B4 receptor (LR KO; B, green). All mice were bred on a wild-type (WT; solid line) or genetically enriched ω-3 PUFA synthesizing Fat-1 (Fat; dashed line) background. All mice were treated with lipopolysaccharide (LPS, 10 μg) via intra-tracheal (i.t.) instillation and were sacrificed at different time points: 0 h, 4 h, 24 h, 72 h, and 120 h p.i. Immunofluorescent staining was used to analyze sections using an antibody for myeloperoxidase. Images were taken and NGs were counted in the 10x field of view. n= 2-5. Due to low n-numbers statistics were not performed but the data was presented as a visually descriptive representation.

A

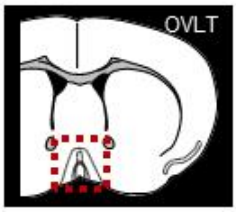

B

Neutrophils OVLT Means per 10x field	0 h	4 h	24 h	72 h	120 h
WT-Norm	0.4	6.3	1.0	1.0	0.4
Fat-Norm	0.2	2.0	1.6	1.5	0.2
WT-CR KO	5.0	4.1	2.4	2.3	2.9
Fat-CR KO	2.2	7.9	1.7	2.8	3.5

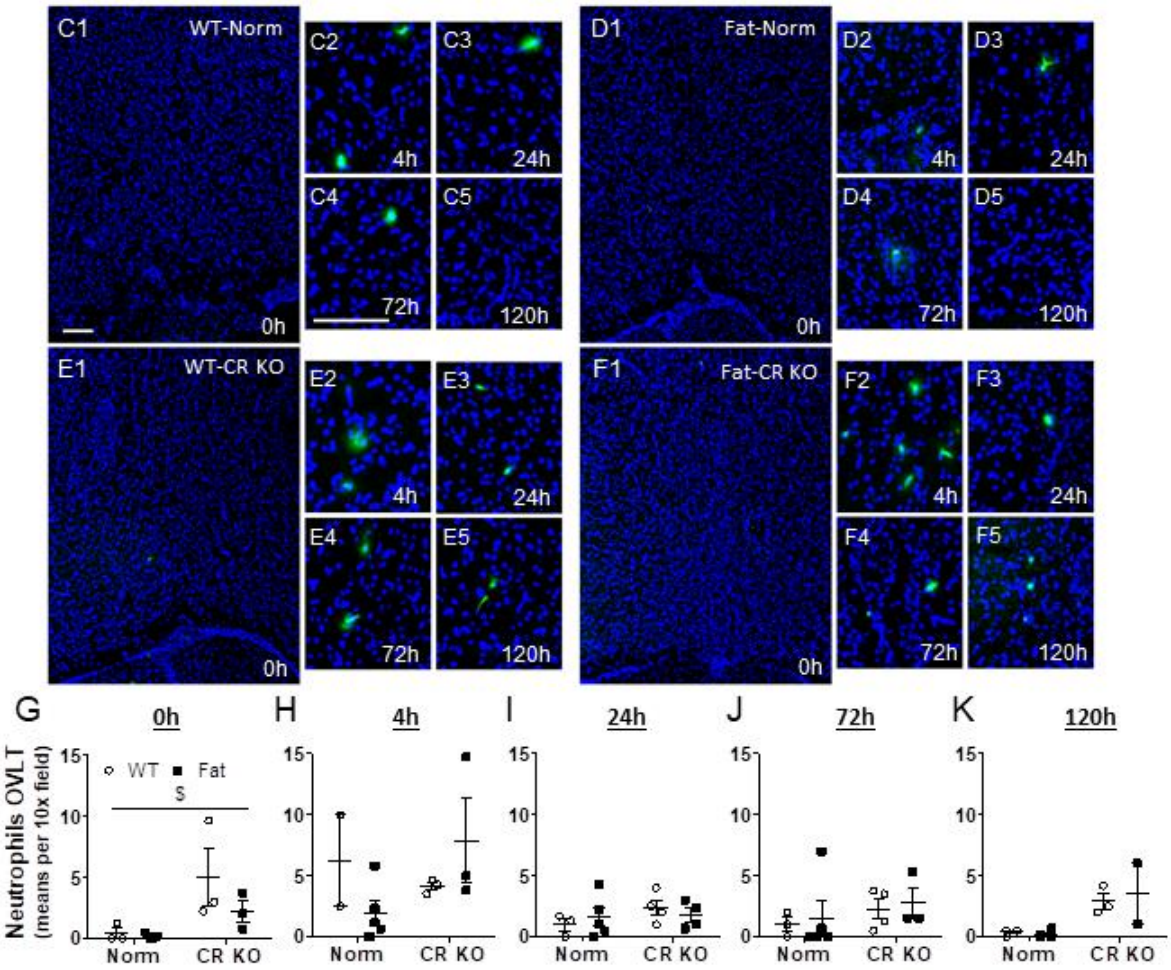

Figure 41: LPS-induced NG recruitment to the OVLT in Norm controls vs. CR KO mice is significantly altered at 0 h p.i.

At the level of the *organum vasculosum of the lamina terminalis* (OVLT; A) recruited neutrophil granulocytes (NG; green, C-F) were counted (B). Unmodified control mice (Norm; C, D) were compared to the RvE1 chemerin receptor 23 knock-out mice (CR KO; E, F) on a wild-type (WT; C, E) or genetically enriched ω-3 PUFA synthesizing Fat-1 (Fat; D, F) background. All mice were treated with lipopolysaccharide (LPS, 10 μg) via intra-tracheal (i.t.) instillation and were sacrificed at different time points: 0 h, 4 h, 24 h, 72 h, and 120 h p.i. At each time point NGs were counted per 10x field of view and compared between Norm (WT-/Fat-) groups vs. CR KO (WT-/Fat-) groups (G-K). Statistics were performed when $n \geq 3$ but the data was presented as a visually descriptive representation when $n < 3$. At 0 h p.i. with LPS CR KO mice had increased NG recruitment in comparison to Norm controls regardless of

ω-3 PUFA enrichment. Staining also shows: DAPI (blue; C-F) visualizes surrounding tissue. n= 2-5. $ Norm vs. CR KO. For C1, D1, E1, and F1 a representative scale bar shown in Figure C1 = 100 μm; For C2-C5, D2-D5, E2-E5, and F2-F5 a representative scale bar shown in Figure C4 = 50 μm. $ p<0.05.

A

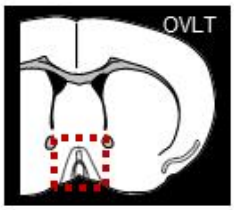

B

Neutrophils OVLT Means per 10x field	0 h	4 h	24 h	72 h	120 h
WT-Norm	0.4	6.3	1.0	1.0	0.4
Fat-Norm	0.2	2.0	1.6	1.5	0.2
WT-LR KO	0.9	5.3	1.2	2.0	1.3
Fat-LR KO	0.8	7.1	1.7	3.3	1.0

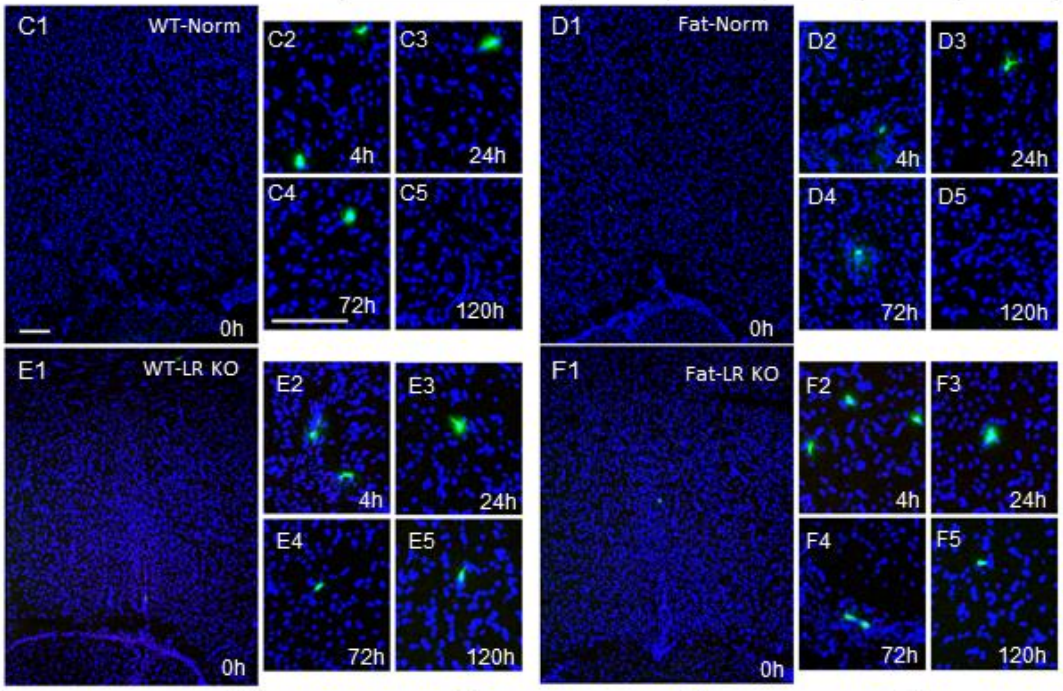

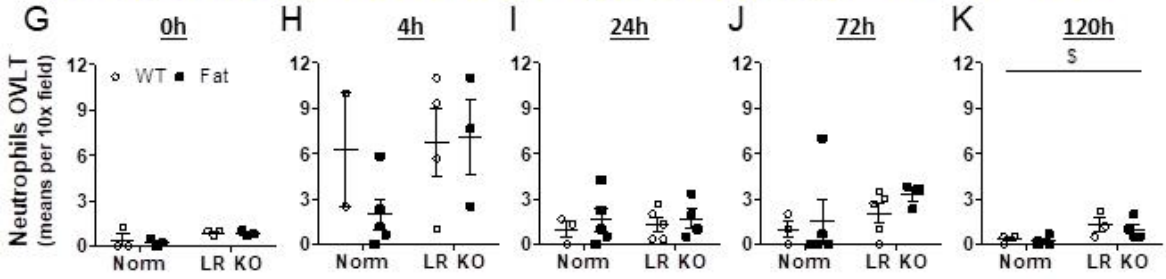

Figure 42: LPS-induced NG recruitment to the OVLT in Norm controls vs. LR KO mice is significantly altered at 120 h p.i.

At the level of the *organum vasculosum of the lamina terminalis* (OVLT; A) recruited neutrophil granulocytes (NG; green, C-F) were counted (B). Unmodified control mice (Norm; C, D) were compared to the RvE1 leukotriene B4 receptor knock-out (LR KO; E, F) on a wild-type (WT; C, E) or genetically

enriched ω-3 PUFA synthesizing Fat-1 (Fat; D, F) background. All mice were treated with lipopolysaccharide (LPS, 10 μg) via intra-tracheal (i.t.) instillation and were sacrificed at different time points: 0 h, 4 h, 24 h, 72 h, and 120 h p.i. At each time point, NGs were counted per 10x field of view and compared between Norm (WT-/Fat-) groups vs. LR KO (WT-/Fat-) groups (G-K). Statistics were performed when n ≥ 3 but the data was presented as a visually descriptive representation when n < 3. At 120 h p.i with LPS LR KO mice had increased NG recruitment in comparison to Norm controls regardless of ω-3 PUFA enrichment. Staining also shows: Intercellular adhesion molecule 1 (ICAM1; red, C, E); DAPI (blue; C-F) visualizes surrounding tissue. n= 2-5. $ main effect Norm vs. LR KO. For C1, D1, E1, and F1 a representative scale bar shown in Figure C1 = 100 μm; For C2-C5, D2-D5, E2-E5, and F2-F5 a representative scale bar shown in Figure C4 = 50 μm. $ $p<0.05$. Please note the data on WT-Norm and Fat-Norm controls is displayed again from Figure 41 for comparison.

As previously mentioned, over the course of LPS-induced ARDS, the BIF showed a similar peak in NG recruitment at 4 h p.i. in WT-Norm controls that was not observed in other groups aside from the Fat-LR KO mice (Figure 43). Once again, ω-3 PUFA enrichment seemed to eliminate the 4 h peak in Fat-Norm controls but also partially recovered the effect in RvE1 receptor deficient groups. To better understand the impact of ω-3 PUFAs, further immunohistochemical analysis at the level of the BIF were analyzed for each time point. I found that while ω-3 PUFAs did not significantly affect NG recruitment over time at 0 h ($p = 0.0441$) and 72 h p.i. ($p = 0.0274$) Fat-CR KO mice did have increased NG levels compared to Fat-Norm controls. Additionally, at 0 h ($p = 0.0025$), 24 h ($p = 0.0339$), and 72 h p.i. ($p = 0.0216$) CR deficiency caused an overall increase in NG recruitment, regardless of ω-3 PUFA enrichment (Figure 44). Notably, no significant differences due to of ω-3 PUFAs or RvE1 receptors were evident in LR KO mice (Figure 45)

Like the OVLT, ω-3 PUFAs may inhibit NG recruitment to the BIF during ARDS; however, in combination with LR deficiency, the expression may enhance recruitment (since Fat-LR KO also showed a peak in NG recruitment). Taken together, the observed influence of CR deficiency on NG recruitment to the BIF suggests that Rv modulation of NG recruitment may be mediated through CR and not LR.

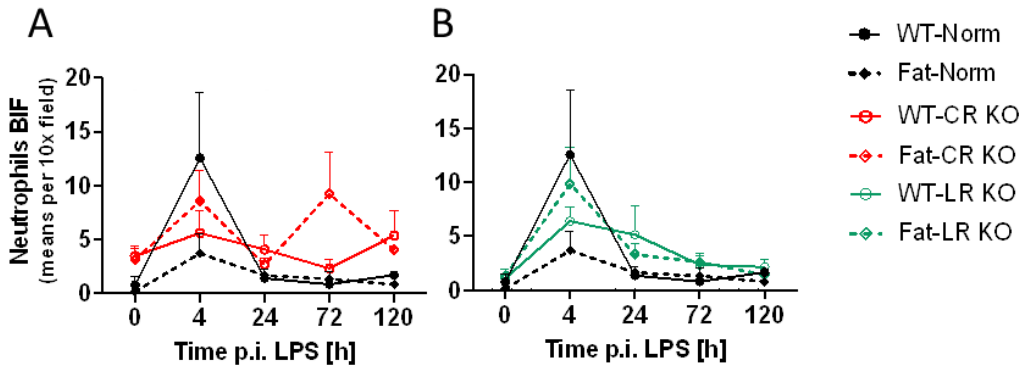

Figure 43: NG recruitment at the level of the BIF in Norm, CR KO, and LR KO mice over time after LPS-induced ARDS

Analysis of the bifurcation (BIF) for neutrophil granulocyte (NG) recruitment to the brain (A-B). Unmodified control mice (Norm; black) were compared to two different RvE1 receptor knock-out (KO) mice, i.e., chemerin receptor 23 (CR KO; A, red) or leukotriene B4 receptor (LR KO; B, green). All mice were bred on a wild-type (WT; solid line) or genetically enriched ω-3 PUFA synthesizing Fat-1 (Fat; dashed line) background. All mice were treated with lipopolysaccharide (LPS, 10 μg) via intra-tracheal (i.t.) instillation and were sacrificed at different time points: 0 h, 4 h, 24 h, 72 h, and 120 h p.i. Immunofluorescent staining was used to analyze sections using an antibody for myeloperoxidase. Images were taken and NGs were counted per 10x field of view. n= 2-6. Due to low n-numbers statistics were not performed but the data was presented as a visually descriptive representation.

A

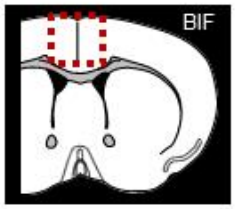

B

Neutrophils BIF Means per 10x field	0 h	4 h	24 h	72 h	120 h
WT-Norm	0.8	12.6	1.4	0.8	1.7
Fat-Norm	0.1	3.7	2.0	1.3	0.8
WT-CR KO	3.4	5.6	4.1	2.3	5.4
Fat-CR KO	3.1	8.6	2.6	9.2	4

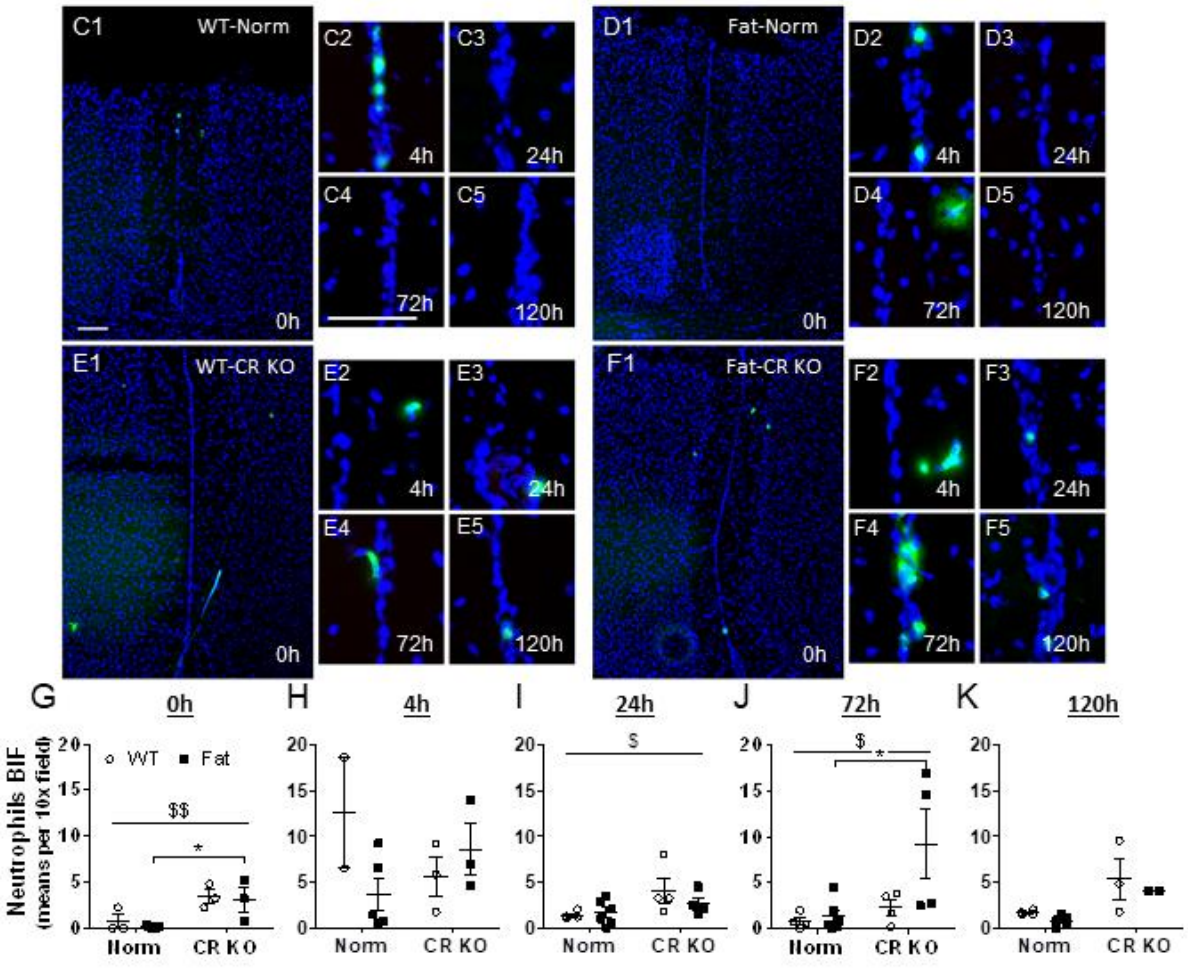

Figure 44: LPS-induced ARDS NG recruitment at the level of the BIF in Norm vs. CR KO mice is significantly altered at multiple time points

At the level of the bifurcation (BIF; A) recruited neutrophil granulocytes (NG; green, C-F) were counted (B). Unmodified control mice (Norm; C) were compared to the RvE1 chemerin receptor 23 knock-out mice (CR KO; E) on a wild-type (WT; C, E) or genetically enriched ω-3 PUFA synthesizing Fat-1 (Fat; D, F) background. All mice were treated with lipopolysaccharide (LPS, 10 μg) via intra-tracheal (i.t.) instillation and were sacrificed at different time points: 0 h, 4 h, 24 h, 72 h, and 120 h p.i. At each time point, NGs were counted per 10x field of view and compared between Norm (WT-/Fat-) groups vs. CR KO (WT-/Fat-) groups (G-K). Statistics were performed when n ≥ 3 but the data was presented as a visually descriptive representation when n < 3. At 0 h, 24 h, and 72 h p.i. with LPS, CR KO mice had increased NG recruitment in comparison to Norm controls regardless of ω-3 PUFA enrichment. Additionally, at 0 h and 72 h p.i.

with LPS, ω-3 PUFA enrichment in CR KO mice (Fat-CR KO) induced enhanced NG recruitment than in Fat-Norm controls. Staining also shows: DAPI (blue; C-F) visualizes surrounding tissue. n= 2-6. $ main effect Norm vs. CR KO. For C1, D1, E1, and F1 a representative scale bar shown in Figure C1 = 100 μm; For C2-C5, D2-D5, E2-E5, and F2-F5 a representative scale bar shown in Figure C4 = 50 μm. *p<0.05, $ p<0.05, $$ p<0.01.

A

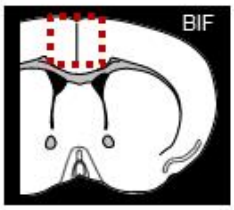

B

Neutrophils BIF Means per 10x field	0 h	4 h	24 h	72 h	120 h
WT-Norm	0.8	12.6	1.4	0.8	1.7
Fat-Norm	0.1	3.7	2.0	1.3	0.8
WT-LR KO	1.1	6.4	5.2	2.4	2.2
Fat-LR KO	1.3	9.9	3.4	2.6	1.4

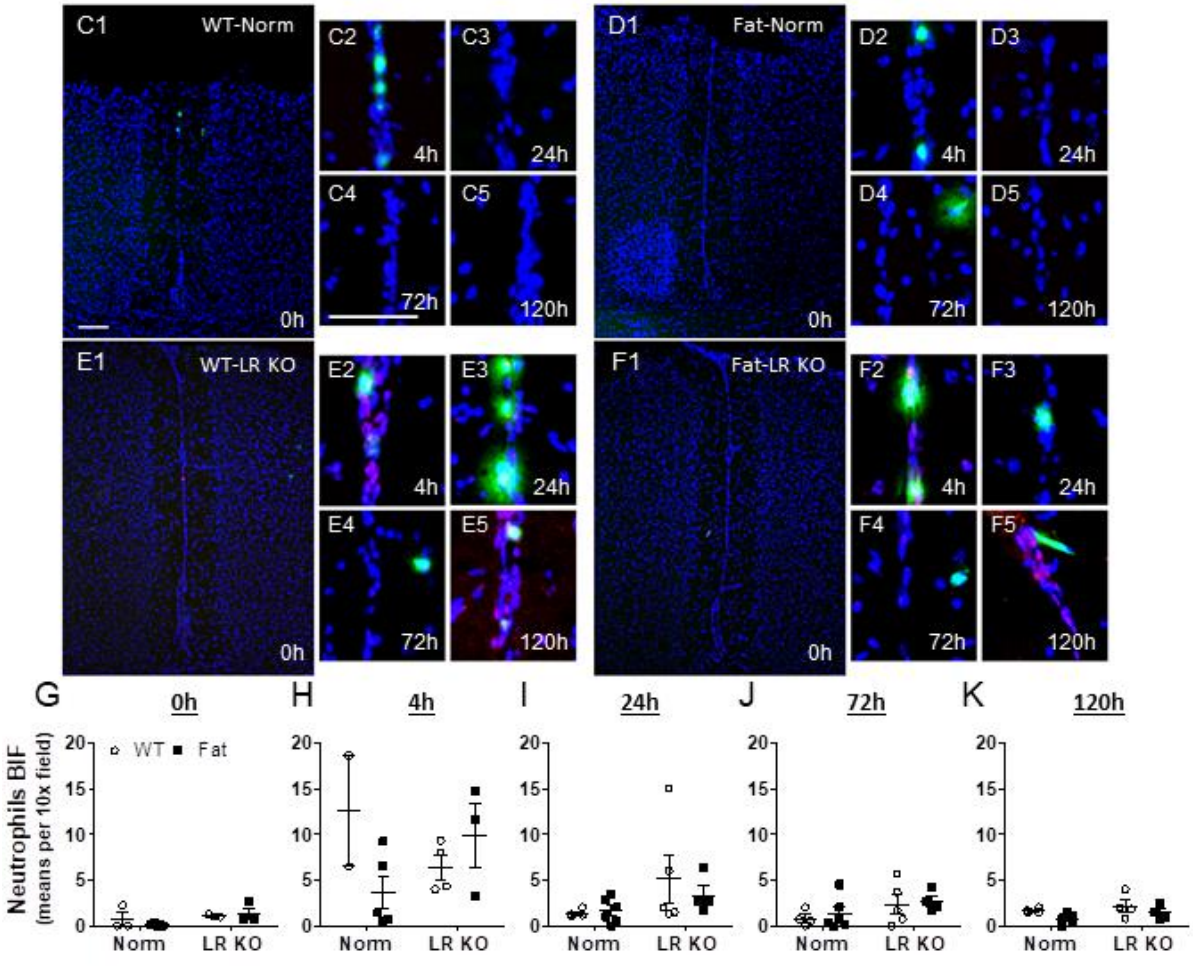

Figure 45: LPS-induced ARDS NG recruitment at the level of the BIF in Norm vs. LR KO mice is not significantly altered

At the level of the bifurcation (BIF; A) recruited neutrophil granulocytes (NG; green, C-F) were counted (B). Unmodified control mice (Norm; C, D) were compared to the RvE1 leukotriene B4 receptor knock-out mice (LR KO; E, F) on a wild-type (WT; C, E) or genetically enriched ω-3 PUFA synthesizing Fat-1 (Fat; D, F) background. All mice were treated with lipopolysaccharide (LPS, 10 μg) via intra-tracheal (i.t.) instillation and were sacrificed at different time points: 0 h, 4 h, 24 h, 72 h, and 120 h p.i. At each time point, NGs were counted per 10x field of view and compared between Norm (WT-/Fat-) groups vs. CR KO (WT-/Fat-) groups (G-K). Statistics were performed when $n \geq 3$ but the data was presented as a visually descriptive representation when $n < 3$. No differences were observed between groups. Staining also shows: Nuclear factor interleukin 6 (NF-IL6; red, E, F); DAPI (blue; C-F) visualizes surrounding tissue. n= 2-6. For C1, D1, E1, and F1 a representative scale bar shown in Figure C1 = 100 μm; For C2-C5, D2-D5, E2-E5, and F2-F5 a representative scale bar shown in Figure C4 = 50 μm. Please note the data on WT-Norm and Fat-Norm controls is displayed again from Figure 44 for comparison.

IV. Discussion

4.1 Impact of neutropenia on the brain and peripheral inflammatory response during LPS-induced severe systemic inflammation

My investigation on NGs during LPS-induced severe systemic inflammation is a novel examination into their potential anti-inflammatory properties on sickness behavior and inflammation in the brain and periphery. Inflammatory mediators, immune cell trafficking, and HPA activation were used as readouts. Indeed, NG recruitment to the brain is a probable route for immune-to-brain communication (Pflieger et al. 2018). I showed that not only cytokine profiles were altered in the periphery during inflammation but signaling pathways and enzymes in the hypothalamus were also impacted by neutropenia. Pro-inflammatory cytokines like IL-6, TNFα, and chemokines such as CXCL1, and CXCL2 as well as anti-inflammatory IL-10 showed exacerbated circulating levels in neutropenic mice during severe LPS-induced inflammation. Although cytokine profiles in the hypothalamus were unchanged, inflammatory signaling via NFκB and STAT3/SOCS3 and inflammatory enzymes COX-2 and mPGES were increased by neutropenia regardless of treatment. LPS-induced activation of the HPA axis was impaired resulting in a dampened response that remained elevated during later stage inflammation in neutropenic mice. Moreover, neutropenia alone exacerbated hypothermia during systemic LPS-induced inflammation. These results indicate that NGs, directly or indirectly, are important mediators of the sickness response that also contribute to an anti-inflammatory profile during severe inflammation and whose therapeutic potential should be further explored.

4.1.1 Role of neutrophil granulocytes in the development of sickness behavior

By combining the use of the transmitter implant with a telemetric system, I was able to show a detailed account of how neutropenia affects physiological parameters at baseline and sickness behavior during LPS-induced inflammation including core body temperature, activity, and food and water intake. The connection between inflammation and sickness behavior has been well established but the role of NGs remain to be clearly understood (Dantzer and Kelley 2007, Pflieger et al. 2018). Previous studies

have focused on the pro-inflammatory role NGs play and have found that an elevated ratio of NGs to lymphocytes could be used as an indicator for major depressive disorders in patients (Demir et al. 2015). Others correlated NG infiltration into the brain with increased depression-like behavior during systemic inflammation and were able to abolish symptoms through acute NG depletion using the same type of antiserum as in the present dissertation project (Aguilar-Valles et al. 2014).

As a prominent cell of the inflammatory response, the accumulation of NGs can have effects beyond their phagocytic actions at the site of inflammation. While unable to produce the same level of cytokines as monocytes or other lymphocytes, it is important to remember that NGs vastly outnumber these other cells and, therefore, are able to influence the APR through their own cytokines (Cassatella 1995). Human isolated NGs stimulated with LPS or a variety of cytokines, such as GM-CSF, IL-1β, and TNFα, have been shown to secrete TNFα, IL-1β, and IL-6 (Lindemann et al. 1988, Dubravec et al. 1990, Marucha et al. 1990, Cicco et al. 1990). Of these cytokines, IL-1β is an inducer of such behavioral effects like anorexia and reduced social exploration as shown by Kent et al. (1992) in rats where IP administration of IL-1ra prevented the development of these sickness behavior components (Kent et al. 1992a). Similar symptoms were also observed following IP administration of TNFα in mice that as well resulted in anorexia and reduced exploration behaviors (Bluthé et al. 1994). Interestingly, Lewkowicz et al. (2016) have also shown that anti-inflammatory IL-10 producing NGs can be induced following interactions with LPS-stimulated regulatory T cells *in vitro* (Lewkowicz et al. 2016). The cytokines released by NGs will activate endothelial cells through their respective receptors, which plays an essential role in NG recruitment to the vasculature of the CNS (Maloney et al. 1998, Wright et al. 2010, Zhou et al. 2009).

On the one hand, in my own experiments I found exacerbated LPS-induced hypothermia in neutropenic compared to immunocompetent mice while both immunocompetent and neutropenic mice displayed, to a similar extent, several brain-controlled responses including reduced locomotor activity, anorexia, and adipsia. On the other hand, neutropenia alone in PBS-stimulated control animals did not have an effect.

4.1.1.1 Influence of neutropenia on locomotor activity

Systemic inflammation causes a reduction in locomotor activity that is thought to aid in recovery such as by conserving energy and reducing heat loss (Schöbitz et al. 1994, Kelley et al. 2003). Several LPS-induced cytokines such as IL-1 and TNFα have been associated with inducing this reduction in activity as well as other components of sickness behavior (Schöbitz et al. 1994, Dantzer 2001, Kelley et al. 2003). Given that NGs are able to produce these same cytokines as mentioned above, and have previously been shown to influence depressive-like sickness behaviors through trafficking to the brain, I was interested to see what effects NGs could have on the progression of locomotor activity following LPS treatment (Lindemann et al. 1988, Dubravec et al. 1990, Aguilar-Valles et al. 2014).

Indeed, previous studies found that NG recruitment to the brain can influence locomotor activity in severe models of brain inflammation as seen in a mouse model of bacterial meningitis. NG infiltration to the meninges reduced locomotor activity while NG depletion abrogated the effect, although, NG depletion was accompanied by increased mortality in infected mice (Too et al. 2016). Similarly, using NOD-like receptor *nlrc3l*$^{-/-}$ larval zebrafish, which lack microglia and maintain an activated macrophage profile, Kwon and colleagues (2022) also found that infiltrating NGs caused a reduction in locomotor activity (Kwon et al. 2022). The accumulation of NGs in the brain, interaction with cells of the BBB, and/or subsequent release of pro-inflammatory cytokines may be responsible for the reductions in locomotor activity observed in these studies.

In my current experiment, I found evidence for NG recruitment to the brain, but I did not observe a strong influence of neutropenia on locomotor activity during LPS-induced inflammation. However, it was of note that a short-lived reduction in locomotor activity occurred immediately following an injection with PMN suggesting some inflammatory reaction during NG depletion. Moreover, pretreatment with PMN alone also induced a short lasting fever response; both effects could be attributed to a low-grade inflammatory response related to the break down and phagocytosis of NGs. A possible reason why in my own experiments neutropenia did not induce increased locomotor activity may be related to the severity of the LPS model, the extent of NG recruitment to the brain, and

level of NG depletion. Indeed, LPS-induced septic models do increase circulating levels of TNFα and IL-1β as well as BBB permeability in mice but also have a very severe almost abolishing effect on locomotor activity that could be masking any differences that would be otherwise observed between groups (Waage et al. 1989, Lv et al. 2014, Gamal et al. 2015). It should also be kept in mind that evidence suggests that LPS-induced reduced locomotor activity and food intake occur independently of other sickness-type behaviors, i.e., decreased sucrose preference and immobility in a forced swim test in mice (O'Connor et al. 2009, Walker et al. 2013) suggesting that NGs may only be involved in some of these behaviors.

4.1.1.2 Influence of neutropenia on food and water intake

Anorexia and adipsia are common effects observed during LPS-induced inflammation (Bluthe´ et al. 1992, Dantzer 2001). LPS signaling through the TLR4 receptor in particular leads to pro-inflammatory cytokine release that contributes to anorexia and weight loss during systemic inflammation in mice (Burfeind et al. 2018). As stated above, the same circulating cytokines, namely IL-1 and TNFα, not only contribute to reduced locomotor activity but also impact food and water intake by suppressing feeding and drinking during LPS-induced inflammation (Bluthe´ et al. 1992, Schöbitz et al. 1994, Dantzer 2001, Kelley et al. 2003). Food consumption is regulated through certain hypothalamic structures (Jang et al. 2010). Treatment with LPS results in stimulation of appetite suppressing pathways via NFκB mediated pro-inflammatory cytokine induction (Jang et al. 2010). In my current experiment, the results mirrored these established findings as reductions in food and water intake began immediately following LPS treatment. Unique to food intake, there was a point during the mouse's active phase when neutropenia alone caused an increase in food intake in the control group. Although brief (~2 h), the neutropenic controls experienced a distinctive uptick in food consumption that was lacking in their immunocompetent counterparts. Further studies will be necessary to gain more insights into potential mechanism and the relevance of this observation. Despite this small discrepancy, indirectly or directly neutropenia did cause a slight reduction in bodyweights (~1 %). Since pretreatment with PMN alone induced a fever response and reduced locomotor activity, the effect cannot be directly linked to neutropenia and may be due to low-grade inflammation elicited during

depletion of NG by processes related to the antiserum and the removal of NG. The PMN dependent reduction in body weights was no longer apparent after LPS or PBS treatments. From the results of my dissertation project, it is likely that NGs do not have a significant impact on locomotor activity or food and water intake as components of the sickness response during severe LPS-induced systemic inflammation. Discrepancies to previous studies may be linked to model systems (meningitis vs. systemic inflammation), experimental length (24 h vs. 240 h) (Too et al. 2016), and the severity of neutropenia.

4.1.2 Influence of neutropenia on systemic inflammatory mediators

The complex septic response includes aberrant production of both pro- and anti-inflammatory cytokines that can result in immunosuppression and poor outcomes (Boomer et al. 2011, Hotchkiss et al. 2013). Under non-neutropenic septic conditions, NGs become dysregulated and experience altered functions, such as impaired migration and reduced phagocytosis and apoptosis (Danikas et al. 2008, Alves-Filho et al. 2009, Alves-Filho et al. 2010). Indeed, sepsis suppresses the expression of genes associated with NG inflammatory mediation; correlations have been made between diminished NG activity and worse outcomes (Danikas et al. 2008, Tang et al. 2007). Given the connections between weakened NG function and poor prognosis as well as the severity of neutropenia during systemic inflammation (Danikas et al. 2008, Tang et al. 2007, Lyman et al. 2014), I initially assessed several inflammatory mediators in circulation to identify how the levels of pro- and anti-inflammatory cytokines and NG chemoattractants could be affected. Previous studies have already found that several circulating cytokines including IL-6, IL-8, and G-CSF were elevated in neutropenic septic patients and contributed to enhanced disease such as a higher risk of acute kidney injury (Reilly et al. 2016). A significant alteration to peripheral cytokines would also have implications for the humoral communication pathway between circulating mediators and the brain, particularly during the severe systemic inflammatory status due to the increased permeability of the BBB (Tsao et al. 2001, Mina et al. 2014). In accordance with previous studies, treatment with LPS upregulated inflammatory mediators in circulation (Levy 1996, Hu and Pasare 2013, Lasselin et al. 2020), while in the present study, neutropenia exacerbated these inflammatory mediators as compared to immunocompetent mice. This intensified inflammation occurred in the absence of enhanced bacterial growth even

though previous studies hypothesized increased bacterial growth was a factor in mortality for those patients in clinical studies (Abe et al. 2008, Li et al. 2017, van Vught et al. 2017). Moreover, when determining a dose response relation of PMN and mortality; the more severe neutropenia often resulted in higher mortality, as shown here, following treatment with LPS.

Interestingly, analysis of inflammatory mediators during early stages of inflammation (4 h) revealed that only production of the anti-inflammatory cytokine IL-10 was exacerbated by neutropenia following treatment with LPS. This elevation is highly significant since overproduction of IL-10 can be used as a predictor for severity and mortality (Abe et al. 2008, Wu et al. 2009, Li et al. 2017, van Vught et al. 2017). In contrast, the immunocompetent mice did not appear to have generated the same strong immunosuppressive response. Thus, such data is indicative that the neutropenic mice were experiencing more severe symptoms than their immunocompetent counterparts. Other chemoattractants like CXCL1, CXCL2, and CCL5 and pro-inflammatory cytokines IL-6 and TNFα were elevated at the early stages of inflammation by LPS treatment. At the later stage of inflammation (24 h), IL-10 remained elevated in neutropenic mice but was now joined by higher levels of the pro-inflammatory cytokines IL-6 and TNFα as well as the chemoattractants CXCL1 and CXCL2 in neutropenic compared to immunocompetent LPS-treated mice. PMN-dependent alterations to the inflammatory response could be contributing to mortalities observed in dosage experiments and would indicate that neutropenia itself and not enhanced bacterial load are contributing to worse outcomes. The potential significance of these changes is discussed below.

4.1.2.1 Anti-inflammatory mediators

As an anti-inflammatory cytokine, IL-10 suppresses the immune system, but during sepsis this dampening of the immune response can exacerbate disease progression (Wu et al. 2009). Previously observed at increased levels in neutropenic patients, elevated production of IL-10 could be a consequence of the failure of NGs as the first line of defense and a weakened overall inflammatory response (Yin et al. 2021). Indeed, an early immunosuppressive reaction brought on by neutropenia could enhance levels of bacterial pathogens as has been observed in influenza infected mice (Bradley et al.

2012). Alterations to other immune cells also contribute to the cytokine shift, and not only T cell populations are impaired during sepsis but there is also a subsequent increase in the percentage of IL-10 producing immunosuppressive regulatory T cells (Joseph et al. 2017, Yu et al. 2019, Boomer et al. 2011). Additionally, monocytes are a major source of IL-10 and during sepsis a combination of monocyte anergy and leukocyte reprogramming contribute to the elevated levels of this important cytokine (Fabri et al. 2020). Similar to LPS-induced tolerance that has been observed in human endotoxemia models, monocytes isolated from septic patients and exposed to an endotoxin *in vitro* have reduced production of pro-inflammatory cytokines like TNFα and induce a shift toward anti-inflammatory cytokines like IL-10 contributing to endotoxin tolerance (Sfeir et al. 2001, van 't Veer et al. 2007).

In addition to lymphocyte exhaustion, reprogramming of APC also contributes to the immunosuppression that occurs during sepsis (Hotchkiss et al. 2013). A notable reduction in dendritic cells, due to IL-10 induced apoptosis, and an overall diminished surface expression of human leukocyte antigen (HLA)-DR inhibits their functions (Fumeaux and Pugin 2002, Pastille et al. 2011). The reduced expression of HLA-DR means that dendritic cells cannot effectively present antigen to other cells and plays a role in the failed development of an adequate immune response (Fumeaux and Pugin 2002, Pastille et al. 2011). Moreover, TLR4 stimulation will induce myeloid dendritic cells to release IL-10 (Boonstra et al. 2006). Together, the interplay between the innate and adaptive immune system contribute to immunosuppression during sepsis.

Though the circulating levels of IL-10 had reduced by the later stage of inflammation, they were still significantly elevated compared to the immunocompetent counterparts. The prolonged “immunosuppressive” status in the neutropenic mice continued to serve as an indicator of their disease severity (Abe et al. 2008, Wu et al. 2009, Li et al. 2017, van Vught et al. 2017). Together, exacerbated septic symptoms and subsequent shift in cell function is most likely responsible for the elevated levels of IL-10 observed here. Nonetheless, increased IL-10 levels during systemic inflammation may as well just reflect counteraction to the stronger pro-inflammatory response in neutropenic animals compared to the immunocompetent counterparts to the systemic LPS-challenge.

Finally, although I was unable to analyze circulating levels here, NG secretion of the anti-inflammatory cytokine IL-1ra could also prove to be an important modulatory cytokine during severe systemic inflammation. Tamassia et al. (2008) found that IL-10 induces the IL-1ra gene expression in LPS-treated NGs from septic but not healthy patients (Tamassia et al. 2008). Lower circulating levels of IL-1ra have been observed in neutropenic patients with bacteremia and correlate with an exacerbated inflammatory response and poor outcome (Hynninen et al. 1995). Indeed, IL-1ra could be an important contribution of NGs during severe systemic inflammation but further investigations in future studies are still required.

4.1.2.2 Pro-inflammatory mediators

In addition to IL-10, the pro-inflammatory cytokine IL-6 has also been identified as a marker during sepsis (Wu et al. 2009) and was elevated in the neutropenic mice compared to immunocompetent ones but only during the later stage of inflammation i.e., 24 h post LPS-stimulation. Characteristic of early inflammation, IL-6 plays a beneficial role in curbing the spread of infection by contributing to the pro-inflammatory cytokine profile. In the present study, LPS did increase IL-6 already at the early time point (4 h) in both neutropenic and immunocompetent groups. However, during sepsis, overexpression can produce an excessive inflammatory state and, therefore, has value as a marker of severity (Damas et al. 1992, Oda et al. 2005, Song et al. 2019). Song et al. (2019) have shown that elevated levels of IL-6, in comparison to pentraxin 3 and procalcitonin, is a superior diagnostic and prognostic marker of disease severity for sepsis and septic shock in humans (Song et al. 2019). Elevated levels of circulating IL-6 are also common among neutropenic patients with sepsis and, as mentioned above, associated with more severe outcomes (Reilly et al. 2016, Song et al. 2019). Typically released by monocytes, macrophages, and T-cells (Spittler et al. 2000, Ma et al. 2016), acute inflammation can also stimulate IL-6 release from other cells like endothelial cells, mesenchymal cells, or hepatocytes such as during a severe septic condition or after LPS treatment (Akira et al. 1993, Norris et al. 2014). Indeed, a rapid release of IL-6 has broad effects throughout the body including activation of liver cells responsible for APP, weakening of vascular endothelium resulting in vascular leakage, and promoting initiation of the coagulation cascade (Heinrich et al. 1990, Neumann et al. 1997, Gruys

et al. 2005, Kang et al. 2020). IL-6 also contributes to NG recruitment by stimulating production from the bone marrow and elevated levels are consistent with an attempt to recruit NGs to fight infection (Kopf et al. 1994, Reilly et al. 2016). In addition to being a potent pro-inflammatory cytokine, it is also important to recognize that IL-6 can also induce anti-inflammatory responses. Schindler et al (1990) noted that IL-6 released from human PBMCs stimulated with LPS would suppress transcription of IL-1β and TNFα (Schindler et al. 1990). There have also been significant connections, which indicate that IL-6 amplifies anti-inflammatory mediators like IL-10 production form T cells and cortisol release in humans (Steensberg et al. 2003, Zarković et al. 2008, Jin et al. 2013). Therefore, elevated IL-6 could also contribute to the prolonged exacerbated IL-10 response also observed as well as other physiological functions.

Another leading pro-inflammatory cytokine during sepsis that was elevated in the neutropenic mice is TNFα. One of the first cytokines released during sepsis, high circulating values have also been associated with mortality (Debets et al. 1989, Baghel et al. 2014, Quinto et al. 2015). During LPS-induced systemic inflammation, both IL-6 and TNFα contribute to the breakdown of the BBB such as through the disruption of tight junctions and loss of endothelial cell integrity (Cheng et al. 2018, Voirin et al. 2020). As a result of the weakened BBB, there is an increased interaction of circulating inflammatory mediators with the brain (Tsao et al. 2001, Mina et al. 2014, Annane and Sharshar 2015, Sharshar et al. 2007). In the present experiment, TNFα levels were elevated during early inflammation in neutropenic and immunocompetent mice. By the later time point, though the values had decreased, TNFα was still detectable and neutropenia now maintained a higher circulating value than the immunocompetent counterparts. The quick release of TNFα is the most probable reason why previous studies have routinely reported low levels of production during later stages of sepsis and failed to identify differences between neutropenic and immunocompetent patients (Janský et al. 1995, Araujo et al. 2017, Dinc et al. 2020, Yin et al. 2021). Primarily released by monocytes and macrophages, TNFα will push forward the inflammatory cascade by activating other immune cells to then release their own inflammatory mediators as well as through apoptotic signaling (Lewis et al. 1991, Ordás et al. 2007, Drewry et al. 2016). Like with IL-10, these elevated values, although levels did decrease over the course of the

experiment, could indicate an increased risk of mortality in neutropenic mice. However, though associations have been made linking high TNFα levels with increased mortality, no connection has been made between TNFα and sepsis severity indicating that TNFα itself may associate with severity while not being responsible for the deleterious effects (Quinto et al. 2015, Gharamti et al. 2022).

4.1.2.3 Neutrophil granulocyte chemoattractants

In addition to the pro- and anti-inflammatory cytokines present, chemoattractants like CXCL1 and CXCL2 will also mediate the release of NG from the bone marrow into circulation through CXC receptor (CXCR) 2 interactions (Eash et al. 2010, Delano et al. 2011). During instances of bacterial sepsis, CXCL1 and CXCL2 are released from resident and myeloid cells, such as epithelial cells and macrophages, in an attempt to eliminate bacteria through NG recruitment and activation (Jin et al. 2014, Wang et al. 2021a, Huebener et al. 2015). However, progression to severe sepsis has been shown to downregulate CXCR2 and prevent CXCL1 and CXCL2 mediated NG recruitment and subsequent pathogen clearance, which is associated with worse outcomes (Huebener et al. 2015, Sawant et al. 2015).

Interestingly, even without live bacteria, I found that the neutropenic mice in my experimental model had elevated levels of CXCL1 and CXCL2 as well as exacerbated inflammation compared to the immunocompetent counterparts. Other studies have reported links between diminished NG activity, such as experienced by neutropenic mice, and severity of inflammation (Danikas et al. 2008, Tang et al. 2007, Lyman et al. 2014, Craciun et al. 2010). Additionally, during sepsis, a rapid recruitment of NGs from the bone marrow will also lead to increased levels of a specific subpopulation of NGs in circulation (Parthasarathy et al. 2023), an effect that would be exaggerated in the NG depleted mice used here. Experiments performed by Parthasarathy and colleagues (2023), analyzed blood samples from patients and found that during sepsis the levels of immature NGs were increased in circulation and identified an inverse relationship between NG maturity and soluble factors like pentraxin 3 and metabolic functions via fatty acid levels in circulation (Parthasarathy et al. 2023). These data indicated that immature NGs could exacerbate endothelial dysfunction and vascular leaking as well as

aberrant metabolic activities (Parthasarathy et al. 2023). Therefore, by enhancing the recruitment of immature NGs from the bone marrow elevated levels of these chemoattractants could be exacerbating septic inflammation. It is important to note that in instances of myelosuppression, such as after chemotherapy (Lyman et al. 2014, Schiel et al. 2003), patients may experience more prolonged neutropenia (Moore 2016) and the immature NG subset may not be present to the same extent.

4.1.3 Influence of neutropenia on inflammation in the brain

Several different pathological conditions can lead to the development of inflammation in the brain during which astrocytes and microglia are primarily responsible for defending the brain (Afridi et al. 2022). Astrocytes will modulate barrier functions to restrict permeability and transmit inflammatory signals to regulate inflammation in the brain through the recruitment of immune cells or activation of the brain immune response (Gimenez et al. 2004, Wanner et al. 2013, Norden et al. 2016, Klein and Hunter 2017). Moreover, microglia are the innate immune cells of the CNS and, as with macrophages, they will polarize towards a pro-inflammatory (M1) or anti-inflammatory (M2) phenotype following stimulation (Orihuela et al. 2016). Additional research has even found that other cells of the CNS such as endothelial cells can also release inflammatory mediators that activate microglial and mediate inflammation in the brain (Liu et al. 2019, Handa et al. 2008). Finally, the immune cells that have been recruited to the brain, like NGs, have been identified as contributors to certain neuroinflammatory disease states through their own release of inflammatory mediators and cellular components such as in Alzheimer's disease and ischemic brain injury (Dinkel et al. 2004, Nguyen et al. 2007, Herz et al. 2015, Zenaro et al. 2015). In the case of Alzheimer's disease, Zenaro and colleagues (2015) noted the presence of NGs and NETs within the brain venules and parenchyma of Alzheimer's patients. Moreover, NG depletion improved memory and neuropathology in a transgenic Alzheimer's mouse model (Zenaro et al. 2015).

Early production of cytokines in the brain and sepsis-associated encephalopathy (SAE) is a common neuroinflammatory event characteristic of sepsis. This response affects consciousness, cognition inducing an altered mental state, and depressive-like symptoms; it can even result in significant long term impacts on cognitive functions

including memory, mood disorders, and verbal fluency (Iwashyna et al. 2010, Aguilar-Valles et al. 2014, Annane and Sharshar 2015, Comim et al. 2011b). Direct infection of the brain is not necessary for SAE to develop but the exact mechanisms remain unclear as several pathways could be involved. Particularly important seems to be damage caused by an exaggerated immune response to the cells comprising the BBB resulting in a break down and augmented interactions of circulating mediators and immune cells with the brain (Tsao et al. 2001, Mina et al. 2014, Annane and Sharshar 2015, Sharshar et al. 2007). The severity of the inflammatory response in the brain indicates that patients suffering from SAE have a severe clinical condition associated with increased mortality (Kafa et al. 2010).

I was interested in the role NGs could play in brain inflammation and SAE. Evidence that NGs in the periphery can cause depression-like behaviors during LPS-induced inflammation through NET-dependent increases in pro-inflammatory cytokines or via direct NG-to-brain signaling suggests two possible pathways (Aguilar-Valles et al. 2014, Kong et al. 2021). In this manner, a peripheral- or central brain action of NGs is utilized to alter immune-to-brain communication (Aguilar-Valles et al. 2014, Kong et al. 2021). So far, the present experiment has shown that neutropenia is able to exacerbate the circulating cytokine response during LPS-induced severe systemic inflammation. Therefore, I examined the hypothalamus to determine if neutropenia could also cause alterations to inflammatory mediators, transcription factors, PG generation, and NG markers in the hypothalamus, an important center for immune-to-brain communication and for controlling homeostasis. During the early stages of inflammation, LPS caused an increase in inflammatory mediators, transcription factors, precursors of PG synthesis, and NG markers in the hypothalamus but no effect of neutropenia was apparent. These LPS-induced effects disappeared by 24 h p.i. but interestingly, during the later stages of inflammation, a minor impact of neutropenia was now observed among the transcription factors and PG precursors. Overall, these results suggest that a peripheral effect of neutropenia may be more important than their direct effect on the brain at least in the model and conditions investigated here.

4.1.3.1 Inflammatory mediators in the brain

In order to have an accurate description of the cytokine profile in the hypothalamus, I analyzed the expression of several important mediators including IL-6, TNFα, and IL-10. We know that during brain inflammation inflammatory mediators can enter into the brain through the permeabilized BBB (Tsao et al. 2001). Additionally, activated neuroglial and immune cells like NGs, which are recruited to the brain during sepsis, can locally produce similar mediators (Burguillos et al. 2011, Lee et al. 1993, Nguyen et al. 2007, Herz et al. 2015, Zenaro et al. 2015, Rummel et al. 2010, Aguilar-Valles et al. 2014). Indeed, a characteristic of SAE is microglia mediated neuroinflammation (Yan et al. 2022). Activated through interactions with local cytokines and other inflammatory signals within the brain, these microglia will then release cytokines (Yan et al. 2022). This response has been replicated using LPS and TLR4 signaling to polarize microglia towards an M1 activation profile and release pro-inflammatory cytokines including IL-6 and TNFα (Orihuela et al. 2016, Moraes et al. 2021). IL-6 and TNFα have also been detected being released from endothelial cells treated with a septic-like dose of LPS *in vitro* and astrocytes isolated from LPS-treated mice (Norden et al. 2016, Yi et al. 2022). Additionally, perivascular macrophages in key structures like the CVOs, which interact more closely with inflammatory mediators in circulation, can respond to inflammation by producing pro-inflammatory cytokines (Quan et al. 1998). Regarding IL-10, during the resolution stage of brain inflammation, polarization of microglia to an M2 phenotype generates one of the key producers of anti-inflammatory IL-10 (Norden et al. 2016, Moraes et al. 2021). However, as with the pro-inflammatory cytokines, other neuroglia such as astrocytes, macrophages, and endothelial cells will also contribute to local production of IL-10 in the brain (Hulshof et al. 2002, Norden et al. 2016, Yi et al. 2022). In my own experimental model, a combination of peripheral and locally produced cytokines could explain the early increase in expression of IL-10, IL-6, and TNFα observed in immunocompetent and neutropenic mice.

During inflammation in the brain, both IL-6 and TNFα maintain pro-inflammatory actions to mediate physiological responses and sickness behavior (see section 1.7) brought on by a systemic inflammatory insult (Norden et al. 2016). Numerous studies have identified that IL-6 and TNFα production in the brain will upregulate chemokine production,

depressive-like sickness behavior and, in the case of SAE, delirium (Dantzer et al. 2008, Orhun et al. 2019, Klawonn et al. 2021). It has also been observed by Michels and colleagues (2015) that sepsis induced BBB permeability leads to elevated levels of IL-6 and TNFα in the brain and contributed to microglia activation and oxidative stress in rats subjected to CLP (Michels et al. 2015). TNFα in particular significantly impacts the development of SAE through the TNFα-TNFR1 complex and mediation of NG recruitment, astrocytosis, and cellular death (Alexander et al. 2008). I have already covered the detrimental effects of IL-10 overproduction in the periphery (see section 4.1.3.1) but in the brain, the IL-10 immunosuppressive profile benefits neuronal and glial cell survival as well as preventing microglia overstimulation (Strle et al. 2002, Shemer et al. 2020). It has traditionally been reported that brain IL-10 production is delayed and follows an early elevation in the pro-inflammatory cytokines. However, a recent study showed that *in vitro* LPS-stimulated mouse mixed glial cultures release IL-10 already as early as 1 h following treatment (Wang et al. 2021b). Cellular immune-to-brain communication can also contribute to local brain levels of IL-10. Given their increased recruitment to the brain (Rummel et al. 2010, Aguilar-Valles et al. 2014, Neumann et al. 2018, Kim et al. 2020), NGs could be a source of cytokine production including IL-10. Altogether, altered levels of IL-6, TNFα, and IL-10 in the brain can have severe consequences that impair protective immune functions or exacerbate symptoms and disease severity (Strle et al. 2002, Dantzer et al. 2008, Orhun et al. 2019, Shemer et al. 2020, Klawonn et al. 2021).

The present experiment shows a cytokine profile consistent with what can be expected in a septic model of inflammation. Although I did not see an impact of neutropenia on hypothalamic cytokine expression, data of other studies indicates that NGs could influence microglia. Using a mouse model of ischemic stroke, Neumann and colleagues (2018) have shown that NGs are not only present in the brain but that they will interact with activated microglia in a significant manner (Neumann et al. 2018). Similar findings were also reported by Kim et al. (2020) following LPS-induced neuroinflammation where microglia activation was associated with NG infiltration (Kim et al. 2020). Since this microglia-NG interaction is not yet fully understood, it remains to be seen what are the consequences of their crosstalk and how it could impact microglia function. Further

investigations should be pursued, for example, using *in vitro* methods of co-culturing NGs and microglia; following treatment with LPS, it would be possible to analyze any alterations to the cytokines being released.

4.1.3.2 Transcription factors and signaling pathways in the brain

In addition to cytokines, the activation of certain signaling pathways related to brain-controlled sickness responses like, NF-IL6, NFκB, and STAT3, were also used as markers of severity during brain inflammation (Rummel 2016, Schneiders et al. 2015, Shih et al. 2015, Damm et al. 2013). In fact enhanced NFκB activity is associated with increased mortality during sepsis (Liu and Malik 2006). Following treatment with LPS, subsequent transcription factor activation can occur due to several factors including: the breakdown of the BBB, interactions at the CVOs, elevated levels of pro-inflammatory cytokines, and activation via TLR4 in the brain (Gautron et al. 2002, Harré et al. 2002, Rummel et al. 2006, Damm et al. 2011, Damm et al. 2013, Fuchs et al. 2013). Notably, all three transcription factors have displayed some capacity for regulation of immune cells and recruitment, specifically NGs. By using NF-IL6 deficient mice, Schneiders and colleagues (2015) were able to demonstrate an NF-IL6 dependent reduction in NG recruitment to the brain during LPS-induced systemic inflammation (Schneiders et al. 2015). Both NFκB and STAT3 are also able to induce expression of the adhesion molecule ICAM1 while NF-IL6 has been identified as a modulator of NFκB dependent ICAM1 expression as has been seen in *in vitro* cultures of epithelial cells (Wung et al. 2005, Manzel et al. 2009). Moreover, NF-IL6, NFκB, and STAT3 are all contributors to NG function and can activate such pathways like cytokine expression, as has been shown for IL-8 (NF-IL6/NFκB), and granulopoiesis (STAT3) (Panopoulos et al. 2006, Cloutier et al. 2009).

In the present study, as expected, I saw a clear early effect of LPS on NF-IL6, NFκB, and STAT3 expression consistent with what previous studies have shown (Rummel 2016, Schneiders et al. 2015, Shih et al. 2015, Damm et al. 2013). However, what was particularly interesting was at 24 h p.i., where, regardless of treatment with LPS, neutropenia alone may be enough to increase the expression of NFκB and STAT3. Although I could not detect a difference in hypothalamic cytokine mRNA expression, the

elevated levels of peripheral cytokines experienced by neutropenic mice may contribute to the exacerbated pro-inflammatory signaling. On one hand, LPS and pro-inflammatory cytokines like TNFα, which I found to be elevated in the circulation of neutropenic mice, are both strong activators of NFκB in endothelial cells (J. W. Fuseler 2006, Schlegel et al. 2012). On the other hand, STAT3 expression in endothelial and glial cells could be induced by IL-6 and in astrocytes by TNFα (Beurel and Jope 2009, Kim et al. 2022, Uddin et al. 2022, Rummel et al. 2006). Increased interactions with glial cells at brain structures with a leaky BBB like the CVOs, which have previously shown strong transcriptional activation during LPS-induced inflammation, could also impact transcription factor expression (Harré et al. 2003, Roth et al. 2004, Pflieger et al. 2022). An amplified expression of NFκB would be an indicator of an enhanced inflammatory response associated with worse clinical outcomes demonstrated by the fact that inhibition of NFκB has been shown to have positive therapeutic effects that ameliorate some sepsis-induced symptoms and prevent lethality (Bernard et al. 2001, Altavilla et al. 2002, Ikezoe et al. 2003, Sheehan et al. 2003). In addition, IL-10 can inhibit NFκB, therefore, the presence of IL-10 producing NGs could contribute to attenuation of NFκB (Fan et al. 2001, Lewkowicz et al. 2016). Over activation of STAT3 would also contribute to impairments of the BBB as seen by Chen et al. (2020) in rats treated with CLP (Chen et al. 2020).

Further analysis of enzymes required for the synthesis of PGE2, namely COX-2 and mPGES, revealed similar results to the transcription factors as expected since the NFκB dependent production of both enzymes and NF-IL6 mediated expression of mPGES are both known to be upregulated in models of sepsis (Uematsu et al. 2002, Schneiders et al. 2015, Kikuchi et al. 2019, Båge et al. 2010). Indeed, as a key moderator of the sickness response, an increased expression of PGE2 in the brain is associated with severe inflammation (Akanuma et al. 2011). Dalvi and colleagues (2015) have also shown that PGE2 production can increase the permeability of the BBB as shown in *in vitro* cultures of human brain microvascular endothelial cells treated with AA (Dalvi et al. 2015). Together, alterations to the transcription factors and signaling pathways in the hypothalamus could indicate a role for NGs in modulation of the sickness response. If neutropenia can induce an elevation in NFκB, STAT3, COX-2, and mPGES, as

implicated in the present experiment, it could indicate a latent modulatory impact of NGs during the later stages of inflammation. However, additional investigations still need to be performed in order to better understand this effect. By co-culturing glial cells with NGs and individually inhibiting the respective signaling pathways it would be possible to measure changes in inflammatory mediators such as PGE2. Moreover, the same technique could be applied *in vivo* using the neutropenic mouse model and inhibiting pivotal inflammatory signaling pathways to evaluate any differences in the sickness response.

4.1.3.3 Immune cell recruitment to the brain

If, as I hypothesize, NG interactions with the brain are modulating inflammatory mediators, then the local expression of chemoattractants could be an indicator of their recruitment. Production of CXCL1, for instance, by brain endothelial cells enhanced ICAM1 mediated NG binding during CLP-induced SAE in mice (Wang et al. 2015a). Augmented NG binding would support the association observed during LPS-induced systemic inflammation between upregulated brain levels of CXCL1 transcription and NG recruitment to the brain (Thomson et al. 2020). Indeed, in the present experiment, I found that CXCL1 expression was elevated in the hypothalamus during LPS-induced inflammation and varying degrees of NG recruitment to the SFO and PVN occurred. Although NG recruitment to the SFO was not as high as the PVN, it was at this brain structure that neutropenia (reduction by ~25%) in the present study reduced NG levels during inflammation. An early interaction between NGs and brain endothelial cells has already been identified as a contributing factor to the dysfunction of the CNS as seen in mice following CLP where increased MPO activity and BBB permeability were observed (Comim et al. 2011b). However, the previously mentioned significant interactions between NGs and microglia, that did not involve phagocytosis, observed by Neumann et al. (2018) and Kim et al. (2020) provide a promising direction for future studies (Neumann et al. 2018, Kim et al. 2020). Thus, NG-mediated modulation of microglial activation could impact brain inflammation since long term activation of microglia can lead to neuronal death and increased pro-inflammatory cytokine levels (Arai et al. 2004, Kim et al. 2020).

Following interactions with microglia, Kim and colleagues (2020) also found that NGs were re-entering the bloodstream by reverse transendothelial migration and could represent another route for communication between the brain and periphery via NG signaling (Kim et al. 2020). The few studies conducted on NG reverse transendothelial migration during sepsis tend to indicate that re-entry may exaggerate inflammation in the periphery (Ode et al. 2018, Jin et al. 2019) but the data is limited and further investigations are still required. Given the reduced NG recruitment to the SFO it may be at the CVO structures that significant interactions between microglial and NG or reverse transendothelial migration are occurring during severe systemic inflammation.

The inflammatory protease Elane is another important NG migration enzyme that eases passage through the endothelium, however, it can also be an indicator of NETosis as it is released during NET formation (Papayannopoulos et al. 2010, Singh et al. 2012). Translocation of Elane from azurophilic granules to the nucleus contributes to chromatin decondensation through the cleaving of histones and, eventual, break-down of the plasma membrane (Papayannopoulos et al. 2010). During septic inflammation, NETs in the periphery help to control pathogen levels but excessive formation can cause organ dysfunction and predict worse outcomes as shown by Czaikoski and colleagues (2016) using two different septic mouse models, namely, CLP and LPS-induced endotoxemia (Czaikoski et al. 2016). Moreover, PAD4 KO mice that are unable to form NETs have reduced levels of circulating pro-inflammatory cytokines, fewer activated microglia, reduced astrocyte loss, and improved depressive-like behaviors following treatment with LPS (Kong et al. 2021). Even though NG recruitment to the brain has been established during septic inflammation (Nguyen et al. 2007, Aguilar-Valles et al. 2014, Herz et al. 2015, Rummel et al. 2010) and circulating NETs are able to transfer inflammatory information to the brain (Kong et al. 2021), the role NETs play in the brain during SAE remains vague. Recently, Zhu et al. (2023) found increased NET formation in the hippocampus using a CLP-model to induce SAE in mice. Moreover, inhibition of NETs attenuated symptoms including memory impairment, BBB integrity, neuronal apoptosis, and microglia activation (Zhu et al. 2023).

In my own experiments, I did find that during early inflammation treatment with LPS increased the expression of Elane in the hypothalamus but this alone could be indicative

of NG migration or NETosis (Papayannopoulos et al. 2010, Singh et al. 2012). However, further analysis of the NET markers H3Cit and DNA/His at the level of the MnPO, a key hypothalamic structure for fever induction pathways (McKinley et al. 2003, Lazarus et al. 2007), did not show any differences between control groups and groups treated with LPS or PMN. An *in vitro* analysis of NGs also indicated that LPS was a poor inducer of NETs in mice. From these results, I would imply that the upregulation in Elane expression is most likely indicative of enhanced NG recruitment. Nonetheless, the negative NET result could also be due to the brain structure selected for analysis or the area analyzed. In order to maximize the analyses that could be performed using the brain tissue, I selected an early section of the MnPO for immunofluorescent staining that might not be representative of the entire brain. In addition, using quiescent mature NGs isolated from the plasma of uninfected mice, as opposed to NGs derived from bone marrow, which may have larger populations of immature cells, may increase the magnitude of NETosis. Indeed, human plasma derived NGs primed by LPS-activated factors and cytokines have demonstrated more rapid NET formation (Clark et al. 2007, Yousefi et al. 2009). Therefore, a more comprehensive analysis of other hypothalamic structures is still needed before NETs in the brain can be ruled out as modulators of inflammation in this model of severe systemic inflammation.

Other immune cells surrounding the brain, such as perivascular macrophages, can also be a source of pro-inflammatory cytokines (Quan et al. 1998). Their close contact with brain endothelial cells predisposes transfer of information between the immune system and the brain. As such, Serrats et al. (2010) revealed that perivascular macrophages generate PGE2 and stimulate endothelial cell PGE2 production when treated with IL-1β or LPS, respectively (Serrats et al. 2010). Moreover, during psychological restraint stress, the perivascular macrophages of rats contributed to brain levels of PGE2 via local production of COX-2. In the same experiment, ablation of the perivascular macrophages reduced PVN activation (Serrats et al. 2017). Interestingly, evaluations of the brain tissue from patients that passed away under septic conditions have shown a moderate increase in brain perivascular macrophages (Zrzavy et al. 2019). In my own experiments, I found that LPS overall modestly reduced CD163 mRNA expression, a marker protein for perivascular macrophages in mice, regardless of neutropenic status 4

h after stimulation suggesting that perivascular macrophages may not play a major role during severe systemic inflammation and neutropenia. It should be noted that the anti-inflammatory CD163 marker I used to identify perivascular macrophages has also been found on M2 microglia at low levels and was downregulated during acute sepsis (Orihuela et al. 2016, Zrzavy et al. 2019, Cherry et al. 2014).

4.1.4 Influence of neutropenia on activation of the HPA axis

Septic inflammation induced immune dysregulation can also extend to regulatory systems of the stress response through immune-to-brain communication via the HPA axis and glucocorticoid generation. Under normal circumstances, glucocorticoids (cortisol humans; corticosterone rodents) have a modulatory role that both suppresses the immune response and utilizes energy during illness to attempt a return to homeostasis (Chrousos 1995, Fuchs et al. 2013, Damm et al. 2011). Enhanced circulating glucocorticoids will regulate PRRs, cytokine generation, leukocyte recruitment, and promote an anti-inflammatory M2 macrophage phenotype (Cain and Cidlowski 2017). The disruption of HPA axis function and reduced glucocorticoid metabolism can lead to further elevation as shown by Boonen et al. (2013) where plasma cortisol levels were higher in critically ill patients compared to demographically matched controls (Boonen et al. 2013). In the present study, my results were consistent with the existing literature as I found that LPS did increase circulating levels of corticosterone in both groups. Interestingly, further comparisons between neutropenic and immunocompetent mice revealed that neutropenic mice experienced dysregulation of their HPA axis with a dampened but prolonged activity.

There is evidence that glucocorticoid modulation can be beneficial during sepsis since depletion of glucocorticoid receptors increased inflammation and/or mortality in several mouse models of sepsis including CLP- and LPS-induced inflammation (Kleiman et al. 2012, Goodwin et al. 2013, Jenniskens et al. 2018, van Looveren et al. 2020). Therefore, the initial reduced levels of corticosterone in neutropenic mice could represent an insufficient response of the HPA axis during early inflammation (4 h) due to an insufficient innate response of NGs. Similarly, an attenuated cortisol response in relation to C-reactive protein and procalcitonin has been observed in patients with

neutropenic fever and severe sepsis (Juutilainen et al. 2011). The lack of early corticosterone modulation may go on to influence the increase in circulating inflammatory mediators (24 h) I previously discussed. These pro-inflammatory cytokines could subsequently act through the CVOs and disrupted BBB in other brain structures to activate neurons of the PVN and boost HPA activation (Silverman et al. 2005). Indeed, cytokine activation of the inflammatory signaling by STAT3 and NFκB, which I also observed to be enhanced in the hypothalamus of neutropenic mice, can contribute to the expression of ACTH as has been seen *in vitro* with mice and in *in vivo* rat models during LPS-induced systemic inflammation or under chronic stress (Gautron et al. 2003, Takayasu et al. 2010, Mehet et al. 2012, Girotti et al. 2013).

Although there are benefits of circulating glucocorticoids, during later stages of inflammation, the prolonged exposure to high levels of corticosterone may become detrimental. Excessive production of corticosterone has been observed in rats that died following CLP while cortisol functioned as a predictor of mortality in human patients diagnosed with septic shock (Bollaert et al. 2003, Carlson and Chiu 2008). Ultimately, during neutropenia, the disruption of the HPA axis could be a further indicator of severity during early and later stage inflammation. Indeed, my own results showed dampened (4 h) but prolonged (24 h) elevated corticosterone levels highlighting the severity of a neutropenic status during septic-like inflammation even without bacterial overgrowth and another possible contributor to the increased mortality that took place in mice treated with higher doses of PMN.

4.1.5 Influence of neutropenia on thermoregulation

Core body temperature is an important signal of health and ineffectual thermoregulation in sepsis can be a strong indicator of severity (Gao et al. 2017, Rumbus et al. 2017). Although fever and hypothermia can each occur as a clinical manifestation during sepsis, and serious complications can develop from both, patients suffering from hypothermia have notoriously higher mortality rates than those with fever (Kushimoto et al. 2013, Drewry et al. 2015, Rumbus et al. 2017, Rumbus and Garami 2019). Indeed, hypothermia is often associated with a decline in organ function and progression to move severe clinical status (Kushimoto et al. 2013, Rumbus et al. 2017). In order to

improve treatment and survivability of septic infections it is important to determine the mechanics behind this thermoregulatory response. For instance, an exaggerated inflammatory response including overproduction of the circulating cytokines TNFα, IL-6, and IL-10 have all been observed in hypothermic mice and rats during different models of sepsis (Töllner et al. 2000, Saito et al. 2003, Corrigan et al. 2014, Mul Fedele et al. 2020). In my own experiments, I also found enhanced circulating peripheral cytokines accompanied by hypothermia following systemic treatment with a high dose of LPS.

High dose LPS treatment mimics a severe systemic inflammation and commonly results in hypothermia (Töllner et al. 2000, Leon 2004, Steiner et al. 2009, Mul Fedele et al. 2020, Souza et al. 2020). Previous studies in my own lab have also reported a drop in core body temperature using the same dosage of LPS (2.5 mg/kg) in mice (Pflieger 2021). In the present experiment, both groups treated with LPS became hypothermic. However, while the temperature drop of immunocompetent mice was similar to what was previously observed in rodents, about 1.5°C (Töllner et al. 2000, Leon 2004, Pflieger 2021), the temperature of the neutropenic mice continued to fall until it was nearly 3°C below their normal temperature. An exacerbated circulating cytokine response could point toward peripheral cytokines as likely contributors to this process. Given that there was a limited impact of neutropenia within the brain, an action of these cytokines on endothelial cells or at the level of the CVOs could be the driving force in generating the hypothermic response.

Interactions at the BBB, endothelial cells, and/or CVOs of LPS, TNFα, and IL-6 (Mallard 2012, Johnson et al. 2018, Laflamme and Rivest 2001, Chakravarty and Herkenham 2005) could ultimately transfer signals to thermosensitive regions of the hypothalamus. Subsequent glia activation and local production of inflammatory mediators would initiate signaling pathways such as that of TNFα-TNFR1 via transcription factor NFκB (Akira et al. 1993, Quan et al. 1998, Wajant and Scheurich 2011, Schlegel et al. 2012, Norden et al. 2016). In particular, cryogenic effects of TNFα have long been known to reduce body temperatures during LPS-induced inflammation in rats (Long et al. 1992, Klir et al. 1995). Indeed, during hypothermic septic inflammation, Fedele and colleagues (2020) identified enhanced TNFα and TNFR1 expression in the thermoregulatory preoptic area

of the hypothalamus of mice, similar to the heightened TNFα expression I also observed. In their experiment, more severe hypothermia was associated with higher levels of circulating TNFα and depletion of TNFR1 improved survival rates after treatment with LPS (Mul Fedele et al. 2020). Interestingly, depletion of TNFR1 did not improve hypothermia, although, mice with intact TNFα signaling pathways did have greater neuronal activation (Mul Fedele et al. 2020). Since the depletion of TNFR1 failed to abolish hypothermia in Fedele's experiment, it can be inferred that additional signaling must also contribute to this thermoregulatory response.

As previously discussed (see section 1.9.1), IL-6 is another well-known mediator of the febrile response capable of activating the COX pathway via STAT3 in endothelial cells of the brain during LPS-induced inflammation (Rummel et al. 2006, Eskilsson et al. 2014, Wilhelms et al. 2014). Other studies have found compelling evidence that the interaction between TNFα and IL-6 can switch TNFα from a pyrogen to become a cryogen. In IL-6 or TNFR KO mice with CLP-induced sepsis, depletion of the TNFR attenuated early hypothermia followed by fever but IL-6 depletion abolished the febrile response entirely and instead mice maintained a hypothermic status (Leon et al. 1998). Remick et al. (2005) found that during more severe CLP-induced sepsis IL-6 KO mice did not become hypothermic as was seen in WT control mice (Remick et al. 2005). Based on the existing data and what I observed in my own experiment, it is through signaling pathways such as those discussed here that circulating inflammatory mediators, like TNFα and IL-6, exacerbated hypothermia in neutropenic mice. In the future, culturing brain endothelial cells in the presence of NGs or cytokines shown to be upregulated in neutropenic mice during LPS-induced systemic inflammation could be useful in identifying anti-inflammatory pathways of NGs.

4.1.6 Conclusions and perspectives for further investigations

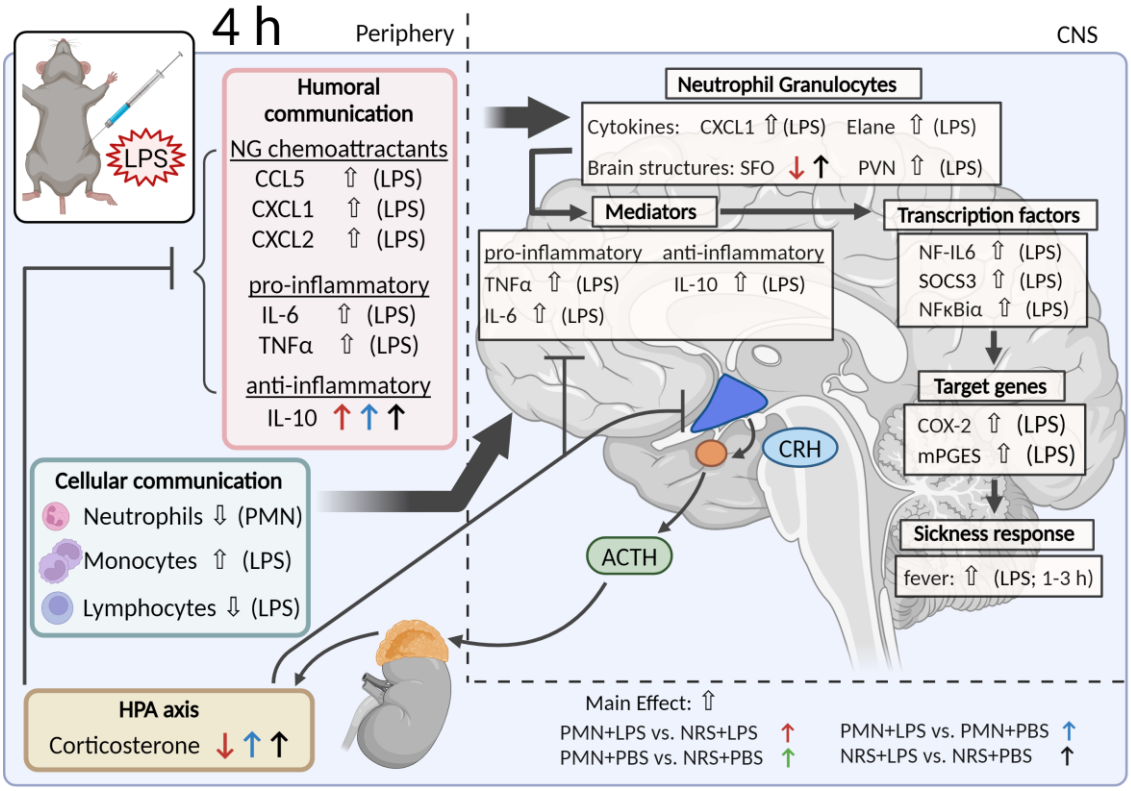

Figure 46 Influence of neutropenia on peripheral and brain inflammation at 4 h p.i. during LPS-induced severe systemic inflammation.

Schematic summary of the main findings: The inflammatory response in the plasma and hypothalamus following intraperitoneal instillation with lipopolysaccharide (LPS, 2.5 mg/kg) induced severe systemic inflammation includes the expression of inflammatory mediators, immune cells, transcription factors, and activation markers at 4 h p.i. with LPS. Further telemetric analyses were used to record activity, core body temperature, and food and water intake. Immunofluorescent analysis of neutrophil granulocyte (NG) recruitment to two brain structures, the subfornical organ (SFO) and paraventricular nucleus (PVN), were also carried out. Comparisons were made between groups that received normal rabbit serum (NRS, 1 ml/kg) or anti-polymorphonuclear serum (PMN, 1 ml/kg) as well as phosphate buffered saline (PBS) or LPS. Changes are shown between: PMN+LPS vs. NRS+LPS (**red**), PMN+PBS vs. NRS+PBS (**green**), PMN+LPS vs. PMN+PBS (**blue**), and NRS+LPS vs. NRS+PBS (**black**). Main effects are represented by an open arrow (⇧) and followed by the factor causing the effect. Arrows in the corresponding colors signify an increase (↑) or decrease (↓). Thick black arrows were used to show immune-to-brain communication from the periphery and thinner black arrows, outside of text boxes, showed pathways of activation in the brain. Other arrows were used to outline the route of the hypothalamic pituitary adrenal axis (HPA). Mediators in the periphery were predominantly increased by treatment with LPS at this stage of inflammation regardless of PMN or NRS pretreatment except for IL-10, which was elevated in mice that received PMN prior to LPS. PMN depleted the circulating level of NGs regardless of LPS treatment while monocytes were increased and lymphocytes were decreased after LPS regardless of neutropenic status, respectively. In the brain, NG chemoattractants were up-regulated by LPS treatment. LPS-induced NG recruitment to the SFO, but not the PVN, was attenuated by pretreatment with PMN. Other

inflammatory mediators, transcription factors, and target genes were increased by LPS compared to PBS and resulted in a short-lived febrile response from 1-3 h p.i. regardless of PMN or NRS pretreatment. While LPS increased corticosterone production, activation of the HPA was dampened during LPS-induced inflammation by pretreatment with PMN. A deficiency in NGs altered the anti-inflammatory response during early inflammation through increased IL-10 production and inhibition of corticosterone production via the HPA axis indicating a possible modulatory role for NGs during severe systemic inflammation. Abbreviations: chemokine (C-C motif) ligand (CCL), chemokine (C-X-C motif) ligand (CXCL), interleukin (IL), tumor necrosis factor (TNF), elastase, neutrophil expressed (Elane), nuclear factor (NF), suppressor of cytokine signaling (SOCS), cyclooxygenase (COX), microsomal prostaglandin E synthase (mPGES), main effect (ME). Figure created with BioRender.com.

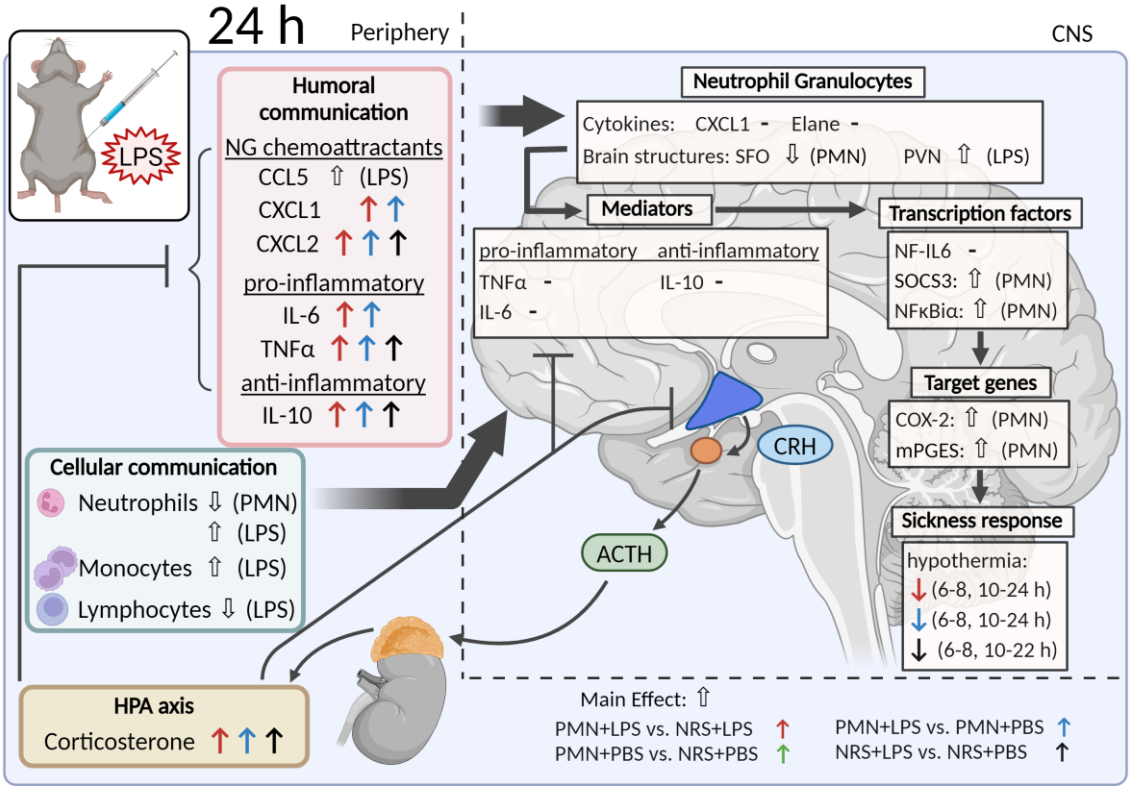

Figure 47 Influence of neutropenia on peripheral and brain inflammation at 24 h p.i. during LPS-induced severe systemic inflammation.

Schematic summary of the main findings: The inflammatory response in the plasma and hypothalamus following intraperitoneal instillation with lipopolysaccharide (LPS, 2.5 mg/kg) induced severe systemic inflammation includes the expression of inflammatory mediators, immune cells, transcription factors, and activation markers at 24 h p.i. with LPS. Further telemetric analyses were used to record activity, core body temperature, and food and water intake as well as immunofluorescent analysis of neutrophil granulocyte (NG) recruitment to two brain structures, the subfornical organ (SFO) and paraventricular nucleus (PVN), were also carried out. Comparisons were made between groups that received normal rabbit serum (NRS, 1 ml/kg) or anti-polymorphonuclear serum (PMN, 1 ml/kg) as well as phosphate buffered saline (PBS) or LPS. Changes are shown between: PMN+LPS vs. NRS+LPS (**red**), PMN+PBS vs. NRS+PBS (**green**), PMN+LPS vs. PMN+PBS (**blue**), and NRS+LPS vs. NRS+PBS (**black**). Main effects are

represented by an open arrow (⇧) and followed by the factor causing the effect. Arrows in the corresponding colors signify an increase (↑) or decrease (↓). Thick black arrows were used to show immune-to-brain communication from the periphery and thinner black arrows, outside of text boxes, showed pathways of activation in the brain. Other arrows were used to outline the route of the hypothalamic pituitary adrenal axis (HPA). Mediators in the periphery were predominantly increased by treatment with LPS at this stage of inflammation and exacerbated by pretreatment with PMN. Though significant differences were not detected between groups, main effects of LPS (increase) and PMN (decrease) indicated an overall impact on circulating NGs. The main effect of LPS further indicated increased circulating monocyte and decreased lymphocyte populations, respectively. In the brain, NG chemoattractants were no longer up-regulated by LPS treatment but a main effect of PMN signified reduced NG recruitment to the SFO remained overall. Other transcription factors and target genes were exacerbated by PMN pretreatment and, ultimately, PMN exacerbated the LPS-induced hypothermic response experienced by the mice from approximately 6 h p.i. At this later time point, corticosterone levels were now elevated in comparison to immunocompetent controls also treated with LPS indicating prolonged activation of the HPA. A deficiency in NGs intensified the peripheral inflammatory response and resulted in severe hypothermia signifying a potential anti-inflammatory role for NGs during severe systemic inflammation. However, minimal hypothalamic activation could imply that this role is not the result of immune cell trafficking to the brain but rather due to a peripheral or brain endothelial cell interaction. Abbreviations: chemokine (C-C motif) ligand (CCL), chemokine (C-X-C motif) ligand (CXCL), interleukin (IL), tumor necrosis factor (TNF), elastase, neutrophil expressed (Elane), nuclear factor (NF), suppressor of cytokine signaling (SOCS), cyclooxygenase (COX), microsomal prostaglandin E synthase (mPGES). Figure created with BioRender.com.

In summary, by analyzing the effects of neutropenia during LPS-induced severe systemic inflammation I found that NG depletion reduced recruitment of NGs to certain brain structures (SFO) and exacerbated the sickness response. I confirm that neutropenia increases mortality in severe cases, amplifies inflammatory responses in the periphery, dysregulates the HPA axis, and intensifies hypothermia. Minimal differences in activation markers of the hypothalamus between neutropenic and immunocompetent mice suggest that a peripheral action is largely responsible for the observed changes in sickness response severity. In particular, elevated levels of TNFα and IL-6 may contribute to hypothermia through interactions at the BBB and CVOs. Together, these data indicate an anti-inflammatory role of NGs and potentially partially explains the high mortality seen in clinical cases of neutropenia even independent of bacterial growth. While the treatment strategy remains largely the same for patients with or without neutropenia by tailoring treatments for neutropenic patients there could be hope to improve their overall outcome.

Limitations of the present study include the technique of NG depletion used. Although an established model for studying neutropenia (Aguilar-Valles et al. 2014) by using an anti-serum, I depleted circulating NGs but could not prevent the production of new NGs. Additionally, I was not able to check for endothelial cell activation or perform experiments, which blocked the actions of brain endothelial cells and therefore could not verify pathways of communication with the periphery. Future studies should expand on the present findings, for example, utilizing TNFα or IL-6 depleted mice to establish metabolic pathways and assessing humoral interactions with endothelial cells and CVOs. NETs should also be explored in a more dynamic manner in the periphery and brain to understand their contributions, if any, to the sickness response. Nevertheless, I have identified a significant role of NGs in modulating inflammation and thermoregulation during severe systemic inflammation and believe that the present data are meaningful in recognizing the beneficial role NGs can play during severe systemic inflammation.

4.2 Role of RvE1 receptors and ω-3 PUFA enrichment on LPS-induced ARDS

To understand the underlying mechanisms of lung-to-brain communication during LPS-induced ARDS, I investigated cytokines, lipid mediators, and the trafficking of NGs to the brain. I found that LPS-induced ARDS was sufficient to induce signs of inflammatory signaling in the brain such as NFκB. However, other inflammatory markers and genomic NF-IL6 activation in brain structures with (BIF) and without (OVLT) a complete BBB were not detected at significant levels to influence the lung-to-brain axis. Minimal humoral communication with the brain could indicate a larger role for immune cells, such as NGs, in lung-brain communication. Interestingly, descriptive NG data demonstrated a peak at 4 h p.i. within the BIF, an effect that was eliminated by ω-3 PUFA enrichment in Norm control mice but rescued in ω-3 PUFA enriched CR depleted mice during later stage inflammation. Further analysis revealed that genetic ω-3 PUFA enrichment and RvE1 receptor depletions altered mediators of inflammation in tissue from the lung, liver, and hypothalamus. In the periphery, RvE1 receptor deficient mice enriched with ω-3 PUFAs showed overall reduced pro- inflammatory cytokines including IL-17, IL-1β, and TNFα as well as anti-inflammatory IL-10. The NG markers GM-CSF and CXCL5 were similarly reduced in the periphery in Fat-LR KO mice compared to Fat-Norm controls. Signs of ω-3 PUFA enrichment altering inflammation in the brain were revealed for TFAM, NF-IL6, and PGC1α while ω-3 PUFA enrichment and RvE1 receptor deficiencies both affected CXCL1, IL-1β, IL-1ra, and GFAP. Though basal effects of LR deficiency were detected in the lung, it was ultimately the CR deficiency that showed more significant effects on pro-inflammatory cytokines and NG markers in the lung during inflammation. In the brain, depletion of CR once again impacted the BIF, here both NF-IL6 immunoreactivity and NG recruitment were altered and, for NGs, ω-3 PUFA enrichment enhanced their recruitment in CR but not LR deficient mice.

4.2.1 Systemic inflammation during ARDS

It has already been shown that inflammatory mediators produced in the lungs during ARDS can effect peripheral levels of circulating mediators and even reach the brain

(Pelosi and Rocco 2011). In fact, certain pro-inflammatory cytokines like IL-1β, TNFα, and IL-6 that are detectable in the BALF of ARDS patients are also able to cross the BBB, particularly when permeability increases such as during severe inflammation (Banks 2015, Carson et al. 2006, Wang et al. 2014a, Meduri et al. 2009). The influence of these cytokines is not restricted to those that support a pro-inflammatory profile and, in fact, decreased levels of anti-inflammatory IL-10 have even been correlated with increased mortality in ARDS patients (Aisiku et al. 2016). In the present experiment, a reduction in IL-10 was observed in CR deficient mice during later stages of inflammation and, though not fatal, may have been a contributing factor to the exacerbated NG recruitment observed in the same groups. By assessing a range of cytokines typically produced during inflammation in a variety of tissues, I hoped to identify pathways of lung-to-brain communication effected by RvE1 receptor deficiencies and/or ω-3 PUFA enrichment. To accomplish this, I first profiled the inflammatory response at the primary site of LPS-induced inflammation, i.e., the lung, before analyzing the liver as a proxy for the systemic inflammatory response. A descriptive peak in cytokines was observed at 24 h p.i. in the lung along with basal reductions in several inflammatory mediators by the LR and delayed effects of CR during late inflammation (i.e., 72 h p.i.). The same peak was absent in the liver and minor effects of RvE1 receptor deficiencies or ω-3 PUFA enrichment could be detected.

4.2.1.1 Influence of RvE1 receptors and ω-3 PUFA enrichment on inflammatory mediators in the lung

Due to the regulatory role that endogenous RvE1 can play in the resolution of inflammation, its actions through two different receptors (CR or LR) were the focus of this study. Both receptors can be competitively bound by RvE1 and modulate inflammation as has been observed in a mouse model of zymosan A-induced peritonitis and *E. coli* induced lung injury (Arita et al. 2007, El Kebir et al. 2012). The expression of these receptors on immune cells, and for CR in the lung, strongly indicates their presence during ARDS and makes them ideal targets to study (Bondue et al. 2011). For example, RvE1 can reduce TNFα related NFκB activation through CR while the RvE1-LR complex dampens pro-inflammatory signals by acting as an antagonist for this receptor (Arita et al. 2005, Arita et al. 2007, Lämmermann et al. 2013).

The organ-specific inflammatory responses investigated here revealed that nearly all effects of the RvE1 receptors were localized to lung tissue. Beginning at basal levels, the production of pro-inflammatory IL-1β and TNFα, as well as anti-inflammatory IL-10, were reduced in ω-3 PUFA enriched LR depleted mice. However, over the course of the experiment, only deficiency of the CR consistently altered any inflammatory markers. Indeed, depletion of CR caused reduced expression of IL-10 during inflammation and is suggestive of a complex regulation between the pro- and anti-inflammatory responses. The multifaceted interactions between RvE1 and each receptor could be due, in part, to continued formation of the LTB_4-BLT1 and chemerin-CR complexes. For one, though reduced, LTB_4 can still signal and exacerbate inflammation through the LR as has been observed by Horii and colleagues (2020) using a model of myocardial infarction (Horii et al. 2020). Moreover, interactions between chemerin and CR will foster viral clearance and attenuate levels of inflammation such that, in a mouse model of pneumonia, CR KO mice had higher mortality rates than controls with intact RvE1 receptors (Bondue et al. 2011). Taken together, in addition to the beneficial actions of RvE1 through the receptors, the LR and CR each maintain their pro- and anti-inflammatory capacities, respectively, indicating a broader implication and significance of each KO. In mice with depleted Rv receptors and reduced anti-inflammatory Rv signaling, I anticipated a dampened anti-inflammatory response similar to what has previously been shown in a mouse model of peritonitis by Arita et al. (2007), as well as enhanced inflammation as shown by Bondue et al. (2011) using a mouse model of pneumonia (Arita et al. 2007, Bondue et al. 2011). Indeed, in the present study, the reduction of lung IL-10 levels initially supports the concept of receptor depleted mice experiencing a dampened anti-inflammatory response due to defective Rv signaling. In combination with diminished IL-10, I would have expected upregulation of pro-inflammatory cytokines since acute neutralization of circulating IL-10 is known to exacerbate pro-inflammatory responses during severe LPS-induced system inflammation (Harden et al. 2014). However, reduced lung IL-1β and TNFα levels directly contradict such notions of reduced anti-inflammatory singling. The explanation for these discrepancies are likely linked to complexities of the inflammatory response and could suggest enhanced inflammation at other time points. I would propose that at basal levels the LR may exert a stronger influence on inflammation due to its pro-inflammatory capacities than the CR, which,

during later stages of inflammation, continues to significantly impact IL-10 production. However, since IL-1β and TNFα reductions were dependent on ω-3 PUFA enrichment in LR KO mice and Norm control mice did not show any effect of ω-3 PUFA enrichment, it remains to be investigated to what extent the receptor contributes to this process.

Interestingly, SPMs, and specifically the E series Rv, are capable of reducing IL-1β in lung tissue, in part by diminishing NG accumulation, as demonstrated in mice during a combination of ALI and bacterial pneumonia (Seki et al. 2010). Moreover, the RvE1 precursor 18-HEPE has been identified as a possible regulator of TNFα and NFκB in transgenic *fat-1* mice, contributing to the prevention of streptozocin-induced diabetes (Bellenger et al. 2011). Since IL-1β and TNFα are both produced by activated NGs during ARDS (Shokry et al. 2022, Huang et al. 2017), it is possible that RvE1 dependent reduction of NG levels in the lung lead to the reduction in pro-inflammatory cytokines found in the present study. Indeed, RvE1 dependent generation of ROS and depression of anti-apoptotic signals through LRs increases NG apoptosis and clearance during ALI (El Kebir et al. 2012). Apoptotic NGs are then phagocytosed by macrophages, which in turn increases production of pro-resolving anti-inflammatory mediators like IL-10 (El Kebir et al. 2012). This process has been documented by Herová and colleagues (2015) who found an increase IL-10 production after RvE1 treatment (10nM) in *in vitro* cultures of human primary macrophages expressing CR (Herová et al. 2015). Overall, functional NG regulation is one therapeutic effect of RvE1 that can be observed during ARDS (Seki et al. 2010, El Kebir et al. 2012). Such action may partially explain the cytokine profile of the lungs observed in the present study.

As inflammation progressed, i.e., 72 h p.i., CR deficiency was exerting a greater impact on pro-inflammatory cytokines (IL-17, IL-1β, TNFα, CXCL5, and GM-CSF) in the lung. Since CR is expressed by a wider variety of cell types than LR (Arita et al. 2005, Gantz et al. 1996, Samson et al. 1998a, Goralski et al. 2007, Mastroianni et al. 1991, Kaur et al. 2010), it is probable that the impact of this receptor extends beyond the initial phases of inflammation and continues even after inflammatory leukocytes have dissipated. Altogether, the combination of RvE1 receptor depletion and genetic ω-3 PUFA enrichment seemed to dampen the overall immune response in mice. However, mice with intact Rv receptors did not experience the same differences between WT and Fat

groups. The fact that differences in these mice with intact receptors were not observed may be due to several factors. In addition to the actions of chemerin and LTB_4 (Horii et al. 2020, Bondue et al. 2011), the low dose of LPS used or the time points analyzed should be considered.

4.2.1.2 Influence of RvE1 receptors and ω-3 PUFA enrichment on neutrophil granulocyte markers in the lung

Substantial recruitment and infiltration of NGs into the lungs is a major contributor to pathogenesis during ARDS (Ware and Matthay 2000, Mikacenic et al. 2016, Sawant et al. 2015). Thus, measuring markers associated with recruitment and activation NGs is an important and reliable way to monitor lung inflammation (Parsey et al. 1998, Matute-Bello et al. 2000, Ware and Matthay 2000, Jeyaseelan et al. 2004, Ballinger et al. 2006, Bhatia et al. 2012, Sawant et al. 2015, Mikacenic et al. 2016). IL-17 in particular has been identified as a key modulator of inflammation in the lung, such as during H1N1 influenza where IL-17 deficiency improved ALI in mice (Li et al. 2012). IL-17 can also be modulated through ω-3 PUFAs, which inhibits its production as demonstrated in several mouse models including experimental autoimmune encephalomyelitis, colitis, and psoriasis (Unoda et al. 2013, Monk et al. 2012, Qin et al. 2014). Another driving force during lung inflammation is GM-CSF, which polarizes cells to a pro-inflammatory phenotype and initiates myelopoiesis (Lang et al. 2020). Similarly to IL-17, long term dietary supplementation with ω-3 PUFAs reduced circulating levels of GM-CSF in insulin resistant patients with obesity (Hernandez et al. 2021). Consistent with previous studies, I found both IL-17 and GM-CSF to be reduced in the lungs of mice with genetic ω-3 PUFA enrichment. However, although the effects of ω-3 PUFAs are apparent, this only seemed to occur in combination with LR deficiency. As hypothesized for IL-1β, TNFα, and IL-10, complex regulatory signaling pathways and other binding partners aside from RvE1, such as LTB_4 or chemerin, could help to explain discrepancies between groups. Nevertheless, reduced BALF levels of pro-inflammatory cytokines, including CCL5 and CXCL1, and elevated lung tissue levels of both RvE1 and PD1 have been recorded in ω-3 PUFA enriched Fat mice during allergic airway inflammation (Bilal et al. 2011). Research by Haworth and colleagues (2008) also identified that RvE1 treatment decreased levels of IL-17 in BALF and suppressed IL-17 producing T helper cells using

a mouse model of allergic airway inflammation (Haworth et al. 2008). Moreover, modulation of CXCL1 by ω-3 PUFAs can influence the outcome during early lung infection (Tiesset et al. 2009). However, the present results only found a moderate impact of ω-3 PUFAs on CXCL1 among Norm and CR deficient mice that reached significance only at a later stage of lung inflammation.

4.2.1.3 Influence of RvE1 receptors and ω-3 PUFA enrichment on inflammatory mediators in the liver

In comparison to the lung, far fewer alterations to NG marker expression were detectable in the liver. Here, I did observe an ω-3 PUFA dependent reduction of IL-17 in the Norm control group with intact Rv receptors, which is in line with what others have previously reported (Unoda et al. 2013, Monk et al. 2012, Qin et al. 2014). Differences between inflammatory mediator profiles in the lung and liver might again signify a delay in the inflammatory dynamics originating in the lung with some moderate spillover to the circulation eliciting a minor response in the liver. For instance, in the liver, RvE1 seems to require the CR, or in the case of IL-10 CR or LR, in order to modulate inflammation with an overall more robust impact of the CR similar to what we observed for the lung. Overall, the lack of a strong effect of LPS to increase inflammatory mediators in the liver indicates weak contributions of humoral mediators between lung-organ interactions in our ARDS model.

4.2.2 Inflammation in the brain during ARDS

During lung inflammation, the lungs are capable of producing a wide range of inflammatory mediators (Moldoveanu et al. 2009). In particular, LPS models of ARDS show an increase in the permeability of endothelial barriers and the accumulation of leukocytes and other signaling molecules, including NGs in the lung (Matthay et al. 2012, Schulte et al. 2011, Williams et al. 2017). As a consequence of enhanced leukocyte accumulation and activation, high cytokine synthesis occurs (Darwish et al. 2011). Notably, IL-1β is a key mediator of the inflammatory process in the lungs (Goodman et al. 2003b). Additionally, and as previously mentioned, the impact of ARDS can reach beyond the lungs and cause harm to other organs such as the liver and brain (Li et al. 2022). Indeed, bi-directional communication exists between the lungs and brain,

and injuries or insults to either organ can impact the other (Gonzalvo et al. 2007, Sahu et al. 2018, Li et al. 2022, Rummel et al. 2022). This pathway was exemplified in a study by Sahu and colleagues (2018) using a two-hit model to mimic ALI. In this study, mice were treated with an i.t. instillation of hydrochloric acid and LPS, after which the animals displayed cognitive impairments and had elevated levels of circulating pro-inflammatory cytokines (Sahu et al. 2018). It is likely that during ALI/ARDS inflammatory mediators are responsible for some form of cross talk between the lung and brain resulting in these deleterious effects of cognitive impairments. The transmission of information via cytokines and immune cells allows for a possible circuit of communication between the lung and the brain. Previous studies have even shown how upregulation of NGs and neutrophilic NADPH oxidase activation, for example, can contribute to neurological symptoms in a mouse model of ALI (Pelosi and Rocco 2011, Nadeem et al. 2017, Li et al. 2022).

4.2.2.1 Influence of RvE1 receptors and ω-3 PUFA enrichment on inflammatory mediators in the brain

Since anti-inflammatory effects in the brain have been established for ω-3 PUFA and their derivatives and given the impact ARDS can have on the brain, I was particularly interested to see if ω-3 PUFAs affected inflammation in the brain during LPS-induced ARDS. Previously, it has been shown that genetic ω-3 PUFA enrichment accelerates recovery from CNS controlled sickness responses, such as fever, after i.t LPS-installation (Mayer et al. 2009). Moreover, others have also shown that RvE1 specifically can suppress LPS-induced depressive- like symptoms when infused into the brain (Deyama et al. 2018). In combination with work done by Wang and colleagues (2015), which showed that patients with Alzheimer's disease had upregulated glial expression of CR (Wang et al. 2015b), these data suggest the need for further investigations into the applications of ω-3 PUFAs during brain inflammation as some form of counter regulation to inflammation.

To outline pathways of lung-to-brain communication during ARDS contributing to inflammation, further analyses of the brain were performed. Indeed, I discovered evidence that LPS-induced ARDS was already sufficient to alter inflammatory mediators

in the hypothalamus as well as NG recruitment to different brain structures. Significant differences were found in markers of oxidative stress, NGs, mitochondrial activity, cytokines, and astrocyte activation but little to no changes was detected in key signaling pathways, PG synthesis, and markers of neuroplasticity in the hypothalamus. Additionally, assessments of NG recruitment and NF-IL6 immunoreactivity were performed (I) at the OVLT, a brain structure with a leaky BBB predisposed to detecting inflammatory mediators (Roth and Blatteis 2014, Roth et al. 2004), and (II) the BIF, a brain structure with a complete BBB. In comparing these two brain structures, I was able to evaluate the significance of blood borne signaling during lung-to-brain communication.

4.2.2.2 Influence of RvE1 receptors and ω-3 PUFA enrichment on oxidative stress in the brain

It is already known that oxidative stress plays an important role in the brain's inflammatory response during LPS-induced inflammation (Bernhardi et al. 2015, Hritcu et al. 2011, Garcia et al. 2018, Hritcu and Ciobica 2013). The extent that oxidative stress occurs can be determined by analyzing the production of antioxidants (i.e., Cat, SOD1, and SOD2) and microglial expression of NOS2 (Younus 2018, Badshah et al. 2019, Nandi et al. 2019). While these enzymes are important to maintain homeostasis, exorbitant NOS2 production or inadequate regulation by antioxidants can lead to oxidative stress and cellular damage (Loh et al. 2006, Mariani et al. 2005, Moreira et al. 2005). Given the anti-inflammatory capacities of RvE1 and the expression by glial cells of CR, there has been increased interest in the applications of RvE1 during brain inflammation (Fries et al. 2005, Chalon 2006, Wang et al. 2015b, Zhang et al. 2018). Indeed, Zhang et al. (2022) recently found that signaling through CR by RvE1 improved oxidative stress in the brains of a mouse model of diabetes (Zhang et al. 2022). My initial evaluation of the hypothalamus revealed that CR deficiency had an overall impact and WT-CR KO mice, in particular, experienced reduced production of NOS2 at later time points after LPS-induced ARDS. Moreover, the expression of TFAM, which plays a significant role in mitochondrial biogenesis and maintenance as well as other additional antioxidant effects, was altered in mice deficient for CR (Zhang and Wang 2018, Kang et al. 2007). Since previous studies have already found that TFAM can to a certain extent protect against cognitive impairments in neurological disorders like Alzheimer's disease

(Alawdi et al. 2017), CR dependent alterations to its expression seem be of importance during inflammation. To confirm the observed results on hypothalamic NOS2 expression, further analyses on protein level were performed in collaboration with the lab of Prof. Dr. Carsten Culmsee (Institute for Pharmacology and Clinical Pharmacy, Philipps University Marburg; data not shown) (Hernandez et al. 2023). Interestingly, these analyses revealed that neither ω-3 PUFA enrichment nor CR receptor deficiency had an effect on protein carbonylation or protein levels of SOD2 and Cat. Even though ROS generation had some connections with LR deficiency, my preliminary analysis of the hypothalamus indicated greater differences with CR deficient mice. Therefore, additional assessments were limited to these groups i.e., CR KO mice.

4.2.2.3 Influence of RvE1 receptors and ω-3 PUFA enrichment on neutrophil granulocyte recruitment to the brain

As with the periphery, NGs role in the brain continued to be a primary interest. Recently, recruitment of NGs to the brain has been emphasized as an important pathway in immune-to-brain communication in the course of systemic and localized organ-specific lung inflammation (Pflieger et al. 2018, Nadeem et al. 2017). Since ARDS causes substantial recruitment of NGs to the lungs (Ware and Matthay 2000, Parsey et al. 1998), I aimed to investigate if these cells were also transmitting information from the lung to the brain. Unexpectedly, the initial results revealed that the chemoattractant CXCL1 was enhanced by ω-3 PUFAs but such an increase was lacking in both Rv receptor-deficient groups although ω-3 PUFAs did significantly reduce production of CXCL1 in CR KO mice compared to Fat-Norm. These results directly conflicted with what was expected since ω-3 PUFAs should reduce NG infiltration and increase phagocytosis as previously shown (Marcheselli et al. 2003, Serhan et al. 2009). Nonetheless, previous studies did not include detailed analyses of the dynamics of NG recruitment and its modulation by ω-3 PUFAs, which remains to be investigated in the future.

To more accurately visualize NG recruitment to the brain, immunofluorescence analyses allowed me to assess recruitment to different brain structures. Here, the results more accurately reflected what has been shown previously (Marcheselli et al. 2003, Serhan et

al. 2009, Caputo et al. 2019). Enrichment with ω-3 PUFAs eliminated the LPS-induced NG peak detected in the WT-Norm mice. By itself, RvE1 has been previously shown to exert a significant impact on human NGs *in vitro* by weakening LTB4s pro-inflammatory properties (Arita et al. 2007). Arita and colleagues (2005) demonstrated that after a combination treatment of aspirin and EPA, patients had increased levels of RvE1 in circulation in a manner consistent with EPA derived 18R-HEPE being converted to RvE1 by means of leukocyte and endothelial cells (Serhan et al. 2000, Arita et al. 2005). Building on this information, using a dorsal air pouch mouse model of TNFα-induced local inflammation, treatment with a combination of aspirin and 18R-HEPE attenuated NGs recruitment to the inflammatory site (Serhan et al. 2000, Arita et al. 2005). Recently, experiments performed in my own lab have even detected increased production of 18-HEPE in the supernatants of primary CVO cultures following stimulation with LPS, stressing 18-HEPE as a promising endogenously produced lead to potentially treat inflammation in the brain (Pflieger et al. 2022). Even though explicit differences were not detected amongst WT groups, increased NG recruitment to the BIF was detected in ω-3 PUFA enriched CR KO mice in comparison to Norm in my present study. Additionally, a stronger effect was seen in mice deficient in CR as opposed to a LR deficiency suggesting that modulation of NG during ARDS may primarily occur through this receptor. As it happens, the RvE1/CR axis is known to prompt NG apoptosis and phagocytosis (Flesher et al. 2014, Serhan 2014). Together, previous studies and my present results support a role for RvE1/CR in NG recruitment to the brain.

4.2.2.4 Influence of RvE1 receptors and ω-3 PUFA enrichment on the humoral communication pathway

Additional attention was placed on the possibility for lung-to-brain communication and the capacity for cytokines, such as those induced in the lungs by LPS, to modulate inflammation in the hypothalamus. Indeed, brain endothelial cytokine production and the compromised integrity of the BBB during LPS-induced inflammation (Biesmans et al. 2013) can increase the impact of inflammatory mediators on the brain. As such, IL-1β, which can lead to its local production by microglia, may contribute to such effects (Banks 2015, Hoogland et al. 2015, Prinz and Priller 2014). I found that ω-3 PUFAs and RvE1

receptor deficiencies differently altered mRNA expression of IL-1β and IL-1ra. Initially, basal levels were increased in an ω-3 PUFA-dependent manner for IL-1ra in CR KO mice, which may well be related to RvE1 expression by microglial. Although it is uncertain why CR KO mice alone experienced this effect in my study, early microglial-dependent production of IL-1ra (Pinteaux et al. 2006), could attenuate NG emigration and, thus, limit LPS-induced inflammation (Ulich et al. 1991) and modulate pro-inflammatory activity of IL-1β (Pinteaux et al. 2006, Plata-Salamán and ffrench-Mullen 1994, Seckinger et al. 1987). To further expand on the present mRNA expression data, additional analyses are necessary to confirm a role for Rv signaling in brain IL-1β/IL-1ra action on protein levels.

4.2.2.5 Influence of RvE1 receptors and ω-3 PUFA enrichment on transcription factors and signaling pathways

Downstream of cytokine action, several signaling pathways contribute to brain inflammation including NF-IL6, NFκB, and PPARγ (Rummel 2016, Schneiders et al. 2015, Shih et al. 2015, Villapol 2018). Each of these pathways can be influenced by ω-3 PUFAs as has been demonstrated in different models of inflammation (Arita et al. 2005, Liang and Ward 2006, Draper et al. 2011, Bredehöft et al. 2019). However, in my study, mRNA expression of NF-IL6 and the PPARγ signal regulator PGC1α, had only minor impacts due to ω-3 PUFAs (Liang and Ward 2006). Moreover, despite the fact that RvE1 can limit activation of the prominent pro-inflammatory transcription factor NFκB (Arita et al. 2005, Tak and Firestein 2001) I did not reveal any significant differences between groups. Given that my working group has previously shown that LPS treatment in Fat mice can induce unique lipid mediator production patterns in the OVLT in combination with NF-IL6 expression (Bredehöft et al. 2019); I decided to pursue an additional NF-IL6 analysis.

NF-IL6 has been shown to behave as a transcription factor for both, early pro-inflammatory and late anti-inflammatory mediators during systemic inflammation, and is broadly used as a marker for genomic brain cell activation (Rummel 2016, Schneiders et al. 2015). Additional spatiotemporal immunohistochemical analysis of NF-IL6 at the level of the OVLT and BIF allowed for more detailed results to be obtained regarding the

transcription factor. Interestingly, I did not observe significant differences in the immunoreactivity of NF-IL6 between groups or by genetic ω-3 PUFA enrichment at the OVLT. However, subtle alterations due to ω-3 PUFAs and RvE1 receptor deficiencies were detected at the BIF, suggestive of some impact on brain cell activity. The Fat-CR KO mice possibly experienced a prolonged state of NF-IL6 activation than other groups, but the high variability in immunoreactivity and low n-numbers should be taken into account. Indeed, such data remains descriptive for large parts. Nonetheless, unaffected mRNA expression of mPGES, i.e., the terminal enzyme for PGE2 production, reinforces a limited impact of NF-IL6 being involved in regulating mPGES expression (Uematsu et al. 2002, Schneiders et al. 2015). Overall, while some changes to the brain cell activation marker NF-IL6 validate modest brain alterations during LPS-induced ARDS, these minor changes once more suggest that humoral signals refrained from playing a major role in lung-brain signaling.

4.2.2.6 Influence of RvE1 receptors and ω-3 PUFA enrichment on glial cell activation

Since microglia functions have been shown to be affected by asthma, as well as by changes to the lungs microbiome (Lewkowich et al. 2020, Hosang et al. 2022), the activation of glial cells was also assessed. During brain inflammation, glial cells can release cytokines, lipid mediators, or even ROS to regulate local inflammation (Hoogland et al. 2015, Xie et al. 2002, Chhor et al. 2013, Cherry et al. 2014). By assessing different therapeutic techniques in an attempt to modulate the activation of certain glia like microglia or astrocytes, damage could potentially be attenuated (Michaud et al. 2013). On the one hand, work done by Ji et al (2012) found that ω-3 PUFA supplementation inhibited microglia activation in rats during LPS-induced inflammation (Ji et al. 2012). On the other hand, microglia depletion studies performed in mice and rats failed to inhibit the expression of pro-inflammatory cytokines in the brain following treatment with LPS (Vichaya et al. 2020). Another study by Kawashima and colleagues (2008) found that IL-1β-induced IL-6 secretion could be attenuated in glioma cells treated with EPA *in vitro* in an astrocyte dependent manner (Kawashima et al. 2008). Taken together, the brain inflammatory response is a complex network with multiple contributing factors. While I did not detect significant changes to CD68, a

marker for microglial activation (Supplementary Figure 1), the astrocytic activation marker GFAP was impacted by CR deficiency. Further analysis performed in collaboration with the lab of Prof. Dr. Christiane Herden (Institute for Veterinary Pathology, JLU; data not shown) confirmed that, at the level of the PVN, astrocyte area was increased at 24 h p.i. in mice deficient in the CR regardless of ω-3 PUFAs (Hernandez et al. 2023). Using a mouse model of Parkinson's disease, Bousquet and colleagues (2011) already found that GFAP expression is reduced in Fat mice (Bousquet et al. 2011). Since inflammation in the brain can increase the astrocytic expression of CR (Wang et al. 2015b, Emre et al. 2020) the actions of RvE1 through this receptor may be able to modulate astrocyte activation, however future studies are necessary before these observations can be confirmed.

4.2.3 Lipid mediators in the lung and brain during LPS-induced ARDS

In addition to the profiles of inflammatory mediators in the lung and brain new insights into the alterations of lipid mediators following LPS-induced ARDS were also investigated in collaboration with the lab of Prof. Dr. Natascha Sommer (Excellence Cluster Cardio-Pulmonary Institute, Universities of Giessen and Marburg Lung Center, JLU; data not shown) (Hernandez et al. 2023). It is already well understood that EPA and SPMs, namely Rvs, participate in the return to homeostasis during lung inflammation (Schaefer et al. 2007, Mayer et al. 2009, Seki et al. 2010, Luo et al. 2022). Moreover, given the high levels of PUFAs like DHA and AA in the brain (25-30%) (Joffre et al. 2019) alterations to the brain's lipid profile by genetic ω-3 PUFA enrichment, deficiency of the RvE1 receptors, and/or LPS-induced ARDS could have broad effects on the inflammatory response. Previous studies have shown that circulating levels of both ω-3 and ω-6 PUFAs can be elevated during severe inflammation and/or infection (Weissman 1990, Mayer et al. 2003, Mayer et al. 2009). Mayer et al. (2003, 2009) for one, saw that the increased plasma levels of DHA and EPA during inflammation or infection in both human patients and in a mouse model could be further elevated by genetic ω-3 PUFA enrichment (mice) or following treatment with ω-3 PUFA emulsion (human patients) (Mayer et al. 2003, Mayer et al. 2009). Indeed, in the present study, most PUFAs in the lung and brain were time-dependently increased by genetic ω-3 PUFA enrichment and partially altered RvE1 receptor deficiencies.

Here, depletion of RvE1 receptors, and in particular LR, tended to increase PUFAs in both the lung and brain. However, in combination with ω-3 PUFA enrichment LR deficiencies caused an overall reduction in brain PUFAs. In comparison, at basal levels and 24 h p.i. with LPS, ω-3 PUFA enrichment alone increased PUFAs and their derivatives in both Norm and CR deficient groups compared to their respective WT controls in a manner consistent with the existing data (Weissman 1990, Mayer et al. 2003, Mayer et al. 2009). Although Fat mice did show higher levels of several lipid mediators than WT controls, it remains unclear why more anti-inflammatory effects were not detected in either the lungs or brains.

A comprehensive analysis of AA, EPA, DHA, and their respective derivatives was performed but, due to the aim of the present study, I will focus on RvE1 and its precursor 18-HEPE. As with previous studies (Schaefer et al. 2007, Mayer et al. 2009, Bilal et al. 2011), ω-3 PUFA enrichment increased EPA at basal levels in the lungs compared to the Norm controls; however, an interesting trend observed here was that these levels decreased over time as inflammation progressed (i.e., 24 h and 72 h p.i.). Consecutively, as EPA decreased in the lungs, the metabolites RvE1 and its precursor 18-HEPE were detected at increasing levels in the genetically ω-3 PUFA enriched mice. Taken together, the decrease in EPA is likely indicative of its conversion into RvE1 in the lungs. This effect was not observed for the brain but considering the brains higher expression of DHA compared to EPA (Ostermann et al. 2017, Joffre et al. 2019) 18-HEPE and RvE1 were not expected to be as prevalent. In combination with instability and rapid conversion to its inactive products, RvE1 could be especially difficult to detect in the brain as has been seen in other biological samples (Serhan 2014, Schebb et al. 2022).

Analysis of DHA and its derivatives (17(S)-HDHA, 14(S)-HDHA, NPD1/PDX, and Mar1) in the brain showed that all values were increased after 24 h p.i. in ω-3 PUFA enriched Norm and CR deficient groups. In comparison, ω-3 PUFA enriched mice deficient in LR showed far fewer elevated PUFAs in the brain than both Norm and CR deficient groups. Attenuated PUFA levels in the brains of these LR KO mice could be in part due to a reduced inflammatory response in these mice to LPS as has been previously reported in mouse models of sterile injury and infection and myocardial infarction (Lämmermann et

al. 2013, Horii et al. 2020). Given the capacity of 17(S)- and 14(S)-HDHA as leukocyte regulators, their upregulation could contribute to reduced NG recruitment and possibly block glial production of cytokines (Hong et al. 2003). Altogether, the present results suggest that high levels of EPA and EPA derivatives in the lung and DHA and DHA derivatives in the brain may have some functional significance in lung-brain communication.

4.2.4 Conclusions and perspectives for further investigations

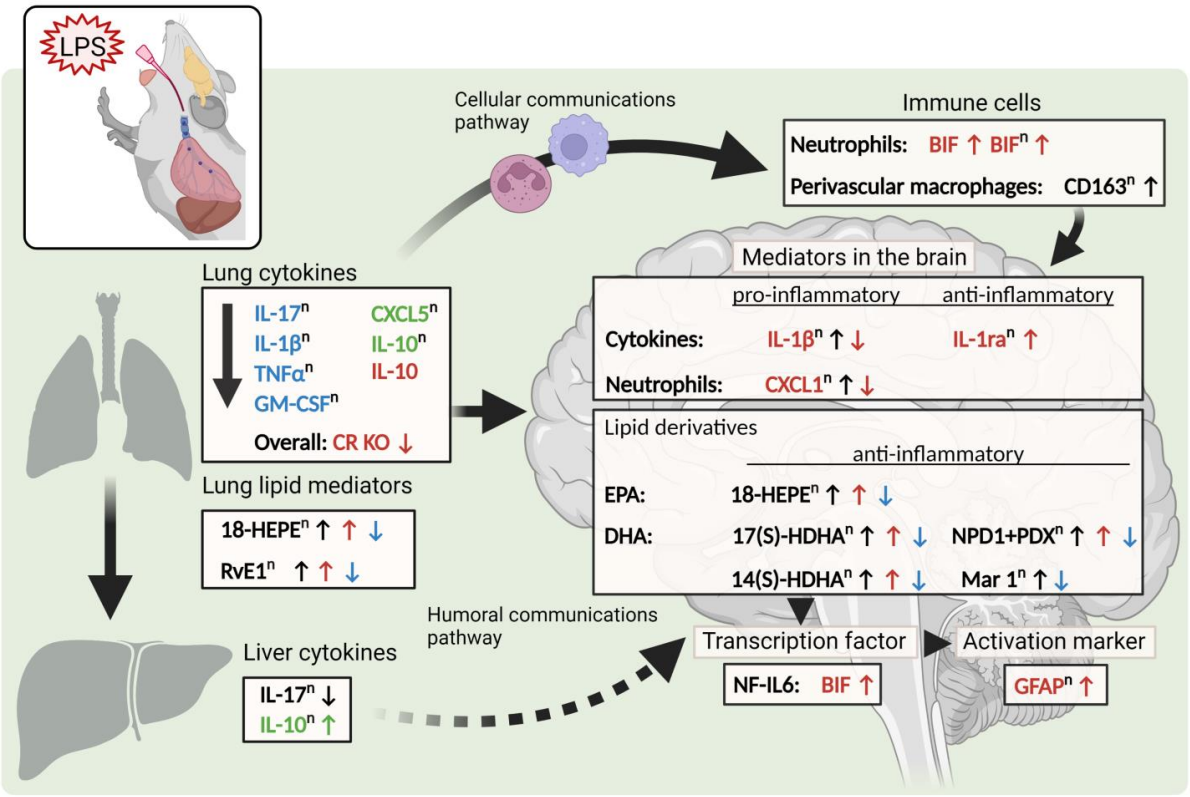

Figure 48 Influence of ω-3 PUFAs and RvE1 receptor knock-outs on inflammatory marker proteins and lung-brain signaling pathways during LPS-induced ARDS

Schematic summary: Analysis of the inflammatory response in the periphery (lung, liver) and brain (hypothalamus) after intra-tracheal instillation of lipopolysaccharide (LPS, 10µg) induced ARDS. The mRNA-expression of inflammatory mediators was assessed including: cytokines, transcription factors, immune cells, activation markers, and lipid mediators at 0 h, 24 h, and 72 h p.i. with LPS. Additional analysis of neutrophil granulocyte (NG) recruitment and nuclear factor (NF) interleukin (IL) 6 immunoreactivity in two brain structures, the bifurcation (BIF) and the *organum vasculosum of the lamina terminalis* (OVLT) were carried out by immunofluorescent staining at 0h, 4 h, 24 h, 72 h, and 120 h p.i. Changes are presented compared to unmodified controls (Norm) on a wild-type (WT) background. Different colors were used to show effects in resolvin (Rv) receptor knock-out (KO) groups: **red**-chemerin receptor 23 (CR) KO, **blue**- leukotriene B4 receptor (LR) KO, or **green**- both KOs. Comparisons

between Norm and genetically enriched ω-3 PUFA synthesizing Fat-1 KO mice (Fat) are identified with an 'n' symbol and **black** represents comparisons between Fat-Norm and WT-Norm groups. Arrows in the corresponding colors indicate an increase (↑) or decrease (↓) in that genotype. Within the lung cytokine box, a large arrow indicates that all cytokines were decreased. Mediators in the brain were primarily impacted in CR KO groups but other effects between Fat-Norm and WT-Norm were also present. Due to extensive effects between groups, the lipid mediators are written in black and arrows indicate genotype-specific alterations. To simplify the image, changes are not shown by time. Therefore, all significant differences for all time points are shown together. Please refer to section 3.3 for alterations at specific time points. Weak effects of the RvE1 receptor KOs in Fat mice were detected in the lung and liver. In the brain, I found that both RvE1 receptor KOs may increase recruitment of NGs at the OVLT, a brain structure with a leaky BBB while only the CR KO group had an impact at the BIF. Minor CR KO dependent alterations in inflammatory mediators were detected in the hypothalamus, and it was here that I also detected an effect of Fat in Norm controls. EPA and DHA and their derivatives in the hypothalamus were, overall, increased in Fat-Norm and Fat-CR KO mice but decreased in Fat-LR KO mice. The inflammatory transcription factor NF-IL6 was increased in the BIF of RvE1 receptor KO mice. Lastly, GFAP expression was increased in the Fat-CR KO group alone. Taken together, LPS-induced ARDS caused low levels of inflammatory signaling in the periphery and hypothalamus where immune-to-brain communication occurred via humoral signaling and NG recruitment. A deficiency in RvE1 receptors, particularly CR in the hypothalamus, and enhanced production of ω-3 PUFAs altered several of these inflammatory mediators and lipid mediators indicating a possible role for RvE1 to modulate immune-to-brain communication during ARDS via recruitment of NGs. Abbreviations: granulocyte-macrophage colony-stimulating factor (GM-CSF), chemokine (C-X-C motif) ligand (CXCL), cluster of differentiation (CD), hydroxyeicosapentaenoic acid (HEPE), hydroxy docosahexaenoic acid (HDHA), neuroprotection D1 (NPD1), protectin DX (PDX), maresin 1 (Mar1), nuclear factor (NF), glial fibrillary acidic protein (GFAP). Figure created with BioRender.com.

In summary I revealed, in part through descriptive results, that LPS-induced ARDS increased peripheral inflammatory signaling in the lung, and was even apparent in the hypothalamus where minor humoral signaling and immune cell recruitment to the brain facilitated immune-to-brain communication. A deficiency of RvE1 receptors and enhanced production of ω-3 PUFAs was able to modify the profile of several inflammatory mediators, to alter astrocytic activation (CR deficiency), and to change lipid mediators in the brain. I have presented evidence that RvE1 receptor deficiencies and genetic enrichment of ω-3 PUFAs can modify the brains lipid profile during LPS-induced ARDS. In particular, genetic ω-3 PUFAs enrichment may be capable of modulating lung-brain communication through NG recruitment, and to a lesser extent via the humoral pathway by acting through RvE1 actions on CR during ARDS. Overall, ω-3 PUFAs and SPMs i.e., NPD1/PDX or Mar1 and certain SPM precursors i.e., 18-HEPE, 17(S)-HDHA, or 14(S)-HDHA, may well represent targets for future therapeutic investigations to

modulate inflammation for individuals dealing with or at risk of developing brain inflammation due to ARDS.

Limitations of the present study consist of technical challenges causing low numbers per group. However, the experiment did employ the RRR principle of Russel and Burch (Russell and Burch 1960) and analyzed tissue harvested in collaboration with another ongoing experiment with a separate purpose. To further reduce the amount of animals required for scientific purposes, the experiment focused only on LPS-treated mice and, therefore, LPS-induced effects compared to PBS controls remain to be further analyzed in the future. Moreover, to take full advantage of transgenic animals being produced, both males and females were utilized for the experiment. The use of both sexes may have altered some assessments, due to the fact that gender specific alterations cannot be excluded. However, due to low n-numbers, I was unable to analyze by gender and subsequently rule out these effects. Future studies should expand on these findings, for example, regarding metabolic pathways, assessing NGs in a more dynamic manner, along with testing additional doses of LPS and gender effects. Nevertheless, I believe that the present data are meaningful and identify an important role for the precursors and receptors of RvE1 and NGs in lung-to-brain communication and explore, for the first time, the impact of lung inflammation, Rv receptor deficiency, and genetic ω-3 PUFA enrichment on the brain during LPS-induced ARDS.

V. Summary

The brain inflammatory response and brain-controlled sickness symptoms, such as fever, involve innate immune system activation through immune-to-brain signaling during systemic inflammatory insults. Neutrophil granulocytes (NG) are a crucial part of the carefully regulated immune system and contribute to the transmission of inflammatory information. Dysregulation of the immune response during an infection can have severe consequences, such as progression to septic inflammation. Indeed, sepsis is characterized by an overwhelming inflammatory response to infection and can be life-threatening or result in long-term impairments due, in part, to poor treatment options. Moreover, neutropenic fever is a severe life threatening condition in immunocompromised patients, such as those that have undergone chemotherapy. Therefore, an anti-inflammatory role for NGs during such inflammatory conditions was hypothesized. This hypothesis is supported by NG-dependent production of specialized pro-resolving mediators (SPM), like resolvin (Rv) E1. For my dissertation project, the role of NGs in two different mouse models of systemic and localized organ-specific lung inflammation was investigated.

The first inflammatory model evaluated the effects of neutropenia during severe systemic inflammation. Mice received an intraperitoneal (IP) dose of anti-polymorphonuclear serum (PMN; 1 ml/kg), or normal rabbit serum (NRS) as a control, followed by an IP dose of lipopolysaccharide (LPS; 2.5 mg/kg) or phosphate buffered saline (PBS) 24 h later. The effects on sickness symptoms and peripheral and brain inflammation were investigated. Using a telemetric system, the following physiological parameters were continuously recorded: core body temperature, locomotor activity, and food and water intake. Mice were sacrificed at 4 h or 24 h post-inoculation (p.i.) with LPS and brain and plasma samples were collected. Alterations to peripheral and brain inflammation were assessed by hematological measurements, immunohistochemistry, immunoassays, and RT-qPCR.

The second inflammatory model evaluated the effects of genetic omega (ω)-3 polyunsaturated fatty acid (PUFA) enrichment and two different RvE1 receptor (chemerin receptor 23 [CR] or leukotriene B4 receptor [LR]) deficiencies during acute

respiratory distress syndrome (ARDS). To investigate the therapeutic potential of SPMs and the role of NGs during ARDS, C57BL/6N mice were bred with (Fat) or without (WT) fat-1 genetic ω-3 PUFA enrichment and crossbred with the RvE1 receptor knock-out (CR KO/LR KO) or unmodified (Norm) mice. Mice were treated with an intra-tracheal (i.t.) instillation of LPS (10 μg/mouse in 50 μl saline) and sacrificed at five different time points: 0 h, 4 h, 24 h, 72 h, or 120 h p.i. Lung, liver, and brain tissues were collected and analyzed by RT-qPCR, multiplex, Western blot, liquid chromatography-tandem mass spectrometry (LC-MS/MS), and immunohistochemistry to assess the peripheral and brain inflammatory response.

Interestingly, during severe systemic inflammation, pretreatment with PMN not only reduced circulating levels of NGs but, at higher doses, increased lethality. Moreover, NG recruitment to the brain was attenuated by PMN. All physiological parameters were strongly affected by LPS, but only LPS-induced hypothermia was exacerbated and prolonged in PMN pretreated mice. Indeed, while LPS did increase circulating cytokines, neutropenic mice showed enhanced production of IL-10 as early as 4 h p.i. and by 24 h p.i. plasma levels of CXCL1, CXCL2, IL-10, IL-6, and tumor necrosis factor (TNF) α were all exacerbated in these mice compared to the immunocompetent controls. LPS-induced inflammation in the brain was detectable at 4 h p.i. for inflammatory mediators, enzymes for prostaglandin (PG) E2 synthesis, and markers for activation of inflammatory transcription factors, but these did not persist to 24 h p.i. and were unaffected by PMN pretreatment. However, at 24 h p.i., the mRNA expression of marker proteins for NFκB, STAT3, as well as the enzymes microsomal PGE synthase (mPGES), and cyclooxygenase (COX)2 were generally increased by pretreatment with PMN regardless of LPS treatment. Despite an overall weak PMN effect in the brain, LPS-induced circulating levels of corticosterone were dampened at 4 h but showed a prolonged increase in PMN pretreated compared to NRS pretreated mice. Taken together, these data suggest a peripheral action may be largely responsible for observed alterations in sickness symptoms in neutropenic animals.

LPS-induced ARDS resulted in milder inflammation compared to the severe LPS-induced systemic model. The inflammatory response was largely localized to the lung where mediators of inflammation appeared enhanced at 24 h p.i., and alterations by

genetic ω-3 PUFA enrichment and RvE1 receptor deficiencies changed over time. These data indicate that both ω-3 PUFA enrichment and RvE1 receptor deficiencies were enough to cause minor alterations in LPS-induced lung inflammation. In contrast, LPS-induced production of inflammatory mediators in the liver was less pronounced. Despite low inflammatory signaling in the periphery (liver), signs of inflammation in the brain were detected in the hypothalamus, similar to the lung with a peak at 24 h p.i. Overall, deficiency in CR had a stronger effect than LR deficiency in the hypothalamus as evidenced by reduced expression of CXCL1 and IL-1β in Fat-CR KO mice compared to Fat-Norm controls. In addition, GFAP expression was increased by CR deficiency regardless of ω-3 PUFA enrichment. Immunohistochemical staining also revealed that NG recruitment to different brain structures were present during inflammation. In combination with the liver's modest inflammatory response, these effects suggest a minor role of circulating cytokines in lung-to-brain communication. However, NGs trafficking to the brain may contribute to inflammatory signaling from the lung to the brain. Enrichment with ω-3 PUFA and RvE1 receptor deficiencies modulated lipid mediator profiles in the lung and hypothalamus. Such changes in lipids may significantly contribute to lung-brain communication and inflammatory resolution during LPS-induced ARDS.

In summary, by analyzing NGs during two different models of inflammation, I found that NGs can be recruited to different brain structures during LPS-induced severe systemic inflammation and ARDS, and potentially participate in immune-to-brain communication. In the case of severe systemic inflammation, neutropenia increases mortality, exacerbates peripheral inflammation, prolongs HPA activation, and worsens inflammatory hypothermia. In this model of inflammation, a peripheral anti-inflammatory action of NGs is most likely contributing to alterations in disease severity. Exaggerated peripheral inflammation during neutropenia could be instrumental in exacerbating sickness symptoms, possibly through interactions with the blood-brain barrier (BBB) or at brain structures with a leaky BBB such as the so-called circumventricular organs. In the milder inflammatory ARDS model, lung-to-brain communication includes low humoral signaling and recruitment of NGs. Both genetic ω-3 PUFA enrichment and RvE1 receptor deficiencies had an effect on the inflammatory response in the lung and

hypothalamus. Within the hypothalamus, CR deficiency enhanced GFAP immunoreactivity. The actions of RvE1, as well as ω-3 PUFA enrichment, modulate NG recruitment to the brain most likely through CR. Further investigations into the anti-inflammatory roles of NGs and their ability to participate in immune-to-brain communication are warranted. This will help to gain further insights into underlying mechanisms of the pathophysiology in individuals suffering from neutropenia or when being at risk for brain inflammatory insults as a complication of ARDS.

VI. Zusammenfassung

Das angeborene Immunsystem ist im Rahmen der bidirektionalen Kommunikation zwischen Immun- und Nervensystem maßgeblich an der Entwicklung entzündlicher Prozesse im Gehirn und der daraus resultierenden Entstehung von Krankheitssymptomen, wie Fieber beteiligt. Neutrophile Granulozyten (NG) sind ein wichtiger Bestandteil des streng regulierten Immunsystems und tragen zur Übermittlung von Entzündungsinformationen bei. Eine Dysregulation der Immunantwort während einer Infektion kann schwerwiegende Folgen haben. Dies geschieht zum Beispiel bei der Entwicklung einer septischen Entzündung. Dabei handelt es sich um eine überschießende Entzündungsreaktion, die während Infektionen auftreten kann. Sie kann lebensbedrohlich sein oder zu langfristigen Beeinträchtigungen führen. Nach wie vor existieren nur eingeschränkte Behandlungsmöglichkeiten. Die Beeinflussung von NG stellt in diesem Kontext einen vielversprechenden Ansatz dar. Dafür spricht eine NG-abhängige Produktion von „specialized pro-resolving mediators" (SPM), wie Resolvin (Rv) E1. Im Rahmen meines Dissertationsprojekts wurde die Rolle der NGs in zwei verschiedenen Mausmodellen für systemische und lokale, organspezifische Lungenentzündungen untersucht.

Im ersten Entzündungsmodell wurden die Auswirkungen einer Neutropenie während einer schweren systemischen Entzündung untersucht. Zur Induktion der Neutropenie wurde Mäusen „antipolymorphonuclear serum" (PMN; 1 ml/kg) oder „normal rabbit serum" (NRS) als Kontrolle intraperitoneal (IP) injiziert. Die systemische Entzündung wurde 24 Stunden später durch Lipopolysaccharid (LPS; 2,5 mg/kg; IP) induziert, während Kontrolltieren phosphatgepufferte Kochsalzlösung (PBS) appliziert wurde. Die Auswirkungen wurden auf Krankheitssymptome (Fieber, Apathie, Anorexie, Adipsie) sowie auf zellulär-molekularer Ebene im Gehirn und der Peripherie untersucht. Mit Hilfe eines Telemetriesystems wurden die folgenden physiologischen Parameter kontinuierlich aufgezeichnet: Körperkerntemperatur, lokomotorische Aktivität sowie Nahrungs- und Wasseraufnahme. Die Mäuse wurden 4 bzw. 24 Stunden post Inokulation (p.i.) mit LPS perfundiert, woraufhin Gehirn- und Plasmaproben entnommen wurden. Die Veränderungen der peripheren Entzündung und der Entzündung im Gehirn

wurden durch hämatologische Messungen, Immunhistochemie, Immunoassays und RT-qPCR untersucht.

In einem weiteren Entzündungsmodell des „acute respiratory distress syndrome" (ARDS) wurden die Auswirkungen einer genetischen Anreicherung mit mehrfach ungesättigten Omega-(ω)-3-Fettsäuren sowie der Einfluss der Defizienz zweier RvE1-Rezeptoren (Chemerin-Rezeptor 23 [CR] oder Leukotrien-B4-Rezeptor [LR]) untersucht. Um das therapeutische Potenzial von SPMs und die Rolle von NGs während des ARDS zu analysieren, wurden Fat-1-Mäuse, die genetisch mit ω-3 PUFA angereichert sind (Fat) sowie der C57BL/6N Hintergrundstamm (WT), mit RvE1-Rezeptor „knock-out" (CR KO/LR KO) oder unmodifizierten (Norm) Mäusen gekreuzt. Die Mäuse wurden einer intratrachealen (i.t.) Instillation mit LPS (10 μg/Maus in 50 μl Saline) unterzogen und zu fünf verschiedenen Zeitpunkten perfundiert: 0 h, 4 h, 24 h, 72 h oder 120 h p.i.. Lungen-, Leber- und Hirngewebe wurden entnommen. Die Entzündungsreaktion in der Peripherie und im Gehirn wurden mittels RT-qPCR, Multiplex, Western Blot, Flüssigchromatographie mit Tandem Massenspektrometrie (LC-MS/MS) und Immunhistochemie untersucht.

Interessanterweise verringerte die Vorbehandlung mit PMN bei schweren systemischen Entzündungen nicht nur die zirkulierenden NG-Spiegel, sondern erhöhte bei höherer Dosierung auch die Sterblichkeit. Außerdem wurde die NG-Rekrutierung ins Gehirn durch PMN abgeschwächt. LPS hatte starke Auswirkungen auf alle physiologischen Parameter, aber nur die LPS-induzierte Hypothermie war bei den mit PMN vorbehandelten Mäusen im Vergleich zu den NRS vorbehandelten Tieren verstärkt und verlängert. Obwohl die zirkulierenden Zytokine in beiden LPS-Gruppen erhöht waren, wiesen die neutropenen Mäuse bereits nach 4 Stunden p.i. eine erhöhte Produktion von IL-10 auf. Nach 24 Stunden p.i. waren auch die LPS-induzierten Plasmaspiegel von CXCL1, CXCL2, IL-10, IL-6 und Tumornekrosefaktor (TNF) α bei neutropenen Mäusen im Vergleich zu den immunkompetenten Kontrolltieren erhöht. Anzeichen einer Entzündung im Gehirn waren 4 Stunden p.i. durch gesteigerte mRNA Expression von Entzündungsmediatoren, Enzymen der Prostaglandin (PG) E2-Synthese und Markern für entzündliche Transkriptionsfaktoren nachweisbar. Allerdings hielten diese Effekte nicht bis 24 Stunden p.i. an und wurden durch die PMN-Vorbehandlung weitgehend

nicht beeinflusst. Darüber hinaus war die mRNA Expression von Markerproteinen für NFκB, STAT3 sowie der Enzyme mikrosomale PGE-Synthase (mPGES) und Zyklooxygenase (COX)2 nach 24 Stunden p.i durch die Vorbehandlung mit PMN, unabhängig von der LPS-Behandlung, generell erhöht. Trotz des insgesamt schwachen PMN-Effektes im Gehirn waren die LPS-induzierten zirkulierenden Corticosteronplasmakonzentrationen nach 4 Stunden vermindert, zeigten hingegen einen verlängerten Anstieg in den mit PMN vorbehandelten Mäusen im Vergleich zu NRS vorbehandelten Tieren. Insgesamt deuten diese Daten darauf hin, dass eine periphere Wirkung weitgehend für die beobachteten Veränderungen der Krankheitssymptome in den neutropenen Tiere verantwortlich ist.

LPS-induziertes ARDS führte verglichen mit dem schweren systemischen LPS-induzierten Modell zu einer milderen Entzündung. Die Entzündungsreaktion war weitgehend auf die Lunge beschränkt. Dort traten 24 h p.i. LPS-induziert verstärkt Entzündungsmediatoren auf und die Veränderungen durch die genetische ω-3 PUFA-Anreicherung und den Mangel an RvE1-Rezeptoren variierten über die Zeit. Diese Daten deuten darauf hin, dass sowohl die ω-3 PUFA-Anreicherung als auch der Mangel an RvE1-Rezeptoren ausreichen, um eine geringfügige Veränderung der LPS-induzierten Lungenentzündung zu bewirken. Im Gegensatz dazu war die LPS-induzierte Produktion von Entzündungsmediatoren in der Leber weniger ausgeprägt. Trotz geringerer Entzündungssignale in der Peripherie (Leber) wurden im Hypothalamus Anzeichen einer Gehirnentzündung festgestellt, ähnlich wie in der Lunge mit einem Peak bei 24 h p.i.. Insgesamt hatte die Defizienz des CR im Hypothalamus eine stärkere Wirkung, als die LR Defizienz. Belege hierfür finden sich in der geringeren Expression von CXCL1 und IL-1β in den unveränderten Fat-Kontrolltieren verglichen mit Fat-CR KO Mäusen. Zusätzlich war die GFAP-Expression durch die CR-Defizienz unabhängig von der ω-3 PUFA-Anreicherung erhöht. Immunfluoreszenzuntersuchungen zeigten eine Rekrutierung von NG in verschiedenen Gehirnstrukturen während der Inflammation. In Kombination mit der geringgradigen Entzündungsreaktion der Leber legen diese Effekte eine untergeordnete Rolle der zirkulierenden Zytokine in der Kommunikation zwischen Immunsystem und Gehirn nahe. Allerdings könnte die Migration von NG in das Gehirn einen wesentlichen Bestandteil der Entzündungsweiterleitung von der Lunge zum

Gehirn darstellen. Anreicherung mit ω-3 PUFA sowie RvE1 Rezeptordefizienz modulierten Lipidmediatorprofile in Lunge und Hypothalamus. Diese Veränderung der Lipide könnte wesentlich zur Kommunikation zwischen Lunge und Gehirn und zur Auflösung der Entzündung bei LPS-induziertem ARDS beitragen.

Zusammenfassend habe ich durch die Untersuchung von NGs in zwei verschiedenen Entzündungsmodellen herausgefunden, dass NGs bei LPS-induzierter schwerer systemischer Entzündung und ARDS in verschiedene Gehirnstrukturen rekrutiert werden können und an der Kommunikation zwischen Immunsystem und Gehirn maßgeblich beteiligt sind. Im Falle einer schweren systemischen Entzündung erhöht eine Neutropenie die Sterblichkeit, verschlimmert die periphere Entzündung, verlängert die HPA-Aktivierung und verstärkt die entzündungsbedingte Hypothermie. In diesem Entzündungsmodell trägt eine periphere entzündungshemmende Wirkung von NGs höchstwahrscheinlich zu den Veränderungen der Schwere des Krankheitsverlaufes bei. Eine übermäßige periphere Entzündung während der Neutropenie ist wahrscheinlich an einer verstärkten Krankheitsreaktion beteiligt, möglicherweise durch Interaktionen mit Zellen der Blut-Hirn-Schranke (BHS) oder an Gehirnstrukturen mit einer durchlässigen BHS wie beispielsweise die zirkumventrikulären Organe. Im milderen inflammatorischen ARDS-Modell beinhaltet die Kommunikation von der Lunge zum Gehirn den geringgradigen humoralen Signalweg und die Rekrutierung von NG. Sowohl die genetische ω-3 PUFA-Anreicherung als auch die Defizienz der RvE1-Rezeptoren hatten einen Einfluss auf die Entzündungsreaktion in der Lunge und im Hypothalamus. Im Hypothalamus erhöhte der CR-Mangel die GFAP-Immunreaktivität. Die Wirkung von RvE1 sowie die ω-3 PUFA-Anreicherung über CR könnten die Rekrutierung von NG im Gehirn beeinflussen. Weitere Untersuchungen der entzündungshemmenden Rolle der NGs und ihrer Beteiligung an der Kommunikation zwischen Immunsystem und Gehirn sind notwendig. Dies wird zukünftig dazu beitragen, weitere Einblicke in die zugrundeliegenden Mechanismen der Pathophysiologie bei Personen zu gewinnen, die an Neutropenie leiden oder bei denen das Risiko einer entzündlichen Gehirnschädigung als Komplikation von ARDS besteht.

VII. Abbreviations list

Abbreviation	Definition
AA	Arachidonic acid
ACTH	Adrenal corticotropin hormone
ALI	Acute lung injury
ALOX	Arachidonate lipoxygenase
ALOX5-ap	Arachidonate 5-lipoxygenase activating protein
ALX	Lipoxin A4 receptor
ANOVA	Analysis of variance
AP	*Area postrema*
APP	Acute phase proteins
APR	Acute phase response
ARDS	Acute respiratory distress syndrome
aSN	Sensory afferent neurons
AVP	Arginine vasopressin
B9	B9 hybridoma cell line
BAT	Brown adipose tissue
BBB	Blood-brain barrier
BDNF	Brain-derived neurotrophic factor
BIF	Bifurcation
C	Cold-sensitive
Cat	Catalase
CCL	Chemokine [C-C motif] ligand
CCR	Chemokine [C-C motif] receptor
CD	Cluster of differentiation
cDNA	Complementary DNA
CLP	Cecal ligation and puncture
CNS	Central nervous system
COVID-19	Coronavirus disease 2019
COX	Cyclooxygenase
CRH	Corticotropin-releasing hormone
CR	Chemerin receptor 23
CSF	Cerebrospinal fluid
ct	Cycle threshold
CVO	Circumventricular organ
CXCL	Chemokine [C-X-C motif] ligand
CXCR	Chemokine [C-X-C motif] receptor
CYP450	Cytochrome P450
DAMP	Damage-associated molecular pattern
DAPI	4',6-Diamidin-2-phenylindol
DEPC	Diethylpyrocarbonate
DHA	Docosahexaenoic acid
DMH	Dorsomedial hypothalamic nucleus
DNA	Deoxyribonucleic acid

DNA/His	DNA/Histone
dNTPs	Deoxynucleotide mix
DTT	Dithiothreitol
eAN	Efferent neurons
EDTA	Ethylenediaminetetraacetic acid
Elane	Elastase, neutrophil expressed
ELISA	Enzyme-linked immunosorbent assay
EP	Prostaglandin E2 receptor
EPA	Eicosapentaenoic acid
EtOH	Ethanol
Fat	Fat-1 mice endogenously expressing omega-3 fatty acids
FCS	Fetal calf serum
FSC	Forward scatter
GABA	Gamma-aminobutyric acid
G-CSF	Granulocyte colony-stimulating factor
GM-CSF	Granulocyte-macrophage colony-stimulating factor
GPCR	G protein coupled receptor
h	Hour
H3Cit	Citrullinated histone H3
HCl	Hydrochloric acid
HEPE	Hydroxyeicosapentaenoic acid
HLA	Human leukocyte antigen
HPA	Hypothalamus-pituitary-adrenal axis
HpDHA	Hydroperoxydocosahexaenoic acid
IP	Intraperitoneal
iα	Inhibitor alpha
ICAM	Intercellular adhesion molecule
IFN	Interferon
IL	Interleukin
JAK-STAT	Janus kinase-signal transducer and activator of transcription
KO	Knock-out
Kc	Kupffer cells
LEDs	Light-emitting diodes
LOX	Lipoxygenase
LPS	Lipopolysaccharide
LR	Leukotriene B4 receptor 1
LT	Leukotriene
LX	Lipoxin
MD	Myeloid differentiation factor
MF	Murine fibrosarcoma cell line
MnPO	Median preoptic nucleus
mPGES	Microsomal prostaglandin E synthase
MPO	Myeloperoxidase
MS	Multiple sclerosis
MTT	3-[4,5-Dimethylthiazol-2yl] 2,5-Diphenyl-Tetrazolliumbromide
NaCl	Sodium chloride

NADPH	Nicotinamide adenine dinucleotide phosphate
NDS	Normal donkey serum
NET	Neutrophil extracellular trap
NF	Nuclear factor
NFκB	Nuclear-factor-"kappa -light-chain-enhancer of activated B-cells"
NG	Neutrophil granulocytes
nM	Nanomolar
Norm	Unmodified mice
NOS	Inducible nitric oxide
NOX	NADPH oxidase enzyme
NPD1	Neuroprotectin D1
NRS	Normal rabbit serum
NSAIDs	Nonsteroidal anti-inflammatory drugs
NSB	Non-specific binding
OVLT	*Organum vasculosum of the lamina terminalis*
P/S	Penicillin-Streptomycin
PAB	Primary antibody
PAMP	Pathogen-associated molecular pattern
PBMCs	Peripheral blood mononuclear cells
PBS	Phosphate buffered saline
PD	Panic disorder
PD1	Protectin D1
PFA	Paraformaldehyde
PG	Prostaglandin
PGC	Peroxisome proliferator-activated receptor-α coactivator
PLA2	Phospholipase A2
plexus	Choroid plexus
PMA	Phorbol 12-myristate 13-acetate
PMN	Anti-polymorphonuclear serum
p.i.	Post inoculation
POA	Preoptic-anterior hypothalamic area
post-op	Postoperative
PRRs	Pattern-recognition receptors
Ptgds	Prostaglandin D2 synthase
PTSD	Post-traumatic stress disorder
PUFA	Polyunsaturated fatty acids
PVN	Paraventricular nucleus
RT-qPCR	Reverse transcription real-time polymerase chain reaction
ra	Receptor antagonist
Raw IntDen	Raw integrated density
RNA	Ribonucleic acid
ROS	Reactive oxygen species
RPA	Raphe pallidus nucleus
RPMI	Roswell Park Memorial Institute
RQ	Relative quantification
RSV	Respiratory syncytial virus

RT	Room temperature
RT-enzyme	Reverse transcriptase enzyme
Rv	Resolvin
SAB	Secondary antibody
SAE	Sepsis-associated encephalopathy
SFO	Subfornical organ
SOCS3	Suppressor of cytokine signaling 3
SOD	Superoxide dismutase
SPMs	Specialized pro-resolving mediators
SSC	Side scatter
STAT3	Signal transducer and activator of transcription 3
TAN	Tumor-associated neutrophils
TFAM	Transcription factor A, mitochondrial
TGF	Transforming growth factor
TLR	Toll-like receptors
TMB	Tetramethylbenzidine
TNF-α	Tumor necrosis factor a
TNFR	Tumor necrosis factor receptor
vital mitochondrial	Vital NETosis with the release of mitochondrial DNA
vital nuclear	Vital NETosis with the release of nuclear DNA
vWF	von Willebrand factor
W	Warm-sensitive
WT	C57BL/6N wild-type mice
ω-3	Omega-3
ω-6	Omega-6

VIII. Publication bibliography

Abbott NJ, Patabendige AAK, Dolman DEM, Yusof SR, Begley DJ (2010) Structure and function of the blood-brain barrier. Neurobiology of disease 37:13–25

Abdel-Halim M, Hamberg M, Sjöquist B, Ångård E (1977) Identification of prostaglandin D2 as a major prostaglandin in homogenates of rat brain. Prostaglandins 14:633–643

Abdolmaleki F, Kovanen PT, Mardani R, Gheibi-Hayat SM, Bo S, Sahebkar A (2020) Resolvins: Emerging Players in Autoimmune and Inflammatory Diseases. Clinical reviews in allergy & immunology 58:82–91

Abe R, Hirasawa H, Oda S, Sadahiro T, Nakamura M, Watanabe E, Nakada T-A, Hatano M, Tokuhisa T (2008) Up-regulation of interleukin-10 mRNA expression in peripheral leukocytes predicts poor outcome and diminished human leukocyte antigen-DR expression on monocytes in septic patients. The Journal of surgical research 147:1–8

Actor JK (ed) (2012) Elsevier's integrated review. Immunology and microbiology, 2nd ed. Elsevier's integrated series. Elsevier/Saunders, Philadelphia, PA

Afridi R, Tsuda M, Ryu H, Suk K (2022) The Function of Glial Cells in the Neuroinflammatory and Neuroimmunological Responses. Cells 11

Aggarwal BB (2003) Signalling pathways of the TNF superfamily: a double-edged sword. Nature reviews. Immunology 3:745–756

Aguilar-Valles A, Aguliar-Valles A, Kim J, Jung S, Woodside B, Luheshi GN (2014) Role of brain transmigrating neutrophils in depression-like behavior during systemic infection. Molecular psychiatry 19:599–606

Aisiku IP, Yamal J-M, Doshi P, Benoit JS, Gopinath S, Goodman JC, Robertson CS (2016) Plasma cytokines IL-6, IL-8, and IL-10 are associated with the development of acute respiratory distress syndrome in patients with severe traumatic brain injury. Critical care (London, England) 20:288

Akanuma S-I, Uchida Y, Ohtsuki S, Tachikawa M, Terasaki T, Hosoya K-I (2011) Attenuation of prostaglandin E2 elimination across the mouse blood-brain barrier in lipopolysaccharide-induced inflammation and additive inhibitory effect of cefmetazole. Fluids and barriers of the CNS 8:24

Akashi S, Ogata H, Kirikae F, Kirikae T, Kawasaki K, Nishijima M, Shimazu R, Nagai Y, Fukudome K, Kimoto M, Miyake K (2000) Regulatory roles for CD14 and phosphatidylinositol in the signaling via toll-like receptor 4-MD-2. Biochemical and biophysical research communications 268:172–177

Akira S, Taga T, Kishimoto T (1993) Interleukin-6 in biology and medicine. Advances in immunology 54:1–78

Akira S, Takeda K (2004) Toll-like receptor signalling. Nature reviews. Immunology 4:499–511

Akira S, Uematsu S, Takeuchi O (2006) Pathogen recognition and innate immunity. Cell 124:783–801

Alawdi SH, El-Denshary ES, Safar MM, Eidi H, David M-O, Abdel-Wahhab MA (2017) Neuroprotective Effect of Nanodiamond in Alzheimer's Disease Rat Model: a Pivotal Role for Modulating NF-κB and STAT3 Signaling. Mol Neurobiol 54:1906–1918

Alexander JJ, Jacob A, Cunningham P, Hensley L, Quigg RJ (2008) TNF is a key mediator of septic encephalopathy acting through its receptor, TNF receptor-1. Neurochemistry international 52:447–456

Al-Kuraishy HM, Al-Gareeb AI, Al-Hussaniy HA, Al-Harcan NAH, Alexiou A, Batiha GE-S (2022) Neutrophil Extracellular Traps (NETs) and Covid-19: A new frontiers for therapeutic modality. International immunopharmacology 104:108516

Allgire E, McAlees JW, Lewkowich IP, Sah R (2021) Asthma and posttraumatic stress disorder (PTSD): Emerging links, potential models and mechanisms. Brain, behavior, and immunity 97:275–285

Almeida MC, Steiner AA, Branco LGS, Romanovsky AA (2006) Cold-seeking behavior as a thermoregulatory strategy in systemic inflammation. The European journal of neuroscience 23:3359–3367

Altavilla D, Squadrito G, Minutoli L, Deodato B, Bova A, Sardella A, Seminara P, Passaniti M, Urna G, Venuti SF, Caputi AP, Squadrito F (2002) Inhibition of nuclear factor-kappaB activation by IRFI 042, protects against endotoxin-induced shock. Cardiovascular research 54:684–693

Alves-Filho JC, Freitas A, Souto FO, Spiller F, Paula-Neto H, Silva JS, Gazzinelli RT, Teixeira MM, Ferreira SH, Cunha FQ (2009) Regulation of chemokine receptor by Toll-like receptor 2 is critical to neutrophil migration and resistance to polymicrobial sepsis. Proceedings of the National Academy of Sciences of the United States of America 106:4018–4023

Alves-Filho JC, Spiller F, Cunha FQ (2010) Neutrophil paralysis in sepsis. Shock 34 Suppl 1:15–21

Andersson PB, Perry VH, Gordon S (1992a) Intracerebral injection of proinflammatory cytokines or leukocyte chemotaxins induces minimal myelomonocytic cell recruitment to the parenchyma of the central nervous system. J Exp Med 176:255–259

Andersson P-B, Perry VH, Gordon† S (1992b) The acute inflammatory response to lipopolysaccharide in cns parenchyma differs from that in other body tissues. Neuroscience 48:169–186

Annane D, Sharshar T (2015) Cognitive decline after sepsis. The Lancet. Respiratory medicine 3:61–69

Anthony DC, Bolton SJ, Fearn S, Perry VH (1997) Age-related effects of interleukin-1 beta on polymorphonuclear neutrophil-dependent increases in blood-brain barrier permeability in rats. Brain : a journal of neurology 120 (Pt 3):435–444

Arai H, Furuya T, Yasuda T, Miura M, Mizuno Y, Mochizuki H (2004) Neurotoxic effects of lipopolysaccharide on nigral dopaminergic neurons are mediated by microglial activation, interleukin-1beta, and expression of caspase-11 in mice. Journal of Biological Chemistry 279:51647–51653

Araujo OR de, Salomão R, Brunialti MKC, da Silva DCB, Senerchia AA, Moraes Costa Carlesse FA de, Petrilli AS (2017) Cytokine Kinetics in Febrile Neutropenic Children: Insights on the Usefulness as Sepsis Biomarkers, Influence of Filgrastim, and Behavior of the IL-23/IL-17 Pathway. Mediators of inflammation 2017:8291316

Ariel A, Fredman G, Sun Y-P, Kantarci A, van Dyke TE, Luster AD, Serhan CN (2006) Apoptotic neutrophils and T cells sequester chemokines during immune response resolution through modulation of CCR5 expression. Nat Immunol 7:1209–1216

Arita M, Bianchini F, Aliberti J, Sher A, Chiang N, Hong S, Yang R, Petasis NA, Serhan CN (2005) Stereochemical assignment, antiinflammatory properties, and receptor for the omega-3 lipid mediator resolvin E1. J Exp Med 201:713–722

Arita M, Ohira T, Sun Y-P, Elangovan S, Chiang N, Serhan CN (2007) Resolvin E1 selectively interacts with leukotriene B4 receptor BLT1 and ChemR23 to regulate inflammation. Journal of immunology (Baltimore, Md. : 1950) 178:3912–3917

Assi LK, Wong SH, Ludwig A, Raza K, Gordon C, Salmon M, Lord JM, Scheel-Toellner D (2007) Tumor necrosis factor alpha activates release of B lymphocyte stimulator by neutrophils infiltrating the rheumatoid joint. Arthritis and rheumatism 56:1776–1786

Auffray C, Fogg D, Garfa M, Elain G, Join-Lambert O, Kayal S, Sarnacki S, Cumano A, Lauvau G, Geissmann F (2007) Monitoring of blood vessels and tissues by a population of monocytes with patrolling behavior. Science (New York, N.Y.) 317:666–670

Badshah H, Ikram M, Ali W, Ahmad S, Hahm JR, Kim MO (2019) Caffeine May Abrogate LPS-Induced Oxidative Stress and Neuroinflammation by Regulating Nrf2/TLR4 in Adult Mouse Brains. Biomolecules 9

Baeuerle PA, Baltimore D (1988) Activation of DNA-binding activity in an apparently cytoplasmic precursor of the NF-κB transcription factor. Cell 53:211–217

Båge T, Lindberg J, Lundeberg J, Modéer T, Yucel-Lindberg T (2010) Signal pathways JNK and NF-kappaB, identified by global gene expression profiling, are involved in regulation of TNFalpha-induced mPGES-1 and COX-2 expression in gingival fibroblasts. BMC Genomics 11:241

Bagga D, Wang L, Farias-Eisner R, Glaspy JA, Reddy ST (2003) Differential effects of prostaglandin derived from omega-6 and omega-3 polyunsaturated fatty acids on COX-2 expression and IL-6 secretion. Proc. Natl. Acad. Sci. U.S.A. 100:1751–1756

Baghel K, Srivastava RN, Chandra A, Goel SK, Agrawal J, Kazmi HR, Raj S (2014) TNF-α, IL-6, and IL-8 cytokines and their association with TNF-α-308 G/A polymorphism and postoperative sepsis. Journal of gastrointestinal surgery : official journal of the Society for Surgery of the Alimentary Tract 18:1486–1494

Ballinger MN, Paine R, Serezani CHC, Aronoff DM, Choi ES, Standiford TJ, Toews GB, Moore BB (2006) Role of granulocyte macrophage colony-stimulating factor during gram-negative lung infection with Pseudomonas aeruginosa. American journal of respiratory cell and molecular biology 34:766–774

Banks WA (2005) Blood-brain barrier transport of cytokines: a mechanism for neuropathology. Current pharmaceutical design 11:973–984

Banks WA (2012) Brain meets body: the blood-brain barrier as an endocrine interface. Endocrinology 153:4111–4119

Banks WA (2015) The blood-brain barrier in neuroimmunology: Tales of separation and assimilation. Brain, behavior, and immunity 44:1–8

Banks WA (2016) From blood-brain barrier to blood-brain interface: new opportunities for CNS drug delivery. Nature reviews. Drug discovery 15:275–292

Banks WA (2019) The blood-brain barrier as an endocrine tissue. Nature reviews. Endocrinology 15:444–455

Basil MC, Levy BD (2016) Specialized pro-resolving mediators: endogenous regulators of infection and inflammation. Nat Rev Immunol 16:51–67

Bauer J, Sminia T, Wouterlood FG, Dijkstra CD (1994) Phagocytic activity of macrophages and microglial cells during the course of acute and chronic relapsing experimental autoimmune encephalomyelitis. Journal of neuroscience research 38:365–375

Bauer N, Moritz A (2008) Evaluation of three methods for measurement of hemoglobin and calculated hemoglobin parameters with the ADVIA 2120 and ADVIA 120 in dogs, cats, and horses. Veterinary clinical pathology 37:173–179

Baumann H, Gauldie J (1994) The acute phase response. Immunology Today 15:74–80

Bazan NG, Rodriguez de Turco EB, Gordon WC (1993) Pathways for the uptake and conservation of docosahexaenoic acid in photoreceptors and synapses: biochemical and autoradiographic studies. Canadian journal of physiology and pharmacology 71:690–698

Bechmann I, Priller J, Kovac A, Böntert M, Wehner T, Klett FF, Bohsung J, Stuschke M, Dirnagl U, Nitsch R (2001) Immune surveillance of mouse brain perivascular spaces by blood-borne macrophages. The European journal of neuroscience 14:1651–1658

Bellenger J, Bellenger S, Bataille A, Massey KA, Nicolaou A, Rialland M, Tessier C, Kang JX, Narce M (2011) High pancreatic n-3 fatty acids prevent STZ-induced diabetes in fat-1 mice: inflammatory pathway inhibition. Diabetes 60:1090–1099

Bellocq A, Antoine M, Flahault A, Philippe C, Crestani B, Bernaudin JF, Mayaud C, Milleron B, Baud L, Cadranel J (1998) Neutrophil alveolitis in bronchioloalveolar carcinoma: induction by tumor-derived interleukin-8 and relation to clinical outcome. The American Journal of Pathology 152:83–92

Benveniste EN, Benos DJ (1995) TNF-alpha- and IFN-gamma-mediated signal transduction pathways: effects on glial cell gene expression and function. FASEB journal : official publication of the Federation of American Societies for Experimental Biology 9:1577–1584

Bernard GR, Vincent JL, Laterre PF, LaRosa SP, Dhainaut JF, Lopez-Rodriguez A, Steingrub JS, Garber GE, Helterbrand JD, Ely EW, Fisher CJ (2001) Efficacy and safety of recombinant human activated protein C for severe sepsis. The New England journal of medicine 344:699–709

Bernardini R, Kamilaris TC, Calogero AE, Johnson EO, Gomez MT, Gold PW, Chrousos GP (1990) Interactions between tumor necrosis factor-alpha, hypothalamic corticotropin-releasing hormone, and adrenocorticotropin secretion in the rat. Endocrinology 126:2876–2881

Bernhardi R von, Eugenín-von Bernhardi L, Eugenín J (2015) Microglial cell dysregulation in brain aging and neurodegeneration. Frontiers in aging neuroscience 7:124

Beurel E, Jope RS (2009) Lipopolysaccharide-induced interleukin-6 production is controlled by glycogen synthase kinase-3 and STAT3 in the brain. J Neuroinflammation 6:9

Bhatia M, Zemans RL, Jeyaseelan S (2012) Role of chemokines in the pathogenesis of acute lung injury. American journal of respiratory cell and molecular biology 46:566–572

Bibby DC, Grimble RF (1989) Temperature and metabolic changes in rats after various doses of tumour necrosis factor alpha. The Journal of physiology 410:367–380

Bienvenu OJ, Colantuoni E, Mendez-Tellez PA, Dinglas VD, Shanholtz C, Husain N, Dennison CR, Herridge MS, Pronovost PJ, Needham DM (2012) Depressive symptoms and impaired physical function after acute lung injury: a 2-year longitudinal study. American journal of respiratory and critical care medicine 185:517–524

Biesmans S, Meert TF, Bouwknecht JA, Acton PD, Davoodi N, Haes P de, Kuijlaars J, Langlois X, Matthews LJR, Ver Donck L, Hellings N, Nuydens R (2013) Systemic immune activation leads to neuroinflammation and sickness behavior in mice. Mediators of inflammation 2013:271359

Biff D, Petronilho F, Constantino L, Vuolo F, Zamora-Berridi GJ, Dall'Igna DM, Comim CM, Quevedo J, Kapczinski F, Dal-Pizzol F (2013) Correlation of acute phase inflammatory and oxidative markers with long-term cognitive impairment in sepsis survivors rats. Shock 40:45–48

Bilal S, Haworth O, Wu L, Weylandt KH, Levy BD, Kang JX (2011) Fat-1 transgenic mice with elevated omega-3 fatty acids are protected from allergic airway responses. Biochimica et biophysica acta 1812:1164–1169

Blanqué R, Meakin C, Millet S, Gardner CR (1996) Hypothermia as an indicator of the acute effects of lipopolysaccharides: comparison with serum levels of IL1β, IL6 and TNFα. General Pharmacology: The Vascular System 27:973–977

Blatteis CM, Bealer SL, Hunter WS, Llanos J-Q, Ahokas RA, Mashburn TA (1983) Suppression of fever after lesions of the anteroventral third ventricle in guinea pigs. Brain Research Bulletin 11:519–526

Blatteis CM, Hales JR, McKinley MJ, Fawcett AA (1987) Role of the anteroventral third ventricle region in fever in sheep. Canadian journal of physiology and pharmacology 65:1255–1260

Blatteis CM, Li S, Li Z, Perlik V, Feleder C (2004a) Complement is required for the induction of endotoxic fever in guinea pigs and mice. Journal of Thermal Biology 29:369–381

Blatteis CM, Li S, Li Z, Perlik V, Feleder C (2004b) Signaling the brain in systemic inflammation: the role of complement. Frontiers in bioscience : a journal and virtual library 9:915–931

Blomqvist A, Engblom D (2018) Neural Mechanisms of Inflammation-Induced Fever. The Neuroscientist : a review journal bringing neurobiology, neurology and psychiatry 24:381–399

Bluthé RM, Pawlowski M, Suarez S, Parnet P, Pittman Q, Kelley KW, Dantzer R (1994) Synergy between tumor necrosis factor alpha and interleukin-1 in the induction of sickness behavior in mice. Psychoneuroendocrinology 19:197–207

Bluthe´ R-M, Dantzer R, Kelley KW (1992) Effects of interleukin-1 receptor antagonist on the behavioral effects of lipopolysaccharide in rat. Brain Research 573:318–320

Bockman RS (1981) Prostaglandin production by human blood monocytes and mouse peritoneal macrophages : Synthesis dependent on in vitro culture conditions. Prostaglandins 21:9–31

Boeltz S, Amini P, Anders H-J, Andrade F, Bilyy R, Chatfield S, Cichon I, Clancy DM, Desai J, Dumych T, Dwivedi N, Gordon RA, Hahn J, Hidalgo A, Hoffmann MH, Kaplan MJ, Knight JS, Kolaczkowska E, Kubes P, Leppkes M, Manfredi AA, Martin SJ, Maueröder C, Maugeri N, Mitroulis I, Munoz LE, Nakazawa D, Neeli I, Nizet V, Pieterse E, Radic MZ, Reinwald C, Ritis K, Rovere-Querini P, Santocki M, Schauer C, Schett G, Shlomchik MJ, Simon H-U, Skendros P, Stojkov D, Vandenabeele P, Berghe TV, van der Vlag J, Vitkov L, Köckritz-Blickwede M von, Yousefi S, Zarbock A, Herrmann M (2019) To NET or not to NET:current opinions and state of the science regarding the formation of neutrophil extracellular traps. Cell death and differentiation 26:395–408

Bohatschek M, Werner A, Raivich G (2001) Systemic LPS injection leads to granulocyte influx into normal and injured brain: effects of ICAM-1 deficiency. Experimental neurology 172:137–152

Bollaert P-E, Fieux F, Charpentier C, Lévy B (2003) Baseline cortisol levels, cortisol response to corticotropin, and prognosis in late septic shock. Shock (Augusta, Ga.) 19:13–15

Bondue B, Vosters O, Nadai P de, Glineur S, Henau O de, Luangsay S, van Gool F, Communi D, Vuyst P de, Desmecht D, Parmentier M (2011) ChemR23 dampens lung inflammation and enhances anti-viral immunity in a mouse model of acute viral pneumonia. PLoS Pathogens 7:e1002358

Bone RC, Grodzin CJ, Balk RA (1997) Sepsis: a new hypothesis for pathogenesis of the disease process. Chest 112:235–243

Boomer JS, To K, Chang KC, Takasu O, Osborne DF, Walton AH, Bricker TL, Jarman SD, Kreisel D, Krupnick AS, Srivastava A, Swanson PE, Green JM, Hotchkiss RS (2011) Immunosuppression in patients who die of sepsis and multiple organ failure. JAMA 306:2594–2605

Boonen E, Vervenne H, Meersseman P, Andrew R, Mortier L, Declercq PE, Vanwijngaerden Y-M, Spriet I, Wouters PJ, Vander Perre S, Langouche L, Vanhorebeek I, Walker BR, van den Berghe G (2013) Reduced cortisol metabolism during critical illness. The New England journal of medicine 368:1477–1488

Boonstra A, Rajsbaum R, Holman M, Marques R, Asselin-Paturel C, Pereira JP, Bates EEM, Akira S, Vieira P, Liu Y-J, Trinchieri G, O'Garra A (2006) Macrophages and myeloid dendritic cells, but not plasmacytoid dendritic cells, produce IL-10 in response to MyD88- and TRIF-dependent TLR signals, and TLR-independent signals. J Immunol 177:7551–7558

Borland G, Bird RJ, Palmer TM, Yarwood SJ (2009) Activation of protein kinase Calpha by EPAC1 is required for the ERK- and CCAAT/enhancer-binding protein beta-dependent induction of the SOCS-3 gene by cyclic AMP in COS1 cells. Journal of Biological Chemistry 284:17391–17403

Boro M, Balaji KN (2017) CXCL1 and CXCL2 Regulate NLRP3 Inflammasome Activation via G-Protein-Coupled Receptor CXCR2. The Journal of Immunology 199:1660–1671

Boulant JA (2000) Role of the preoptic-anterior hypothalamus in thermoregulation and fever. Clinical infectious diseases : an official publication of the Infectious Diseases Society of America 31 Suppl 5:S157-61

Bousquet M, Gue K, Emond V, Julien P, Kang JX, Cicchetti F, Calon F (2011) Transgenic conversion of omega-6 into omega-3 fatty acids in a mouse model of Parkinson's disease. Journal of lipid research 52:263–271

Bradley JR, Pober JS (1996) Prolonged cytokine exposure causes a dynamic redistribution of endothelial cell adhesion molecules to intercellular junctions. Laboratory investigation; a journal of technical methods and pathology 75:463–472

Bradley LM, Douglass MF, Chatterjee D, Akira S, Baaten BJG (2012) Matrix metalloprotease 9 mediates neutrophil migration into the airways in response to influenza virus-induced toll-like receptor signaling. PLoS Pathogens 8:e1002641

Brandau S, Dumitru CA, Lang S (2013) Protumor and antitumor functions of neutrophil granulocytes. Seminars in immunopathology 35:163–176

Branitzki-Heinemann K, Brogden G, Köckritz-Blickwede M von (2020) Influence of Oxygen on Function and Cholesterol Composition of Murine Bone Marrow-Derived Neutrophils. Methods in molecular biology (Clifton, N.J.) 2087:223–233

Branitzki-Heinemann K, Möllerherm H, Völlger L, Husein DM, Buhr N de, Blodkamp S, Reuner F, Brogden G, Naim HY, Köckritz-Blickwede M von (2016) Formation of Neutrophil Extracellular Traps under Low Oxygen Level. Front. Immunol. 7:518

Braun DA, Fribourg M, Sealfon SC (2013) Cytokine response is determined by duration of receptor and signal transducers and activators of transcription 3 (STAT3) activation. The Journal of biological chemistry 288:2986–2993

Bredehöft J, Bhandari DR, Pflieger FJ, Schulz S, Kang JX, Layé S, Roth J, Gerstberger R, Mayer K, Spengler B, Rummel C (2019) Visualizing and Profiling Lipids in the OVLT of Fat-1 and Wild Type Mouse Brains during LPS-Induced Systemic Inflammation Using AP-SMALDI MSI. ACS chemical neuroscience 10:4394–4406

Brinkmann V, Reichard U, Goosmann C, Fauler B, Uhlemann Y, Weiss DS, Weinrauch Y, Zychlinsky A (2004) Neutrophil extracellular traps kill bacteria. Science (New York, N.Y.) 303:1532–1535

Bucklin SE, Silverstein R, Morrison DC (1993) An interleukin-6-induced acute-phase response does not confer protection against lipopolysaccharide lethality. Infection and Immunity 61:3184–3189

Buhr N de, Köckritz-Blickwede M von (2020) Detection, Visualization, and Quantification of Neutrophil Extracellular Traps (NETs) and NET Markers. Methods in molecular biology (Clifton, N.J.) 2087:425–442

Burfeind KG, Zhu X, Levasseur PR, Michaelis KA, Norgard MA, Marks DL (2018) TRIF is a key inflammatory mediator of acute sickness behavior and cancer cachexia. Brain, behavior, and immunity 73:364–374

Burguillos MA, Deierborg T, Kavanagh E, Persson A, Hajji N, Garcia-Quintanilla A, Cano J, Brundin P, Englund E, Venero JL, Joseph B (2011) Caspase signalling controls microglia activation and neurotoxicity. Nature 472:319–324

Cain DW, Cidlowski JA (2017) Immune regulation by glucocorticoids. Nat Rev Immunol 17:233–247

Calder PC (2006a) n-3 polyunsaturated fatty acids, inflammation, and inflammatory diseases. The American journal of clinical nutrition 83:1505S-1519S

Calder PC (2006b) Polyunsaturated fatty acids and inflammation. Prostaglandins, Leukotrienes and Essential Fatty Acids 75:197–202

Cannon B, Houstek J, Nedergaard J (1998) Brown adipose tissue. More than an effector of thermogenesis? Annals of the New York Academy of Sciences 856:171–187

Cappello C, Zwergal A, Kanclerski S, Haas SC, Kandemir JD, Huber R, Page S, Brand K (2009) C/EBPbeta enhances NF-kappaB-associated signalling by reducing the level of IkappaB-alpha. Cellular signalling 21:1918–1924

Caputo MP, Radlowski EC, Lawson MA, Antonson AM, Watson JE, Matt SM, Leyshon BJ, Das A, Johnson RW (2019) Herring roe oil supplementation alters microglial cell gene expression and reduces peripheral inflammation after immune activation in a neonatal piglet model. Brain, behavior, and immunity 81:455–469

Carbone F, Crotty S, Heath B, Jenkins M, Rudensky A, Sakaguchi S, Cancro M, Haberman A, Kearney J, Randall T, Ravetch J, Tucker H, Kaech S, McSorley S, Cerf-Bensussan N, MacDonald T, Rescigno M, Russell M, Stappenbeck T (2017) Janeway's Immunobiolgy. Part IV The Adaptive Immune Response, 9th. Garland Science, Taylor and Francis Group, LLC, New York NY

Carlson DE, Chiu WC (2008) The absence of circadian cues during recovery from sepsis modifies pituitary-adrenocortical function and impairs survival. Shock (Augusta, Ga.) 29:127–132

Carson MJ, Doose JM, Melchior B, Schmid CD, Ploix CC (2006) CNS immune privilege: hiding in plain sight. Immunological reviews 213:48–65

Carswell EA, Old LJ, Kassel RL, Green S, Fiore N, Williamson B (1975) An endotoxin-induced serum factor that causes necrosis of tumors. Proceedings of the National Academy of Sciences of the United States of America 72:3666–3670

Cash JL, Hart R, Russ A, Dixon JPC, Colledge WH, Doran J, Hendrick AG, Carlton MBL, Greaves DR (2008) Synthetic chemerin-derived peptides suppress inflammation through ChemR23. The Journal of experimental medicine 205:767–775

Cassatella MA (1995) The production of cytokines by polymorphonuclear neutrophils. Immunology Today 16:21–26

Cassatella MA, Meda L, Gasperini S, Calzetti F, Bonora S (1994) Interleukin 10 (IL-10) upregulates IL-1 receptor antagonist production from lipopolysaccharide-stimulated human polymorphonuclear leukocytes by delaying mRNA degradation. J Exp Med 179:1695–1699

Cedergren J, Forslund T, Sundqvist T, Skogh T (2007) Intracellular oxidative activation in synovial fluid neutrophils from patients with rheumatoid arthritis but not from other arthritis patients. The Journal of Rheumatology 34:2162–2170

Chakravarty S, Herkenham M (2005) Toll-like receptor 4 on nonhematopoietic cells sustains CNS inflammation during endotoxemia, independent of systemic cytokines. J. Neurosci. 25:1788–1796

Chalon S (2006) Omega-3 fatty acids and monoamine neurotransmission. Prostaglandins, Leukotrienes and Essential Fatty Acids 75:259–269

Chavan SS, Pavlov VA, Tracey KJ (2017) Mechanisms and Therapeutic Relevance of Neuro-immune Communication. Immunity 46:927–942

Chen Q, Wang H, Liu Y, Song Y, Lai L, Han Q, Cao X, Wang Q (2012) Inducible microRNA-223 down-regulation promotes TLR-triggered IL-6 and IL-1β production in macrophages by targeting STAT3. PloS one 7:e42971

Chen S-L, Cai G-X, Ding H-G, Liu X-Q, Wang Z-H, Jing Y-W, Han Y-L, Jiang W-Q, Wen M-Y (2020) JAK/STAT signaling pathway-mediated microRNA-181b promoted blood-brain barrier impairment by targeting sphingosine-1-phosphate receptor 1 in septic rats. Annals of translational medicine 8:1458

Cheng X, Yang Y-L, Yang H, Wang Y-H, Du G-H (2018) Kaempferol alleviates LPS-induced neuroinflammation and BBB dysfunction in mice via inhibiting HMGB1 release and down-regulating TLR4/MyD88 pathway. International immunopharmacology 56:29–35

Cherry JD, Olschowka JA, O'Banion MK (2014) Neuroinflammation and M2 microglia: the good, the bad, and the inflamed. J Neuroinflammation 11:98

Chhor V, Le Charpentier T, Lebon S, Oré M-V, Celador IL, Josserand J, Degos V, Jacotot E, Hagberg H, Sävman K, Mallard C, Gressens P, Fleiss B (2013) Characterization of phenotype markers and neuronotoxic potential of polarised primary microglia in vitro. Brain, behavior, and immunity 32:70–85

Chou SH-Y, Beghi E, Helbok R, Moro E, Sampson J, Altamirano V, Mainali S, Bassetti C, Suarez JI, McNett M (2021) Global Incidence of Neurological Manifestations Among Patients Hospitalized With COVID-19-A Report for the GCS-NeuroCOVID Consortium and the ENERGY Consortium. JAMA network open 4:e2112131

Chow JC, Young DW, Golenbock DT, Christ WJ, Gusovsky F (1999) Toll-like receptor-4 mediates lipopolysaccharide-induced signal transduction. Journal of Biological Chemistry 274:10689–10692

Chrousos GP (1995) The hypothalamic-pituitary-adrenal axis and immune-mediated inflammation. The New England journal of medicine 332:1351–1362

Chrousos GP (2009) Stress and disorders of the stress system. Nature reviews. Endocrinology 5:374–381

Cicco NA, Lindemann A, Content J, Vandenbussche P, Lubbert M, Gauss J, Mertelsmann R, Herrmann F (1990) Inducible production of interleukin-6 by human polymorphonuclear neutrophils: role of granulocyte-macrophage colony-stimulating factor and tumor necrosis factor-alpha. Blood 75:2049–2052

Cinamon G, Shinder V, Shamri R, Alon R (2004) Chemoattractant signals and beta 2 integrin occupancy at apical endothelial contacts combine with shear stress signals to promote transendothelial neutrophil migration. Journal of immunology (Baltimore, Md. : 1950) 173:7282–7291

Clark SR, Ma AC, Tavener SA, McDonald B, Goodarzi Z, Kelly MM, Patel KD, Chakrabarti S, McAvoy E, Sinclair GD, Keys EM, Allen-Vercoe E, Devinney R, Doig CJ, Green FHY, Kubes P (2007) Platelet TLR4 activates neutrophil extracellular traps to ensnare bacteria in septic blood. Nat Med 13:463–469

Claushuis TAM, van Vught LA, Scicluna BP, Wiewel MA, Klein Klouwenberg PMC, Hoogendijk AJ, Ong DSY, Cremer OL, Horn J, Franitza M, Toliat MR, Nürnberg P, Zwinderman AH, Bonten MJ, Schultz MJ, van der Poll T (2016) Thrombocytopenia is associated with a dysregulated host response in critically ill sepsis patients. Blood 127:3062–3072

Cloutier A, Guindi C, Larivée P, Dubois CM, Amrani A, McDonald PP (2009) Inflammatory cytokine production by human neutrophils involves C/EBP transcription factors. The Journal of Immunology 182:563–571

Coceani F, Bishai I, Lees J, Sirko S (1986) Prostaglandin E2 and fever: a continuing debate. The Yale Journal of Biology and Medicine 59:169–174

Cohen S, Janicki-Deverts D, Doyle WJ, Miller GE, Frank E, Rabin BS, Turner RB (2012) Chronic stress, glucocorticoid receptor resistance, inflammation, and disease risk. Proceedings of the National Academy of Sciences of the United States of America 109:5995–5999

Comim CM, Cassol OJ, Constantino LS, Felisberto F, Petronilho F, Rezin GT, Scaini G, Daufenbach JF, Streck EL, Quevedo J, Dal-Pizzol F (2011a) Alterations in inflammatory mediators, oxidative stress parameters and energetic metabolism in the brain of sepsis survivor rats. Neurochemical research 36:304–311

Comim CM, Vilela MC, Constantino LS, Petronilho F, Vuolo F, Lacerda-Queiroz N, Rodrigues DH, Da Rocha JL, Teixeira AL, Quevedo J, Dal-Pizzol F (2011b) Traffic of leukocytes and cytokine up-regulation in the central nervous system in sepsis. Intensive Care Med 37:711–718

Cooney GM, Dwan K, Greig CA, Lawlor DA, Rimer J, Waugh FR, McMurdo M, Mead GE (2013) Exercise for depression. The Cochrane database of systematic reviews:CD004366

Cooper KE, Cranston WI, Honour AJ (1967) Observations on the site & mode of action of pyrogens in the rabbit brain. The Journal of physiology 191:325–337

Corraliza I (2014) Recruiting specialized macrophages across the borders to restore brain functions. Frontiers in Cellular Neuroscience 8:262

Corrêa TD, Rocha LL, Pessoa CMS, Silva E, Assuncao MSC de (2015) Fluid therapy for septic shock resuscitation: which fluid should be used? Einstein (Sao Paulo, Brazil) 13:462–468

Corrigan JJ, Fonseca MT, Flatow EA, Lewis K, Steiner AA (2014) Hypometabolism and hypothermia in the rat model of endotoxic shock: independence of circulatory hypoxia. The Journal of physiology 592:3901–3916

Craciun FL, Schuller ER, Remick DG (2010) Early enhanced local neutrophil recruitment in peritonitis-induced sepsis improves bacterial clearance and survival. The Journal of Immunology 185:6930–6938

Crispe IN (2009) The liver as a lymphoid organ. Annual review of immunology 27:147–163

Czaikoski PG, Mota JMSC, Nascimento DC, Sônego F, Castanheira FVeS, Melo PH, Scortegagna GT, Silva RL, Barroso-Sousa R, Souto FO, Pazin-Filho A, Figueiredo F, Alves-Filho JC, Cunha FQ (2016) Neutrophil Extracellular Traps Induce Organ Damage during Experimental and Clinical Sepsis. PLOS ONE 11:e0148142

da Silva Correia J, Soldau K, Christen U, Tobias PS, Ulevitch RJ (2001) Lipopolysaccharide is in close proximity to each of the proteins in its membrane receptor complex. transfer from CD14 to TLR4 and MD-2. Journal of Biological Chemistry 276:21129–21135

Dalvi S, Nguyen HH, On N, Mitchell RW, Aukema HM, Miller DW, Hatch GM (2015) Exogenous arachidonic acid mediates permeability of human brain microvessel endothelial cells through prostaglandin E2 activation of EP3 and EP4 receptors. Journal of neurochemistry 135:867–879

Damas P, Ledoux D, Nys M, Vrindts Y, Groote D de, Franchimont P, Lamy M (1992) Cytokine serum level during severe sepsis in human IL-6 as a marker of severity. Annals of surgery 215:356–362

Damm J, Harden LM, Gerstberger R, Roth J, Rummel C (2013) The putative JAK-STAT inhibitor AG490 exacerbates LPS-fever, reduces sickness behavior, and alters the expression of pro- and anti-inflammatory genes in the rat brain. Neuropharmacology 71:98–111

Damm J, Luheshi GN, Gerstberger R, Roth J, Rummel C (2011) Spatiotemporal nuclear factor interleukin-6 expression in the rat brain during lipopolysaccharide-induced fever is linked to sustained hypothalamic inflammatory target gene induction. The Journal of comparative neurology 519:480–505

Damm J, Wiegand F, Harden LM, Gerstberger R, Rummel C, Roth J (2012) Fever, sickness behavior, and expression of inflammatory genes in the hypothalamus after systemic and localized subcutaneous stimulation of rats with the Toll-like receptor 7 agonist imiquimod. Neuroscience 201:166–183

Damoiseaux JG, Döpp EA, Calame W, Chao D, MacPherson GG, Dijkstra CD (1994) Rat macrophage lysosomal membrane antigen recognized by monoclonal antibody ED1. Immunology 83:140–147

Danikas DD, Karakantza M, Theodorou GL, Sakellaropoulos GC, Gogos CA (2008) Prognostic value of phagocytic activity of neutrophils and monocytes in sepsis. Correlation to CD64 and CD14 antigen expression. Clin Exp Immunol 154:87–97

Dantzer R (2001) Cytokine-induced sickness behavior: mechanisms and implications. Annals of the New York Academy of Sciences 933:222–234

Dantzer R, Bluthé R-M, Gheusi G, Cremona S, Layé S, Parnet P, Kelley KW (1998) Molecular basis of sickness behavior. Annals of the New York Academy of Sciences 856:132–138

Dantzer R, Kelley KW (1989) Stress and immunity: An integrated view of relationships between the brain and the immune system. Life Sciences 44:1995–2008

Dantzer R, Kelley KW (2007) Twenty years of research on cytokine-induced sickness behavior. Brain, behavior, and immunity 21:153–160

Dantzer R, Konsman J-P, Bluthé R-M, Kelley KW (2000) Neural and humoral pathways of communication from the immune system to the brain: parallel or convergent? Autonomic Neuroscience 85:60–65

Dantzer R, O'Connor JC, Freund GG, Johnson RW, Kelley KW (2008) From inflammation to sickness and depression: when the immune system subjugates the brain. Nature reviews. Neuroscience 9:46–56

Darnell JE, Kerr IM, Stark GR (1994) Jak-STAT pathways and transcriptional activation in response to IFNs and other extracellular signaling proteins. Science (New York, N.Y.) 264:1415–1421

Darwish I, Mubareka S, Liles WC (2011) Immunomodulatory therapy for severe influenza. Expert review of anti-infective therapy 9:807–822

Debets JM, Kampmeijer R, van der Linden MP, Buurman WA, van der Linden CJ (1989) Plasma tumor necrosis factor and mortality in critically ill septic patients. Critical Care Medicine 17:489–494

Deeter LB, Martin LW, Lipton JM (1989) Age- and sex-related differences in febrile response to peripheral pyrogens in the rabbit. Gerontology 35:297–304

Delano MJ, Kelly-Scumpia KM, Thayer TC, Winfield RD, Scumpia PO, Cuenca AG, Harrington PB, O'Malley KA, Warner E, Gabrilovich S, Mathews CE, Laface D, Heyworth PG, Ramphal R, Strieter RM, Moldawer LL, Efron PA (2011) Neutrophil mobilization from the bone marrow during polymicrobial sepsis is dependent on CXCL12 signaling. The Journal of Immunology 187:911–918

Delgado-Rizo V, Martínez-Guzmán MA, Iñiguez-Gutierrez L, García-Orozco A, Alvarado-Navarro A, Fafutis-Morris M (2017) Neutrophil Extracellular Traps and Its Implications in Inflammation: An Overview. Frontiers in immunology 8:81

Demir S, Atli A, Bulut M, İbiloğlu AO, Güneş M, Kaya MC, Demirpençe Ö, Sır A (2015) Neutrophil-lymphocyte ratio in patients with major depressive disorder undergoing no pharmacological therapy. Neuropsychiatric disease and treatment 11:2253–2258

Deng B, Wang C-W, Arnardottir HH, Li Y, Cheng C-YC, Dalli J, Serhan CN (2014) Maresin biosynthesis and identification of maresin 2, a new anti-inflammatory and pro-resolving mediator from human macrophages. PLOS ONE 9:e102362

Derijk RH, van Kampen M, van Rooijen N, Berkenbosch F (1994) Hypothermia to endotoxin involves reduced thermogenesis, macrophage-dependent mechanisms, and prostaglandins. The American journal of physiology 266:R1-8

Deyama S, Shimoda K, Suzuki H, Ishikawa Y, Ishimura K, Fukuda H, Hitora-Imamura N, Ide S, Satoh M, Kaneda K, Shuto S, Minami M (2018) Resolvin E1/E2 ameliorate lipopolysaccharide-induced depression-like behaviors via ChemR23. Psychopharmacology 235:329–336

Diana J, Simoni Y, Furio L, Beaudoin L, Agerberth B, Barrat F, Lehuen A (2013) Crosstalk between neutrophils, B-1a cells and plasmacytoid dendritic cells initiates autoimmune diabetes. Nat Med 19:65–73

Dinarello CA (1996) Biologic basis for interleukin-1 in disease. Blood 87:2095–2147

Dinarello CA (2004a) Infection, fever, and exogenous and endogenous pyrogens: some concepts have changed. Journal of endotoxin research 10:201–222

Dinarello CA (2004b) Therapeutic strategies to reduce IL-1 activity in treating local and systemic inflammation. Current opinion in pharmacology 4:378–385

Dinarello CA, Cannon JG, Wolff SM, Bernheim HA, Beutler B, Cerami A, Figari IS, Palladino MA, O'Connor JV (1986) Tumor necrosis factor (cachectin) is an endogenous pyrogen and induces production of interleukin 1. J Exp Med 163:1433–1450

Dinc G, Eren E, Kontas O, Doganay M (2020) The efficacy of mesenchymal stem cell therapy in experimental sepsis induced by carbapenem-resistant K. pneumoniae in neutropenic mice model. European journal of clinical microbiology & infectious diseases : official publication of the European Society of Clinical Microbiology 39:1739–1744

Ding ZM, Babensee JE, Simon SI, Lu H, Perrard JL, Bullard DC, Dai XY, Bromley SK, Dustin ML, Entman ML, Smith CW, Ballantyne CM (1999) Relative contribution of LFA-1 and Mac-1 to neutrophil adhesion and migration. Journal of immunology (Baltimore, Md. : 1950) 163:5029–5038

Dinkel K, Dhabhar FS, Sapolsky RM (2004) Neurotoxic effects of polymorphonuclear granulocytes on hippocampal primary cultures. Proc. Natl. Acad. Sci. U.S.A. 101:331–336

D'Mello C, Le T, Swain MG (2009) Cerebral microglia recruit monocytes into the brain in response to tumor necrosis factoralpha signaling during peripheral organ inflammation. The Journal of neuroscience : the official journal of the Society for Neuroscience 29:2089–2102

Donnelly SC, Strieter RM, Reid PT, Kunkel SL, Burdick MD, Armstrong I, Mackenzie A, Haslett C (1996) The association between mortality rates and decreased concentrations of interleukin-10 and interleukin-1 receptor antagonist in the lung fluids of patients with the adult respiratory distress syndrome. Annals of internal medicine 125:191–196

Draper E, Reynolds CM, Canavan M, Mills KH, Loscher CE, Roche HM (2011) Omega-3 fatty acids attenuate dendritic cell function via NF-κB independent of PPARγ. The Journal of nutritional biochemistry 22:784–790

Drewry AM, Ablordeppey EA, Murray ET, Beiter ER, Walton AH, Hall MW, Hotchkiss RS (2016) Comparison of monocyte human leukocyte antigen-DR expression and stimulated tumor necrosis factor alpha production as outcome predictors in severe sepsis: a prospective observational study. Critical care (London, England) 20:334

Drewry AM, Fuller BM, Skrupky LP, Hotchkiss RS (2015) The presence of hypothermia within 24 hours of sepsis diagnosis predicts persistent lymphopenia. Critical Care Medicine 43:1165–1169

Dubravec DB, Spriggs DR, Mannick JA, Rodrick ML (1990) Circulating human peripheral blood granulocytes synthesize and secrete tumor necrosis factor alpha. Proceedings of the National Academy of Sciences of the United States of America 87:6758–6761

Dustin ML, Rothlein R, Bhan AK, Dinarello CA, Springer TA (1986) Induction by IL 1 and interferon-gamma: tissue distribution, biochemistry, and function of a natural adherence molecule (ICAM-1). Journal of immunology (Baltimore, Md. : 1950) 137:245–254

Eash KJ, Greenbaum AM, Gopalan PK, Link DC (2010) CXCR2 and CXCR4 antagonistically regulate neutrophil trafficking from murine bone marrow. J Clin Invest 120:2423–2431

El Kebir D, Gjorstrup P, Filep JG (2012) Resolvin E1 promotes phagocytosis-induced neutrophil apoptosis and accelerates resolution of pulmonary inflammation. Proceedings of the National Academy of Sciences of the United States of America 109:14983–14988

Emre C, Hjorth E, Bharani K, Carroll S, Granholm A-C, Schultzberg M (2020) Receptors for pro-resolving mediators are increased in Alzheimer's disease brain. Brain pathology (Zurich, Switzerland) 30:614–640

Endres S, Ghorbani R, Kelley VE, Georgilis K, Lonnemann G, van der Meer JW, Cannon JG, Rogers TS, Klempner MS, Weber PC (1989) The effect of dietary supplementation with n-3 polyunsaturated fatty acids on the synthesis of interleukin-1 and tumor necrosis factor by mononuclear cells. The New England journal of medicine 320:265–271

Engblom D, Saha S, Engström L, Westman M, Audoly LP, Jakobsson P-J, Blomqvist A (2003) Microsomal prostaglandin E synthase-1 is the central switch during immune-induced pyresis. Nature neuroscience 6:1137–1138

Engel A, Kern WV, Mürdter G, Kern P (1994) Kinetics and correlation with body temperature of circulating interleukin-6, interleukin-8, tumor necrosis factor alpha and interleukin-1 beta in patients with fever and neutropenia. Infection 22:160–164

Engelhardt B (2006) Molecular mechanisms involved in T cell migration across the blood-brain barrier. Journal of neural transmission (Vienna, Austria : 1996) 113:477–485

Erridge C, Bennett-Guerrero E, Poxton IR (2002) Structure and function of lipopolysaccharides. Microbes and infection 4:837–851

Eskilsson A, Mirrasekhian E, Dufour S, Schwaninger M, Engblom D, Blomqvist A (2014) Immune-induced fever is mediated by IL-6 receptors on brain endothelial cells coupled to STAT3-dependent induction of brain endothelial prostaglandin synthesis. J. Neurosci. 34:15957–15961

Espevik T, Nissen-Meyer J (1986) A highly sensitive cell line, WEHI 164 clone 13, for measuring cytotoxic factor/tumor necrosis factor from human monocytes. Journal of immunological methods 95:99–105

Fabri A, Kandara K, Coudereau R, Gossez M, Abraham P, Monard C, Cour M, Rimmelé T, Argaud L, Monneret G, Venet F (2020) Characterization of Circulating IL-10-Producing Cells in Septic Shock Patients: A Proof of Concept Study. Front. Immunol. 11:615009

Fan J, Malik AB (2003) Toll-like receptor-4 (TLR4) signaling augments chemokine-induced neutrophil migration by modulating cell surface expression of chemokine receptors. Nature medicine 9:315–321

Fan J, Ye RD, Malik AB (2001) Transcriptional mechanisms of acute lung injury. American journal of physiology. Lung cellular and molecular physiology 281:L1037-50

Fiorentino DF, Zlotnik A, Mosmann TR, Howard M, O'Garra A (1991) IL-10 inhibits cytokine production by activated macrophages. Journal of immunology (Baltimore, Md. : 1950) 147:3815–3822

Flesher RP, Herbert C, Kumar RK (2014) Resolvin E1 promotes resolution of inflammation in a mouse model of an acute exacerbation of allergic asthma. Clinical science (London, England : 1979) 126:805–814

Flower RJ, Harvey EA, Kingston WP (1976) Inflammatory effects of prostaglandin D2 in rat and human skin. British journal of pharmacology 56:229–233

Follin P, Dahlgren C (1992) Phagocytosis by lipopolysaccharide-primed human neutrophils is associated with increased extracellular release of reactive oxygen metabolites. Inflammation 16:83–91

Fonseca MT, Rodrigues AC, Cezar LC, Fujita A, Soriano FG, Steiner AA (2016) Spontaneous hypothermia in human sepsis is a transient, self-limiting, and nonterminal response. Journal of applied physiology (Bethesda, Md. : 1985) 120:1394–1401

Ford-Hutchinson AW, Bray MA, Doig MV, Shipley ME, Smith MJ (1980) Leukotriene B, a potent chemokinetic and aggregating substance released from polymorphonuclear leukocytes. Nature 286:264–265

Fortier M-E, Kent S, Ashdown H, Poole S, Boksa P, Luheshi GN (2004) The viral mimic, polyinosinic:polycytidylic acid, induces fever in rats via an interleukin-1-dependent mechanism. American journal of physiology. Regulatory, integrative and comparative physiology 287:R759-66

Freudenberg MA, Galanos C (1990) Bacterial lipopolysaccharides: structure, metabolism and mechanisms of action. International reviews of immunology 6:207–221

Frey EA, Miller DS, Jahr TG, Sundan A, Bazil V, Espevik T, Finlay BB, Wright SD (1992) Soluble CD14 participates in the response of cells to lipopolysaccharide. J Exp Med 176:1665–1671

Fridlender ZG, Sun J, Kim S, Kapoor V, Cheng G, Ling L, Worthen GS, Albelda SM (2009) Polarization of tumor-associated neutrophil phenotype by TGF-beta: "N1" versus "N2" TAN. Cancer cell 16:183–194

Fries M, Bickenbach J, Henzler D, Beckers S, Dembinski R, Sellhaus B, Rossaint R, Kuhlen R (2005) S-100 protein and neurohistopathologic changes in a porcine model of acute lung injury. Anesthesiology 102:761–767

Fuchs F, Damm J, Gerstberger R, Roth J, Rummel C (2013) Activation of the inflammatory transcription factor nuclear factor interleukin-6 during inflammatory and psychological stress in the brain. J Neuroinflammation 10:140

Fuchs TA, Abed U, Goosmann C, Hurwitz R, Schulze I, Wahn V, Weinrauch Y, Brinkmann V, Zychlinsky A (2007) Novel cell death program leads to neutrophil extracellular traps. The Journal of cell biology 176:231–241

Fujishima S, Hoffman AR, Vu T, Kim KJ, Zheng H, Daniel D, Kim Y, Wallace EF, Larrick JW, Raffin TA (1993) Regulation of neutrophil interleukin 8 gene expression and protein secretion by LPS, TNF-alpha, and IL-1 beta. Journal of cellular physiology 154:478–485

Fujitani Y, Kanaoka Y, Aritake K, Uodome N, Okazaki-Hatake K, Urade Y (2002) Pronounced eosinophilic lung inflammation and Th2 cytokine release in human lipocalin-type prostaglandin D synthase transgenic mice. Journal of immunology (Baltimore, Md. : 1950) 168:443–449

Fumeaux T, Pugin J (2002) Role of interleukin-10 in the intracellular sequestration of human leukocyte antigen-DR in monocytes during septic shock. American journal of respiratory and critical care medicine 166:1475–1482

Galea I, Felton LM, Waters S, van Rooijen N, Perry VH, Newman TA (2008) Immune-to-brain signalling: the role of cerebral CD163-positive macrophages. Neuroscience letters 448:41–46

Gamal M, Moawad J, Rashed L, El-Eraky W, Saleh D, Lehmann C, Sharawy N (2015) Evaluation of the effects of Eserine and JWH-133 on brain dysfunction associated with experimental endotoxemia. Journal of neuroimmunology 281:9–16

Gantz I, Konda Y, Yang YK, Miller DE, Dierick HA, Yamada T (1996) Molecular cloning of a novel receptor (CMKLR1) with homology to the chemotactic factor receptors. Cytogenetics and cell genetics 74:286–290

Gao Y, Zhu J, Yin C, Zhu J, Zhu T, Liu L (2017) Effects of Target Temperature Management on the Outcome of Septic Patients with Fever. BioMed Research International 2017:3906032

Garami A, Steiner AA, Romanovsky AA (2018) Fever and hypothermia in systemic inflammation. Handbook of clinical neurology 157:565–597

Garcia IJP, Kinoshita PF, Oliveira Braga I de, Parreira GM, Mignaco JA, Scavone C, Barbosa LA, Lima Santos H de (2018) Ouabain attenuates the oxidative stress induced by lipopolysaccharides in the cerebellum of rats. Journal of cellular biochemistry 119:2156–2167

Garcia-Bonilla L, Moore JM, Racchumi G, Zhou P, Butler JM, Iadecola C, Anrather J (2014) Inducible nitric oxide synthase in neutrophils and endothelium contributes to ischemic brain injury in mice. Journal of immunology (Baltimore, Md. : 1950) 193:2531–2537

Gaudreault E, Thompson C, Stankova J, Rola-Pleszczynski M (2005) Involvement of BLT1 endocytosis and Yes kinase activation in leukotriene B4-induced neutrophil degranulation. Journal of immunology (Baltimore, Md. : 1950) 174:3617–3625

Gautron L, Lafon P, Chaigniau M, Tramu G, Layé S (2002) Spatiotemporal analysis of signal transducer and activator of transcription 3 activation in rat brain astrocytes and pituitary following peripheral immune challenge. Neuroscience 112:717–729

Gautron L, Lafon P, Tramu G, Layé S (2003) In vivo activation of the interleukin-6 receptor/gp130 signaling pathway in pituitary corticotropes of lipopolysaccharide-treated rats. Neuroendocrinology 77:32–43

Gazzinelli RT, Wysocka M, Hieny S, Scharton-Kersten T, Cheever A, Kühn R, Müller W, Trinchieri G, Sher A (1996) In the absence of endogenous IL-10, mice acutely infected with Toxoplasma gondii succumb to a lethal immune response dependent on CD4+ T cells and accompanied by overproduction of IL-12, IFN-gamma and TNF-alpha. Journal of immunology (Baltimore, Md. : 1950) 157:798–805

Gentile F, Bocci T, Coppola S, Pozzi T, Modafferi L, Priori A, Chiumello D (2022) Putative Role of the Lung-Brain Axis in the Pathogenesis of COVID-19-Associated Respiratory Failure: A Systematic Review. Biomedicines 10

Gentile LF, Cuenca AG, Efron PA, Ang D, Bihorac A, McKinley BA, Moldawer LL, Moore FA (2012) Persistent inflammation and immunosuppression: a common syndrome and new horizon for surgical intensive care. The journal of trauma and acute care surgery 72:1491–1501

Gharamti AA, Samara O, Monzon A, Montalbano G, Scherger S, DeSanto K, Chastain DB, Sillau S, Montoya JG, Franco-Paredes C, Henao-Martínez AF, Shapiro L (2022) Proinflammatory cytokines levels in sepsis and healthy volunteers, and tumor necrosis factor-alpha associated sepsis mortality: A systematic review and meta-analysis. Cytokine 158:156006

Ghosh S, May MJ, Kopp EB (1998) NF-kappa B and Rel proteins: evolutionarily conserved mediators of immune responses. Annual review of immunology 16:225–260

Gibney MJ, Hunter B (1993) The effects of short- and long-term supplementation with fish oil on the incorporation of n-3 polyunsaturated fatty acids into cells of the immune system in healthy volunteers. European journal of clinical nutrition 47:255–259

Gilroy DW, Colville-Nash PR, McMaster S, Sawatzky DA, Willoughby DA, Lawrence T (2003) Inducible cyclooxygenase-derived 15-deoxy(Delta)12-14PGJ2 brings about acute inflammatory resolution in rat pleurisy by inducing neutrophil and macrophage apoptosis. FASEB journal : official publication of the Federation of American Societies for Experimental Biology 17:2269–2271

Gilroy DW, Colville-Nash PR, Willis D, Chivers J, Paul-Clark MJ, Willoughby DA (1999) Inducible cyclooxygenase may have anti-inflammatory properties. Nat Med 5:698–701

Gimenez MAT, Sim JE, Russell JH (2004) TNFR1-dependent VCAM-1 expression by astrocytes exposes the CNS to destructive inflammation. Journal of neuroimmunology 151:116–125

Girotti M, Donegan JJ, Morilak DA (2013) Influence of hypothalamic IL-6/gp130 receptor signaling on the HPA axis response to chronic stress. Psychoneuroendocrinology 38:1158–1169

Godson C, Mitchell S, Harvey K, Petasis NA, Hogg N, Brady HR (2000) Cutting edge: lipoxins rapidly stimulate nonphlogistic phagocytosis of apoptotic neutrophils by monocyte-derived macrophages. Journal of immunology (Baltimore, Md. : 1950) 164:1663–1667

Goehler LE, Gaykema RP, Hansen MK, Anderson K, Maier SF, Watkins LR (2000) Vagal immune-to-brain communication: a visceral chemosensory pathway. Autonomic Neuroscience 85:49–59

Goldman DW, Pickett WC, Goetzl EJ (1983) Human neutrophil chemotactic and degranulating activities of leukotriene B5 (LTB5) derived from eicosapentaenoic acid. Biochemical and biophysical research communications 117:282–288

Gonzalvo R, Martí-Sistac O, Blanch L, López-Aguilar J (2007) Bench-to-bedside review: brain-lung interaction in the critically ill--a pending issue revisited. Crit Care 11:216

Goodman RB, Pugin J, Lee JS, Matthay MA (2003a) Cytokine-mediated inflammation in acute lung injury. Cytokine & growth factor reviews 14:523–535

Goodman RB, Pugin J, Lee JS, Matthay MA (2003b) Cytokine-mediated inflammation in acute lung injury. Cytokine & growth factor reviews 14:523–535

Goodwin JE, Feng Y, Velazquez H, Sessa WC (2013) Endothelial glucocorticoid receptor is required for protection against sepsis. Proceedings of the National Academy of Sciences of the United States of America 110:306–311

Goralski KB, McCarthy TC, Hanniman EA, Zabel BA, Butcher EC, Parlee SD, Muruganandan S, Sinal CJ (2007) Chemerin, a novel adipokine that regulates adipogenesis and adipocyte metabolism. Journal of Biological Chemistry 282:28175–28188

Gordon CJ (1985) Relationship between autonomic and behavioral thermoregulation in the mouse. Physiology & Behavior 34:687–690

Graeber MB, Streit WJ, Kreutzberg GW (1989) Identity of ED2-positive perivascular cells in rat brain. Journal of neuroscience research 22:103–106

Gruys E, Toussaint MJM, Niewold TA, Koopmans SJ (2005) Acute phase reaction and acute phase proteins. Journal of Zhejiang University. Science. B 6:1045–1056

Gu M, Li Y, Tang H, Zhang C, Li W, Zhang Y, Li Y, Zhao Y, Song C (2018) Endogenous Omega (n)-3 Fatty Acids in Fat-1 Mice Attenuated Depression-Like Behavior, Imbalance between Microglial M1 and M2 Phenotypes, and Dysfunction of Neurotrophins Induced by Lipopolysaccharide Administration. Nutrients 10:1351

Guo RF, Huber-Lang M, Wang X, Sarma V, Padgaonkar VA, Craig RA, Riedemann NC, McClintock SD, Hlaing T, Shi MM, Ward PA (2000) Protective effects of anti-C5a in sepsis-induced thymocyte apoptosis. J Clin Invest 106:1271–1280

Guo R-F, Ward PA (2005) Role of C5a in inflammatory responses. Annual review of immunology 23:821–852

Hailman E, Lichenstein HS, Wurfel MM, Miller DS, Johnson DA, Kelley M, Busse LA, Zukowski MM, Wright SD (1994) Lipopolysaccharide (LPS)-binding protein accelerates the binding of LPS to CD14. J Exp Med 179:269–277

Hall WD, Hurst JW, Walker HK (1990) Clinical methods. The history, physical, and laboratory examinations, 3. ed. Butterworths, Boston

Han B, Yu L, Geng Y, Shen L, Wang H, Wang Y, Wang J, Wang M (2016) Chronic Stress Aggravates Cognitive Impairment and Suppresses Insulin Associated Signaling Pathway in APP/PS1 Mice. Journal of Alzheimer's disease : JAD 53:1539–1552

Handa O, Stephen J, Cepinskas G (2008) Role of endothelial nitric oxide synthase-derived nitric oxide in activation and dysfunction of cerebrovascular endothelial cells during early onsets of sepsis. American journal of physiology. Heart and circulatory physiology 295:H1712-9

Haqqani AS, Sandhu JK, Birnboim HC (1999) A myeloperoxidase-specific assay based upon bromide-dependent chemiluminescence of luminol. Analytical biochemistry 273:126–132

Harden LM, Rummel C, Laburn HP, Damm J, Wiegand F, Poole S, Gerstberger R, Roth J (2014) Critical role for peripherally-derived interleukin-10 in mediating the thermoregulatory manifestations of fever and hypothermia in severe forms of lipopolysaccharide-induced inflammation. Pflugers Archiv : European journal of physiology 466:1451–1466

Harré E-M, Roth J, Gerstberger R, Hübschle T (2003) Interleukin-6 mediates lipopolysaccharide-induced nuclear STAT3 translocation in astrocytes of rat sensory circumventricular organs. Brain Research 980:151–155

Harré E-M, Roth J, Pehl U, Kueth M, Gerstberger R, Hübschle T (2002) Selected contribution: role of IL-6 in LPS-induced nuclear STAT3 translocation in sensory circumventricular organs during fever in rats. Journal of applied physiology (Bethesda, Md. : 1985) 92:2657–2666

Hart BL (1988) Biological basis of the behavior of sick animals. Neuroscience & Biobehavioral Reviews 12:123–137

Hasturk H, Kantarci A, Ohira T, Arita M, Ebrahimi N, Chiang N, Petasis NA, Levy BD, Serhan CN, van Dyke TE (2006) RvE1 protects from local inflammation and osteoclast- mediated bone destruction in periodontitis. The FASEB Journal 20:401–403

Haworth O, Cernadas M, Yang R, Serhan CN, Levy BD (2008) Resolvin E1 regulates interleukin 23, interferon-gamma and lipoxin A4 to promote the resolution of allergic airway inflammation. Nat Immunol 9:873–879

Heinrich PC, Castell JV, Andus T (1990) Interleukin-6 and the acute phase response. The Biochemical journal 265:621–636

Heller A, Koch T, Schmeck J, van Ackern K (1998) Lipid mediators in inflammatory disorders. Drugs 55:487–496

Henkel T, Machleidt T, Alkalay I, Krönke M, Ben-Neriah Y, Baeuerle PA (1993) Rapid proteolysis of I kappa B-alpha is necessary for activation of transcription factor NF-kappa B. Nature 365:182–185

Henneck T, Mergani A, Clever S, Seidler AE, Brogden G, Runft S, Baumgärtner W, Branitzki-Heinemann K, Köckritz-Blickwede M von (2022) Formation of Neutrophil Extracellular Traps by Reduction of Cellular Cholesterol Is Independent of Oxygen and HIF-1α. International journal of molecular sciences 23

Herman JP, Tasker JG (2016) Paraventricular Hypothalamic Mechanisms of Chronic Stress Adaptation. Frontiers in endocrinology 7:137

Hernandez J, Schäffer J, Herden C, Pflieger FJ, Reiche S, Körber S, Kitagawa H, Welter J, Michels S, Culmsee C, Bier J, Sommer N, Kang JX, Mayer K, Hecker M, Rummel C (2023) n-3 Polyunsaturated Fatty Acids Modulate LPS-Induced ARDS and the Lung–Brain Axis of Communication in Wild-Type versus Fat-1 Mice Genetically Modified for Leukotriene B4 Receptor 1 or Chemerin Receptor 23 Knockout. IJMS 24:13524

Hernandez JD, Li T, Rau CM, LeSuer WE, Wang P, Coletta DK, Madura JA, Jacobsen EA, Filippis E de (2021) ω-3PUFA supplementation ameliorates adipose tissue inflammation and insulin-stimulated glucose disposal in subjects with obesity: a potential role for apolipoprotein E. International journal of obesity (2005) 45:1331–1341

Herová M, Schmid M, Gemperle C, Hersberger M (2015) ChemR23, the receptor for chemerin and resolvin E1, is expressed and functional on M1 but not on M2 macrophages. The Journal of Immunology 194:2330–2337

Hertwig L, Pache F, Romero-Suarez S, Stürner KH, Borisow N, Behrens J, Bellmann-Strobl J, Seeger B, Asselborn N, Ruprecht K, Millward JM, Infante-Duarte C, Paul F (2016) Distinct functionality of neutrophils in multiple sclerosis and neuromyelitis optica. Multiple sclerosis (Houndmills, Basingstoke, England) 22:160–173

Herz J, Sabellek P, Lane TE, Gunzer M, Hermann DM, Doeppner TR (2015) Role of Neutrophils in Exacerbation of Brain Injury After Focal Cerebral Ischemia in Hyperlipidemic Mice. Stroke 46:2916–2925

Hespeling U, Püschel GP, Jungermann K, Götze O, Zwirner J (1995) Stimulation of glycogen phosphorylase in rat hepatocytes via prostanoid release from Kupffer cells by recombinant rat anaphylatoxin C5a but not by native human C5a in hepatocyte/Kupffer cell co-cultures. FEBS Letters 372:108–112

Hirche TO, Gaut JP, Heinecke JW, Belaaouaj A (2005) Myeloperoxidase plays critical roles in killing Klebsiella pneumoniae and inactivating neutrophil elastase: effects on host defense. Journal of immunology (Baltimore, Md. : 1950) 174:1557–1565

Hirose A, Terauchi M, Akiyoshi M, Owa Y, Kato K, Kubota T (2016) Depressive symptoms are associated with oxidative stress in middle-aged women: a cross-sectional study. BioPsychoSocial Med 10:12

Honda T, Matsuoka T, Ueta M, Kabashima K, Miyachi Y, Narumiya S (2009) Prostaglandin E(2)-EP(3) signaling suppresses skin inflammation in murine contact hypersensitivity. The Journal of allergy and clinical immunology 124:809-18.e2

Hong S, Gronert K, Devchand PR, Moussignac R-L, Serhan CN (2003) Novel docosatrienes and 17S-resolvins generated from docosahexaenoic acid in murine brain, human blood, and glial cells. Autacoids in anti-inflammation. Journal of Biological Chemistry 278:14677–14687

Hong W, Yang J, Zou J, Bi Z, He C, Lei H, He X, Li X, Alu A, Ren W, Wang Z, Jiang X, Zhong K, Jia G, Yang Y, Yu W, Huang Q, Yang M, Zhou Y, Zhao Y, Kuang D, Wang J, Wang H, Chen S, Luo M, Zhang Z, Lu T, Chen L, Que H, He Z, Sun Q, Wang W, Shen G, Lu G, Zhao Z, Yang L, Yang J, Wang Z, Li J, Song X, Dai L, Chen C, Geng J, Gou M, Chen L, Dong H, Peng Y, Huang C, Qian Z, Cheng W, Fan C, Wei Y, Su Z, Tong A, Lu S, Peng X, Wei X (2022) Histones released by NETosis enhance the infectivity of SARS-CoV-2 by bridging the spike protein subunit 2 and sialic acid on host cells. Cellular & molecular immunology

Hoogland ICM, Houbolt C, van Westerloo DJ, van Gool WA, van de Beek D (2015) Systemic inflammation and microglial activation: systematic review of animal experiments. J Neuroinflammation 12:114

Hoover RL, Karnovsky MJ, Austen KF, Corey EJ, Lewis RA (1984) Leukotriene B4 action on endothelium mediates augmented neutrophil/endothelial adhesion. Proc. Natl. Acad. Sci. U.S.A. 81:2191–2193

Hopkins RO, Weaver LK, Chan KJ, Orme JF (2004) Quality of life, emotional, and cognitive function following acute respiratory distress syndrome. Journal of the International Neuropsychological Society : JINS 10:1005–1017

Hoppenbrouwers T, Autar ASA, Sultan AR, Abraham TE, van Cappellen WA, Houtsmuller AB, van Wamel WJB, van Beusekom HMM, van Neck JW, Maat MPM de (2017) In vitro induction of NETosis: Comprehensive live imaging comparison and systematic review. PLOS ONE 12:e0176472

Horii Y, Nakaya M, Ohara H, Nishihara H, Watari K, Nagasaka A, Nakaya T, Sugiura Y, Okuno T, Koga T, Tanaka A, Yokomizo T, Kurose H (2020) Leukotriene B4 receptor 1 exacerbates inflammation following myocardial infarction. The FASEB Journal 34:8749–8763

Hosang L, Canals RC, van der Flier FJ, Hollensteiner J, Daniel R, Flügel A, Odoardi F (2022) The lung microbiome regulates brain autoimmunity. Nature 603:138–144

Hotchkiss RS, Monneret G, Payen D (2013) Sepsis-induced immunosuppression: from cellular dysfunctions to immunotherapy. Nat Rev Immunol 13:862–874

Hritcu L, Ciobica A (2013) Intranigral lipopolysaccharide administration induced behavioral deficits and oxidative stress damage in laboratory rats: relevance for Parkinson's disease. Behavioural brain research 253:25–31

Hritcu L, Ciobica A, Stefan M, Mihasan M, Palamiuc L, Nabeshima T (2011) Spatial memory deficits and oxidative stress damage following exposure to lipopolysaccharide in a rodent model of Parkinson's disease. Neuroscience research 71:35–43

Hsi ED, Remick DG (1995) Monocytes are the major producers of interleukin-1 beta in an ex vivo model of local cytokine production. Journal of interferon & cytokine research : the official journal of the International Society for Interferon and Cytokine Research 15:89–94

Hu W, Pasare C (2013) Location, location, location: tissue-specific regulation of immune responses. Journal of Leukocyte Biology 94:409–421

Huang F, Kao C-Y, Wachi S, Thai P, Ryu J, Wu R (2007) Requirement for both JAK-mediated PI3K signaling and ACT1/TRAF6/TAK1-dependent NF-kappaB activation by IL-17A in enhancing cytokine expression in human airway epithelial cells. Journal of immunology (Baltimore, Md. : 1950) 179:6504–6513

Huang L, Zhao A, Wong F, Ayala JM, Struthers M, Ujjainwalla F, Wright SD, Springer MS, Evans J, Cui J (2004) Leukotriene B4 strongly increases monocyte chemoattractant protein-1 in human monocytes. Arteriosclerosis, thrombosis, and vascular biology 24:1783–1788

Huang SR, Ma AY, Liu Y, Qu Y (2017) Effects of inflammatory factors including plasma tumor necrosis factor-α in the clinical treatment of acute respiratory distress syndrome. Oncology Letters 13:5016–5020

Huebener P, Pradere J-P, Hernandez C, Gwak G-Y, Caviglia JM, Mu X, Loike JD, Schwabe RF (2015) The HMGB1/RAGE axis triggers neutrophil-mediated injury amplification following necrosis. J Clin Invest 125:539–550

Hughes J, Johnson RJ, Mooney A, Hugo C, Gordon K, Savill J (1997) Neutrophil fate in experimental glomerular capillary injury in the rat. Emigration exceeds in situ clearance by apoptosis. The American Journal of Pathology 150:223–234

Hulshof S, Montagne L, Groot CJA de, van der Valk P (2002) Cellular localization and expression patterns of interleukin-10, interleukin-4, and their receptors in multiple sclerosis lesions. Glia 38:24–35

Hunter WS (1997) Anteroventral third ventricle lesion suppresses fever, but not stress-induced hyperthermia in rats. Annals of the New York Academy of Sciences 813:420–426

Hynninen M, Valtonen M, Vaara M, Markkanen H, Kuusela P, Saxen H, Takkunen O (1995) Plasma endotoxin and cytokine levels in neutropenic and non-neutropenic bacteremic patients. European journal of clinical microbiology & infectious diseases : official publication of the European Society of Clinical Microbiology 14:1039–1045

Ikezoe T, Yang Y, Heber D, Taguchi H, Koeffler HP (2003) PC-SPES: a potent inhibitor of nuclear factor-kappa B rescues mice from lipopolysaccharide-induced septic shock. Molecular pharmacology 64:1521–1529

Innes JK, Calder PC (2018) Omega-6 fatty acids and inflammation. Prostaglandins, leukotrienes, and essential fatty acids 132:41–48

Iwashyna TJ, Ely EW, Smith DM, Langa KM (2010) Long-term cognitive impairment and functional disability among survivors of severe sepsis. JAMA 304:1787–1794

J. W. Fuseler (2006) Analysis and quantitation of NF-κB nuclear translocation in tumor necrosis factor alpha (TNF-α) activated vascular endothelial cells

Jang P-G, Namkoong C, Kang GM, Hur M-W, Kim S-W, Kim GH, Kang Y, Jeon M-J, Kim EH, Lee M-S, Karin M, Baik J-H, Park J-Y, Lee K-U, Kim Y-B, Kim M-S (2010) NF-kappaB activation in hypothalamic pro-opiomelanocortin neurons is essential in illness- and leptin-induced anorexia. The Journal of biological chemistry 285:9706–9715

Janský L, Vybíral S, Pospísilová D, Roth J, Dornand J, Zeisberger E, Kamínková J (1995) Production of systemic and hypothalamic cytokines during the early phase of endotoxin fever. Neuroendocrinology 62:55–61

Jenniskens M, Weckx R, Dufour T, Vander Perre S, Pauwels L, Derde S, Téblick A, Güiza F, van den Berghe G, Langouche L (2018) The Hepatic Glucocorticoid Receptor Is Crucial for Cortisol Homeostasis and Sepsis Survival in Humans and Male Mice. Endocrinology 159:2790–2802

Jeyaseelan S, Chu HW, Young SK, Worthen GS (2004) Transcriptional profiling of lipopolysaccharide-induced acute lung injury. Infection and Immunity 72:7247–7256

Ji A, Diao H, Wang X, Yang R, Zhang J, Luo W, Cao R, Cao Z, Wang F, Cai T (2012) n-3 polyunsaturated fatty acids inhibit lipopolysaccharide-induced microglial activation and dopaminergic injury in rats. Neurotoxicology 33:780–788

Jin H, Aziz M, Ode Y, Wang P (2019) CIRP Induces Neutrophil Reverse Transendothelial Migration in Sepsis. Shock 51:548–556

Jin J-O, Han X, Yu Q (2013) Interleukin-6 induces the generation of IL-10-producing Tr1 cells and suppresses autoimmune tissue inflammation. Journal of autoimmunity 40:28–44

Jin L, Batra S, Douda DN, Palaniyar N, Jeyaseelan S (2014) CXCL1 contributes to host defense in polymicrobial sepsis via modulating T cell and neutrophil functions. The Journal of Immunology 193:3549–3558

Joffre C, Rey C, Layé S (2019) N-3 Polyunsaturated Fatty Acids and the Resolution of Neuroinflammation. Frontiers in pharmacology 10:1022

Johnson AK, Gross PM (1993) Sensory circumventricular organs and brain homeostatic pathways. FASEB journal : official publication of the Federation of American Societies for Experimental Biology 7:678–686

Johnson RH, Kho DT, O' Carroll SJ, Angel CE, Graham ES (2018) The functional and inflammatory response of brain endothelial cells to Toll-Like Receptor agonists. Scientific reports 8:10102

Joseph LC, Kokkinaki D, Valenti M-C, Kim GJ, Barca E, Tomar D, Hoffman NE, Subramanyam P, Colecraft HM, Hirano M, Ratner AJ, Madesh M, Drosatos K, Morrow JP (2017) Inhibition of NADPH oxidase 2 (NOX2) prevents sepsis-induced cardiomyopathy by improving calcium handling and mitochondrial function. JCI insight 2

Juutilainen A, Hämäläinen S, Niemenpää J, Kuittinen T, Pulkki K, Koivula I, Niskanen L, Jantunen E (2011) Serum cortisol and inflammatory response in neutropenic fever. Ann Hematol 90:1467–1475

Kafa IM, Bakirci S, Uysal M, Kurt MA (2010) Alterations in the brain electrical activity in a rat model of sepsis-associated encephalopathy. Brain Research 1354:217–226

Kafrouni MI, Brown GR, Thiele DL (2003) The role of TNF-TNFR2 interactions in generation of CTL responses and clearance of hepatic adenovirus infection. Journal of Leukocyte Biology 74:564–571

Kambas K, Markiewski MM, Pneumatikos IA, Rafail SS, Theodorou V, Konstantonis D, Kourtzelis I, Doumas MN, Magotti P, Deangelis RA, Lambris JD, Ritis KD (2008) C5a and TNF-alpha up-regulate the expression of tissue factor in intra-alveolar neutrophils of patients with the acute respiratory distress syndrome. Journal of immunology (Baltimore, Md. : 1950) 180:7368–7375

Kambas K, Mitroulis I, Apostolidou E, Girod A, Chrysanthopoulou A, Pneumatikos I, Skendros P, Kourtzelis I, Koffa M, Kotsianidis I, Ritis K (2012) Autophagy mediates the delivery of thrombogenic tissue factor to neutrophil extracellular traps in human sepsis. PLOS ONE 7:e45427

Kang D, Kim SH, Hamasaki N (2007) Mitochondrial transcription factor A (TFAM): roles in maintenance of mtDNA and cellular functions. Mitochondrion 7:39–44

Kang JX (2007) Fat-1 transgenic mice: a new model for omega-3 research. Prostaglandins, Leukotrienes and Essential Fatty Acids 77:263–267

Kang JX, Wang J, Wu L, Kang ZB (2004) Transgenic mice: fat-1 mice convert n-6 to n-3 fatty acids. Nature 427:504

Kang S, Tanaka T, Inoue H, Ono C, Hashimoto S, Kioi Y, Matsumoto H, Matsuura H, Matsubara T, Shimizu K, Ogura H, Matsuura Y, Kishimoto T (2020) IL-6 trans-signaling induces plasminogen activator inhibitor-1 from vascular endothelial cells in cytokine release syndrome. Proceedings of the National Academy of Sciences of the United States of America 117:22351–22356

Karampela I, Fragkou PC (2022) Future Perspectives in the Diagnosis and Treatment of Sepsis and Septic Shock. Medicina (Kaunas, Lithuania) 58

Karin M, Ben-Neriah Y (2000) Phosphorylation meets ubiquitination: the control of NF-kappaB activity. Annual review of immunology 18:621–663

Kaur J, Adya R, Tan BK, Chen J, Randeva HS (2010) Identification of chemerin receptor (ChemR23) in human endothelial cells: chemerin-induced endothelial angiogenesis. Biochemical and biophysical research communications 391:1762–1768

Kawashima A, Harada T, Imada K, Yano T, Mizuguchi K (2008) Eicosapentaenoic acid inhibits interleukin-6 production in interleukin-1beta-stimulated C6 glioma cells through peroxisome proliferator-activated receptor-gamma. Prostaglandins, Leukotrienes and Essential Fatty Acids 79:59–65

Kelley KW, Bluthé R-M, Dantzer R, Zhou J-H, Shen W-H, Johnson RW, Broussard SR (2003) Cytokine-induced sickness behavior. Brain, behavior, and immunity 17:112–118

Kelley KW, Kent S (2020) The Legacy of Sickness Behaviors. Frontiers in psychiatry 11:607269

Kelly DP, Scarpulla RC (2004) Transcriptional regulatory circuits controlling mitochondrial biogenesis and function. Genes Dev. 18:357–368

Kenney MJ, Ganta CK (2014) Autonomic nervous system and immune system interactions. Comprehensive Physiology 4:1177–1200

Kent S, Bluthe RM, Dantzer R, Hardwick AJ, Kelley KW, Rothwell NJ, Vannice JL (1992a) Different receptor mechanisms mediate the pyrogenic and behavioral effects of interleukin 1. Proc. Natl. Acad. Sci. U.S.A. 89:9117–9120

Kent S, Bluthé R-M, Kelley KW, Dantzer R (1992b) Sickness behavior as a new target for drug development. Trends in Pharmacological Sciences 13:24–28

Kerola M, Vuolteenaho K, Kosonen O, Kankaanranta H, Sarna S, Moilanen E (2009) Effects of nimesulide, acetylsalicylic acid, ibuprofen and nabumetone on cyclooxygenase-1- and cyclooxygenase-2-mediated prostanoid production in healthy volunteers ex vivo. Basic & Clinical Pharmacology & Toxicology 104:17–21

Kew S, Banerjee T, Minihane AM, Finnegan YE, Williams CM, Calder PC (2003) Relation between the fatty acid composition of peripheral blood mononuclear cells and measures of immune cell function in healthy, free-living subjects aged 25-72 y. The American journal of clinical nutrition 77:1278–1286

Khandpur R, Carmona-Rivera C, Vivekanandan-Giri A, Gizinski A, Yalavarthi S, Knight JS, Friday S, Li S, Patel RM, Subramanian V, Thompson P, Chen P, Fox DA, Pennathur S, Kaplan MJ (2013) NETs are a source of citrullinated autoantigens and stimulate inflammatory responses in rheumatoid arthritis. Science Translational Medicine 5:178ra40

Khatiwada S, Subedi A (2020) Lung microbiome and coronavirus disease 2019 (COVID-19): Possible link and implications. Human microbiome journal 17:100073

Kikuchi DS, Campos ACP, Qu H, Forrester SJ, Pagano RL, Lassègue B, Sadikot RT, Griendling KK, Hernandes MS (2019) Poldip2 mediates blood-brain barrier disruption in a model of sepsis-associated encephalopathy. J Neuroinflammation 16:241

Kim H, Leng K, Park J, Sorets AG, Kim S, Shostak A, Embalabala RJ, Mlouk K, Katdare KA, Rose IVL, Sturgeon SM, Neal EH, Ao Y, Wang S, Sofroniew MV, Brunger JM, McMahon DG, Schrag MS, Kampmann M, Lippmann ES (2022) Reactive astrocytes transduce inflammation in a blood-brain barrier model through a TNF-STAT3 signaling axis and secretion of alpha 1-antichymotrypsin. Nature communications 13:6581

Kim KS (2003) Pathogenesis of bacterial meningitis: from bacteraemia to neuronal injury. Nature reviews. Neuroscience 4:376–385

Kim YR, Kim YM, Lee J, Park J, Lee JE, Hyun Y-M (2020) Neutrophils Return to Bloodstream Through the Brain Blood Vessel After Crosstalk With Microglia During LPS-Induced Neuroinflammation. Frontiers in cell and developmental biology 8:613733

Kishimoto T, Akira S, Taga T (1992) IL-6 receptor and mechanism of signal transduction. International Journal of Immunopharmacology 14:431–438

Klawonn AM, Fritz M, Castany S, Pignatelli M, Canal C, Similä F, Tejeda HA, Levinsson J, Jaarola M, Jakobsson J, Hidalgo J, Heilig M, Bonci A, Engblom D (2021) Microglial activation elicits a negative affective state through prostaglandin-mediated modulation of striatal neurons. Immunity 54:225-234.e6

Kleiman A, Hübner S, Rodriguez Parkitna JM, Neumann A, Hofer S, Weigand MA, Bauer M, Schmid W, Schütz G, Libert C, Reichardt HM, Tuckermann JP (2012) Glucocorticoid receptor dimerization is required for survival in septic shock via suppression of interleukin-1 in macrophages. The FASEB Journal 26:722–729

Klein RS, Hunter CA (2017) Protective and Pathological Immunity during Central Nervous System Infections. Immunity 46:891–909

Klir JJ, McClellan JL, Kozak W, Szelényi Z, Wong GH, Kluger MJ (1995) Systemic but not central administration of tumor necrosis factor-alpha attenuates LPS-induced fever in rats. The American journal of physiology 268:R480-6

Kluger MJ (1979) Phylogeny of fever. Federation proceedings 38:30–34

Kluger MJ, Ringler DH, Anver MR (1975) Fever and survival. Science (New York, N.Y.) 188:166–168

Kobayashi SD, Malachowa N, DeLeo FR (2018) Neutrophils and Bacterial Immune Evasion. Journal of innate immunity 10:432–441

Koenig S, Bredehöft J, Perniss A, Fuchs F, Roth J, Rummel C (2018) Age Dependent Hypothalamic and Pituitary Responses to Novel Environment Stress or Lipopolysaccharide in Rats. Frontiers in behavioral neuroscience 12:55

Koenig S, Luheshi GN, Wenz T, Gerstberger R, Roth J, Rummel C (2014) Leptin is involved in age-dependent changes in response to systemic inflammation in the rat. Brain, behavior, and immunity 36:128–138

Kong Y, He G, Zhang X, Li J (2021) The Role of Neutrophil Extracellular Traps in Lipopolysaccharide-Induced Depression-like Behaviors in Mice. Brain sciences 11

Konstantinos AP, Sheridan JF (2001) Stress and influenza viral infection: modulation of proinflammatory cytokine responses in the lung. Respiration Physiology 128:71–77

Kopf M, Baumann H, Freer G, Freudenberg M, Lamers M, Kishimoto T, Zinkernagel R, Bluethmann H, Köhler G (1994) Impaired immune and acute-phase responses in interleukin-6-deficient mice. Nature 368:339–342

Kozak W, Poli V, Soszynski D, Conn CA, Leon LR, Kluger MJ (1997) Sickness behavior in mice deficient in interleukin-6 during turpentine abscess and influenza pneumonitis. The American journal of physiology 272:R621-30

Krishnamoorthy S, Recchiuti A, Chiang N, Yacoubian S, Lee C-H, Yang R, Petasis NA, Serhan CN (2010) Resolvin D1 binds human phagocytes with evidence for proresolving receptors. Proceedings of the National Academy of Sciences of the United States of America 107:1660–1665

Krüger K, Dischereit G, Seimetz M, Wilhelm J, Weissmann N, Mooren FC (2015) Time course of cigarette smoke-induced changes of systemic inflammation and muscle structure. American journal of physiology. Lung cellular and molecular physiology 309:L119-28

Kuhns DB, Nelson EL, Alvord WG, Gallin JI (2001) Fibrinogen induces IL-8 synthesis in human neutrophils stimulated with formyl-methionyl-leucyl-phenylalanine or leukotriene B(4). Journal of immunology (Baltimore, Md. : 1950) 167:2869–2878

Kunkel SL, Spengler M, May MA, Spengler R, Larrick J, Remick D (1988) Prostaglandin E2 regulates macrophage-derived tumor necrosis factor gene expression. Journal of Biological Chemistry 263:5380–5384

Kurihara Y, Endo H, Akahoshi T, Kondo H (2001) Up-regulation of prostaglandin E receptor EP2 and EP4 subtypes in rat synovial tissues with adjuvant arthritis. Clin Exp Immunol 123:323–330

Kushimoto S, Gando S, Saitoh D, Mayumi T, Ogura H, Fujishima S, Araki T, Ikeda H, Kotani J, Miki Y, Shiraishi S, Suzuki K, Suzuki Y, Takeyama N, Takuma K, Tsuruta R, Yamaguchi Y, Yamashita N, Aikawa N (2013) The impact of body temperature abnormalities on the disease severity and outcome in patients with severe sepsis: an analysis from a multicenter, prospective survey of severe sepsis. Crit Care 17:R271

Kwon D-J, Ju SM, Youn GS, Choi SY, Park J (2013) Suppression of iNOS and COX-2 expression by flavokawain A via blockade of NF-κB and AP-1 activation in RAW 264.7 macrophages. Food and chemical toxicology : an international journal published for the British Industrial Biological Research Association 58:479–486

Kwon V, Cai P, Dixon CT, Hamlin V, Spencer CG, Rojas AM, Hamilton M, Shiau CE (2022) Peripheral NOD-like receptor deficient inflammatory macrophages trigger neutrophil infiltration into the brain disrupting daytime locomotion. Communications biology 5:464

Laflamme N, Rivest S (2001) Toll-like receptor 4: the missing link of the cerebral innate immune response triggered by circulating gram-negative bacterial cell wall components. FASEB journal : official publication of the Federation of American Societies for Experimental Biology 15:155–163

Lämmermann T, Afonso PV, Angermann BR, Wang JM, Kastenmüller W, Parent CA, Germain RN (2013) Neutrophil swarms require LTB4 and integrins at sites of cell death in vivo. Nature 498:371–375

Lang FM, Lee KM-C, Teijaro JR, Becher B, Hamilton JA (2020) GM-CSF-based treatments in COVID-19: reconciling opposing therapeutic approaches. Nat Rev Immunol 20:507–514

Langlet F, Mullier A, Bouret SG, Prevot V, Dehouck B (2013) Tanycyte-like cells form a blood-cerebrospinal fluid barrier in the circumventricular organs of the mouse brain. The Journal of comparative neurology 521:3389–3405

Lansdorp PM, Aarden LA, Calafat J, Zeiljemaker WP (1986) A growth-factor dependent B-cell hybridoma. Current topics in microbiology and immunology 132:105–113

Lasselin J (2021) Back to the future of psychoneuroimmunology: Studying inflammation-induced sickness behavior. Brain, behavior, & immunity - health 18:100379

Lasselin J, Schedlowski M, Karshikoff B, Engler H, Lekander M, Konsman JP (2020) Comparison of bacterial lipopolysaccharide-induced sickness behavior in rodents and humans: Relevance for symptoms of anxiety and depression. Neuroscience and biobehavioral reviews 115:15–24

Law AHY, Lee DCW, Cheung BKW, Yim HCH, Lau ASY (2007) Role for nonstructural protein 1 of severe acute respiratory syndrome coronavirus in chemokine dysregulation. Journal of virology 81:416–422

Lawrence MB, Bainton DF, Springer TA (1994) Neutrophil tethering to and rolling on E-selectin are separable by requirement for L-selectin. Immunity 1:137–145

Lazarus M, Yoshida K, Coppari R, Bass CE, Mochizuki T, Lowell BB, Saper CB (2007) EP3 prostaglandin receptors in the median preoptic nucleus are critical for fever responses. Nature neuroscience 10:1131–1133

Le Bel M, Brunet A, Gosselin J (2014) Leukotriene B4, an endogenous stimulator of the innate immune response against pathogens. Journal of innate immunity 6:159–168

Ledeboer A, Brevé JJP, Wierinckx A, van der Jagt S, Bristow AF, Leysen JE, Tilders FJH, van Dam A-M (2002) Expression and regulation of interleukin-10 and interleukin-10 receptor in rat astroglial and microglial cells. The European journal of neuroscience 16:1175–1185

Lee SC, Liu W, Dickson DW, Brosnan CF, Berman JW (1993) Cytokine production by human fetal microglia and astrocytes. Differential induction by lipopolysaccharide and IL-1 beta. J Immunol 150:2659–2667

Lee TH, Hoover RL, Williams JD, Sperling RI, Ravalese J, Spur BW, Robinson DR, Corey EJ, Lewis RA, Austen KF (1985) Effect of dietary enrichment with eicosapentaenoic and docosahexaenoic acids on in vitro neutrophil and monocyte leukotriene generation and neutrophil function. The New England journal of medicine 312:1217–1224

Lee TH, Menica-Huerta JM, Shih C, Corey EJ, Lewis RA, Austen KF (1984) Characterization and biologic properties of 5,12-dihydroxy derivatives of eicosapentaenoic acid, including leukotriene B5 and the double lipoxygenase product. Journal of Biological Chemistry 259:2383–2389

Lehmann C, Homann J, Ball A-K, Blöcher R, Kleinschmidt TK, Basavarajappa D, Angioni C, Ferreirós N, Häfner A-K, Rådmark O, Proschak E, Haeggström JZ, Geisslinger G, Parnham MJ, Steinhilber D, Kahnt AS (2015) Lipoxin and resolvin biosynthesis is dependent on 5-lipoxygenase activating protein. The FASEB Journal 29:5029–5043

Leon LR (2004) Hypothermia in systemic inflammation: role of cytokines. Frontiers in bioscience : a journal and virtual library 9:1877–1888

Leon LR, Kozak W, Peschon J, Kluger MJ (1997) Exacerbated febrile responses to LPS, but not turpentine, in TNF double receptor-knockout mice. The American journal of physiology 272:R563-9

Leon LR, White AA, Kluger MJ (1998) Role of IL-6 and TNF in thermoregulation and survival during sepsis in mice. The American journal of physiology 275:R269-77

Levi M, van der Poll T (2017) Coagulation and sepsis. Thrombosis research 149:38–44

Levy JH (1996) The Human Inflammatory Response. Journal of Cardiovascular Pharmacology 27:31

Lewis M, Tartaglia LA, Lee A, Bennett GL, Rice GC, Wong GH, Chen EY, Goeddel DV (1991) Cloning and expression of cDNAs for two distinct murine tumor necrosis factor receptors demonstrate one receptor is species specific. Proc. Natl. Acad. Sci. U.S.A. 88:2830–2834

Lewis RA, Austen KF, Soberman RJ (1990) Leukotrienes and other products of the 5-lipoxygenase pathway. Biochemistry and relation to pathobiology in human diseases. The New England journal of medicine 323:645–655

Lewkowich I, Ahlbrand R, Johnson E, McAlees J, Nawreen N, Raman R, Lingel I, Hargis J, Hoover C, Sah R (2020) Modulation of fear behavior and neuroimmune alterations in house dust mite exposed A/J mice, a model of severe asthma. Brain, behavior, and immunity 88:688–698

Lewkowicz N, Mycko MP, Przygodzka P, Ćwiklińska H, Cichalewska M, Matysiak M, Selmaj K, Lewkowicz P (2016) Induction of human IL-10-producing neutrophils by LPS-stimulated Treg cells and IL-10. Mucosal immunology 9:364–378

Ley K, Laudanna C, Cybulsky MI, Nourshargh S (2007) Getting to the site of inflammation: the leukocyte adhesion cascade updated. Nature reviews. Immunology 7:678–689

Li C, Chen W, Lin F, Li W, Wang P, Liao G, Zhang L (2022) Functional Two-Way Crosstalk Between Brain and Lung: The Brain-Lung Axis. Cellular and molecular neurobiology

Li C, Yang P, Sun Y, Li T, Wang C, Wang Z, Zou Z, Yan Y, Wang W, Chen Z, Xing L, Tang C, Ju X, Guo F, Deng J, Zhao Y, Yang P, Tang J, Wang H, Zhao Z, Yin Z, Cao B, Wang X, Jiang C (2012) IL-17 response mediates acute lung injury induced by the 2009 pandemic influenza A (H1N1) virus. Cell research 22:528–538

Li P, Li M, Lindberg MR, Kennett MJ, Xiong N, Wang Y (2010) PAD4 is essential for antibacterial innate immunity mediated by neutrophil extracellular traps. The Journal of experimental medicine 207:1853–1862

Li X, Xu Z, Pang X, Huang Y, Yang B, Yang Y, Chen K, Liu X, Mao P, Li Y (2017) Interleukin-10/lymphocyte ratio predicts mortality in severe septic patients. PLOS ONE 12:e0179050

Li Z, Blatteis CM (2004) Fever onset is linked to the appearance of lipopolysaccharide in the liver. Journal of endotoxin research 10:39–53

Li Z, Perlik V, Feleder C, Tang Y, Blatteis CM (2006) Kupffer cell-generated PGE2 triggers the febrile response of guinea pigs to intravenously injected LPS. American journal of physiology. Regulatory, integrative and comparative physiology 290:R1262-70

Liang H, Ward WF (2006) PGC-1alpha: a key regulator of energy metabolism. Advances in physiology education 30:145–151

Lindemann A, Riedel D, Oster W, Meuer SC, Blohm D, Mertelsmann RH, Herrmann F (1988) Granulocyte/macrophage colony-stimulating factor induces interleukin 1 production by human polymorphonuclear neutrophils. Journal of immunology (Baltimore, Md. : 1950) 140:837–839

Liu E, Lewis K, Al-Saffar H, Krall CM, Singh A, Kulchitsky VA, Corrigan JJ, Simons CT, Petersen SR, Musteata FM, Bakshi CS, Romanovsky AA, Sellati TJ, Steiner AA (2012) Naturally occurring hypothermia is more advantageous than fever in severe forms of lipopolysaccharide- and Escherichia coli-induced systemic inflammation. American journal of physiology. Regulatory, integrative and comparative physiology 302:R1372-83

Liu M, Shen J, Yuan H, Chen F, Song H, Qin H, Li Y, Xu J, Ye Q, Li S, Saeki K, Yokomizo T (2018) Leukotriene B4 receptor 2 regulates the proliferation, migration, and barrier integrity of bronchial epithelial cells. Journal of cellular physiology 233:6117–6124

Liu SF, Malik AB (2006) NF-kappa B activation as a pathological mechanism of septic shock and inflammation. American journal of physiology. Lung cellular and molecular physiology 290:L622-L645

Liu T, Zhang L, Joo D, Sun S-C (2017) NF-κB signaling in inflammation. Signal transduction and targeted therapy 2

Liu X, Nemeth DP, McKim DB, Zhu L, DiSabato DJ, Berdysz O, Gorantla G, Oliver B, Witcher KG, Wang Y, Negray CE, Vegesna RS, Sheridan JF, Godbout JP, Robson MJ, Blakely RD, Popovich PG, Bilbo SD, Quan N (2019) Cell-Type-Specific Interleukin 1 Receptor 1 Signaling in the Brain Regulates Distinct Neuroimmune Activities. Immunity 50:317-333.e6

Loh KP, Huang SH, Silva R de, Tan BKH, Zhu YZ (2006) Oxidative stress: apoptosis in neuronal injury. Current Alzheimer research 3:327–337

Long NC, Morimoto A, Nakamori T, Murakami N (1992) Systemic injection of TNF-alpha attenuates fever due to IL-1 beta and LPS in rats. The American journal of physiology 263:R987-91

Lowell CA, Berton G (1999) Integrin signal transduction in myeloid leukocytes. Journal of Leukocyte Biology 65:313–320

Lukiw WJ, Cui J-G, Marcheselli VL, Bodker M, Botkjaer A, Gotlinger K, Serhan CN, Bazan NG (2005) A role for docosahexaenoic acid-derived neuroprotectin D1 in neural cell survival and Alzheimer disease. J Clin Invest 115:2774–2783

Luo J, Zhang W-Y, Li H, Zhang P-H, Tian C, Wu C-H, Zhao A-N, Chen M-L, Guo Y-F, Cho Y-C, Jin S-W, Hao Y (2022) Pro-Resolving Mediator Resolvin E1 Restores Alveolar Fluid Clearance in Acute Respiratory Distress Syndrome. Shock 57:565–575

Lv S, Han M, Yi R, Kwon S, Dai C, Wang R (2014) Anti-TNF-α therapy for patients with sepsis: a systematic meta-analysis. International journal of clinical practice 68:520–528

Lyman GH, Abella E, Pettengell R (2014) Risk factors for febrile neutropenia among patients with cancer receiving chemotherapy: A systematic review. Critical reviews in oncology/hematology 90:190–199

Ma L, Zhang H, Yin Y-L, Guo W-Z, Ma Y-Q, Wang Y-B, Shu C, Dong L-Q (2016) Role of interleukin-6 to differentiate sepsis from non-infectious systemic inflammatory response syndrome. Cytokine 88:126–135

Machado NLS, Bandaru SS, Abbott SBG, Saper CB (2020) EP3R-Expressing Glutamatergic Preoptic Neurons Mediate Inflammatory Fever. J. Neurosci. 40:2573–2588

Machado NLS, Saper CB (2022) Genetic identification of preoptic neurons that regulate body temperature in mice. Temperature (Austin, Tex.) 9:14–22

Maddox JF, Hachicha M, Takano T, Petasis NA, Fokin VV, Serhan CN (1997) Lipoxin A4 stable analogs are potent mimetics that stimulate human monocytes and THP-1 cells via a G-protein-linked lipoxin A4 receptor. Journal of Biological Chemistry 272:6972–6978

Madore C, Yin Z, Leibowitz J, Butovsky O (2020) Microglia, Lifestyle Stress, and Neurodegeneration. Immunity 52:222–240

Mallard C (2012) Innate immune regulation by toll-like receptors in the brain. ISRN neurology 2012:701950

Maloney CG, Kutchera WA, Albertine KH, McIntyre TM, Prescott SM, Zimmerman GA (1998) Inflammatory agonists induce cyclooxygenase type 2 expression by human neutrophils. Journal of immunology (Baltimore, Md. : 1950) 160:1402–1410

Manzel LJ, Chin CL, Behlke MA, Look DC (2009) Regulation of bacteria-induced intercellular adhesion molecule-1 by CCAAT/enhancer binding proteins. American journal of respiratory cell and molecular biology 40:200–210

Mao L, Jin H, Wang M, Hu Y, Chen S, He Q, Chang J, Hong C, Zhou Y, Wang D, Miao X, Li Y, Hu B (2020) Neurologic Manifestations of Hospitalized Patients With Coronavirus Disease 2019 in Wuhan, China. JAMA neurology 77:683–690

Mao Y, Bajinka O, Tang Z, Qiu X, Tan Y (2022) Lung-brain axis: Metabolomics and pathological changes in lungs and brain of respiratory syncytial virus-infected mice. Journal of medical virology

Marcheselli VL, Hong S, Lukiw WJ, Tian XH, Gronert K, Musto A, Hardy M, Gimenez JM, Chiang N, Serhan CN, Bazan NG (2003) Novel docosanoids inhibit brain ischemia-reperfusion-mediated leukocyte infiltration and pro-inflammatory gene expression. Journal of Biological Chemistry 278:43807–43817

Marcon R, Bento AF, Dutra RC, Bicca MA, Leite DFP, Calixto JB (2013) Maresin 1, a proresolving lipid mediator derived from omega-3 polyunsaturated fatty acids, exerts protective actions in murine models of colitis. The Journal of Immunology 191:4288–4298

Marfaing-Koka A, Maravic M, Humbert M, Galanaud P, Emilie D (1996) Contrasting effects of IL-4, IL-10 and corticosteroids on RANTES production by human monocytes. Int Immunol 8:1587–1594

Mariani E, Polidori MC, Cherubini A, Mecocci P (2005) Oxidative stress in brain aging, neurodegenerative and vascular diseases: an overview. Journal of chromatography. B, Analytical technologies in the biomedical and life sciences 827:65–75

Marucha PT, Zeff RA, Kreutzer DL (1990) Cytokine regulation of IL-1 beta gene expression in the human polymorphonuclear leukocyte. Journal of immunology (Baltimore, Md. : 1950) 145:2932–2937

Mastroianni CM, Liuzzi GM, Vullo V, Jirillo E, Delia S, Riccio P (1991) Detection of cerebrospinal fluid antibodies against myelin basic protein in patients with AIDS dementia complex. Molecular and chemical neuropathology 14:227–236

Matsuda T, Hori T, Nakashima T (1992) Thermal and PGE2 sensitivity of the organum vasculosum lamina terminalis region and preoptic area in rat brain slices. The Journal of physiology 454:197–212

Matsumura K, Kobayashi S (2004) Signaling the brain in inflammation: the role of endothelial cells. Frontiers in bioscience : a journal and virtual library 9:2819–2826

Matsusaka T, Fujikawa K, Nishio Y, Mukaida N, Matsushima K, Kishimoto T, Akira S (1993) Transcription factors NF-IL6 and NF-kappa B synergistically activate transcription of the inflammatory cytokines, interleukin 6 and interleukin 8. Proc. Natl. Acad. Sci. U.S.A. 90:10193–10197

Matthay MA, Ware LB, Zimmerman GA (2012) The acute respiratory distress syndrome. J Clin Invest 122:2731–2740

Matute-Bello G, Liles WC, Radella F, Steinberg KP, Ruzinski JT, Hudson LD, Martin TR (2000) Modulation of neutrophil apoptosis by granulocyte colony-stimulating factor and granulocyte/macrophage colony-stimulating factor during the course of acute respiratory distress syndrome. Critical Care Medicine 28:1–7

Mayer K, Fegbeutel C, Hattar K, Sibelius U, Krämer H-J, Heuer K-U, Temmesfeld-Wollbrück B, Gokorsch S, Grimminger F, Seeger W (2003) Omega-3 vs. omega-6 lipid emulsions exert differential influence on neutrophils in septic shock patients: impact on plasma fatty acids and lipid mediator generation. Intensive care medicine 29:1472–1481

Mayer K, Kiessling A, Ott J, Schaefer MB, Hecker M, Henneke I, Schulz R, Günther A, Wang J, Wu L, Roth J, Seeger W, Kang JX (2009) Acute lung injury is reduced in fat-1 mice endogenously synthesizing n-3 fatty acids. American journal of respiratory and critical care medicine 179:474–483

McColl BW, Rothwell NJ, Allan SM (2007) Systemic inflammatory stimulus potentiates the acute phase and CXC chemokine responses to experimental stroke and exacerbates brain damage via interleukin-1- and neutrophil-dependent mechanisms. The Journal of neuroscience : the official journal of the Society for Neuroscience 27:4403–4412

McCurdy JD, Lin T-J, Marshall JS (2001) Toll-like receptor 4-mediated activation of murine mast cells. Journal of Leukocyte Biology 70:977–984

McDonald B, Pittman K, Menezes GB, Hirota SA, Slaba I, Waterhouse CCM, Beck PL, Muruve DA, Kubes P (2010) Intravascular danger signals guide neutrophils to sites of sterile inflammation. Science (New York, N.Y.) 330:362–366

McEwen BS, Sapolsky RM (1995) Stress and cognitive function. Current Opinion in Neurobiology 5:205–216

McKim DB, Weber MD, Niraula A, Sawicki CM, Liu X, Jarrett BL, Ramirez-Chan K, Wang Y, Roeth RM, Sucaldito AD, Sobol CG, Quan N, Sheridan JF, Godbout JP (2018) Microglial recruitment of IL-1β-producing monocytes to brain endothelium causes stress-induced anxiety. Molecular psychiatry 23:1421–1431

McKinley MJ, McAllen RM, Davern P, Giles ME, Penschow J, Sunn N, Uschakov A, Oldfield BJ (2003) The sensory circumventricular organs of the mammalian brain. Advances in anatomy, embryology, and cell biology 172:III-XII, 1-122, back cover

Medawar PB (1946) Immunity to homologous grafted skin; the relationship between the antigens of blood and skin. British Journal of Experimental Pathology 27:15–24

Meduri GU, Annane D, Chrousos GP, Marik PE, Sinclair SE (2009) Activation and regulation of systemic inflammation in ARDS: rationale for prolonged glucocorticoid therapy. Chest 136:1631–1643

Medzhitov R, Janeway CA (1997) Innate immunity: impact on the adaptive immune response. Current Opinion in Immunology 9:4–9

Medzhitov R, Preston-Hurlburt P, Janeway CA (1997) A human homologue of the Drosophila Toll protein signals activation of adaptive immunity. Nature 388:394–397

Mehet DK, Philip J, Solito E, Buckingham JC, John CD (2012) Evidence from in vitro and in vivo studies showing that nuclear factor-κB within the pituitary folliculostellate cells and corticotrophs regulates adrenocorticotrophic hormone secretion in experimental endotoxaemia. Journal of neuroendocrinology 24:862–873

Meneses G, Cárdenas G, Espinosa A, Rassy D, Pérez-Osorio IN, Bárcena B, Fleury A, Besedovsky H, Fragoso G, Sciutto E (2019) Sepsis: developing new alternatives to reduce neuroinflammation and attenuate brain injury. Annals of the New York Academy of Sciences 1437:43–56

Metz R, Ziff E (1991) cAMP stimulates the C/EBP-related transcription factor rNFIL-6 to trans-locate to the nucleus and induce c-fos transcription. Genes Dev. 5:1754–1766

Michaud J-P, Hallé M, Lampron A, Thériault P, Préfontaine P, Filali M, Tribout-Jover P, Lanteigne A-M, Jodoin R, Cluff C, Brichard V, Palmantier R, Pilorget A, Larocque D, Rivest S (2013) Toll-like receptor 4 stimulation with the detoxified ligand monophosphoryl lipid A improves Alzheimer's disease-related pathology. Proceedings of the National Academy of Sciences of the United States of America 110:1941–1946

Michels M, Vieira AS, Vuolo F, Zapelini HG, Mendonça B, Mina F, Dominguini D, Steckert A, Schuck PF, Quevedo J, Petronilho F, Dal-Pizzol F (2015) The role of microglia activation in the development of sepsis-induced long-term cognitive impairment. Brain, behavior, and immunity 43:54–59

Mikacenic C, Hansen EE, Radella F, Gharib SA, Stapleton RD, Wurfel MM (2016) Interleukin-17A Is Associated With Alveolar Inflammation and Poor Outcomes in Acute Respiratory Distress Syndrome. Critical Care Medicine 44:496–502

Mina F, Comim CM, Dominguini D, Cassol OJ, Dall Igna DM, Ferreira GK, Silva MC, Galant LS, Streck EL, Quevedo J, Dal-Pizzol F (2014) Il1-β involvement in cognitive impairment after sepsis. Mol Neurobiol 49:1069–1076

Miñano FJ, Tavares E, Maldonado R (2004) Role of endogenous macrophage inflammatory protein-2 in regulating fever induced by bacterial endotoxin in normal and immunosuppressed rats. Clinical and experimental pharmacology & physiology 31:723–731

Mishalian I, Bayuh R, Levy L, Zolotarov L, Michaeli J, Fridlender ZG (2013) Tumor-associated neutrophils (TAN) develop pro-tumorigenic properties during tumor progression. Cancer immunology, immunotherapy : CII 62:1745–1756

Mitroulis I, Kambas K, Anyfanti P, Doumas M, Ritis K (2011a) The multivalent activity of the tissue factor-thrombin pathway in thrombotic and non-thrombotic disorders as a target for therapeutic intervention. Expert opinion on therapeutic targets 15:75–89

Mitroulis I, Kambas K, Chrysanthopoulou A, Skendros P, Apostolidou E, Kourtzelis I, Drosos GI, Boumpas DT, Ritis K (2011b) Neutrophil extracellular trap formation is associated with IL-1β and autophagy-related signaling in gout. PloS one 6:e29318

Miyahara N, Miyahara S, Takeda K, Gelfand EW (2006) Role of the LTB4/BLT1 pathway in allergen-induced airway hyperresponsiveness and inflammation. Allergology international : official journal of the Japanese Society of Allergology 55:91–97

Moldoveanu B, Otmishi P, Jani P, Walker J, Sarmiento X, Guardiola J, Saad M, Yu J (2009) Inflammatory mechanisms in the lung. Journal of inflammation research 2:1–11

Monk JM, Hou TY, Turk HF, Weeks B, Wu C, McMurray DN, Chapkin RS (2012) Dietary n-3 polyunsaturated fatty acids (PUFA) decrease obesity-associated Th17 cell-mediated inflammation during colitis. PLOS ONE 7:e49739

Moore DC (2016) Drug-Induced Neutropenia: A Focus on Rituximab-Induced Late-Onset Neutropenia. Pharmacy and Therapeutics 41:765–768

Moraes CA, Zaverucha-do-Valle C, Fleurance R, Sharshar T, Bozza FA, d'Avila JC (2021) Neuroinflammation in Sepsis: Molecular Pathways of Microglia Activation. Pharmaceuticals (Basel, Switzerland) 14

Moreira PI, Siedlak SL, Aliev G, Zhu X, Cash AD, Smith MA, Perry G (2005) Oxidative stress mechanisms and potential therapeutics in Alzheimer disease. Journal of neural transmission (Vienna, Austria : 1996) 112:921–932

Morrison SF, Nakamura K (2019) Central Mechanisms for Thermoregulation. Annual review of physiology 81:285–308

Motulsky HJ, Brown RE (2006) Detecting outliers when fitting data with nonlinear regression - a new method based on robust nonlinear regression and the false discovery rate. BMC bioinformatics 7:123

Mouihate A, Chen X, Pittman QJ (1998) Interleukin-1beta fever in rats: gender difference and estrous cycle influence. The American journal of physiology 275:R1450-4

Mouihate A, Pittman QJ (2003) Neuroimmune response to endogenous and exogenous pyrogens is differently modulated by sex steroids. Endocrinology 144:2454–2460

Mukherjee PK, Marcheselli VL, Serhan CN, Bazan NG (2004) Neuroprotectin D1: a docosahexaenoic acid-derived docosatriene protects human retinal pigment epithelial cells from oxidative stress. Proc. Natl. Acad. Sci. U.S.A. 101:8491–8496

Mul Fedele ML, Aiello I, Caldart CS, Golombek DA, Marpegan L, Paladino N (2020) Differential Thermoregulatory and Inflammatory Patterns in the Circadian Response to LPS-Induced Septic Shock. Frontiers in Cellular and Infection Microbiology 10:100

Nadeem A, Siddiqui N, Al-Harbi NO, Attia SM, AlSharari SD, Ahmad SF (2017) Acute lung injury leads to depression-like symptoms through upregulation of neutrophilic and neuronal NADPH oxidase signaling in a murine model. International immunopharmacology 47:218–226

Nadjar A, Bluthé R-M, May MJ, Dantzer R, Parnet P (2005) Inactivation of the cerebral NFkappaB pathway inhibits interleukin-1beta-induced sickness behavior and c-Fos expression in various brain nuclei. Neuropsychopharmacology : official publication of the American College of Neuropsychopharmacology 30:1492–1499

Naegele M, Tillack K, Reinhardt S, Schippling S, Martin R, Sospedra M (2012) Neutrophils in multiple sclerosis are characterized by a primed phenotype. Journal of neuroimmunology 242:60–71

Nakamura K (2011) Central circuitries for body temperature regulation and fever. American journal of physiology. Regulatory, integrative and comparative physiology 301:R1207-28

Nandi A, Yan L-J, Jana CK, Das N (2019) Role of Catalase in Oxidative Stress- and Age-Associated Degenerative Diseases. Oxidative medicine and cellular longevity 2019:9613090

Nathan C (2002) Points of control in inflammation. Nature 420:846–852

Natsuka S, Akira S, Nishio Y, Hashimoto S, Sugita T, Isshiki H, Kishimoto T (1992) Macrophage differentiation-specific expression of NF-IL6, a transcription factor for interleukin-6. Blood 79:460–466

Neubert E, Senger-Sander SN, Manzke VS, Busse J, Polo E, Scheidmann SEF, Schön MP, Kruss S, Erpenbeck L (2019) Serum and Serum Albumin Inhibit in vitro Formation of Neutrophil Extracellular Traps (NETs). Front. Immunol. 10:12

Neumann A, Brogden G, Jerjomiceva N, Brodesser S, Naim HY, Köckritz-Blickwede M von (2014) Lipid alterations in human blood-derived neutrophils lead to formation of neutrophil extracellular traps. European Journal of Cell Biology 93:347–354

Neumann FJ, Ott I, Marx N, Luther T, Kenngott S, Gawaz M, Kotzsch M, Schömig A (1997) Effect of human recombinant interleukin-6 and interleukin-8 on monocyte procoagulant activity. Arteriosclerosis, thrombosis, and vascular biology 17:3399–3405

Neumann J, Henneberg S, Kenne S von, Nolte N, Müller AJ, Schraven B, Görtler MW, Reymann KG, Gunzer M, Riek-Burchardt M (2018) Beware the intruder: Real time observation of infiltrated neutrophils and neutrophil-Microglia interaction during stroke in vivo. PLOS ONE 13:e0193970

Nguyen HX, O'Barr TJ, Anderson AJ (2007) Polymorphonuclear leukocytes promote neurotoxicity through release of matrix metalloproteinases, reactive oxygen species, and TNF-alpha. Journal of neurochemistry 102:900–912

Nicholson SE, Souza D de, Fabri LJ, Corbin J, Willson TA, Zhang JG, Silva A, Asimakis M, Farley A, Nash AD, Metcalf D, Hilton DJ, Nicola NA, Baca M (2000) Suppressor of cytokine signaling-3 preferentially binds to the SHP-2-binding site on the shared cytokine receptor subunit gp130. Proceedings of the National Academy of Sciences of the United States of America 97:6493–6498

Niiro H, Otsuka T, Izuhara K, Yamaoka K, Ohshima K, Tanabe T, Hara S, Nemoto Y, Tanaka Y, Nakashima H, Niho Y (1997) Regulation by Interleukin-10 and Interleukin-4 of Cyclooxygenase-2 Expression in Human Neutrophils. Blood 89:1621–1628

Niiro H, Otsuka T, Kuga S, Nemoto Y, Abe M, Hara N, Nakano T, Ogo T, Niho Y (1994) IL-10 inhibits prostaglandin E2 production by lipopolysaccharide-stimulated monocytes. Int Immunol 6:661–664

Norden DM, Trojanowski PJ, Villanueva E, Navarro E, Godbout JP (2016) Sequential activation of microglia and astrocyte cytokine expression precedes increased Iba-1 or GFAP immunoreactivity following systemic immune challenge. Glia 64:300–316

Norris CA, He M, Kang L-I, Ding MQ, Radder JE, Haynes MM, Yang Y, Paranjpe S, Bowen WC, Orr A, Michalopoulos GK, Stolz DB, Mars WM (2014) Synthesis of IL-6 by hepatocytes is a normal response to common hepatic stimuli. PLOS ONE 9:e96053

Nozawa H, Chiu C, Hanahan D (2006) Infiltrating neutrophils mediate the initial angiogenic switch in a mouse model of multistage carcinogenesis. Proc. Natl. Acad. Sci. U.S.A. 103:12493–12498

Obermeyer Z, Samra JK, Mullainathan S (2017) Individual differences in normal body temperature: longitudinal big data analysis of patient records. BMJ (Clinical research ed.) 359:j5468

O'Connor JC, Lawson MA, André C, Moreau M, Lestage J, Castanon N, Kelley KW, Dantzer R (2009) Lipopolysaccharide-induced depressive-like behavior is mediated by indoleamine 2,3-dioxygenase activation in mice. Molecular psychiatry 14:511–522

Oda S, Hirasawa H, Shiga H, Nakanishi K, Matsuda K, Nakamua M (2005) Sequential measurement of IL-6 blood levels in patients with systemic inflammatory response syndrome (SIRS)/sepsis. Cytokine 29:169–175

Ode Y, Aziz M, Wang P (2018) CIRP increases ICAM-1+ phenotype of neutrophils exhibiting elevated iNOS and NETs in sepsis. Journal of Leukocyte Biology 103:693–707

Ogoina D (2011) Fever, fever patterns and diseases called 'fever'--a review. Journal of infection and public health 4:108–124

Oh SF, Pillai PS, Recchiuti A, Yang R, Serhan CN (2011) Pro-resolving actions and stereoselective biosynthesis of 18S E-series resolvins in human leukocytes and murine inflammation. J Clin Invest 121:569–581

Ohira T, Arita M, Omori K, Recchiuti A, van Dyke TE, Serhan CN (2010) Resolvin E1 receptor activation signals phosphorylation and phagocytosis. The Journal of biological chemistry 285:3451–3461

O'Neill GP, Ford-Hutchinson AW (1993) Expression of mRNA for cyclooxygenase-1 and cyclooxygenase-2 in human tissues. FEBS Letters 330:157–160

Opp MR, Krueger JM (1991) Interleukin 1-receptor antagonist blocks interleukin 1-induced sleep and fever. The American journal of physiology 260:R453-7

Ordás MC, Costa MM, Roca FJ, López-Castejón G, Mulero V, Meseguer J, Figueras A, Novoa B (2007) Turbot TNFalpha gene: molecular characterization and biological activity of the recombinant protein. Molecular Immunology 44:389–400

Orhun G, Tüzün E, Özcan PE, Ulusoy C, Yildirim E, Küçükerden M, Gürvit H, Ali A, Esen F (2019) Association Between Inflammatory Markers and Cognitive Outcome in Patients with Acute Brain Dysfunction Due to Sepsis. Noro psikiyatri arsivi 56:63–70

Orihuela R, McPherson CA, Harry GJ (2016) Microglial M1/M2 polarization and metabolic states. British journal of pharmacology 173:649–665

Orr SK, Tong JYM, Kang JX, Ma DWL, Bazinet RP (2010) The fat-1 mouse has brain docosahexaenoic acid levels achievable through fish oil feeding. Neurochemical research 35:811–819

Osaka T (2022) The EP3 and EP4 Receptor Subtypes both Mediate the Fever-producing Effects of Prostaglandin E2 in the Rostral Ventromedial Preoptic Area of the Hypothalamus in Rats. Neuroscience 494:25–37

Osterhout JA, Kapoor V, Eichhorn SW, Vaughn E, Moore JD, Liu D, Lee D, DeNardo LA, Luo L, Zhuang X, Dulac C (2022) A preoptic neuronal population controls fever and appetite during sickness. Nature 606:937–944

Ostermann AI, Waindok P, Schmidt MJ, Chiu C-Y, Smyl C, Rohwer N, Weylandt K-H, Schebb NH (2017) Modulation of the endogenous omega-3 fatty acid and oxylipin profile in vivo-A comparison of the fat-1 transgenic mouse with C57BL/6 wildtype mice on an omega-3 fatty acid enriched diet. PLOS ONE 12:e0184470

Ott D, Murgott J, Rafalzik S, Wuchert F, Schmalenbeck B, Roth J, Gerstberger R (2010) Neurons and glial cells of the rat organum vasculosum laminae terminalis directly respond to lipopolysaccharide and pyrogenic cytokines. Brain Research 1363:93–106

Padgett LE, Broniowska KA, Hansen PA, Corbett JA, Tse HM (2013) The role of reactive oxygen species and proinflammatory cytokines in type 1 diabetes pathogenesis. Annals of the New York Academy of Sciences 1281:16–35

Palmer R, Stepney RJ, Higgs GA, Eakins KE (1980) Chemokinetic activity of arachidonic acid lipoxygenase products on leuocyctes of different species. Prostaglandins 20:411–418

Panopoulos AD, Zhang L, Snow JW, Jones DM, Smith AM, El Kasmi KC, Liu F, Goldsmith MA, Link DC, Murray PJ, Watowich SS (2006) STAT3 governs distinct pathways in emergency granulopoiesis and mature neutrophils. Blood 108:3682–3690

Papayannopoulos V, Metzler KD, Hakkim A, Zychlinsky A (2010) Neutrophil elastase and myeloperoxidase regulate the formation of neutrophil extracellular traps. The Journal of cell biology 191:677–691

Park J, Langmead CJ, Riddy DM (2020) New Advances in Targeting the Resolution of Inflammation: Implications for Specialized Pro-Resolving Mediator GPCR Drug Discovery. ACS pharmacology & translational science 3:88–106

Park JY, Pillinger MH, Abramson SB (2006) Prostaglandin E2 synthesis and secretion: the role of PGE2 synthases. Clinical immunology (Orlando, Fla.) 119:229–240

Parolini S, Santoro A, Marcenaro E, Luini W, Massardi L, Facchetti F, Communi D, Parmentier M, Majorana A, Sironi M, Tabellini G, Moretta A, Sozzani S (2007) The role of chemerin in the colocalization of NK and dendritic cell subsets into inflamed tissues. Blood 109:3625–3632

Parrillo JE (1993) Pathogenetic mechanisms of septic shock. The New England journal of medicine 328:1471–1477

Parsey MV, Tuder RM, Abraham E (1998) Neutrophils are major contributors to intraparenchymal lung IL-1 beta expression after hemorrhage and endotoxemia. J Immunol 160:1007–1013

Parthasarathy U, Kuang Y, Thakur G, Hogan JD, Wyche TP, Norton JE, Killough JR, Sana TR, Beakes C, Shyong B, Zhang RN, Gutierrez DA, Filbin M, Christiani DC, Therien AG, Woelk CH, White CH, Martinelli R (2023) Distinct subsets of neutrophils crosstalk with cytokines and metabolites in patients with sepsis. iScience 26:105948

Pastille E, Didovic S, Brauckmann D, Rani M, Agrawal H, Schade FU, Zhang Y, Flohé SB (2011) Modulation of dendritic cell differentiation in the bone marrow mediates sustained immunosuppression after polymicrobial sepsis. The Journal of Immunology 186:977–986

Paul BZ, Jin J, Kunapuli SP (1999) Molecular mechanism of thromboxane A(2)-induced platelet aggregation. Essential role for p2t(ac) and alpha(2a) receptors. Journal of Biological Chemistry 274:29108–29114

Peek V, Neumann E, Inoue T, Koenig S, Pflieger FJ, Gerstberger R, Roth J, Matsumura K, Rummel C (2020) Age-Dependent Changes of Adipokine and Cytokine Secretion From Rat Adipose Tissue by Endogenous and Exogenous Toll-Like Receptor Agonists. Frontiers in immunology 11:1800

Pelosi P, Rocco PRM (2011) The lung and the brain: a dangerous cross-talk. Crit Care 15:168

Perianayagam MC, Balakrishnan VS, Pereira BJG, Jaber BL (2004) C5a delays apoptosis of human neutrophils via an extracellular signal-regulated kinase and Bad-mediated signalling pathway. European journal of clinical investigation 34:50–56

Perlstein RS (1993) Synergistic roles of interleukin-6, interleukin-1, and tumor necrosis factor in the adrenocorticotropin response to bacterial lipopolysaccharide in vivo. Endocrinology 132:946–952

Perry VH, Cunningham C, Holmes C (2007) Systemic infections and inflammation affect chronic neurodegeneration. Nature reviews. Immunology 7:161–167

Perry VH, Teeling J (2013) Microglia and macrophages of the central nervous system: the contribution of microglia priming and systemic inflammation to chronic neurodegeneration. Seminars in immunopathology 35:601–612

Peters-Golden M, Henderson WR (2007) Leukotrienes. The New England journal of medicine 357:1841–1854

Petrova TV, Akama KT, van Eldik LJ (1999) Selective modulation of BV-2 microglial activation by prostaglandin E(2). Differential effects on endotoxin-stimulated cytokine induction. Journal of Biological Chemistry 274:28823–28827

Pflieger FJ (2021) <Multimodale Analysen von Lipiden, Lipid-Metaboliten und relevanten Enzymen im Gehirn der Maus unter dem Einfluss von omega-3-Fettsäuren während systemischer Entzündung>. Edition Scientifique. VVB Laufersweiler Verlag, Gießen, Lahn

Pflieger FJ, Hernandez J, Schweighöfer H, Herden C, Rosengarten B, Rummel C (2018) The role of neutrophil granulocytes in immune-to-brain communication. Temperature (Austin, Tex.) 5:296–307

Pflieger FJ, Wolf J, Feldotto M, Nockher A, Wenderoth T, Hernandez J, Roth J, Ott D, Rummel C (2022) Norepinephrine Inhibits Lipopolysaccharide-Stimulated TNF-α but Not Oxylipin Induction in n-3/n-6 PUFA-Enriched Cultures of Circumventricular Organs. International journal of molecular sciences 23

Pham CTN (2006) Neutrophil serine proteases: specific regulators of inflammation. Nature reviews. Immunology 6:541–550

Phillipson M, Heit B, Colarusso P, Liu L, Ballantyne CM, Kubes P (2006) Intraluminal crawling of neutrophils to emigration sites: a molecularly distinct process from adhesion in the recruitment cascade. The Journal of experimental medicine 203:2569–2575

Pinteaux E, Rothwell NJ, Boutin H (2006) Neuroprotective actions of endogenous interleukin-1 receptor antagonist (IL-1ra) are mediated by glia. Glia 53:551–556

Pittman K, Kubes P (2013) Damage-associated molecular patterns control neutrophil recruitment. Journal of innate immunity 5:315–323

Pizzo PA (1993) Management of fever in patients with cancer and treatment-induced neutropenia. The New England journal of medicine 328:1323–1332

Plata-Salamán CR, ffrench-Mullen JM (1994) Interleukin-1 beta inhibits Ca2+ channel currents in hippocampal neurons through protein kinase C. European Journal of Pharmacology 266:1–10

Poltorak A, He X, Smirnova I, Liu MY, van Huffel C, Du X, Birdwell D, Alejos E, Silva M, Galanos C, Freudenberg M, Ricciardi-Castagnoli P, Layton B, Beutler B (1998) Defective LPS signaling in C3H/HeJ and C57BL/10ScCr mice: mutations in Tlr4 gene. Science (New York, N.Y.) 282:2085–2088

Powell ND, Sloan EK, Bailey MT, Arevalo JMG, Miller GE, Chen E, Kobor MS, Reader BF, Sheridan JF, Cole SW (2013) Social stress up-regulates inflammatory gene expression in the leukocyte transcriptome via β-adrenergic induction of myelopoiesis. Proceedings of the National Academy of Sciences of the United States of America 110:16574–16579

Prinz M, Priller J (2014) Microglia and brain macrophages in the molecular age: from origin to neuropsychiatric disease. Nature reviews. Neuroscience 15:300–312

Pylaeva E, Lang S, Jablonska J (2016) The Essential Role of Type I Interferons in Differentiation and Activation of Tumor-Associated Neutrophils. Front. Immunol. 7:629

Qin S, Wen J, Bai X-C, Chen T-Y, Zheng R-C, Zhou G-B, Ma J, Feng J-Y, Zhong B-L, Li Y-M (2014) Endogenous n-3 polyunsaturated fatty acids protect against imiquimod-induced psoriasis-like inflammation via the IL-17/IL-23 axis. Molecular medicine reports 9:2097–2104

Quan N, Whiteside M, Herkenham M (1998) Time course and localization patterns of interleukin-1β messenger rna expression in brain and pituitary after peripheral administration of lipopolysaccharide. Neuroscience 83:281–293

Queen MM, Ryan RE, Holzer RG, Keller-Peck CR, Jorcyk CL (2005) Breast cancer cells stimulate neutrophils to produce oncostatin M: potential implications for tumor progression. Cancer research 65:8896–8904

Quinto BMR, Iizuka IJ, Monte JCM, Santos BF, Pereira V, Durão MS, Dalboni MA, Cendoroglo M, Santos OFP, Batista MC (2015) TNF-α depuration is a predictor of mortality in critically ill patients under continuous veno-venous hemodiafiltration treatment. Cytokine 71:255–260

Rambault M, Doz-Deblauwe É, Le Vern Y, Carreras F, Cunha P, Germon P, Rainard P, Winter N, Remot A (2021) Neutrophils Encompass a Regulatory Subset Suppressing T Cells in Apparently Healthy Cattle and Mice. Front. Immunol. 12:625244

Ramji DP, Foka P (2002) CCAAT/enhancer-binding proteins: structure, function and regulation. The Biochemical journal 365:561–575

Redl H, Bahrami S, Schlag G, Traber DL (1993) Clinical detection of LPS and animal models of endotoxemia. Immunobiology 187:330–345

Rees D, Miles EA, Banerjee T, Wells SJ, Roynette CE, Wahle KW, Calder PC (2006) Dose-related effects of eicosapentaenoic acid on innate immune function in healthy humans: a comparison of young and older men. The American journal of clinical nutrition 83:331–342

Reilly JP, Anderson BJ, Hudock KM, Dunn TG, Kazi A, Tommasini A, Charles D, Shashaty MGS, Mikkelsen ME, Christie JD, Meyer NJ (2016) Neutropenic sepsis is associated with distinct clinical and biological characteristics: a cohort study of severe sepsis. Critical care (London, England) 20:222

Remick DG, Bolgos G, Copeland S, Siddiqui J (2005) Role of interleukin-6 in mortality from and physiologic response to sepsis. Infection and Immunity 73:2751–2757

Rett BS, Whelan J (2011) Increasing dietary linoleic acid does not increase tissue arachidonic acid content in adults consuming Western-type diets: a systematic review. Nutrition & metabolism 8:36

Reul JM, Kloet ER de (1985) Two receptor systems for corticosterone in rat brain: microdistribution and differential occupation. Endocrinology 117:2505–2511

Rey C, Nadjar A, Buaud B, Vaysse C, Aubert A, Pallet V, Layé S, Joffre C (2016) Resolvin D1 and E1 promote resolution of inflammation in microglial cells in vitro. Brain, behavior, and immunity 55:249–259

Ricciotti E, FitzGerald GA (2011) Prostaglandins and inflammation. Arteriosclerosis, thrombosis, and vascular biology 31:986–1000

Rinaldo JE, Borovetz H (1985) Deterioration of oxygenation and abnormal lung microvascular permeability during resolution of leukopenia in patients with diffuse lung injury. The American review of respiratory disease 131:579–583

Rola-Pleszczynski M, Lemaire I (1985) Leukotrienes augment interleukin 1 production by human monocytes. Journal of immunology (Baltimore, Md. : 1950) 135:3958–3961

Romanovsky AA (2004) Do fever and anapyrexia exist? Analysis of set point-based definitions. American journal of physiology. Regulatory, integrative and comparative physiology 287:R992-5

Romanovsky AA, Shido O, Sakurada S, Sugimoto N, Nagasaka T (1996) Endotoxin shock: thermoregulatory mechanisms. The American journal of physiology 270:R693-703

Romanovsky AA, Shido O, Sakurada S, Sugimoto N, Nagasaka T (1997) Endotoxin shock-associated hypothermia. How and why does it occur? Annals of the New York Academy of Sciences 813:733–737

Ross G, Roth J, Störr B, Voigt K, Zeisberger E (2000) Afferent nerves are involved in the febrile response to injection of LPS into artificial subcutaneous chambers in guinea pigs. Physiology & Behavior 71:305–313

Roth J, Blatteis CM (2014) Mechanisms of fever production and lysis: lessons from experimental LPS fever. Comprehensive Physiology 4:1563–1604

Roth J, Harré E-M, Rummel C, Gerstberger R, Hübschle T (2004) Signaling the brain in systemic inflammation: role of sensory circumventricular organs. Frontiers in bioscience : a journal and virtual library 9:290–300

Roth J, Souza GE de (2001) Fever induction pathways: evidence from responses to systemic or local cytokine formation. Brazilian journal of medical and biological research = Revista brasileira de pesquisas medicas e biologicas 34:301–314

Rudaya AY, Steiner AA, Robbins JR, Dragic AS, Romanovsky AA (2005) Thermoregulatory responses to lipopolysaccharide in the mouse: dependence on the dose and ambient temperature. American journal of physiology. Regulatory, integrative and comparative physiology 289:R1244-52

Rumbus Z, Garami A (2019) Fever, hypothermia, and mortality in sepsis: Comment on: Rumbus Z, Matics R, Hegyi P, Zsiboras C, Szabo I, Illes A, Petervari E, Balasko M, Marta K, Miko A, Parniczky A, Tenk J, Rostas I, Solymar M, Garami A. Fever is associated with reduced, hypothermia with increased mortality in septic patients: a meta-analysis of clinical trials. PLoS One. 2017;12(1):e0170152. DOI: 10.1371/journal.pone.0170152. Temperature (Austin, Tex.) 6:101–103

Rumbus Z, Matics R, Hegyi P, Zsiboras C, Szabo I, Illes A, Petervari E, Balasko M, Marta K, Miko A, Parniczky A, Tenk J, Rostas I, Solymar M, Garami A (2017) Fever Is Associated with Reduced, Hypothermia with Increased Mortality in Septic Patients: A Meta-Analysis of Clinical Trials. PLOS ONE 12:e0170152

Rummel C (2016) Inflammatory transcription factors as activation markers and functional readouts in immune-to-brain communication. Brain, behavior, and immunity 54:1–14

Rummel C, Del Rey A, Bähr L, Krüger K, Peters E (2022) 1st European Psychoneuroimmunology Network (EPN) Autumn School: Lung-Brain Axis in Health and Disease. Neuroimmunomodulation 29 Suppl 2:3–8

Rummel C, Hübschle T, Gerstberger R, Roth J (2004) Nuclear translocation of the transcription factor STAT3 in the guinea pig brain during systemic or localized inflammation. The Journal of physiology 557:671–687

Rummel C, Inoue W, Poole S, Luheshi GN (2010) Leptin regulates leukocyte recruitment into the brain following systemic LPS-induced inflammation. Molecular psychiatry 15:523–534

Rummel C, Matsumura K, Luheshi GN (2011) Circulating IL-6 contributes to peripheral LPS-induced mPGES-1 expression in the rat brain. Brain Research Bulletin 86:319–325

Rummel C, Sachot C, Poole S, Luheshi GN (2006) Circulating interleukin-6 induces fever through a STAT3-linked activation of COX-2 in the brain. American journal of physiology. Regulatory, integrative and comparative physiology 291:R1316-26

Rummel C, Voss T, Matsumura K, Korte S, Gerstberger R, Roth J, Hübschle T (2005) Nuclear STAT3 translocation in guinea pig and rat brain endothelium during systemic challenge with lipopolysaccharide and interleukin-6. The Journal of comparative neurology 491:1–14

Russell W, Burch RL (1960) The Principles of Humane Experimental Technique. Medical Journal of Australia 1:500

Saadoun S, Waters P, MacDonald C, Bell BA, Vincent A, Verkman AS, Papadopoulos MC (2012) Neutrophil protease inhibition reduces neuromyelitis optica-immunoglobulin G-induced damage in mouse brain. Annals of neurology 71:323–333

Saeki K, Yokomizo T (2017) Identification, signaling, and functions of LTB4 receptors. Seminars in immunology 33:30–36

Sagiv JY, Voels S, Granot Z (2016) Isolation and Characterization of Low- vs. High-Density Neutrophils in Cancer. Methods in molecular biology (Clifton, N.J.) 1458:179–193

Sahu B, Sandhir R, Naura AS (2018) Two hit induced acute lung injury impairs cognitive function in mice: A potential model to study cross talk between lung and brain. Brain, behavior, and immunity 73:633–642

Saito H, Sherwood ER, Varma TK, Evers BM (2003) Effects of aging on mortality, hypothermia, and cytokine induction in mice with endotoxemia or sepsis. Mechanisms of ageing and development 124:1047–1058

Sakamoto Y, Koike K, Kiyama H, Konishi K, Watanabe K, Tsurufuji S, Bicknell R, Hirota K, Miyake A (1996) A stress-sensitive chemokinergic neuronal pathway in the hypothalamo-pituitary system. Neuroscience 75:133–142

Salomao R, Brunialti MKC, Rapozo MM, Baggio-Zappia GL, Galanos C, Freudenberg M (2012) Bacterial sensing, cell signaling, and modulation of the immune response during sepsis. Shock 38:227–242

Samson M, Edinger AL, Stordeur P, Rucker J, Verhasselt V, Sharron M, Govaerts C, Mollereau C, Vassart G, Doms RW, Parmentier M (1998a) ChemR23, a putative chemoattractant receptor, is expressed in monocyte-derived dendritic cells and macrophages and is a coreceptor for SIV and some primary HIV-1 strains. Eur. J. Immunol. 28:1689–1700

Samson M, Edinger AL, Stordeur P, Rucker J, Verhasselt V, Sharron M, Govaerts C, Mollereau C, Vassart G, Doms RW, Parmentier M (1998b) ChemR23, a putative chemoattractant receptor, is expressed in monocyte-derived dendritic cells and macrophages and is a coreceptor for SIV and some primary HIV-1 strains. Eur. J. Immunol. 28:1689–1700

Saper CB, Breder CD (1994) The neurologic basis of fever. The New England journal of medicine 330:1880–1886

Sapolsky R, Rivier C, Yamamoto G, Plotsky P, Vale W (1987) Interleukin-1 stimulates the secretion of hypothalamic corticotropin-releasing factor. Science (New York, N.Y.) 238:522–524

Sauter C, Wolfensberger C (1980) INTERFERON IN HUMAN SERUM AFTER INJECTION OF ENDOTOXIN. The Lancet 316:852–853

Savill JS, Wyllie AH, Henson JE, Walport MJ, Henson PM, Haslett C (1989) Macrophage phagocytosis of aging neutrophils in inflammation. Programmed cell death in the neutrophil leads to its recognition by macrophages. The Journal of clinical investigation 83:865–875

Sawada A, Niiyama Y, Ataka K, Nagaishi K, Yamakage M, Fujimiya M (2014) Suppression of bone marrow-derived microglia in the amygdala improves anxiety-like behavior induced by chronic partial sciatic nerve ligation in mice. Pain 155:1762–1772

Sawant KV, Xu R, Cox R, Hawkins H, Sbrana E, Kolli D, Garofalo RP, Rajarathnam K (2015) Chemokine CXCL1-Mediated Neutrophil Trafficking in the Lung: Role of CXCR2 Activation. Journal of innate immunity 7:647–658

Scammell TE, Elmquist JK, Griffin JD, Saper CB (1996a) Ventromedial Preoptic Prostaglandin E2 Activates Fever-Producing Autonomic Pathways. J. Neurosci. 16:6246–6254

Scammell TE, Elmquist JK, Saper CB (1996b) Inhibition of nitric oxide synthase produces hypothermia and depresses lipopolysaccharide fever. The American journal of physiology 271:R333-8

Schaefer MB, Ott J, Mohr A, Bi MH, Grosz A, Weissmann N, Ishii S, Grimminger F, Seeger W, Mayer K (2007) Immunomodulation by n-3- versus n-6-rich lipid emulsions in murine acute lung injury--role of platelet-activating factor receptor. Critical Care Medicine 35:544–554

Schebb NH, Kühn H, Kahnt AS, Rund KM, O'Donnell VB, Flamand N, Peters-Golden M, Jakobsson P-J, Weylandt KH, Rohwer N, Murphy RC, Geisslinger G, FitzGerald GA, Hanson J, Dahlgren C, Alnouri MW, Offermanns S, Steinhilber D (2022) Formation, Signaling and Occurrence of Specialized Pro-Resolving Lipid Mediators-What is the Evidence so far? Frontiers in pharmacology 13:838782

Schiel X, Hebart H, Kern WV, Kiehl MG, Sölch JP, Wilhelm S, Ostermann H (2003) Sepsis in neutropenia--guidelines of the Infectious Diseases Working Party (AGIHO) of the German Society of Hematology and Oncology (DGHO). Annals of hematology 82 Suppl 2:S158-66

Schif-Zuck S, Gross N, Assi S, Rostoker R, Serhan CN, Ariel A (2011) Saturated-efferocytosis generates pro-resolving CD11b low macrophages: modulation by resolvins and glucocorticoids. European journal of immunology 41:366–379

Schiltz JC, Sawchenko PE (2003) Signaling the brain in systemic inflammation: the role of perivascular cells. Frontiers in bioscience : a journal and virtual library 8:s1321-9

Schindler R, Mancilla J, Endres S, Ghorbani R, Clark SC, Dinarello CA (1990) Correlations and interactions in the production of interleukin-6 (IL- 6), IL-1, and tumor necrosis factor (TNF) in human blood mononuclear cells: IL-6 suppresses IL-1 and TNF. Blood 75:40–47

Schlegel N, Leweke R, Meir M, Germer C-T, Waschke J (2012) Role of NF-κB activation in LPS-induced endothelial barrier breakdown. Histochemistry and cell biology 138:627–641

Schneiders J, Fuchs F, Damm J, Herden C, Gerstberger R, Soares DM, Roth J, Rummel C (2015) The transcription factor nuclear factor interleukin 6 mediates pro- and anti-inflammatory responses during LPS-induced systemic inflammation in mice. Brain, behavior, and immunity 48:147–164

Schöbitz B, Kloet ER de, Holsboer F (1994) Gene expression and function of interleukin 1, interleukin 6 and tumor necrosis factor in the brain. Progress in neurobiology 44:397–432

Schönbohn H, Schuler M, Kolbe K, Peschel C, Huber C, Bemb W, Aulitzky WE (1995) Plasma levels of IL-1, TNF alpha, IL-6, IL-8, G-CSF, and IL1-RA during febrile neutropenia: results of a prospective study in patients undergoing chemotherapy for acute myelogenous leukemia. Annals of hematology 71:161–168

Schröder AK, Ohe M von der, Kolling U, Altstaedt J, Uciechowski P, Fleischer D, Dalhoff K, Ju X, Zenke M, Heussen N, Rink L (2006) Polymorphonuclear leucocytes selectively produce anti-inflammatory interleukin-1 receptor antagonist and chemokines, but fail to produce pro-inflammatory mediators. Immunology 119:317–327

Schulte D, Küppers V, Dartsch N, Broermann A, Li H, Zarbock A, Kamenyeva O, Kiefer F, Khandoga A, Massberg S, Vestweber D (2011) Stabilizing the VE-cadherin-catenin complex blocks leukocyte extravasation and vascular permeability. The EMBO Journal 30:4157–4170

Schweighöfer H, Rummel C, Roth J, Rosengarten B (2016) Modulatory effects of vagal stimulation on neurophysiological parameters and the cellular immune response in the rat brain during systemic inflammation. Intensive care medicine experimental 4:19

Seckinger P, Williamson K, Balavoine JF, Mach B, Mazzei G, Shaw A, Dayer JM (1987) A urine inhibitor of interleukin 1 activity affects both interleukin 1 alpha and 1 beta but not tumor necrosis factor alpha. J Immunol 139:1541–1545

Seki H, Fukunaga K, Arita M, Arai H, Nakanishi H, Taguchi R, Miyasho T, Takamiya R, Asano K, Ishizaka A, Takeda J, Levy BD (2010) The anti-inflammatory and proresolving mediator resolvin E1 protects mice from bacterial pneumonia and acute lung injury. The Journal of Immunology 184:836–843

Semmler A, Hermann S, Mormann F, Weberpals M, Paxian SA, Okulla T, Schäfers M, Kummer MP, Klockgether T, Heneka MT (2008) Sepsis causes neuroinflammation and concomitant decrease of cerebral metabolism. J Neuroinflammation 5:38

Serhan CN (2005) Lipoxins and aspirin-triggered 15-epi-lipoxins are the first lipid mediators of endogenous anti-inflammation and resolution. Prostaglandins, Leukotrienes and Essential Fatty Acids 73:141–162

Serhan CN (2014) Pro-resolving lipid mediators are leads for resolution physiology. Nature 510:92–101

Serhan CN (2017) Treating inflammation and infection in the 21st century: new hints from decoding resolution mediators and mechanisms. FASEB journal : official publication of the Federation of American Societies for Experimental Biology 31:1273–1288

Serhan CN, Brain SD, Buckley CD, Gilroy DW, Haslett C, O'Neill LAJ, Perretti M, Rossi AG, Wallace JL (2007) Resolution of inflammation: state of the art, definitions and terms. FASEB journal : official publication of the Federation of American Societies for Experimental Biology 21:325–332

Serhan CN, Chiang N, Dalli J (2015) The resolution code of acute inflammation: Novel pro-resolving lipid mediators in resolution. Seminars in immunology 27:200–215

Serhan CN, Chiang N, Dalli J, Levy BD (2014) Lipid mediators in the resolution of inflammation. Cold Spring Harbor perspectives in biology 7:a016311

Serhan CN, Clish CB, Brannon J, Colgan SP, Chiang N, Gronert K (2000) Novel functional sets of lipid-derived mediators with antiinflammatory actions generated from omega-3 fatty acids via cyclooxygenase 2-nonsteroidal antiinflammatory drugs and transcellular processing. J Exp Med 192:1197–1204

Serhan CN, Dalli J, Karamnov S, Choi A, Park C-K, Xu Z-Z, Ji R-R, Zhu M, Petasis NA (2012) Macrophage proresolving mediator maresin 1 stimulates tissue regeneration and controls pain. The FASEB Journal 26:1755–1765

Serhan CN, Hong S, Gronert K, Colgan SP, Devchand PR, Mirick G, Moussignac R-L (2002) Resolvins: a family of bioactive products of omega-3 fatty acid transformation circuits initiated by aspirin treatment that counter proinflammation signals. J Exp Med 196:1025–1037

Serhan CN, Libreros S, Nshimiyimana R (2022) E-series resolvin metabolome, biosynthesis and critical role of stereochemistry of specialized pro-resolving mediators (SPMs) in inflammation-resolution: Preparing SPMs for long COVID-19, human clinical trials, and targeted precision nutrition. Seminars in immunology:101597

Serhan CN, Yang R, Martinod K, Kasuga K, Pillai PS, Porter TF, Oh SF, Spite M (2009) Maresins: novel macrophage mediators with potent antiinflammatory and proresolving actions. The Journal of experimental medicine 206:15–23

Serrats J, Grigoleit J-S, Alvarez-Salas E, Sawchenko PE (2017) Pro-inflammatory immune-to-brain signaling is involved in neuroendocrine responses to acute emotional stress. Brain, behavior, and immunity 62:53–63

Serrats J, Schiltz JC, García-Bueno B, van Rooijen N, Reyes TM, Sawchenko PE (2010) Dual roles for perivascular macrophages in immune-to-brain signaling. Neuron 65:94–106

Sfeir T, Saha DC, Astiz M, Rackow EC (2001) Role of interleukin-10 in monocyte hyporesponsiveness associated with septic shock. Critical Care Medicine 29:129–133

Sha'afi RI, Naccache PH, Molski TF, Borgeat P, Goetzl EJ (1981) Cellular regulatory role of leukotriene B4: its effects on cation homeostasis in rabbit neutrophils. Journal of cellular physiology 108:401–408

Sharshar T, Carlier R, Bernard F, Guidoux C, Brouland J-P, Nardi O, La Grandmaison GL de, Aboab J, Gray F, Menon D, Annane D (2007) Brain lesions in septic shock: a magnetic resonance imaging study. Intensive care medicine 33:798–806

Sheehan M, Wong HR, Hake PW, Zingarelli B (2003) Parthenolide improves systemic hemodynamics and decreases tissue leukosequestration in rats with polymicrobial sepsis. Critical Care Medicine 31:2263–2270

Shemer A, Scheyltjens I, Frumer GR, Kim J-S, Grozovski J, Ayanaw S, Dassa B, van Hove H, Chappell-Maor L, Boura-Halfon S, Leshkowitz D, Mueller W, Maggio N, Movahedi K, Jung S (2020) Interleukin-10 Prevents Pathological Microglia Hyperactivation following Peripheral Endotoxin Challenge. Immunity 53:1033-1049.e7

Sheng JA, Bales NJ, Myers SA, Bautista AI, Roueinfar M, Hale TM, Handa RJ (2020) The Hypothalamic-Pituitary-Adrenal Axis: Development, Programming Actions of Hormones, and Maternal-Fetal Interactions. Frontiers in behavioral neuroscience 14:601939

Sherwood ER, Burelbach KR, McBride MA, Stothers CL, Owen AM, Hernandez A, Patil NK, Williams DL, Bohannon JK (2022) Innate Immune Memory and the Host Response to Infection. The Journal of Immunology 208:785–792

Shih R-H, Wang C-Y, Yang C-M (2015) NF-kappaB Signaling Pathways in Neurological Inflammation: A Mini Review. Frontiers in molecular neuroscience 8:77

Shimada H, Moriwaki Y, Kurosawa H, Kubota T, Endo I, Togo S, Yamaoka H (1998) Inflammatory mediator and organ dysfunction syndrome. Nihon Geka Gakkai zasshi 99:490–496

Shimazu R, Akashi S, Ogata H, Nagai Y, Fukudome K, Miyake K, Kimoto M (1999) MD-2, a molecule that confers lipopolysaccharide responsiveness on Toll-like receptor 4. J Exp Med 189:1777–1782

Shokry AA, El-Shiekh RA, Kamel G, Bakr AF, Ramadan A (2022) Bioactive phenolics fraction of Hedera helix L. (Common Ivy Leaf) standardized extract ameliorates LPS-induced acute lung injury in the mouse model through the inhibition of proinflammatory cytokines and oxidative stress. Heliyon 8:e09477

SILVERMAN MN, PEARCE BD, Biron CA, MILLER AH (2005) Immune modulation of the hypothalamic-pituitary-adrenal (HPA) axis during viral infection. Viral immunology 18:41–78

Simm B, Ott D, Pollatzek E, Murgott J, Gerstberger R, Rummel C, Roth J (2016) Effects of prostaglandin E2 on cells cultured from the rat organum vasculosum laminae terminalis and median preoptic nucleus. Neuroscience 313:23–35

Singh RK, Liao W, Tracey-White D, Recchi C, Tolmachova T, Rankin SM, Hume AN, Seabra MC (2012) Rab27a-mediated protease release regulates neutrophil recruitment by allowing uropod detachment. Journal of cell science 125:1652–1656

Soares DM, Machado RR, Yamashiro LH, Melo MCC, Souza GEP (2008) Cytokine-induced neutrophil chemoattractant (CINC)-1 induces fever by a prostaglandin-dependent mechanism in rats. Brain Research 1233:79–88

Song J, Park DW, Moon S, Cho H-J, Park JH, Seok H, Choi WS (2019) Diagnostic and prognostic value of interleukin-6, pentraxin 3, and procalcitonin levels among sepsis and septic shock patients: a prospective controlled study according to the Sepsis-3 definitions. BMC infectious diseases 19:968

Souza ALT de, Batalhão ME, Cárnio EC (2020) Study of thermo-regulation as a worsening marker of experimental sepsis in an animal model. Revista latino-americana de enfermagem 28:e3290

Spencer SJ, Mouihate A, Pittman QJ (2007) Peripheral inflammation exacerbates damage after global ischemia independently of temperature and acute brain inflammation. Stroke 38:1570–1577

Sperling RI, Weinblatt M, Robin JL, Ravalese J, Hoover RL, House F, Coblyn JS, Fraser PA, Spur BW, Robinson DR (1987) Effects of dietary supplementation with marine fish oil on leukocyte lipid mediator generation and function in rheumatoid arthritis. Arthritis and rheumatism 30:988–997

Spite M, Norling LV, Summers L, Yang R, Cooper D, Petasis NA, Flower RJ, Perretti M, Serhan CN (2009) Resolvin D2 is a potent regulator of leukocytes and controls microbial sepsis. Nature 461:1287–1291

Spittler A, Razenberger M, Kupper H, Kaul M, Hackl W, Boltz-Nitulescu G, Függer R, Roth E (2000) Relationship between interleukin-6 plasma concentration in patients with sepsis, monocyte phenotype, monocyte phagocytic properties, and cytokine production. Clinical infectious diseases : an official publication of the Infectious Diseases Society of America 31:1338–1342

Spychalla JP, Kinney AJ, Browse J (1997) Identification of an animal omega-3 fatty acid desaturase by heterologous expression in Arabidopsis. Proc. Natl. Acad. Sci. U.S.A. 94:1142–1147

Steensberg A, Fischer CP, Keller C, Møller K, Pedersen BK (2003) IL-6 enhances plasma IL-1ra, IL-10, and cortisol in humans. American journal of physiology. Endocrinology and metabolism 285:E433-7

Steinberg KP, Milberg JA, Martin TR, Maunder RJ, Cockrill BA, Hudson LD (1994) Evolution of bronchoalveolar cell populations in the adult respiratory distress syndrome. American journal of respiratory and critical care medicine 150:113–122

Steiner AA, Dogan MD, Ivanov AI, Patel S, Rudaya AY, Jennings DH, Orchinik M, Pace TWW, O'connor KA, Watkins LR, Romanovsky AA (2004) A new function of the leptin receptor: mediation of the recovery from lipopolysaccharide-induced hypothermia. The FASEB Journal 18:1949–1951

Steiner AA, Hunter JC, Phipps SM, Nucci TB, Oliveira DL, Roberts JL, Scheck AC, Simmons DL, Romanovsky AA (2009) Cyclooxygenase-1 or -2--which one mediates lipopolysaccharide-induced hypothermia? American journal of physiology. Regulatory, integrative and comparative physiology 297:R485-94

Steiner AA, Ivanov AI, Serrats J, Hosokawa H, Phayre AN, Robbins JR, Roberts JL, Kobayashi S, Matsumura K, Sawchenko PE, Romanovsky AA (2006) Cellular and molecular bases of the initiation of fever. PLoS Biology 4:e284

Stephens KE, Ishizaka A, Larrick JW, Raffin TA (1988) Tumor necrosis factor causes increased pulmonary permeability and edema. Comparison to septic acute lung injury. The American review of respiratory disease 137:1364–1370

Stephens MAC, Wand G (2012) Stress and the HPA axis: role of glucocorticoids in alcohol dependence. Alcohol Research : Current Reviews 34:468–483

Stitt JT (1991) Differential sensitivity in the sites of fever production by prostaglandin E1 within the hypothalamus of the rat. The Journal of physiology 432:99–110

Stock JL, Shinjo K, Burkhardt J, Roach M, Taniguchi K, Ishikawa T, Kim HS, Flannery PJ, Coffman TM, McNeish JD, Audoly LP (2001) The prostaglandin E2 EP1 receptor mediates pain perception and regulates blood pressure. The Journal of clinical investigation 107:325–331

Stoolman JS, Duncker PC, Huber AK, Segal BM (2014) Site-specific chemokine expression regulates central nervous system inflammation and determines clinical phenotype in autoimmune encephalomyelitis. The Journal of Immunology 193:564–570

Strle K, Zhou JH, Broussard SR, Venters HD, Johnson RW, Freund GG, Dantzer R, Kelley KW (2002) IL-10 promotes survival of microglia without activating Akt. Journal of neuroimmunology 122:9–19

Sugimoto MA, Vago JP, Perretti M, Teixeira MM (2019) Mediators of the Resolution of the Inflammatory Response. Trends in immunology 40:212–227

Sun Y-P, Oh SF, Uddin J, Yang R, Gotlinger K, Campbell E, Colgan SP, Petasis NA, Serhan CN (2007) Resolvin D1 and its aspirin-triggered 17R epimer. Stereochemical assignments, anti-inflammatory properties, and enzymatic inactivation. Journal of Biological Chemistry 282:9323–9334

Svensson CI, Zattoni M, Serhan CN (2007) Lipoxins and aspirin-triggered lipoxin inhibit inflammatory pain processing. J Exp Med 204:245–252

Szabó K (1983) The vascular architecture of the developing organum vasculosum of the lamina terminalis (OVLT) in the rat. Cell Tissue Res 233:579–592

Tager AM, Dufour JH, Goodarzi K, Bercury SD, Andrian UH von, Luster AD (2000) BLTR mediates leukotriene B(4)-induced chemotaxis and adhesion and plays a dominant role in eosinophil accumulation in a murine model of peritonitis. J Exp Med 192:439–446

Tak PP, Firestein GS (2001) NF-kappaB: a key role in inflammatory diseases. J Clin Invest 107:7–11

Takai E, Tsukimoto M, Kojima S (2013) TGF-β1 downregulates COX-2 expression leading to decrease of PGE2 production in human lung cancer A549 cells, which is involved in fibrotic response to TGF-β1. PLOS ONE 8:e76346

Takano T, Clish CB, Gronert K, Petasis N, Serhan CN (1998) Neutrophil-mediated changes in vascular permeability are inhibited by topical application of aspirin-triggered 15-epi-lipoxin A4 and novel lipoxin B4 stable analogues. J Clin Invest 101:819–826

Takayasu S, Iwasaki Y, Nigawara T, Asai M, Yoshida M, Kageyama K, Suda T (2010) Involvement of nuclear factor-kB and Nurr-1 in cytokine-induced transcription of proopiomelanocortin gene in AtT20 corticotroph cells. Neuroimmunomodulation 17:88–96

Takeda K, Akira S (2000) STAT family of transcription factors in cytokine-mediated biological responses. Cytokine & growth factor reviews 11:199–207

Takei H, Araki A, Watanabe H, Ichinose A, Sendo F (1996) Rapid killing of human neutrophils by the potent activator phorbol 12-myristate 13-acetate (PMA) accompanied by changes different from typical apoptosis or necrosis. Journal of Leukocyte Biology 59:229–240

Tamassia N, Calzetti F, Menestrina N, Rossato M, Bazzoni F, Gottin L, Cassatella MA (2008) Circulating neutrophils of septic patients constitutively express IL-10R1 and are promptly responsive to IL-10. Int Immunol 20:535–541

Tan JC, Indelicato SR, Narula SK, Zavodny PJ, Chou CC (1993) Characterization of interleukin-10 receptors on human and mouse cells. Journal of Biological Chemistry 268:21053–21059

Tang BMP, McLean AS, Dawes IW, Huang SJ, Lin RCY (2007) The use of gene-expression profiling to identify candidate genes in human sepsis. American journal of respiratory and critical care medicine 176:676–684

Tang P, Hung M-C, Klostergaard J (1996) Human pro-tumor necrosis factor is a homotrimer. Biochemistry 35:8216–8225

Tartaglia LA, Ayres T, Wong GH, Goeddel DV (1993) A novel domain within the 55 kd TNF receptor signals cell death. Cell 74:845–853

Tasker JG, Dudek FE (1991) Electrophysiological properties of neurones in the region of the paraventricular nucleus in slices of rat hypothalamus. The Journal of physiology 434:271–293

Thomas RC, Bath MF, Stover CM, Lambert DG, Thompson JP (2014) Exploring LPS-induced sepsis in rats and mice as a model to study potential protective effects of the nociceptin/orphanin FQ system. Peptides 61:56–60

Thomson CA, McColl A, Graham GJ, Cavanagh J (2020) Sustained exposure to systemic endotoxin triggers chemokine induction in the brain followed by a rapid influx of leukocytes. J Neuroinflammation 17:94

Thornberry NA, Bull HG, Calaycay JR, Chapman KT, Howard AD, Kostura MJ, Miller DK, Molineaux SM, Weidner JR, Aunins J (1992) A novel heterodimeric cysteine protease is required for interleukin-1 beta processing in monocytes. Nature 356:768–774

Tiesset H, Pierre M, Desseyn J-L, Guéry B, Beermann C, Galabert C, Gottrand F, Husson M-O (2009) Dietary (n-3) polyunsaturated fatty acids affect the kinetics of pro- and antiinflammatory responses in mice with Pseudomonas aeruginosa lung infection. The Journal of nutrition 139:82–89

Tilley SL, Coffman TM, Koller BH (2001) Mixed messages: modulation of inflammation and immune responses by prostaglandins and thromboxanes. The Journal of clinical investigation 108:15–23

To Y, Dohi M, Matsumoto K, Tanaka R, Sato A, Nakagome K, Nakamura T, Yamamoto K (2002) A two-way interaction between hepatocyte growth factor and interleukin-6 in tissue invasion of lung cancer cell line. American journal of respiratory cell and molecular biology 27:220–226

Töllner B, Roth J, Störr B, Martin D, Voigt K, Zeisberger E (2000) The role of tumor necrosis factor (TNF) in the febrile and metabolic responses of rats to intraperitoneal injection of a high dose of lipopolysaccharide. Pflugers Archiv : European journal of physiology 440:925–932

Too LK, Mitchell AJ, McGregor IS, Hunt NH (2016) Antibody-induced neutrophil depletion prior to the onset of pneumococcal meningitis influences long-term neurological complications in mice. Brain, behavior, and immunity 56:68–83

Tou JS (1986) Acylation of docosahexaenoic acid into phospholipids by intact human neutrophils. Lipids 21:324–327

Trebble TM, Wootton SA, Miles EA, Mullee M, Arden NK, Ballinger AB, Stroud MA, Burdge GC, Calder PC (2003) Prostaglandin E2 production and T cell function after fish-oil supplementation: response to antioxidant cosupplementation. The American journal of clinical nutrition 78:376–382

Triantafilou M, Brandenburg K, Kusumoto S, Fukase K, Mackie A, Seydel U, Triantafilou K (2004) Combinational clustering of receptors following stimulation by bacterial products determines lipopolysaccharide responses. The Biochemical journal 381:527–536

Trivedi SG, Newson J, Rajakariar R, Jacques TS, Hannon R, Kanaoka Y, Eguchi N, Colville-Nash P, Gilroy DW (2006) Essential role for hematopoietic prostaglandin D2 synthase in the control of delayed type hypersensitivity. Proc. Natl. Acad. Sci. U.S.A. 103:5179–5184

Tsao N, Hsu HP, Wu CM, Liu CC, Lei HY (2001) Tumour necrosis factor-alpha causes an increase in blood-brain barrier permeability during sepsis. Journal of Medical Microbiology 50:812–821

Uddin MA, Akhter MS, Kubra K-T, Barabutis N (2022) Hsp90 inhibition protects brain endothelial cells against LPS-induced injury. BioFactors (Oxford, England) 48:926–933

Ueda T, Fukunaga K, Seki H, Miyata J, Arita M, Miyasho T, Obata T, Asano K, Betsuyaku T, Takeda J (2014) Combination therapy of 15-epi-lipoxin A4 with antibiotics protects mice from Escherichia coli-induced sepsis*. Critical Care Medicine 42:e288-95

Uematsu S, Matsumoto M, Takeda K, Akira S (2002) Lipopolysaccharide-dependent prostaglandin E(2) production is regulated by the glutathione-dependent prostaglandin E(2) synthase gene induced by the Toll-like receptor 4/MyD88/NF-IL6 pathway. Journal of immunology (Baltimore, Md. : 1950) 168:5811–5816

Ulevitch RJ, Tobias PS (1995) Receptor-dependent mechanisms of cell stimulation by bacterial endotoxin. Annual review of immunology 13:437–457

Ulich TR, Yin SM, Guo KZ, del Castillo J, Eisenberg SP, Thompson RC (1991) The intratracheal administration of endotoxin and cytokines. III. The interleukin-1 (IL-1) receptor antagonist inhibits endotoxin- and IL-1-induced acute inflammation. The American Journal of Pathology 138:521–524

Unoda K, Doi Y, Nakajima H, Yamane K, Hosokawa T, Ishida S, Kimura F, Hanafusa T (2013) Eicosapentaenoic acid (EPA) induces peroxisome proliferator-activated receptors and ameliorates experimental autoimmune encephalomyelitis. Journal of neuroimmunology 256:7–12

Ushikubi F, Segi E, Sugimoto Y, Murata T, Matsuoka T, Kobayashi T, Hizaki H, Tuboi K, Katsuyama M, Ichikawa A, Tanaka T, Yoshida N, Narumiya S (1998) Impaired febrile response in mice lacking the prostaglandin E receptor subtype EP3. Nature 395:281–284

Valle A, Giamporcaro GM, Scavini M, Stabilini A, Grogan P, Bianconi E, Sebastiani G, Masini M, Maugeri N, Porretti L, Bonfanti R, Meschi F, Pellegrin M de, Lesma A, Rossini S, Piemonti L, Marchetti P, Dotta F, Bosi E, Battaglia M (2013) Reduction of circulating neutrophils precedes and accompanies type 1 diabetes. Diabetes 62:2072–2077

Vallières L, Rivest S (1997) Regulation of the genes encoding interleukin-6, its receptor, and gp130 in the rat brain in response to the immune activator lipopolysaccharide and the proinflammatory cytokine interleukin-1beta. Journal of neurochemistry 69:1668–1683

van Looveren K, Timmermans S, Vanderhaeghen T, Wallaeys C, Ballegeer M, Souffriau J, Eggermont M, Vandewalle J, van Wyngene L, Bosscher K de, Libert C (2020) Glucocorticoids limit lipopolysaccharide-induced lethal inflammation by a double control system. EMBO reports 21:e49762

van 't Veer C, van den Pangaart PS, van Zoelen MAD, Kruif M de, Birjmohun RS, Stroes ES, Vos AF de, van der Poll T (2007) Induction of IRAK-M is associated with lipopolysaccharide tolerance in a human endotoxemia model. J Immunol 179:7110–7120

van Vught LA, Wiewel MA, Hoogendijk AJ, Frencken JF, Scicluna BP, Klein Klouwenberg PMC, Zwinderman AH, Lutter R, Horn J, Schultz MJ, Bonten MMJ, Cremer OL, van der Poll T (2017) The Host Response in Patients with Sepsis Developing Intensive Care Unit-acquired Secondary Infections. American journal of respiratory and critical care medicine 196:458–470

Vane JR (1971) Inhibition of prostaglandin synthesis as a mechanism of action for aspirin-like drugs. Nature: New biology 231:232–235

Vänskä M, Koivula I, Jantunen E, Hämäläinen S, Purhonen A-K, Pulkki K, Juutilainen A (2012) IL-10 combined with procalcitonin improves early prediction of complications of febrile neutropenia in hematological patients. Cytokine 60:787–792

Verma IM, Stevenson JK, Schwarz EM, van Antwerp D, Miyamoto S (1995) Rel/NF-kappa B/I kappa B family: intimate tales of association and dissociation. Genes Dev. 9:2723–2735

Vermeij J-D, Aslami H, Fluiter K, Roelofs JJ, van den Bergh WM, Juffermans NP, Schultz MJ, van der Sluijs K, van de Beek D, van Westerloo DJ (2013) Traumatic brain injury in rats induces lung injury and systemic immune suppression. Journal of neurotrauma 30:2073–2079

Verreck FAW, Boer T de, Langenberg DML, Hoeve MA, Kramer M, Vaisberg E, Kastelein R, Kolk A, Waal-Malefyt R de, Ottenhoff THM (2004) Human IL-23-producing type 1 macrophages promote but IL-10-producing type 2 macrophages subvert immunity to (myco)bacteria. Proceedings of the National Academy of Sciences of the United States of America 101:4560–4565

Vichaya EG, Malik S, Sominsky L, Ford BG, Spencer SJ, Dantzer R (2020) Microglia depletion fails to abrogate inflammation-induced sickness in mice and rats. J Neuroinflammation 17:172

Villapol S (2018) Roles of Peroxisome Proliferator-Activated Receptor Gamma on Brain and Peripheral Inflammation. Cellular and molecular neurobiology 38:121–132

Villar J, Slutsky AS (1993) Effects of induced hypothermia in patients with septic adult respiratory distress syndrome. Resuscitation 26:183–192

Voirin A-C, Perek N, Roche F (2020) Inflammatory stress induced by a combination of cytokines (IL-6, IL-17, TNF-α) leads to a loss of integrity on bEnd.3 endothelial cells in vitro BBB model. Brain Research 1730:146647

Waage A, Halstensen A, Shalaby R, Brandtzaeg P, Kierulf P, Espevik T (1989) Local production of tumor necrosis factor alpha, interleukin 1, and interleukin 6 in meningococcal meningitis. Relation to the inflammatory response. J Exp Med 170:1859–1867

Wajant H, Scheurich P (2011) TNFR1-induced activation of the classical NF-κB pathway. The FEBS journal 278:862–876

Walker AK, Budac DP, Bisulco S, Lee AW, Smith RA, Beenders B, Kelley KW, Dantzer R (2013) NMDA receptor blockade by ketamine abrogates lipopolysaccharide-induced depressive-like behavior in C57BL/6J mice. Neuropsychopharmacology : official publication of the American College of Neuropsychopharmacology 38:1609–1616

Walker J, Dichter E, Lacorte G, Kerner D, Spur B, Rodriguez A, Yin K (2011) Lipoxin a4 increases survival by decreasing systemic inflammation and bacterial load in sepsis. Shock (Augusta, Ga.) 36:410–416

Wang G, Huang W, Wang S, Wang J, Cui W, Zhang W, Lou A, Geng S, Li X (2021a) Macrophagic Extracellular Vesicle CXCL2 Recruits and Activates the Neutrophil CXCR2/PKC/NOX4 Axis in Sepsis. The Journal of Immunology 207:2118–2128

Wang H, Hong L-J, Huang J-Y, Jiang Q, Tao R-R, Tan C, Lu N-N, Wang C-K, Ahmed MM, Lu Y-M, Liu Z-R, Shi W-X, Lai E-Y, Wilcox CS, Han F (2015a) P2RX7 sensitizes Mac-1/ICAM-1-dependent leukocyte-endothelial adhesion and promotes neurovascular injury during septic encephalopathy. Cell research 25:674–690

Wang X, Zhu M, Hjorth E, Cortés-Toro V, Eyjolfsdottir H, Graff C, Nennesmo I, Palmblad J, Eriksdotter M, Sambamurti K, Fitzgerald JM, Serhan CN, Granholm A-C, Schultzberg M (2015b) Resolution of inflammation is altered in Alzheimer's disease. Alzheimer's & dementia : the journal of the Alzheimer's Association 11:40-50.e1-2

Wang Y, Jin S, Sonobe Y, Cheng Y, Horiuchi H, Parajuli B, Kawanokuchi J, Mizuno T, Takeuchi H, Suzumura A (2014a) Interleukin-1β induces blood-brain barrier disruption by downregulating Sonic hedgehog in astrocytes. PLOS ONE 9:e110024

Wang Y, Xiao Y, Zhong L, Ye D, Zhang J, Tu Y, Bornstein SR, Zhou Z, Lam KSL, Xu A (2014b) Increased neutrophil elastase and proteinase 3 and augmented NETosis are closely associated with β-cell autoimmunity in patients with type 1 diabetes. Diabetes 63:4239–4248

Wang Y, Yu P, Li Y, Zhao Z, Wu X, Zhang L, Feng J, Hong J-S (2021b) Early-Released Interleukin-10 Significantly Inhibits Lipopolysaccharide-Elicited Neuroinflammation In Vitro. Cells 10

Wanner IB, Anderson MA, Song B, Levine J, Fernandez A, Gray-Thompson Z, Ao Y, Sofroniew MV (2013) Glial scar borders are formed by newly proliferated, elongated astrocytes that interact to corral inflammatory and fibrotic cells via STAT3-dependent mechanisms after spinal cord injury. J. Neurosci. 33:12870–12886

Ware LB, Matthay MA (2000) The acute respiratory distress syndrome. The New England journal of medicine 342:1334–1349

Watanabe S, Kanada S, Takenaka M, Hamazaki T (2004) Dietary n-3 fatty acids selectively attenuate LPS-induced behavioral depression in mice. Physiology & Behavior 81:605–613

Watkins LR, Maier SF, Goehler LE (1995) Cytokine-to-brain communication: A review & analysis of alternative mechanisms. Life Sciences 57:1011–1026

Wedgwood JF, Hatam L, Bonagura VR (1988) Effect of interferon-γ and tumor necrosis factor on the expression of class I and class II major histocompatibility molecules by cultured human umbilical vein endothelial cells. Cellular Immunology 111:1–9

Weissman C (1990) The metabolic response to stress: an overview and update. Anesthesiology 73:308–327

Weissmann G, Smolen JE, Korchak HM (1980) Release of inflammatory mediators from stimulated neutrophils. The New England journal of medicine 303:27–34

Welch DR, Schissel DJ, Howrey RP, Aeed PA (1989) Tumor-elicited polymorphonuclear cells, in contrast to "normal" circulating polymorphonuclear cells, stimulate invasive and metastatic potentials of rat mammary adenocarcinoma cells. Proc. Natl. Acad. Sci. U.S.A. 86:5859–5863

Wiersinga WJ, Leopold SJ, Cranendonk DR, van der Poll T (2014) Host innate immune responses to sepsis. Virulence 5:36–44

Wilhelms DB, Kirilov M, Mirrasekhian E, Eskilsson A, Kugelberg UÖ, Klar C, Ridder DA, Herschman HR, Schwaninger M, Blomqvist A, Engblom D (2014) Deletion of prostaglandin E2 synthesizing enzymes in brain endothelial cells attenuates inflammatory fever. J. Neurosci. 34:11684–11690

Williams AE, José RJ, Mercer PF, Brealey D, Parekh D, Thickett DR, O'Kane C, McAuley DF, Chambers RC (2017) Evidence for chemokine synergy during neutrophil migration in ARDS. Thorax 72:66–73

Williams CS, DuBois RN (1996) Prostaglandin endoperoxide synthase: why two isoforms? The American journal of physiology 270:G393-400

Wislez M, Rabbe N, Marchal J, Milleron B, Crestani B, Mayaud C, Antoine M, Soler P, Cadranel J (2003) Hepatocyte growth factor production by neutrophils infiltrating bronchioloalveolar subtype pulmonary adenocarcinoma: role in tumor progression and death. Cancer research 63:1405–1412

Wohleb ES, Powell ND, Godbout JP, Sheridan JF (2013) Stress-induced recruitment of bone marrow-derived monocytes to the brain promotes anxiety-like behavior. J. Neurosci. 33:13820–13833

Wolburg H, Wolburg-Buchholz K, Engelhardt B (2005) Diapedesis of mononuclear cells across cerebral venules during experimental autoimmune encephalomyelitis leaves tight junctions intact. Acta neuropathologica 109:181–190

Woo C-H, You H-J, Cho S-H, Eom Y-W, Chun J-S, Yoo Y-J, Kim J-H (2002) Leukotriene B(4) stimulates Rac-ERK cascade to generate reactive oxygen species that mediates chemotaxis. Journal of Biological Chemistry 277:8572–8578

Wright HL, Moots RJ, Bucknall RC, Edwards SW (2010) Neutrophil function in inflammation and inflammatory diseases. Rheumatology 49:1618–1631

Wu H-P, Chen C-K, Chung K, Tseng J-C, Hua C-C, Liu Y-C, Chuang D-Y, Yang C-H (2009) Serial cytokine levels in patients with severe sepsis. Inflamm. Res. 58:385–393

Wu Z, Puigserver P, Andersson U, Zhang C, Adelmant G, Mootha V, Troy A, Cinti S, Lowell B, Scarpulla RC, Spiegelman BM (1999) Mechanisms controlling mitochondrial biogenesis and respiration through the thermogenic coactivator PGC-1. Cell 98:115–124

Wunderlich CA WWB (1871) On the temperature in diseases: a manual of medical thermometry. 2nd. edn. London: New Sydenham Society

Wung BS, Ni CW, Wang DL (2005) ICAM-1 induction by TNFalpha and IL-6 is mediated by distinct pathways via Rac in endothelial cells. Journal of biomedical science 12:91–101

Xie Z, Wei M, Morgan TE, Fabrizio P, Han D, Finch CE, Longo VD (2002) Peroxynitrite mediates neurotoxicity of amyloid beta-peptide1-42- and lipopolysaccharide-activated microglia. J. Neurosci. 22:3484–3492

Xu S, Lu J, Shao A, Zhang JH, Zhang J (2020) Glial Cells: Role of the Immune Response in Ischemic Stroke. Frontiers in immunology 11:294

Yan X, Yang K, Xiao Q, Hou R, Pan X, Zhu X (2022) Central role of microglia in sepsis-associated encephalopathy: From mechanism to therapy. Front. Immunol. 13:929316

Yao C, Sakata D, Esaki Y, Li Y, Matsuoka T, Kuroiwa K, Sugimoto Y, Narumiya S (2009) Prostaglandin E2-EP4 signaling promotes immune inflammation through Th1 cell differentiation and Th17 cell expansion. Nature medicine 15:633–640

Yaqoob P, Pala HS, Cortina-Borja M, Newsholme EA, Calder PC (2000) Encapsulated fish oil enriched in alpha-tocopherol alters plasma phospholipid and mononuclear cell fatty acid compositions but not mononuclear cell functions. European journal of clinical investigation 30:260–274

Ye P, Garvey PB, Zhang P, Nelson S, Bagby G, Summer WR, Schwarzenberger P, Shellito JE, Kolls JK (2001) Interleukin-17 and lung host defense against Klebsiella pneumoniae infection. American journal of respiratory cell and molecular biology 25:335–340

Yi L, Weng T, Nie P, Zhu L, Gao M, Jia H, Yang S, Li X, Zhang L, Xu Y, Ma P, Hu M (2022) Overexpression of interleukin-10 in engineered macrophages protects endothelial cells against LPS-induced injury in vitro. FEBS open bio 12:605–615

Yin F, Xi Y-L, Wang Y, Li B-R, Qian J, Ren H, Zhang J, Tang H-Z, Ning B-T (2021) The clinical outcomes and biomarker features of severe sepsis/septic shock with severe neutropenia: a retrospective cohort study. Translational Pediatrics 10:464–473

Yokomizo T, Izumi T, Chang K, Takuwa Y, Shimizu T (1997) A G-protein-coupled receptor for leukotriene B4 that mediates chemotaxis. Nature 387:620–624

Younus H (2018) Therapeutic potentials of superoxide dismutase. International journal of health sciences 12:88–93

Yousefi S, Mihalache C, Kozlowski E, Schmid I, Simon HU (2009) Viable neutrophils release mitochondrial DNA to form neutrophil extracellular traps. Cell Death Differ 16:1438–1444

Yu CL, Meyer DJ, Campbell GS, Larner AC, Carter-Su C, Schwartz J, Jove R (1995) Enhanced DNA-binding activity of a Stat3-related protein in cells transformed by the Src oncoprotein. Science (New York, N.Y.) 269:81–83

Yu Q, Li Y, Wang H, Xiong H (2019) TSLP induces a proinflammatory phenotype in circulating innate cells and predicts prognosis in sepsis patients. FEBS open bio 9:2137–2148

Yuan JS, Reed A, Chen F, Stewart CN (2006) Statistical analysis of real-time PCR data. BMC bioinformatics 7:85

Zabel U, Baeuerle PA (1990) Purified human IκB can rapidly dissociate the complex of the NF-κB transcription factor with its cognate DNA. Cell 61:255–265

Zabel U, Henkel T, Silva MS, Baeuerle PA (1993) Nuclear uptake control of NF-kappa B by MAD-3, an I kappa B protein present in the nucleus. The EMBO Journal 12:201–211

Zarković M, Ignjatović S, Dajak M, Cirić J, Beleslin B, Savić S, Stojković M, Bulat P, Trbojević B (2008) Cortisol response to ACTH stimulation correlates with blood interleukin 6 concentration in healthy humans. European journal of endocrinology 159:649–652

Zenaro E, Pietronigro E, Della Bianca V, Piacentino G, Marongiu L, Budui S, Turano E, Rossi B, Angiari S, Dusi S, Montresor A, Carlucci T, Nanì S, Tosadori G, Calciano L, Catalucci D, Berton G, Bonetti B, Constantin G (2015) Neutrophils promote Alzheimer's disease-like pathology and cognitive decline via LFA-1 integrin. Nat Med 21:880–886

Zhang F, Sha J, Wood TG, Galindo CL, Garner HR, Burkart MF, Suarez G, Sierra JC, Agar SL, Peterson JW, Chopra AK (2008) Alteration in the activation state of new inflammation-associated targets by phospholipase A2-activating protein (PLAA). Cellular signalling 20:844–861

Zhang J, Liu L, Zhang Y, Yuan Y, Miao Z, Lu K, Zhang X, Ni R, Zhang H, Zhao Y, Wang X (2022) ChemR23 signaling ameliorates cognitive impairments in diabetic mice via dampening oxidative stress and NLRP3 inflammasome activation. Redox biology 58:102554

Zhang R, Wang J (2018) HuR stabilizes TFAM mRNA in an ATM/p38-dependent manner in ionizing irradiated cancer cells. Cancer science 109:2446–2457

Zhang T, Tian X, Wang Q, Tong Y, Wang H, Li Z, Li L, Zhou T, Zhan R, Zhao L, Sun Y, Fan D, Lu L, Zhang J, Jin Y, Xiao W, Guo X, Chui D (2015) Surgical stress induced depressive and anxiety like behavior are improved by dapsone via modulating NADPH oxidase level. Neuroscience letters 585:103–108

Zhang Y, Rom WN (1993) Regulation of the interleukin-1 beta (IL-1 beta) gene by mycobacterial components and lipopolysaccharide is mediated by two nuclear factor-IL6 motifs. Molecular and cellular biology 13:3831–3837

Zhang Y, Xu N, Ding Y, Zhang Y, Li Q, Flores J, Haghighiabyaneh M, Doycheva D, Tang J, Zhang JH (2018) Chemerin suppresses neuroinflammation and improves neurological recovery via CaMKK2/AMPK/Nrf2 pathway after germinal matrix hemorrhage in neonatal rats. Brain, behavior, and immunity 70:179–193

Zhou H, Andonegui G, Wong CHY, Kubes P (2009) Role of endothelial TLR4 for neutrophil recruitment into central nervous system microvessels in systemic inflammation. The Journal of Immunology 183:5244–5250

Zhu C-L, Xie J, Liu Q, Wang Y, Li H-R, Yu C-M, Li P, Deng X-M, Bian J-J, Wang J-F (2023) PD-L1 promotes GSDMD-mediated NET release by maintaining the transcriptional activity of Stat3 in sepsis-associated encephalopathy. International journal of biological sciences 19:1413–1429

Zrzavy T, Höftberger R, Berger T, Rauschka H, Butovsky O, Weiner H, Lassmann H (2019) Pro-inflammatory activation of microglia in the brain of patients with sepsis. Neuropathology and applied neurobiology 45:278–290

IX. Appendix

9.1 Supplementary information

Supplementary Table 1: Mice used for myeloperoxidase staining after LPS-induced severe systemic inflammation

Group	Dose (ml/kg)	Structure	Mice (n)	Sections (#)
NRS	1	OVLT	a	2
			b	1
			c	2
		SFO	a	-
			b	6
			c	4
		PVN	a	6
			b	5
			c	4
		Plexus	a	11
			b	3
			c	6
	2	OVLT	a	5
			b	5
		SFO	a	2
			b	7
		PVN	a	3
			b	1
		Plexus	a	1
			b	11

PMN	1	OVLT	a	3
			b	3
			c	1
		SFO	a	11
			b	12
			c	-
		PVN	a	6
			b	6
			c	7
		Plexus	a	-
			b	-
			c	11
	2	OVLT	a	3
			b	5
			c	5
		SFO	a	3
			b	8
			c	3
		PVN	a	7
			b	8
			c	7
		Plexus	a	6
			b	1
			c	1

Supplementary Table 2: Norm mice used for myeloperoxidase staining after LPS-induced ARDS

Group	Time (h)	Structure	Mice (n)	Sections (#)
WT-Norm	0	OVLT	a	5
			b	3
			c	2
		BIF	a	4
			b	2
			c	2
	4	OVLT	a	10
			b	1
		BIF	a	5
			b	4
	24	OVLT	a	-
			b	3
			c	3
			d	3
		BIF	a	6
			b	1
			c	4
			d	9
	72	OVLT	a	-
			b	2
			c	1
			d	4
		BIF	a	7
			b	2
			c	13
			d	2
	120	OVLT	a	1
			b	4
			c	2
		BIF	a	1
			b	6
			c	4

Fat-Norm	0	OVLT	a	3
			b	-
			c	-
			d	5
			e	2
		BIF	a	6
			b	3
			c	2
			d	10
			e	4
	4	OVLT	a	2
			b	5
			c	8
			d	6
			e	6
		BIF	a	2
			b	5
			c	7
			d	9
			e	7
	24	OVLT	a	5
			b	4
			c	1
			d	4
			e	4
		BIF	a	8
			b	6
			c	1
			d	6
			e	8
	72	OVLT	a	4
			b	5
			c	4
			d	3
			e	1
			f	-
		BIF	a	8
			b	5
			c	8
			d	6
			e	6
			f	1
	120	OVLT	a	3
			b	1
			c	5
			d	-
			e	2
		BIF	a	7
			b	6
			c	7
			d	12
			e	2

Supplementary Table 3: CR KO mice used for myeloperoxidase staining after LPS-induced ARDS

Group	Time (h)	Structure	Mice (n)	Sections (#)
WT-CR KO	0	OVLT	a	3
			b	4
			c	1
		BIF	a	4
			b	4
			c	6
	4	OVLT	a	4
			b	4
			c	3
		BIF	a	5
			b	4
			c	6
	24	OVLT	a	2
			b	2
			c	4
			d	2
		BIF	a	4
			b	2
			c	5
			d	5
	72	OVLT	a	4
			b	2
			c	2
			d	4
		BIF	a	5
			b	2
			c	3
			d	5
	120	OVLT	a	5
			b	4
			c	2
		BIF	a	5
			b	4
			c	4

Fat-CR KO	0	OVLT	a	4
			b	4
			c	5
		BIF	a	4
			b	5
			c	6
	4	OVLT	a	4
			b	5
			c	3
		BIF	a	4
			b	5
			c	6
	24	OVLT	a	3
			b	3
			c	1
			d	2
		BIF	a	4
			b	2
			c	2
			d	4
	72	OVLT	a	2
			b	3
			c	2
			d	-
		BIF	a	4
			b	5
			c	2
			d	5
	120	OVLT	a	1
			b	5
		BIF	a	4
			b	6

Supplementary Table 4: LR KO mice used for myeloperoxidase staining after LPS-induced ARDS

Group	Time (h)	Structure	Mice (n)	Sections (#)
WT-LR KO	0	OVLT	a	2
			b	3
			c	2
		BIF	a	4
			b	4
			c	2
	4	OVLT	a	3
			b	3
			c	3
			d	1
		BIF	a	3
			b	3
			c	3
			d	1
	24	OVLT	a	3
			b	3
			c	3
			d	3
			e	1
		BIF	a	3
			b	4
			c	3
			d	3
			e	1
	72	OVLT	a	3
			b	4
			c	2
			d	2
			e	1
		BIF	a	4
			b	3
			c	3
			d	3
			e	1
	120	OVLT	a	2
			b	5
			c	5
			d	-
		BIF	a	2
			b	6
			c	5
			d	3

Fat-LR KO	0	OVLT	a	3
			b	5
			c	3
		BIF	a	4
			b	5
			c	3
	4	OVLT	a	3
			b	3
			c	4
		BIF	a	3
			b	3
			c	4
	24	OVLT	a	3
			b	3
			c	2
			d	5
		BIF	a	3
			b	3
			c	3
			d	7
	72	OVLT	a	6
			b	3
			c	-
			d	3
		BIF	a	6
			b	3
			c	1
			d	3
	120	OVLT	a	1
			b	3
			c	2
			d	2
		BIF	a	1
			b	3
			c	2
			d	2

Supplementary Table 5: Norm mice used for NF-IL6 staining after LPS-induced ARDS

Group	Time (h)	Structure	Mice (n)	Sections (#)
WT-Norm	0	OVLT	a	3
			b	3
			c	1
		BIF	a	3
			b	2
			c	1
	4	OVLT	a	-
			b	7
		BIF	a	3
			b	3
	24	OVLT	a	4
			b	3
			c	3
			d	1
		BIF	a	3
			b	3
			c	2
			d	4
	72	OVLT	a	5
			b	1
			c	6
			d	1
		BIF	a	3
			b	4
			c	2
			d	7
	120	OVLT	a	3
			b	4
			c	4
			d	2
		BIF	a	2
			b	4
			c	6
			d	4

Fat-Norm	0	OVLT	a	4
			b	-
			c	1
			d	2
			e	2
		BIF	a	5
			b	1
			c	1
			d	2
			e	5
	4	OVLT	a	1
			b	5
			c	5
			d	2
			e	2
		BIF	a	-
			b	6
			c	4
			d	2
			e	4
	24	OVLT	a	3
			b	2
			c	1
			d	3
			e	3
		BIF	a	2
			b	2
			c	-
			d	2
			e	6
	72	OVLT	a	3
			b	1
			c	2
			d	1
			e	1
		BIF	a	4
			b	7
			c	2
			d	2
			e	-
	120	OVLT	a	2
			b	-
			c	2
			d	2
		BIF	a	4
			b	8
			c	1
			d	2

Supplementary Table 6: CR KO mice used for NF-IL6 staining after LPS-induced ARDS

Group	Time (h)	Structure	Mice (n)	Sections (#)
WT-CR KO	0	OVLT	a	1
			b	3
			c	1
		BIF	a	2
			b	2
			c	5
	4	OVLT	a	5
			b	2
			c	2
		BIF	a	4
			b	2
			c	5
	24	OVLT	a	2
			b	2
			c	2
			d	2
		BIF	a	2
			b	5
			c	2
			d	2
	72	OVLT	a	4
			b	2
			c	1
			d	4
		BIF	a	4
			b	2
			c	3
			d	5
	120	OVLT	a	4
			b	-
			c	2
		BIF	a	3
			b	2
			c	4

Fat-CR KO	0	OVLT	a	3
			b	3
			c	5
		BIF	a	2
			b	3
			c	5
	4	OVLT	a	4
			b	3
			c	2
		BIF	a	2
			b	3
			c	6
	24	OVLT	a	4
			b	2
			c	1
			d	2
		BIF	a	3
			b	1
			c	2
			d	3
	72	OVLT	a	2
			b	-
			c	2
			d	3
		BIF	a	2
			b	2
			c	2
			d	5
	120	OVLT	a	1
			b	3
		BIF	a	2
			b	4

Supplementary Table 7: LR KO mice used for NF-IL6 staining after LPS-induced ARDS

Group	Time (h)	Structure	Mice (n)	Sections (#)
WT-LR KO	0	OVLT	a	3
			b	4
			c	2
		BIF	a	4
			b	4
			c	2
	4	OVLT	a	3
			b	3
			c	3
		BIF	a	3
			b	3
			c	3
	24	OVLT	a	3
			b	3
			c	3
		BIF	a	3
			b	4
			c	3
	72	OVLT	a	3
			b	4
			c	2
		BIF	a	3
			b	3
			c	3
	120	OVLT	a	-
			b	4
			c	3
			d	2
		BIF	a	3
			b	3
			c	3
			d	2

Fat-LR KO	0	OVLT	a	3
			b	3
			c	2
		BIF	a	3
			b	3
			c	2
	4	OVLT	a	3
			b	3
			c	3
		BIF	a	3
			b	3
			c	3
	24	OVLT	a	3
			b	3
			c	1
			d	3
		BIF	a	3
			b	3
			c	2
			d	4
	72	OVLT	a	3
			b	3
			c	3
		BIF	a	3
			b	3
			c	3
	120	OVLT	a	2
			b	3
			c	2
		BIF	a	2
			b	3
			c	2

Supplementary Table 8: Main effects of locomotor activity

	Main effects	
Time p.i. (h)	**PMN**	**LPS**
1		<0.0001
2	0.0076	0.0383
3	0.0116	<0.0001
4-6		<0.0001
6-8		<0.0001
8-10		<0.0001
10-12		<0.0001
12-14		<0.0001
14-16		<0.0001
16-18		<0.0001
18-20		<0.0001
20-22		<0.0001
22-24		

Supplementary Table 9: Main effects of food and water intake

	Main effects- Food		Main effects- Water	
Time p.i. (h)	**PMN**	**LPS**	**PMN**	**LPS**
1		0.0145		0.0020
2		0.0126		0.0370
3		0.0075		<0.0001
4-6		0.0174		0.0085
6-8		0.0083		<0.0001
8-10		0.0004		<0.0001
10-12		<0.0001		<0.0001
12-14	0.0014	<0.0001		<0.0001
14-16		0.0002		<0.0001
16-18		<0.0001		<0.0001
18-20		<0.0001		<0.0001
20-22		0.0077		<0.0001
22-24		0.0151		0.0322

Supplementary Table 10: Interactions and main effects of core body temperature

	Interactions				Main effects	
Time p.i. (h)	**NRS+PBS vs. NRS+LPS**	**PMN+PBS vs. PMN+LPS**	**NRS+PBS vs. PMN+PBS**	**NRS+LPS vs. PMN+LPS**	**PMN**	**LPS**
1						0.0030
2						<0.0001
3						
4-6						
6-8	0.0184	<0.0001		0.0053	0.0033	<0.0001
8-10					0.0022	<0.0001
10-12	<0.0001	<0.0001		0.0054	0.0080	<0.0001
12-14	<0.0001	<0.0001		0.0038	0.0087	<0.0001
14-16	<0.0001	<0.0001		0.0017	0.0150	<0.0001
16-18	<0.0001	<0.0001		0.0022	0.0055	<0.0001
18-20	<0.0001	<0.0001		0.0009	0.0009	<0.0001
20-22	0.0007	<0.0001		<0.0001	0.0017	<0.0001
22-24		<0.0001		<0.0001	<0.0001	<0.0001

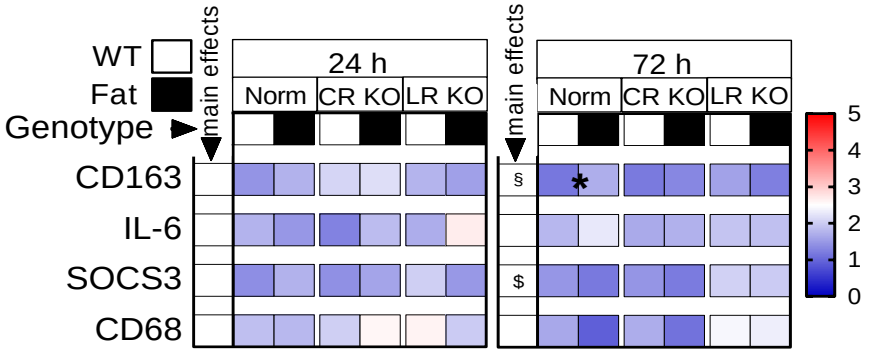

Supplementary Figure 1: Changes in hypothalamic inflammatory mediator mRNA expression following intratracheal LPS-induced ARDS

The hypothalamus was analyzed for expression of markers for macrophage: CD163; cytokine: interleukin (IL)6; signaling pathway: suppressor of cytokine signaling (SOCS)3; and microglia activation: CD68. Mice deficient in chemerin receptor 23 (CR KO) or leukotriene B4 receptor (LR KO) as well as unmodified mice (Norm) were bred on a wild-type (WT) or transgenic ω-3 PUFA synthesizing *fat-1* (Fat) background received an intratracheal (i.t.) instillation with lipopolysaccharide (LPS, 10µg) and were sacrificed at 24 h or 72 h p.i. Preliminary analysis at 24 h and 72 h p.i. showed minor impacts of ω-3 PUFAs and the RvE1 receptors CR and LR at 72 h p.i. but only for CD163 and SOCS3. The average relative expression for each sample set is presented as a value on a heat map. n = 5 per group for all groups except for 72 h WT-Norm (n = 4). Main effect of receptor: $ Norm vs. LR KO. Main effects of n-3 PUFAs: § Norm vs. CR KO. *p<0.05.

9.2 Publications list

9.2.1 Original works in specialized journals

Doctoral studies

- Hernandez J., Schäffer J., Herden C., Pflieger F.J., Reiche S., Körber S., Kitagawa H., Welter J., Michels S., Culmsee C., Bier J., Sommer N., Kang J.X., Mayer K., Hecker M., and Rummel C. (2023). **n-3 polyunsaturated fatty acids modulate LPS-induced ARDS and the lung-brain axis of communication in wild-type versus fat-1 mice genetically modified for leukotriene B4 receptor 1 or chemerin receptor 23 knockout.** Int. J. Mol. Sci. 2023 Aug 31; 24(17), 13524.

- Pflieger F.J., Wolf J., Feldotto M., Nockher A., Wenderoth T., Hernandez J., Roth J., Ott D., and Rummel C. (2022). **Norepinephrine inhibits lipopolysaccharide-stimulated TNF-α but not oxylipin induction in n-3 / n-6 PUFA enriched cultures of circumventricular organs.** Int. J. Mol. Sci:. 2022 Aug 6;23(15):8745.

- Pflieger F.J., Hernandez J., Schweighöfer H., Herden C., Rosengarten B., Rummel C. (2018). **The role of neutrophil granulocytes in immune-to-brain communication.** Temperature (Austin). Nov 1;5(4):296-307.

Masters studies

- Hernandez J., Volland A., Leyshon B.J., Juda M., Ridlon J.M., Johnson R.W., Steelman A.J. (2018). **Effect of imidacloprid ingestion on immune responses to porcine reproductive and respiratory syndrome virus.** Sci. Rep. Aug 2;8(1):11615.

- Blackmore S., Hernandez J., Juda M., Ryder E., Freund G.G., Johnson R.W., and Steelman A.J. (2017). **Influenza infection triggers disease in a genetic model of experimental autoimmune encephalomyelitis.** Proc. Natl. Acad. Sci. USA. Jul 25;114(30):E6107-E6116.

- Klaren R.E., Stasula U., Steelman A.J., Hernandez J., Pence B.D., Woods J.A., Motl R.W. (2016). **Effects of exercise in a relapsing-remitting model of experimental autoimmune encephalomyelitis.** J. Neurosci. Res. Oct;94(10):907-14.

9.2.2 Published abstracts

- Hernandez J., Schäffer J., Herden C., Pflieger F.J., Reiche S., Kitagawa H., Welter J., Culmsee C., Bier J., Sommer N., Kang J.X., Mayer K., Hecker M., and Rummel C. (2023). **n-3 fatty acids modulate LPS-induced ARDS and the lung-brain axis of communication in wild type versus Fat-1 mice genetically modified for leukotriene B4 Receptor 1 or chemerin receptor 23 knock-out.** Brain Behav Immun. *Delayed publication, due in 2024.*

- Hernandez J., Schäffer J., Herden C., Pflieger F.J., Kitagawa H., Welter J., Culmsee C., Sommer N., Hecker M., Mayer K., and Rummel C. (2022). **n-3 fatty acids modulate LPS-induced local lung inflammation and the lung-brain axis in wild type versus Fat-1 mice genetically modified for leukotriene B4 receptor 1 or chemerin receptor 23 knock-out.** Neuroimmunomodulation (2022) 29 (Suppl. 2):17.

- Pflieger F.J., Garikapati V., Bhandari D.R., Bredehöft J., Peek V., Roeb E., Roderfeld M., Hernandez J., Schulz S., Culmsee C., Layé S., Mayer K., Roth J., Spengler B., Rummel C. (2021). **Combined lipidomics in a multimodal pathway analysis revealed Alterations of brain lipid mediator metabolism during the progression of LPS-induced systemic inflammation in wild type and fat-1 mice.** Brain Behav Immun 98 (Suppl.): s22.

- Hernandez J., Pflieger F.J., Schneiders J., Krüger K., Reichel T., and Rummel C. (2021). **Neutropenic mice experience exaggerated hypothermia and brain / peripheral inflammatory responses during LPS-induced systemic inflammation.** Brain Behav Immun 98 (Suppl.).

- Hernandez J., Kitagawa H., Pflieger F., Herden C., Mayer K., and Rummel C. (2019). **The role of neutrophil granulocytes in immune-to-brain**

communication during LPS-induced systemic versus lung inflammation. Brain Behav Immun 81 (Suppl.): s8.

9.2.3 Other conference contributions

- Feldotto M.*, Ott D., Culmsee C., Hernandez J., Slayo M., Spencer S.J., and Rummel C. (2023). **Deciphering neuroprotective effects of n-3 polyunsaturated fatty acids and related impacts of adipokines using organotypic hippocampal slice cultures and primary neuroglial cell cultures.** German-Endochrine-Brain-Immune-Network Conference. Talk*.

- Bähr L.*, Hernandez J., Feldotto M., Marks D., Roth J., and Rummel C. (2023). **Psychological or inflammatory stimulation in mice: investigating how neutropenia affects heart rate variability as a readout parameter.** German-Endochrine-Brain-Immune-Network Conference. Talk*.

- Schaeffer J.*, Hernandez J., Herden C., Pflieger F.J., Reiche S., Kitagawa H., Welter J., Culmsee C., Biers J., Sommer N., Kang J.X., Mayer K., Hecker M., and Rummel C. (2023). **Omega-3 polyunsaturated fatty acids modulate the lung-brain axis of communication during LPS-induced ARDS.** German-Endochrine-Brain-Immune-Network Conference. Talk*.

- Hernandez J.*, Pflieger F.J., Schneiders J., Krüger K., Reichel T., and Rummel, C. (2023). **Neutropenia exaggerates the inflammatory response in the brain and periphery during LPS-induced severe systemic inflammation.** German-Endochrine-Brain-Immune-Network Conference. Talk*.

- Hernandez J., Stoll J.*, Meurer M., Harden L., von köckritz-Blickwede M., and Rummel C. (2023). **An assessment of bacterial induction of mouse neutrophil extracellular traps *in vitro* using lipopolysaccharide or Group B *Streptococcus*.** German-Endochrine-Brain-Immune-Network Conference. Poster*.
- Hernandez J.*, Pflieger F.J., Schneiders J., Krüger K., Reichel T., and Rummel C. (2022). **Severe systemic inflammation induces an exaggerated brain and**

peripheral inflammatory response in neutropenic mice. Deutschen Veterinärmedizinischen Gesellschaft (DVG). Poster*.

- Hernandez J.*, Pflieger F.J., Schneiders J., Krüger K., Reichel T., and Rummel, C. (2021). **Neutropenia enhances the brain and peripheral inflammatory response to LPS-induced hypothermic severe systemic inflammation.** German Physiological Society, Austrian Physiological Society, and Life Sciences Switzerland Physiology Meeting. Poster*.

- Hernandez J.*, Pflieger F.J., Schneiders J., Luheshi G., Krüger K., and Rummel, C. (2020). **Neutropenia exacerbates LPS-induced hypothermia modulating the brain and peripheral inflammatory response.** Virtual Physiology and Pharmacology of Temperature Regulation. Virtual poster*.

9.3 Declaration

I declare that I have completed this dissertation single-handedly without the unauthorized help of a second party and only with the assistance acknowledged therein. I have appropriately acknowledged and referenced all text passages that are derived literally from or are based on the content of published or unpublished work of others, and all information that relates to verbal communications. I have abided by the principles of good scientific conduct laid down in the charter of the Justus Liebig University of Giessen in carrying out the investigations described in the dissertation.

Jessica Kate Hernandez

9.4 Acknowledgement

Thank you to all my colleagues and collaborators without whom the success of these projects and this dissertation would not have been possible.

Namely, I would not have been able to accomplish all that I have in my doctoral program without the support and encouragement of my supervisor Prof. Dr. Christoph Rummel. Thank you for always having confidence in me and for the once in a life time opportunity that allowed me to move abroad and further my academic interests.

Additional thanks to Prof. Dr. Rüdiger Gerstberger for the chance to undertake a doctoral project at the Institute for Veterinary Physiology and Biochemistry and for the support of my work.

I would like to thank Prof Dr. Maren von Köckritz-Blickwede and her lab at the University of Hannover for allowing me to participate in a laboratory rotation that increased my knowledge of NET staining and identification and proved to be a wonderful learning experience. Further thanks for their continued expertise and assistance in immunofluorescent staining.

I would like to thank Prof. Dr. med. Konstantin Mayer's lab for their collaboration and providing tissues from their mice which made the entire ARDS project possible.

I would also like to thank Prof. Dr. Natali Bauer, Prof. Dr. Karsten Krüger, Prof. Dr. Natascha Sommer, Prof. Dr. Carsten Culmsee, Prof. Dr. Christiane Herden, as well as the FCMH initiative for carrying out additional immunoassays and analyses.

For superb technical assistance, I would like to thanks Ms. Doreen Marks and Ms. Jolanta Murgott who were a tremendous help throughout this process.

On a more personal note, few things can adequately prepare someone to leave behind everything they know to start over again in a new city, let alone a new country. I only managed to succeed as much as I did because of my friends and family. Therefore, I would also like to thank everyone at the Institute for Veterinary Physiology and Biochemistry that made me feel welcomed and included. In particular, Fabian thank-you for not only helping me get my project off the ground but also helping with the navigation

of life in Germany. My labmates, Leona and Julia, for always making sure everything was good enough for me. Roberto, thank you for helping me get through the trials and tribulations of everyday life as an expat doctoral student. Most importantly, to my family who never doubted that I would make it, even when it felt like nothing was going right, thank you for the unwavering support.